

Mixed-source community fermentation for ethanol production from municipal solid waste

Priscilla Carrillo Barragán

A thesis submitted to Newcastle University for the degree of
Doctor of Philosophy (Integrated)

School of Natural and Environmental Sciences

Faculty of Science, Agriculture and Engineering



April 2019

Declaration

I hereby certify that this work is the result of the research conducted by the author between September 2014 and April 2019 at Newcastle University, and that no part has been submitted in support for any other degree of qualification at this or any other university.

Abstract

Ethanol from lignocellulosic waste is a sustainable alternative to fossil transport fuels. While most research has been directed towards agricultural and industrial wastes as feedstocks, little attention has been paid to the organic fraction of municipal solid waste (OMSW). The production of bioethanol from OMSW would contribute to the integral solutions of climate change mitigation and transportation energy security, along with the reduction of the increasing amount of municipal solid waste generated, especially in developing countries. Additionally, studies on ethanol (EtOH) production have largely focused on genetically engineering single microorganisms to fully convert lignocellulosic substrates into EtOH. However, mixed culture fermentation (MCF) represents a suitable approach to handle the complexity and variability of organic wastes and to avoid expensive and vulnerable closed-control operational conditions.

In this work, a mixed-source bacterial community, mainly comprised of *Clostridium*, *Pseudomonas*, *Leuconostoc*, *Ruminococcus*, *Petrimonas* and *Leptolinea* genera members, has been reproducibly enriched from sheep rumen and anaerobic granular sludge after testing a range of environmental inocula sources. This community generates $59.8\text{mM} \pm 2.8\text{mM}$ of EtOH in batch microcosms incubated at room temperature under initial aerobic conditions and without further conditioning of the acid pre-treated OMSW used as substrate. The EtOH yield obtained (0.070L/Kg) is about 1/6 of the current corn grain-based EtOH industrial production yield (0.42 L/Kg). EtOH production from such a complex substrate as OMSW in addition to the minimal inputs required by this community, makes it a good candidate for implementation in biorefinery projects in both developed and developing countries.

Despite the reproducibility of these results, where batch cultures were started from the original inocula sources, a drastic loss of EtOH production occurred across successive culture transfers to fresh media conducted at 14 and 3 days after inoculation, where EtOH production decreased by 80% and 50% of the originally inoculated batches, respectively. Nevertheless, during five successive 3-day transfers a functional and structurally stable community was achieved, producing $30.5\text{mM} \pm 1.3\text{mM}$ of EtOH and consistently enriching *Clostridium* and *Pseudomonas* as the most relatively abundant community members. Transfer timing could have played a critical role to maintain organisms with the desired activity before they passed into non-viability, thus having a competitive disadvantage against other more viable bacteria at the time of transfer.

While experimental optimisation and control of EtOH production by these communities remains a challenge, these are promising results encouraging further studies of these communities for their implementation in biorefinery projects. The present study contributes to the scientific literature by presenting the first report of Mixed-source Community Fermentation for Ethanol production from the Organic fraction of Municipal Solid Waste.

Dedication

To Nature, my inexhaustible source of wonder, joy and inspiration.

To México, I am fortunate to have been born in the belly button of the moon, one of your valleys, and to grow up wrapped up by the warmth of your people, whose daily efforts have sponsored this work.

To my mom, Lupita, my role model, my heroine, my first and eternal love.

To my sister, Pau, my reliable source of smiles and laughter.

To my grandparents, Pedro and Cristina, my definition of superheroes

To my family, regardless of the distance I can feel your warmth.

To my father Jorge, I would not have walked so far without you.

To Vali, because the struggle was real, and you have been always there for me.

This is our work.

Acknowledgments

I would like to thank my principal supervisor, Dr. Neil Gray for giving me the opportunity to develop my project proposal, conduct independent work and for always being available for discussion. Equally, I want to thank Dr. Jan Dolfing for his key guidance in critical moments of this project. My thanks are also given to Dr. Paul Sallis for his advice during this work.

I also want to thank Dr. Théodore Bouchez and Dr. Russell Davenport for facilitating an interesting discussion and providing constructive feedback during the *viva voce* examination of this work. I learnt quite a bit from them during that positive experience.

Equally, I would like to thank the Geomicrobiology research group for their support.

I have also received a great amount of guidance and support from the technical team of the former CEGs and now SNES. Special thanks to Paul Donohoe and David Race.

I am profoundly grateful to Berni Bowler, because none of this work would have been possible without his expertise and his friendship.

Warm thanks go out to Patri, for constantly exchanging with me the parts of Don Quijote and Sancho Panza. For sparkling with colours the grey of this adventure. For Duchamp, but really Baroness Elsa von Freytag-Loringhoven, and Ecce Homo.

I would also like to thank Dr. Aleksej Zelezniak and the dry-lab team of Sysbio at Chalmers University. Specially to Filip, for all his selfless help, for the long hours cracking code for this newbie. For encouraging curiosity and for re-teaching me how to learn.

I am sincerely grateful to my sponsor, CONACyT, for their financial support and the trust in this project.

Equally, I appreciate the financial support of SfAM when it was needed the most. I also want to thank FEMS for giving me not only the financial support to do research abroad, but the opportunity to learn and develop new skills.

Table of contents

1.	Introduction	1
1.1	Context	1
1.2	Research problem, aim and objectives	3
2.	Literature review of bioethanol production	5
2.1	Lignocellulosic biomass: the ultimate feedstock	5
2.1.1	Lignocellulosic biomass physicochemical characteristics	6
2.2	Bioethanol production from lignocellulosic waste	7
2.2.1	Overview of research on the production process of lignocellulosic ethanol	7
2.2.2	Commercial-scale bioethanol production from agricultural waste	9
2.3	Municipal solid waste: the problem and the opportunity	11
2.3.1	The organic fraction of municipal solid waste (OMSW) in México and England	12
2.3.2	Research on OMSW as feedstock for EtOH production.	14
2.4	Mixed culture fermentation (MCF): union is strength	20
2.4.1	Environmental control of MCF	24
2.5	MCF modelling	27
2.6	Conclusions	29
3.	Methods	31
3.1	Inocula description and sampling	31
3.2	Organic Municipal Solid Waste (OMSW) analogue composition and preparation	32
3.2.1	OMSW analogue diluted acid pre-treatment	35
3.2.2	OMSW medium basic chemical characterisation	35
3.2.3	OMSW electron milliequivalents content and electron balances	37
3.3	Microcosms set up	37
3.3.1	Culture medium preparation	37
3.3.2	Microcosms inoculation	39
3.3.3	Microcosms liquid sampling and routine analyses overview	39
3.4	Physicochemical analyses of liquid samples	40

3.4.1	pH measurements	40
3.4.2	GC-FID	40
3.4.3	VFAs IC	41
3.5	Statistical analysis of physicochemical data	41
3.6	Molecular biology analysis	41
3.6.1	DNA extraction and purification	42
3.6.2	16s RNA gene PCR amplification	42
3.6.3	Agarose gel electrophoresis	43
3.6.4	Ion-torrent PGM sequencing pooled library preparation	43
3.6.5	Preparation of samples for MiSeq sequencing	45
3.7	Next generation sequencing (NGS) data analysis	46
3.7.1	NGS data pre-treatment	47
3.7.2	Univariate analyses	48
3.7.3	Species richness (S)	48
3.7.4	Inverse Simpson's species diversity and evenness indices	48
3.7.5	Multivariate analyses	49
3.7.6	Bray-Curtis similarity matrix	50
3.7.7	Non-parametric multidimensional scaling (nMDs)	50
3.7.8	Analysis of similarities (ANOSIM)	51
3.7.9	Similarity percentage (SIMPER)	51
4.	Evaluation of inocula source, pH and environmental oxygen for ethanol production from Organic Municipal Solid Waste	53
4.1	Introduction	53
4.2	Objectives	57
4.3	Methods	57
4.3.1	Culture media preparation	57
4.3.2	pH adjustment	58
4.3.3	Microcosms inoculation	58
4.3.4	Experimental design	58
4.3.5	Microcosms incubation and sampling plan	59
4.3.6	GC-FID quantification of soluble fermentation products	60

4.3.7	Statistical analysis of physicochemical data	61
4.4	Results	62
4.4.1	EtOH production by different inocula under initial anaerobic conditions at initial neutral pH	62
4.4.2	EtOH production by different inocula under initial aerobic conditions at initial neutral pH	63
4.4.3	Statistical comparison of maximal EtOH production by the different inocula under initial anaerobic and aerobic conditions at initial neutral pH	65
4.4.4	Microcosms at initial neutral pH time profiles	67
4.4.5	Effect of inocula under initial aerobic and anaerobic conditions at initial acidic pH	69
4.4.6	Statistical comparison of maxima EtOH production by the different inocula under initial anaerobic and aerobic conditions at initial acidic pH	71
4.4.7	Initial acidic pH time profiles	73
4.4.8	Overall comparison of fermentative activity	74
4.4.9	Correlation analysis between pH and EtOH production.	74
4.4.10	Rumen and sludge enrichments electron balances.	77
4.5	Discussion	77
4.5.1	Initial oxygen condition and EtOH production	78
4.5.2	EtOH as major fermentation product	80
4.6	Conclusions	84
5.	Enrichment and characterisation of ethanologenic communities from different inocula sources degrading the organic fraction of municipal solid waste	85
5.1	Introduction	86
5.2	Hypothesis and objectives	87
5.3	Methods	87
5.3.1	Experimental design	87
5.3.2	Microcosms set-up	87
5.3.3	pH adjustment	87
5.3.4	Microcosms incubation and sampling plan	88
5.3.5	GC-FID quantification of soluble ethanol	88
5.3.6	Statistical analysis of physicochemical data	89

5.3.7	DNA extraction and purification	89
5.3.8	Denaturing Gradient Gel Electrophoresis (DGGE)	90
5.3.9	DGGE gels statistical analysis	91
5.3.10	Ion Torrent PGM sequencing pooled library preparation	92
5.3.11	16S rRNA sequencing processing and community composition analyses	92
5.4	Results	93
5.4.1	Ethanologenic activity of the different inocula tested at an initial pH range	93
5.4.2	Statistical comparison of maximal EtOH production by the different inocula at an initial pH range	95
5.4.3	DGGE fungal and bacterial analysis	98
5.4.4	Community composition indices	104
5.4.5	Ordination and statistical comparison of the different inocula before and after enrichment	106
5.4.6	Specific bacterial OTUs typical from the inocula groups before and after enrichment	107
5.4.7	Specific discriminating bacterial OTUs before and after enrichment within single inocula and between the enriched communities from different inocula	111
5.5	Discussion	115
5.5.1	Putative functions of the enriched communities' members	116
5.5.2	Enrichment of a mixed-source novel community	125
5.6	Conclusions	126
6.	Transition of microbial communities during the adaption to fermentation of OMSW at low pH.	129
6.1	Introduction	129
6.2	Objectives	129
6.3	Methods	130
6.3.1	Experimental set-ups	130
6.3.2	Microcosms preparation	130
6.3.3	Microcosms incubation and sampling plan	131
6.3.4	GC-FID quantification of soluble ethanol	131
6.3.5	Statistical analysis of physicochemical data	132

6.3.6	DNA extraction and purification	132
6.3.7	Ion Torrent PGM sequencing pooled library preparation	132
6.3.8	Preparation of samples for MiSeq sequencing	133
6.3.9	16S rRNA sequencing processing and community composition analyses	133
6.3.10	Preparation of samples for Thermogravimetry-Differential Scanning Calorimetry–Quadrupole Mass Spectrometry (TG-DSC-QMS) of Exp B	134
6.4	Results	135
6.4.1	Soluble fermentation products across 14-days transfers (Exp A)	135
6.4.2	Soluble fermentation products across 14-days transfers with initial pH amended after inoculation (Exp B)	137
6.4.3	TG-DSC analysis of OMSW after initial inoculation in Exp B	139
6.4.4	Statistical comparison of maximal fermentative production at the different transfers in Exps A and B	140
6.4.5	Community composition indices of 14-day transfers	141
6.4.6	Ordination and statistical comparison of the communities in 14-days transfers	144
6.4.7	Specific bacterial OTUs typical from the different 14-days transfers	146
6.4.8	Preliminary conclusions leading to the design of Experiment C	153
6.4.9	Soluble fermentation products across 3-days transfers (Exp C)	154
6.4.10	Statistical comparison of maximal fermentative production at the different transfers in Exp C	157
6.4.11	Community composition indices	158
6.4.12	Ordination and statistical comparison of the communities in the 3-days transfers	159
6.4.13	Specific bacterial OTUs typical from the different 3-days transfers	162
6.5	Discussion	169
6.5.1	Putative functions of the most abundant members enriched across transfer experiments	170
6.5.2	Known and unknown selective pressures influencing the bacterial communities enriched	181
6.6	Conclusions	183

7.	Modelling the metabolic interactions within ethanol producing bacterial communities degrading the organic fraction of municipal solid waste	185
7.1	Introduction	185
7.2	Aim and objectives	186
7.3	Methods	187
7.3.1	Identification of the closest species to experimentally determined OTUs	187
7.3.2	Representative genomes retrieval	187
7.3.3	Species-Level genome-scale metabolic model reconstruction	187
7.3.4	Draft GEMs curation and simulation	188
7.3.5	Community metabolic modelling simulation	188
7.4	Results	189
7.4.1	Closest species annotated genomes retrieval to experimentally determined OTUs	189
7.4.2	Draft GEMs manual curation and simulation	190
7.4.3	Communities draft models	192
7.5	Discussion	193
7.6	Conclusions	196
7.7	Acknowledgements	196
8.	Conclusions and recommendations	197
8.1	Conclusions	197
8.1.1	OMSW lab-scale batch reactors operational conditions	197
8.1.2	Mixed-source microbial community characterisation	199
8.1.3	Reproducibility and stability of ethanologenic activity by the mixed-source community	199
8.1.4	Closing remarks	201
8.2	Limitations and Recommendations	202

Appendix A	Statistical analyses of physicochemical data	209
Appendix B	OMSW medium basic chemical characterisation	215
Appendix C	Electron balances	217
Appendix D	Samples and Golay barcodes used for Ion Torrent PGM sequencing	219
Appendix E	TG-DSC data analysis	221
Appendix F	Phylogenetic trees of the most abundant OTUs in the enriched communities of Chapter 6	223
Appendix G	Volatile Suspended Solids content of the R+S inoculum	227
References		229

List of tables

2.1	Commercial-scale operating plants producing lignocellulosic EtOH worldwide.	10
2.2	MSW physical composition in Mexico and England.	13
2.3	Experimental studies of biochemical EtOH production from OMSW.	18
3.1	Composition of the OMSW analogue prepared to be used as substrate for EtOH production throughout this project.	32
3.2	Nutritional values per 100g reported for the food component used to integrate the organics category of the OMSW analogue.	33
4.1	Results of the multiple pairwise-comparison (Tukey HDS test) of the interaction effect of inocula source and initial oxygen conditions on EtOH production at an initial neutral pH.	66
4.2	Results of the multiple pairwise-comparison (Tukey HDS test) of the interaction effect of inocula source and initial oxygen conditions in EtOH production at initial neutral pH.	72
4.3	Correlation analyses results of maximal EtOH production vs initial pH and pH at maximal EtOH concentration.	76
4.4	ATP formation in substrate level phosphorylation	80
5.1	Reagents for the preparation of DGGE denaturing solutions.	91
5.2	Results of the multiple pairwise-comparison (Tukey HDS test) of the interaction effect of inocula source and initial pH conditions on EtOH production.	97
5.3	Most frequent and abundant OTUs found in each inocula group at the beginning of the experiment and after 11 days of enrichment as determined by SIMPER test.	108
5.4	Discriminating OTUs between initial inocula community composition and after 11 days of enrichment as determined by SIMPER test.	112
5.5	Discriminating OTUs between the enriched communities from the different inocula as determined by SIMPER test.	114
6.1	Exps A and B pairwise comparisons of sampling points within and between transfers of each experimental set-up as determined by ANOSIM test.	145
6.2	Most frequent and abundant OTUs found in each sampling point from the initially inoculated microcosms from experimental set-ups A and B as determined by SIMPER test.	148
6.3	Most frequent and abundant OTUs found in each sampling point from the first (Tr1) and last (Tr4) transfers from experimental set-ups A and B as determined by SIMPER test.	151
6.4	Exp C pairwise comparisons of sampling points within and between transfers as determined by ANOSIM test.	161

6.5	Most frequent and abundant OTUs found in each sampling point from the initially inoculated microcosms from experimental set-ups C as determined by SIMPER test.	163
6.6	Most frequent and abundant OTUs found in each sampling point from transfers 1,3 and 5 from experimental set-up C as determined by SIMPER test.	167
7.1	Experimental OTUs phylogenetic alignment results.	190
B1	Table B1. Basic chemical characterisation of food waste fractions and acid pre-treated OMSW.	215
B2	Table B2. Reported and estimated TCOD and BMP values of food waste fractions and acid pre-treated OMSW.	216
C1	Half reactions used to determine electron-equivalent balance and stoichiometry	217
D1	Samples and Golay barcodes used for Ion Torrent PGM sequencing in Chapter5.	219
D2	Samples from EXPs A and B and Golay barcodes used for Ion Torrent PGM sequencing in Chapter 6.	220
E1	Table D1. TG-QDS results	222

List of figures

2.1	General diagram of ethanol production from lignocellulosic biomass.	7
2.2	MCF possible fermentation pathways, taken from Agler et al., (2011).	23
3.1	OMSW analogue preparation and pre-treatment.	34
3.2	Flow diagram of the OMSW analogue culture medium preparation.	36
3.3	General description of the volume of liquid samples and their preparation for the routine analyses performed at different time points for each microcosm.	37
3.4	Flow diagram of the 16S rRNA gene next generation sequencing data analysis.	44
4.1	Experimental designs (EXP1 and EXP2) to test the effects of inocula source, oxygen presence and pH in EtOH production.	59
4.2	Fermentation products by the different inocula tested during 14 days of incubation under initial anaerobic conditions	62
4.3	Fermentation products by the different inocula tested during 14 days of incubation under initial aerobic conditions.	64
4.4	Two-way interaction plot of the means of the maxima EtOH concentrations as a response to the combination of the two factors tested: inocula and initial oxygen conditions	65
4.5	pH changes in each inocula configuration and the blanks during the incubation period under initial aerobic and anaerobic conditions.	67
4.6	Fermentation products and pH curves of the individual sludge inoculated replicates incubated under initial anaerobic conditions.	68
4.7	Fermentation products by the different inocula tested during 30 days of incubation under initial anaerobic conditions.	69
4.8	Fermentation products by the different inocula tested during 30 days of incubation under initial aerobic conditions.	70
4.9	Two-way interaction plot of the means of the maxima EtOH concentrations as a response to the combination of the two factors tested: inocula and initial oxygen conditions.	71
4.10	pH changes in each inocula configuration and the blanks during the incubation period under initial aerobic and anaerobic conditions.	73
4.11	Maximal EtOH production by the different inocula and their initial and pH at max. concentration of EtOH in EXP 1 and EXP2.	75
4.12	Soluble fermentation products as a function of pH in MCF according to the literature.	82
5.1	Experimental design to test the effects of inocula source and initial pH in EtOH production.	87

5.2	Boxplot of the initial pH value groups.	88
5.3	EtOH production profiles and pH curves of the different inocula incubated at a range of initial pH.	94
5.4	Two-way interaction plot of the means of the maxima EtOH concentrations as a response to the combination of the two factors tested: inocula and initial pH conditions.	96
5.5	DGGE fingerprints of fungal ITS region in the rRNA gene fragments amplified from the different inocula under study at the initial pH where their maximal EtOH production was achieved.	99
5.6	DGGE fingerprints of the different inocula under study	102
5.7	nMDS ordination plots of the respective individual DGGE fingerprints in Figure 5.6.	103
5.8	Richness, Simpson's inverse diversity and Simpson's evenness indices of the communities at time 0, represented as boxplots.	105
5.9	A) nMDS of all the inocula at their maximal EtOH production initial pH along with the inocula blanks. B) nMDS of only the inoculated microcosms samples.	106
5.10	Diagram of the putative functionalities of the dominant OTUs enriched from the different inocula under study.	123
6.1	Experimental set-up of the different transfer configurations to test the stability of EtOH production by the R+S community.	130
6.2	Exp A. Fermentation products by the R+S community across transfers tested during 14 days of incubation with no carbonates buffer addition.	135
6.3	Exp B. Fermentation products by the R+S community across transfers tested during 14 days of incubation with initial carbonates buffer addition.	138
6.4	Exps A and B. Richness, Simpson's inverse diversity and Simpson's evenness indices of the communities at the different sampling days across transfers represented as boxplots.	142
6.5	nMDS of Exp A and Exp B replicates including an inocula blank.	144
6.6	Stacked bar plots with different colours representing the average number of OTUs accounting for at least 70% of the cumulative similarity in each transfer/sampling day group from Exp A and Exp B.	147
6.7	Exp C. A) Fermentation products by the R+S community across transfers tested during 3 days of incubation with initial carbonates buffer addition.	155
6.8	ExpC richness, Simpson's inverse diversity and Simpson's evenness indices of the communities at the different sampling days across transfers represented as boxplots.	158
6.9	nMDS of Exp C replicates.	159

6.10	Stacked bar plots with different colours representing the average number of OTUs accounting for at least 70% of the cumulative similarity in each transfer/sampling day group from Exp C.	162
6.11	Diagram of the putative functionalities of the dominant OTUs.	175
6.12	A) Inoculated microcosms at 7 days of incubation. B) Inocula blanks at 7 days of incubation. Images from Exp C.	176
6.13	Soluble fermentation products as a function of pH in MCF according (Rodríguez <i>et al.</i> , 2006) modelling approach.	180
7.1	Workflow diagram of the steps and computational biology/bioinformatic tools employed to construct the metabolic model of the bacterial community starting from 16S ribosomal RNA sequences.	189
7.2	Predictions of interacting subcommunities within the “average” highly ethanologenic community enriched after initial inoculation by the SMETANA pipeline.	192
A1	Workflow diagram for the statistical comparison of variables with n number of levels.	209
A2	Workflow diagram for the statistical correlation analysis of 2 variables.	210
A3	Visual inspection of ANOVA test validity	211
A4	Visual inspection of data for ANOVA test	212
E1	Average TG and DSC and QMS profiles (from top to bottom of OMSW substrate in initially inoculated microcosms and inocula blanks from Exp B after 14 days of incubation (see Chapter 6, section 6.4.3)	221
F1	Neighbour-joining phylogenetic tree based on 16S rRNA gene sequences	223

“...to the eyes of the man of imagination, nature is imagination itself.”

William Blake

Chapter 1. Introduction

1.1 Context

Today, the transport sector worldwide is almost totally dependent on petroleum-based fuels, being responsible for 60% of the world oil consumption and generation of more than 70% of carbon monoxide and 19% of carbon dioxide emissions (Demirbas 2009; Balat 2011)

As result of climate change associated with these greenhouse gases (GHG), the rise of oil prices and the need for energy security; the use of liquid biofuels has gained global support (Balat 2011). Indeed, the United Kingdom and Mexico, being part of G8+5 Climate Change Dialogue, agreed to increasingly employ biofuels for transport to meet their energy targets (GBEP, 2007; Congreso General de los Estados Unidos Mexicanos, 2008; Departament for Transport, 2012).

To achieve these goals alternative fuels must be economically and technically viable and meet the sustainability conditions of reduced GHG emissions and renewable availability.

Within the biomass-derived alternatives to fossil fuels, ethanol (EtOH) seems to be the most promising option for internal combustion engines, which still dominate in transport (Agarwal 2007; Balat 2011; Laser and Lynd 2014).

Bioethanol can be produced from sugars, crops or lignocellulosic materials (Balat 2011). Among these feedstocks, lignocellulosic biomass represents a more sustainable alternative for petroleum, as it has low prices, can be obtained from residual non-food parts of crops, industry and municipal wastes (Mousdale 2008; Demirbas 2009). Importantly, such sources do not compete directly with food production and their obtainment neither requires the deforestation of natural lands nor large quantities of water for growth (wastes), contributing to ecosystems and biodiversity conservation (Mousdale 2008; Demirbas 2009). Therefore, the lignocellulosic waste derived ethanol impact on the environment would be significantly lower than ethanol from crop-based fuels.

In this regard, most efforts have been focused on agricultural (Agrawal et al. 2015; Sarkar et al. 2012; Talebnia et al. 2010) and industrial (Frankó et al. 2016; Kádár et al. 2007) products and wastes as lignocellulosic biomass, whereas the organic fraction of municipal

solid waste (OMSW) has received little attention as feedstock for EtOH production (Ma et al. 2009; Li et al. 2007). OMSW is an attractive feedstock due to its high cellulosic content (Ma et al. 2009; Li et al. 2007) and particularly, to address the international concern to reduce the quantities of waste going to landfill, an issue of especial relevance in urban regions of developing countries, where there is overpopulation, lack of landfill space and generally an MSW treatment/disposal associated negative cost.

However, to make any lignocellulosic fuel affordable, a complex treatment is required, capable of hydrolysing lignocellulose into cellulose and hemicellulose while transforming the resulting mixture of sugars into ethanol (Demirbas 2009; Mousdale 2008). The current trend to face these challenges has been to engineer strains of well-studied ethanologenic and/or industrially friendly microorganisms (e.g. *S. cerevisiae*, *Z. mobilis*, *E. coli*, etc.) to expand their metabolic capabilities, but these processes operate under narrow closed-control conditions, are still limited and the subject of improvement (Carere et al. 2008; Gusakov 2011; Hasunuma et al. 2013).

An alternative approach for the sustainable production of bioethanol could be the application of eco-biotechnology principles, combining the methods of environmental biotechnology with the goals of industrial biotechnology (Johnson et al. 2009), this is to say, the production of metabolic products employing open mixed cultures and ecological selection principles, such as directed natural selection via competition rather than genetic or metabolic engineering, i.e., engineering the ecosystem rather than the microorganisms (Johnson et al. 2009; Varrone et al. 2015).

Indeed, Mixed Culture Fermentation (MCF) is a promising alternative to enzymatic treatment and monoculture fermentation, as it has shown (Kato et al. 2005; Okeke and Lu 2011; Cheng and Zhu 2012; Ronan et al. 2013) enhanced characteristics in the conversion of cellulose to EtOH by virtue of the synergistic combination of metabolic capabilities, reducing problems such as end-product inhibition, incomplete synergistic enzymes, closed-control process and the need for high concentration of enzymes (Zuroff and Curtis 2012). In addition, consortia are more resistant and resilient to perturbation, and close process control is less necessary, making EtOH production more robust and exploitable for operational and maintaining costs (Kato et al. 2005; Okeke and Lu 2011; Ronan et al. 2013).

1.2 Research problem, aim and objectives

The complex structure of OMSW is still today a challenge for microbiological conversion (Steinbusch et al. 2009; Goh et al. 2010; Li and Khraisheh 2010). Indeed, at the time of writing, a Mixed Community Fermentation for EtOH production from OMSW has not yet been reported. Nevertheless, the use of a multiple-species community could be an efficient robust approach to achieve this transformation. However, the complexity of the substrate and of interactions between microorganisms might impose substantial impediments to process manipulation for ethanol production.

The aim of this research was therefore, to enrich a robust microbial community, able to transform the organic fraction of municipal solid waste into ethanol. However, the strength offered by the community diversity and its broad metabolic potential, was at the same time considered the main drawback, as the function of the community would become increasingly difficult to predict and control, and the system switching away from EtOH accumulation as alternative pathways of OMSW degradation are available which may be more thermodynamically and kinetically favourable under in situ conditions. To this extent experiments were conducted with batch microcosms to:

- Evaluate the ubiquity of EtOH fermentation, by monitoring soluble fermentation products profiles of microcosms incubated with different inocula sources where lignocellulose degradation is known to occur (compost piles, woodland soil, rumen, cow faeces and granular anaerobic sludge).
- Compare EtOH production by these inocula under different environmental conditions, such as initial pH and oxygen presence.
- Determine the best combination of inocula/environmental variables (pH/initial O₂) for EtOH production.

Based on the identified best inocula and optimal initial environmental variables, batch microcosms and culture transfers were run and monitored for soluble fermentation products, physicochemical properties and microbial community dynamics to:

- Connect the microbial community composition and possible functionality of the enriched communities to the observed ethanol producing activity.

- Understand the basic thermodynamics and putative functions and relationships between microorganisms and how these might influence the dynamics and robustness of the system to achieve a reliable engineered process.
- Enrich an efficient and stable ethanologenic bacterial community through successive inoculum transfers.

Additionally, microbial community modelling has been used and recognised as a powerful tool to simplify, describe, control and predict the behaviour of complex biological systems (Rodriguez et al., 2005; Zomorodi and Maranas, 2012), and should be considered as part of the holistic approach to engineer biological systems. Therefore, *in silico* experiments using Flux Balance Analysis (FBA) of annotated whole genome sequences were conducted to:

- Obtain representations of the metabolic interactions capable to explain observed fermentation yields by the enriched ethanologenic community.
- Produce a simple model that would serve as a guide for the system operation and optimisation.

Chapter 2. Literature review of bioethanol production

In this literature review, bioethanol production from Organic Municipal Solid (OMSW) waste is discussed by first highlighting the sustainability and social advantages of lignocellulosic wastes as a feedstock when compared to the crop-based current industrial process, to then describe the properties of OMSW among these wastes. The biochemical research approaches for the conversion of these substrates is explored, emphasising the desirability of mixed culture fermentation (MCF) and the use of environmental variables to direct this process towards EtOH production. Finally, the conclusion summarises the relevant information, highlighting the promising areas of research for this field.

2.1 Lignocellulosic biomass: the ultimate feedstock

Nowadays, commercial bioethanol production is led by The United States and Brazil. The former generates around 54 billion litres per year using corn as its main feedstock, whereas the latter bases its production on sugar cane, producing up to 24 billion litres per year (U.S. Energy Information Administration 2015; Barros 2017).

In this respect, numerous studies have been directed to improve these production processes (Kaliyan et al. 2011; de Souza Dias et al. 2015; Dias et al. 2012), as well as to evaluate alternative crops containing a larger proportion of simple sugars to be used for bioethanol production (Bertrand et al. 2016; Barros 2017; Haghighi Mood et al. 2013).

As several reports and life cycle analysis have shown, crop-based bioethanol provides a degree of independence from petroleum in an economically “viable” way, but when considering its energy balance it usually fails to be a sustainable alternative to fossil fuels, as its production can generate higher levels of greenhouse gases (GHG), involves deforestation, damage of biodiversity, erosion and stress of soils, high levels of water demand, fertilisers, and pesticides, thus causing contamination. Moreover, there is direct competition with food production and consequential rise in food prices (Kaliyan et al. 2011; Q. Yang and Chen 2012; Pieragostini et al. 2014; Goldemberg et al. 2008; Cantarella 2018). In consequence, research has moved towards more sustainable feedstocks, such as is waste lignocellulosic biomass, which seems to overcome most of the negative aspects of crop-based ethanol (EtOH) (Singh et al. 2010; Balat 2011; Walker 2011).

2.1.1 Lignocellulosic biomass physicochemical characteristics

Lignocellulose, the most abundant renewable biomass on the planet, is a complex mixture of cellulose, hemicelluloses and lignin (Sluiter et al. 2010; Balat 2011). The carbohydrate polymers (cellulose and hemicellulose), which can be hydrolysed and fermented into EtOH, contribute to about two-thirds of its typical dry mass.

Cellulose can account for 40 – 60% of the dry biomass from the fermentable fraction. Although cellulose is made from glucose monomers just as the starch in corn for EtOH production, its function is to provide structure to the plant biomass, whereas starch is a readily-available glucose reservoir. Therefore, unlike starch, cellulose is a difficult polymer to disrupt (Hendriks and Zeeman 2009; Sluiter et al. 2010).

The other major polymers in lignocellulosic materials are the hemicelluloses (20 – 40% dry biomass), comprised of branched chains of pentoses (xylose and arabinose) and hexoses (glucose, galactose and mannose). The less “organised” structure of hemicelluloses makes them easier to degrade, however different enzymes are required to hydrolyse and ferment the five and six-carbon sugars, imposing a further challenge for lignocellulose biomass optimal use by single organisms such as *S. cerevisiae* (Hendriks and Zeeman 2009; Chundawat et al. 2011).

Meanwhile, lignin (10–25% dry biomass) is a complex polyphenolic compound that cannot be used for ethanol production and therefore, is an unavoidable residue in any ethanologenic process (Thakur et al. 2014). However, despite its recalcitrance, a small number of microorganisms can transform it into high value products (Calvo-Flores and Dobado 2010; Thakur et al. 2014; Larsen et al. 2012). Although this characteristic makes lignocellulosic biomass an even more attractive feedstock, lignin applications and processes are not addressed in this study.

While their chemical composition is what makes lignocellulose materials promising sources for EtOH production, their structure is also the main drawback for its efficient large scale implementation (Sanderson 2011). In this regard, Chundawat and collaborators (2011) presented a comprehensive summary of lignocellulose structure and the problems associated to its biochemical deconstruction from raw biomass to the carbohydrate polymer chain level.

Based on their origin, lignocellulosic waste materials have been classified in four groups: forest residues, municipal solid waste, waste paper, and crop residues (Balat 2011).

Regarding their structure and fermentable sugars that could be obtained from them, Duff and Murray (1996) reviewed the composition and potential of forest residues, whereas Sarkar and colleagues (2012) focussed on agricultural wastes. Sun and Cheng (2002) presented the cellulose, hemicellulose and lignin composition of materials encompassed in forest, paper and crop residues, but failed to include municipal solid waste. The latter has been partially addressed by Li et al. (2012), who investigated the structure, enzymatic hydrolysis and sugar yield from a pre-treated organic fraction of municipal solid waste (OMSW) fibre, reporting a composition of 49% cellulose, 16% hemicelluloses and 10% lignin, while Blake et al.(2017) contribute with the description of some physicochemical properties, such as calorific value and metals content of a fibrous material obtained after pre-treatment of non-segregated OMSW and methane production from it.

2.2 Bioethanol production from lignocellulosic waste

In this section, research and commercial production of EtOH from lignocellulosic waste are broadly reviewed, apart from OMSW, which despite being a lignocellulosic waste, will be discussed in detail in section 2.3.

2.2.1 Overview of research on the production process of lignocellulosic ethanol

The current approach to bioethanol production from lignocellulosic materials can be generalized as follows:

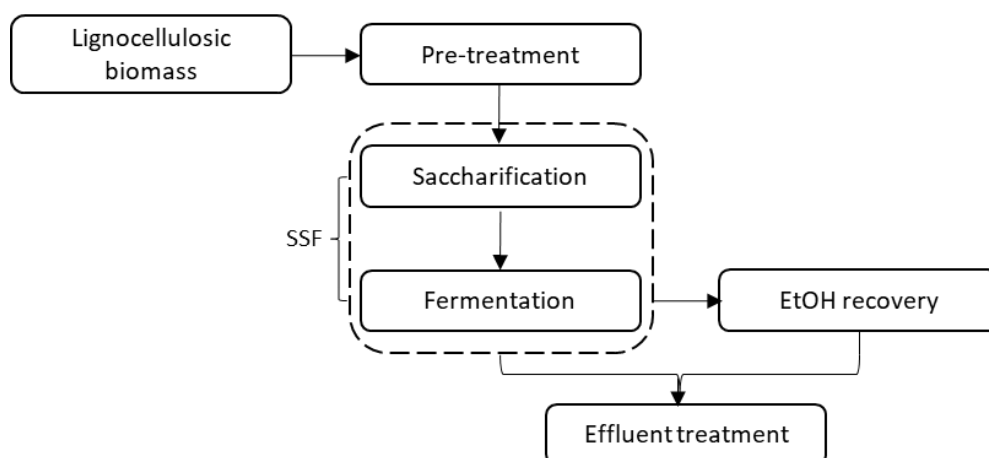


Figure 2.1 General diagram of ethanol production from lignocellulosic biomass. SSF: the saccharification and fermentation steps take place simultaneously.

As Figure 2.1 broadly shows, lignocellulosic materials require a pre-treatment before they can be biologically transformed into EtOH. This can be physical, chemical, physico-chemical or enzymatic, and is considered of prime importance for the maximum optimization of the process. The different pre-treatments, their impact on lignocellulose composition, the release of inhibitory compounds and the consequences for methane and EtOH production have been thoroughly reviewed (Hendriks and Zeeman 2009; Haghighi Mood et al. 2013; Jönsson and Martín 2016).

After the pre-treatment where the lignocellulose structure is disrupted to a certain degree depending on the pre-treatment conditions, the hemicellulose and cellulose are hydrolysed in what is also known as saccharification (Hasunuma et al. 2013). The most common saccharification approach is the addition of fungal recombinant cellulases and hemicellulases enzymes, typically from *Trichoderma reesei*, or mixtures of these enzymes with those from *Saccharomyces cerevisiae* and/or different *Clostridium* species (Das et al. 2013; Bischof et al. 2016). There has also been research in the utilization of thermo-stable enzymes from thermophiles (Gusakov 2011).

The resulting hexoses and pentoses are then fermented to ethanol by the recombinant xylose-degrader *S. cerevisiae* (Mohd Azhar et al. 2017; Martel et al. 2011), or by recombinant bacteria, such as *Escherichia coli*, which expresses *S. cerevisiae* enzymes and tolerates high ethanol concentrations (Das et al. 2013; Balat 2011; Hasunuma and Kondo 2012). *Zymomonas mobilis* is another promising fermentative bacteria (S. Yang et al. 2016), able to convert 90% of the total sugars into EtOH in 18 h (Dewan et al. 2013).

Despite the extensive research conducted to find novel suitable enzymes or to engineer those currently available, and the present offer of commercial enzymes that can effectively hydrolyse lignocellulose to hexoses and pentoses, the typical problems associated with the use of cell-free enzymes remain. For instance: cell free enzymes are subject to product inhibition and high amounts are required, making the process expensive (Teugjas and Väljamäe 2013; Atreya et al. 2016; Q. Zhang and Bao 2017). Indeed, the high cost of enzymatic hydrolysis is a major constraint in the economics of lignocellulosic ethanol and chemicals (B. Yang et al. 2014; Alrumman 2016).

Simultaneous saccharification and fermentation (SSF) is an alternative approach, where these two-unit processes occur in the same reactor as the mixture of hydrolytic enzymes and either the fermentative monoculture or co-culture (hexose and pentose separate fermenters) are combined (Olofsson et al., 2008; Dewan et al., 2013). This process

overcomes the problem of enzyme susceptibility to feedback inhibition by their own products and other compounds, and it has been reported that around 70% of the theoretical EtOH yield can be achieved from total sugars fermentation (Olofsson et al., 2008).

Although the hydrolysis rate is increased, the concentration of enzymes needed is lower and there is less risk of contamination, the main disadvantage of SSF is the difference in optimal conditions for both unit processes (Olofsson et al., 2008; Balat, 2011). This could be overcome using thermostable enzymes from thermophilic and hyperthermophilic bacteria which might be suited to harsh process conditions (Gusakov, 2011). However, the differences in temperature and other environmental conditions for the performance of both processes, today remains a challenge for optimization.

The common approach to EtOH recovery is distillation from the aqueous phase, and subsequent EtOH collection by condensation (Balat, 2011). However, diverse alternatives have been studied and technologies proposed to recover EtOH from the culture broth. For instance, Cadwalader and Dieterle patented an approach where a fraction of the broth recirculates over a system of membranes under reverse osmosis, and then EtOH is recovered (Cadwalader and Dieterle, 2012).

2.2.2 Commercial-scale bioethanol production from agricultural waste

Notwithstanding the challenges previously described, EtOH production from lignocellulosic waste is today a reality. Based on a comparison between the National Renewable Energy Laboratory 2016 Survey of Non-Starch Alcohol (Schwab et al. 2016) and the database Task39 IEA Bioenergy which is elaborated and maintained by Bioenergy2020+ (Bioenergy2020+), table 2.2 summarises commercial-scale lignocellulosic EtOH producing plants. Where a plant is considered at “commercial-scale” if it proves continuous economical production of commercial EtOH volumes (Schwab et al. 2016). For comparison purposes, the current general commercial processes and nation-wide annual production in USA and Brazil are also included in Table 2.2.

To construct Table 2.2 the websites of each of the plants reported was reviewed to determine if they were operating in 2018, and whether lignocellulosic waste was used as feedstock. In this regard, all these projects use agricultural waste, and most of them use enzymatic saccharification and genetically modified yeasts for fermentation. However,

details of their production processes, particularly of the pre-treatment, are generally not disclosed, except for Beta Renewables, creators of the PROESA® pre-treatment, who hint at the use of steam explosion. Among these projects, Beta Renewables, GranBio, Raizen Energia, Shandong LongLive Biotechnology and the Henan Tianguan Group produce lignocellulosic EtOH along with other products, such as crop-based EtOH, feedstocks, high-end chemicals, enzymes and food supplements.

Table 2.1 Commercial-scale operating plants producing lignocellulosic EtOH worldwide

Company	Feedstock	Production Process			EtOH CC	Reference
		Pre-Tr	Sacch.	Fermentation		
POET-DSM (USA)	Corn crop residues	NS	Enzymatic	GMO yeast	76M	(POET-DSM)
GranBio ¹ (Brazil)	Sugarcane straw & bagasse	PROESA®	Enzymatic	GMO yeast	82M	(GrandBio)
Raizen Energia ^{1,2} (Brazil)	Sugarcane straw & bagasse	NS	Enzymatic (Novozymes)	GMO yeast	40M	(Raizen)
Shandong LongLive Bio-Technology ¹ (China)	Corn cob slag	NS	Enzymatic	GMO yeast	63M	(LongLive Bio-Technology)
HenanTianguan ^{1,2} Group (China)	Wheat waste	NS	Enzymatic	GMO yeast	12M	(Henan-Tianguan-Group)
Beta Renewables (Italy)	Rice straw, wheat straw, giant reed	PROESA®	SSF: Enzymatic GMO yeast		51 ^c / 76M	(Beta Renewables)
USA	Corn Particle size 595µm 70-72% starch content	Dry grinding, cooking and liquefaction	Separate batch or SSF Thermostable α-amylase (100°C, pH 6), followed by glucoamylase (pH 4.5)	GMO yeast (32°C, 48 - 72h) + (NH ₄) ₂ SO ₄ or CO(NH ₂) ₂ or proteases to release amino acids, all as nitrogen source	54B	(U.S. Energy Information Administration 2015; Bothast and Schlicher 2005)
Brazil	Sugar cane is milled and sugarcane juice is extracted	Juice pH adjustment, impurities removal and sterilization	Not necessary	GMO yeast	24B	(Barros 2017; Quintero et al. 2008)

Pre-Tr= Pre-treatment, Sacch. = Saccharification, EtOH CC=EtOH commercial capacity production, B= Billions of litres per year, M=Millions of litres per year, NS= Not specified, GMO yeast= Genetically modified strains of *S. cerevisiae*, SSF = Simultaneous Saccharification and Fermentation. ¹Biorefinery, ²1st generation EtOH co-production.

Beta Renewables alone reports its current EtOH annual production to be about 51 million litres from 270 million kilograms of substrate (~ 0.188 L/Kg yield), this is about 34 and 45 % of the crop production processes (overall yield of corn grain EtOH is ~ 0.417 L/Kg, and of 0.556 L/Kg from sugarcane). Nevertheless, Beta Renewables sells its EtOH to Europe for blends with fossil fuels.

Meanwhile, only the maxima EtOH commercial capacity production could be found for the rest of the plants. This could be attributed to the fact that none of these factories are running at their full capacity, likely due to the current low petroleum price and the consequent reduction of government subsidies, together with the relatively high operational costs (Zech et al. 2016).

On this subject, it is worth mentioning the case of the DuPont (USA) lignocellulose ethanol production plant, that despite being at commercial-scale and with comparable production capacity to the other projects listed in Table 2.2, remained in the start-up phase and stopped its operations at the end of 2017. The company declared bioethanol production was out of their business plan, but also confirmed it had not achieved the production of finished bioethanol (Lane 2017). Nevertheless, continuous research is ongoing to improve these and several other pilot and demonstration-scale lignocellulose EtOH production plants.

2.3 Municipal solid waste: the problem and the opportunity

Municipal solid waste (MSW) can be defined as solid or semi-solid waste that is managed (collected and treated) by municipalities (D. Hoornweg and P. Bhada-Tata 2012). It encompasses domestic, commercial and trade, institutional and small-scale industries. It can contain food, yard and park waste; wood, cardboard and paper; textiles; nappies; plastics, metals and glass; and other (e.g. soil, dust, rubber and leather).

According to the World Bank report (D. Hoornweg and P. Bhada-Tata 2012) the Organisation for Economic Co-operation and Development (OECD) members contribute above 50% of global MSW generation. Interestingly, four developing countries (Brazil, China, India, and Mexico) are among the top 10 MSW producers, this is partially due to their big urban areas and adoption of high-consumption lifestyles.

Derived from population growth and current consumption trends, it has been predicted that worldwide MSW generation will double by 2025 (D. Hoornweg and P. Bhada-Tata 2012).

In consequence, the actual struggle of numerous developing nations to manage the growing amount of MSW, in addition to the increasingly demanding waste legislations (European Parliament and Council 2008) set to developed countries, act as drivers for integral MSW management, which should include energy production from MSW (GBEP 2007).

2.3.1 The organic fraction of municipal solid waste (OMSW) in México and England

The almost 120 million of Mexico inhabitants generate around 1Kg MSW/person/day, equivalent to 42.5 million tonnes of MSW per year, composed by 55.58% organics, 20.30% recyclables, 24.12% other materials (INECC 2007; SEMARNAT 2011).

Particularly, Mexico City, with a surface area of 1495 km² (0.1% of the national territory) but home to around 9 million people (INEGI 2015), generates approximately 4.6 million tonnes of MSW per year (Durán-Moreno *et al.*, 2013). From this, 97% are disposed into landfills, a practice that caused the over saturation and final closure of the only remaining landfill “Bordo Poniente” in the city (SMA 2010).

The absolute lack of space for landfill construction within the city has motivated Mexico City’s government to look for the implementation of new approaches to separate, treat and dispose MSW, with a clear intention for energy recovery (AGU 2017).

However, one of the first necessary steps towards this envisioned MSW management was the characterization of the wastes. Durán and colleagues 2013 filled this gap by performing a thorough analysis of the MSW generated in Mexico City, by sampling the 13 transfer stations followed by appropriate chemical tests.

Their weighed average values resulted in the general formula C_{7,125}H_{22,066}O₉₃₈N₃₀₉S (wt% dry basis) for Mexico City’s MSW, with the average moisture and ash content of 33.7% and 13%, respectively. MSW is composed by 49.5% organics, 24% recyclables and 26% other materials. Table 1 shows a more detailed description.

In turn, over 56.1 million people living in England (Park 2016), generate around 28.5 million MSW tonnes per year (DEFRA 2009).

To comply with the EU Waste Framework Directive (European Parliament and Council 2008), the most recent amendment to England and Wales Waste Regulations (2012) stipulates the duty of waste recovery operations.

Chester and colleagues (2008) addressed the necessity of MSW chemical composition information for the United Kingdom (England and Wales) by reviewing numerous surveys and reports conducted by these countries, comprising household and civil amenities waste streams which fell within the broader category of MSW. To homogenize the diverse approaches in the individual reports, the authors grouped the results in comprehensive categories and signaled the possible sources of bias. They concluded that the general formula $C_6H_{10}O_3$ can be used to approximate UK MSW basic chemical composition. Table 2,1 summarizes the physical composition of MSW in Mexico and England.

Table 2.2 MSW physical composition in Mexico and England.

Waste category	Mexico %wt ¹	UK %wt ²
Card	4.03	0.00
Combustibles	0.45 ³	7.51
Ferrous metals	1.16	1.16
Fines	0.8	3.96
Glass	2.65	6.50
Hazardous	0.18	1.06
Non-ferrous metals	0.29	0.53
Organics	49.5	35.09 ⁴
Paper	5.89	18.32
Plastics	13.16	6.47
Textiles	3.64	2.48
Miscellaneous	18.25 ⁵	16.04 ⁶

¹Duran-Moreno et al. (2013) ²Modified from Chester et al. (2008). ³Wood. ⁴Comprises kitchen and garden waste. ⁵Includes construction, sanitary, special and other waste. ⁶Includes non-combustible and electrical and electronic equipment wastes.

Table 2.2 shows that over 60% of MSW is lignocellulosic material. Holtzapple et al. (1992) reported the same proportion for MSW in the US, estimating that if all the lignocellulose in MSW was fermented, over 38 billion liters of EtOH would be produced in the US annually, which would account for around 8% of the transport fuel annual total demand.

The differences in MSW composition within both countries can be explained by the growing reuse/recycling and composting adoption in England, where about 42.2% of the MSW is treated in either way (Thamelis, N. and Bourtsalas 2013).

However, the use of anaerobic digestion to produce biogas is today the main approach of the energy sector in Europe for energy recovery from OMSW. Indeed, based on a life cycle analysis with input data from London, this technology, along with incineration, has been classified as a promising way to treat the organic fraction of MSW at large scale in the UK (Evangelisti et al. 2014).

Undoubtedly, anaerobic digestion and incineration, together with fuel cells and solar, geothermal and nuclear technologies, will help to overcome the threat to energy security in the future (Mousdale 2008). However, what will substitute the liquid transport fuels (petrol and diesel) required for the over 2 billion vehicles expected to be on the roads by 2050 (IEA 2014), when most of them will continue to be powered by the internal combustion engine principle?

The production of bioethanol from MSW would address two major issues, specially in developing countries, namely, climate change and transportation energy security, along with the burden of the increasing amount of MSW generated. Nevertheless, the challenges of any lignocellulosic ethanol production are obstacles that need a solution before EtOH from MSW can become a reality.

2.3.2 Specific research on OMSW as feedstock for potential EtOH production

The earliest study looking at OMSW as a fermentation feedstock, and specifically, appropriate pre-treatments, is that of Holtzapple and collaborators (1992) who proposed ammonia fiber explosion (AFEX) as a suitable pre-treatment for the cardboard and newspaper present in OMSW, as they identified these materials as the most recalcitrant among the paper components in this waste. In their study, they evaluated the digestibility of copy paper, paper towels, cereal boxes, paper bags, etc. individually and mixed (this mixture was obtained from a machine-sorted MSW), as well as before and after AFEX pre-treatment. A mixture of commercial enzymes (Genecor 300P cellulase/hemicellulase and Novo 188 cellobiase) was used to hydrolyze the material. They found a small improvement (~7%) in the hydrolysis of the paper mixture after AFEX, as most of their materials were already de-lignified. However, when treating the separate components, an

important increase (>50%) in the hydrolysis of newspaper was observed, releasing 330mg eq glucose/g dry newspaper. This result was further improved with the addition of H₂O₂/NaOH before AFEX, possibly increasing cellulose solubilization, to render up to 502mg eq glucose/g dry newspaper. However, the authors concluded the latter was not economically viable.

Furthermore, Li et al. (2007) studied the effect of 15 pre-treatments in a substrate integrated with common waste components in OMSW (carrot and potatoes peelings, grass and newspaper), testing different acids (H₂SO₄, HNO₃ and HCl), steam treatment at 121°C and 134°C, microwave treatment (700W), and combinations of these. For the bioconversion of the pre-treated biomass to sugar monomers, they used the fungi *Trichoderma reesei* and *Trichoderma viride* for 96h. A glucose yield of 72.80% was obtained after a combination of diluted acid (H₂SO₄ 1%) and steam pre-treatment (121°C, 15 min) with a maximum enzyme concentration (60 FPU/ g substrate). The authors concluded that high enzyme loading and low substrate concentration (0.5g /50 mL acid) had a higher impact than the steam temperature for optimal glucose yields. Neither of the two previous studies performed fermentation experiments on the hydrolysed carbon.

In turn, Ballesteros et al. (2010) pre-treated OMSW collected from waste containers, by means of active hygienization, a thermal pre-treatment (steam at 160°C, with residence times from 5 to 50 min) conducted by a private company. The resulting biomass was separated and only the organic fiber produced at a 30 min residence time was used as feedstock in SSF, as the glucose and xylose concentrations only increased slightly at higher residence times. The total carbohydrate content on this fiber was about 47-49%. Cellulase and β -glucosidase were used to perform the hydrolysis reactions; the fermentation was carried out by *Saccharomyces cerevisiae* (1g/L). The SSF was run for 72h at pH 5. Producing 25 g/L of EtOH at an initial loading of pre-treated organic fiber of 20% (w/w), equivalent to 60% of the EtOH theoretical yield. However, in this experiment increases in enzyme concentration did not produced a higher sugar content, as in Li et al. (2007), which was attributed to an assumed high starch content in the selected substrate (mostly food waste) versus the more representative nature of the feedstock used by Ballesteros et al. (2010)

Going further in the use of actual OMSW, Mtui and Nakamura (2005) collected samples from diverse dumping sites within Dar es Salaam, Tanzania. They defined lignocellulosic waste as any of plant material, waste paper, straws, bagasse and vegetables and fruits

(usually discarded parts) but removed other organics such as foodstuff remains and decomposed matter. The substrate was then subject to acid steam pre-treatment (H_2SO_4 0.5M / 121°C, 15 min). Saccharification was done with *T. reesei* cellulase and fermentation with *S. cerevisiae*. They observed that EtOH invariably peaked after 48h of incubation after which its production decreased. An absolute maximum 21.45% (w/v) conversion of sugars was achieved, equivalent to 0.15g EtOH/L.

As most of the studies concurred in the effectiveness of steam pre-treatment, Li et al. (2012) used OMSW obtained from a local waste treatment company, through an autoclave high temperature and pressure process (165.5°C, 7 bar, 45 min), and collected the resulting fiber fraction (80% of the original sample). This fiber was milled into a powder and sieved. After a chemical and ultimate analysis, it was found that 65 wt% of the organic material were cellulose and hemicellulose with 10 wt% lignin; the molecular formula of the material was $\text{C}_{100}\text{H}_{171}\text{N}_5\text{O}_{64}$. After the pre-treatment, they evaluated the influence of substrate concentration and particle size, along with the reaction time and enzyme loading, in the hydrolysis using *T. reesei* cellulase (pH 4.8, 40°C, 12-36h).

The optimal operational conditions found were 60g/L of substrate with particle size of 150-300 μm , using 90mg cellulase/g substrate (pH 4.8, 40°C, 12h), obtaining a maximum hydrolysis rate of 53%, equivalent to 385mg sugar/ g substrate. This contradicted previous works, where maximum yields were obtained at low substrate concentrations, although in those other studies the particle size was not reported, and this could explain the differences in results. The fermentation reaction was not actually performed, but it was calculated that 1 ton of fibers obtained from the steam pre-treatment could produce 400kg of sugars, equivalent to 0.152L EtOH/Kg of fibers.

More recently, Ponton-Lozano et al. (2014) investigated the effect of acidic (H_2SO_4 0.75%v/v), alkaline (0.5 g $\text{Ca}(\text{OH})_2$ /g waste) and organosolvent ($\text{EtOH}_{(\text{aq})}$ 50%v/v + H_2SO_4 1.25%v/v) pre-treatments in the bioconversion by *Saccharomyces cerevisiae* of the leachate from the soluble organic fraction of synthetically produced municipal solid waste, with an original COD 16.100mg/L. They observed a sigmoidal curve, with a lag phase of around 35h and a yield of 22.4 mg EtOH/g OMSW (0.028L/Kg) when no pre-treatment was applied. The lag phase disappeared, and the total fermentation time was reduced from 75h to 25h after acid pretreatment at 121°C for 1h, obtaining 52.8 mg EtOH/g OMSW (0.066L/Kg), a yield 2.4 times higher than the one without pre-treatment. No significant difference was observed after alkaline and organosolvent pre-treatments.

Alamanou et al. (2015) found similar high ethanol yields from the fermentation of untreated and microwave/acid pre-treated household food waste, which could allow a more economical production process. However, it is worth highlighting that their feedstock was only composed by food waste, and therefore easier to hydrolyse than the mixtures including paper and cardboard used in other studies.

The experiments described here are compared in Table 2.3 including their yield of litres of EtOH per kilogram of substrate (when appropriate information was supplied). Remarkably, some of these yields were not far from the one currently obtained by Beta Renewables from agricultural waste at commercial scale (0.188 L/Kg. See section 2.2.1), thus showing the potential for OMSW for EtOH production.

In general, steam pre-treatment in combination with acid pre-treatment seems to boost the hydrolysis rate of OMSW, whereas higher enzyme concentrations also tended to enhance this reaction, although the evidence is not conclusive. Furthermore, long retention times appeared to improve the performance up to a certain point, with optima times reported ranging from 12h to 72h. There is no consensus in whether high or low substrate concentration favoured sugar hydrolysis, but the disagreement is probably related to the composition and particle size of the substrates.

Understandably, all the studies described above were focussed in pre-treatment evaluation, as the pre-treatment accounts for around 33% of the total production cost and greatly influences the downstream processes (Lynd 1996). As Table 2.3 shows, the saccharification and fermentation steps were invariably carried out by the conventional enzymatic hydrolysis (*T. reesei*, *T. viride* enzymes), and monoculture fermentation (*S. cerevisiae*) strategy. However, a pre-treatment alone cannot overcome all the challenges presented by the use of OMSW, or any other lignocellulosic biomass, for EtOH production, as for instance, pre-treatments themselves usually produce microbial growth inhibitors (Lynd 1996).

Table 2.3 Experimental studies using OMSW as feedstock for EtOH production.

Substrate description	Pre-treatment	Hydrolysis description	Fermentation description	EtOH yield* (L _{EtOH} /Kg _{substrate})	Reference
MSW paper fraction. Particle size 595- 2000µm	Ammonia fiber explosion (AFEX) 65°C, 10 min, pressure release to 1.5 atm	Substrate 50g/L + Genecor 300P cellulase/hemicellulose 5IU/g _{substrate} , 72h	-	580mg Eq glucose/g substrate	Holtzappple et al. (1992)
MSW biodegradable fraction assembled	H ₂ SO ₄ 1% + Steam 121°C, 15 min	<i>T. viride</i> enzymes ; 60 FPU/g _{substrate} at 50°C, 72h	-	Glucose yield 72.80%	Li et al. (2007)
Fiber from OMSW collected from bins. 47- 49% total carbohydrate content	Active hygienization (steam 160°C, 30 min)	SSF Substrate loading 25% w/w + 20 FPU cellulose + β- glucosidase	<i>S. cerevisiae</i> 1g/L Total t= 72h Opt. t= 24h	0.160	Ballesteros et al. (2010)
Lignocellulose waste from MSW collected from dumping sites in Dar es Salaam	H ₂ SO ₄ 0.5M/ 120 °C / 15 min, 1 atm.	0.5mg substrate/L + 10mg <i>T. reesei</i> cellulase 55°C, 8h	<i>S. cerevisiae</i> 35°C Total t= 72h Opt. t= 48h	0.019	Mtui and Nakamura (2005)

Fiber obtained after pre-treatment of OMSW from a local waste treatment company. Particle size 150-300 µg	Autoclave 165.5°C, 7 bar, 45 min	60g _{substrate} /L + 90mg _{<i>T. reesei</i> cellulase} /g _{substrate} , pH 4.8, 40°C, 12h.	Max. fermentation rate 53% = to 385mg _{sugar} /g _{substrate} (calculated)	0.152 (theoretical)	Li et al. (2012)
Leachate from the organic fraction of synthetically prepared MSW	No pretreatment	NR	COD 1000mg _{substrate} /L + 0.8 g _{<i>S. cerevisiae</i>} /L 35°C, 75h Nitrogen gas to ensure anaerobiosis	0.028	Ponton-Lozano et al. (2014)
	H ₂ SO ₄ 0.75% v/v + 121°C, 1h		COD 1000mg _{substrate} /L + 0.8 g _{<i>S. cerevisiae</i>} /L 35°C, 25h N ₂ to ensure anaerobiosis	0.066	
Dried household food waste, particle size < 3mm	Untreated and microwave digested (700 W, 121°C, 15min) + H ₂ SO ₄ 1%w/w	SSF Celluclast 1.5 L, from <i>Trichoderma reesei</i> ATCC 26921 and β-glucosidase, Novozyme 188	Compressed baker's yeast incubated at 30 ± 0.5 °C, initial pH 5.0 and 80rpm; substrate loading 20% w/v	0.101 untreated/ 0.135 pre-treated	Alamanou et al. (2015)

*When other units are stated is due to the lack of appropriate information to make the calculation (e.g the first two studies evaluated saccharification but not fermentation rates).

Numerous reviews have compiled the formation of inhibitors after lignocellulose pre-treatment (Y. Zhang and Ezeji 2014; Jönsson and Martín 2016; Atreya et al. 2016; Teugjas and Väljamäe 2013) and different strategies to overcome their formation (Parawira and Tekere 2011; Jönsson and Martín 2016).

In this regard, Jönsson et al. (2013) reported weak aliphatic acids, aldehydes, aromatic compounds such as furans and phenolic compounds are the most common inhibitors produced after acid-thermal pre-treatment.

Consistent with the trend of the studies shown in Table 2.3, most of the proposed solutions (Parawira and Tekere 2011; Atreya et al. 2016) focused on the conventional enzymatic hydrolysis/monoculture fermentation process, and involve the addition of further enzymes and/or extensive genetic engineering of *S. cerevisiae* to tolerate the industrial conditions.

2.4 Mixed culture fermentation (MCF): union is strength

Alternatively, with the advancement of simultaneous saccharification and fermentation technologies (SSF) where hydrolysis and fermentation of hexoses and pentoses occur in the same reactor, but the production of hydrolytic enzymes remains as a separate previous step, the emergence of consolidated bioprocessing (CBP; (Lynd 1996)) was supposed as the next logical step to research in ethanologenesis from OMSW. In CPB four basic biochemical events take place simultaneously: Hydrolytic enzymes production, saccharification, hexoses fermentation and pentoses fermentation (Mielenz 2013).

Efforts have been made to engineer microorganisms capable of hydrolysis of both cellulose and hemicellulose and the fermentation of the resulting sugars into EtOH (Martel et al. 2011; Hasunuma and Kondo 2012). However, the development of this “super” microorganism is still subject of extensive research (Hasunuma et al. 2013; Mohd Azhar et al. 2017), and in case such a microorganism were successfully developed, questions about its genetic and phenotypic stability and environment requirements under industrial conditions should arise (Stephanopoulos 2007).

Alternatively, studies have been done in the development of defined natural and/or engineered microbial co-cultures, obtaining results that support the hypothesis of enhanced robustness of consortia over pure culture fermentation. For instance, among

others, a co-culture of engineered *E. coli* strains, has been developed where one strain could degrade glucose and the other xylose efficiently when the substrate loading regime was changed (Eiteman et al. 2008); an immobilized co-culture of *Lactobacillus plantarum* and *S. cerevisiae* has shown high resistance to contamination without closed-control conditions (Abe et al. 2013); and a co-culture of a natural isolated cellulose-degrader *Bacillus* sp. and the fermenter *Klebsiella oxytoca* allowed the efficient EtOH production from different lignocellulosic substrates (Cheng and Zhu 2012). Going further, Mielenz (2013) patented a co-culture of two thermophilic microorganisms to ferment the hexoses and pentoses generated by the degradation of cellulose and hemicelluloses with consequent EtOH production.

Since CBP is still in its early development stages and several aspects of microbial interactions remain unknown, it is understandable to focus on the simplest community configuration: the co-culture. However, most of these have only been tested in commercial defined or complex cellulose/hemicellulose-containing media, but not in the lignocellulosic substrates that would be used at industrial scale. In addition, they have been artificially selected, and/or incubated under strict anaerobic conditions.

A more suitable approach to CBP then, could be the use of a more complex microbial community. In mixed culture or consortia fermentations (MCF), groups of microorganisms ranging from more than two specific species to undefined multispecies communities, perform the required biochemical processes necessary for EtOH production in a single reactor. Thus, the expensive drawbacks of the conventional process i.e. enzyme production and product inhibition, instability, narrow operational conditions, susceptibility to contamination and catabolite repression by means of an engineered super microorganism, could be essentially eliminated (Kleerebezem and van Loosdrecht 2007; Agler et al. 2011; Lynd 1996). This is possible due to the symbiotic relationships occurring between the consortium members, where the high efficiency of the interactions allows the capture of most of the free energy available in the system, giving structure and stability to the community (Zuroff and Curtis 2012).

For instance, Hui et al. (2013) studied the degradation of un-pretreated lignocellulosic feedstocks such as wheat and rice straw, and corn stalk at mesophilic temperature (35°C) and static conditions by the previously isolated undefined consortium XDC-2 (Guo et al. 2010), enriched from vegetal and animal wastes compost-amended soil and comprised of diverse members of the bacterial phyla *Clostridiales*, *Proteobacteria*, and *Bacteroidetes*.

After 12 days of cultivation, ~14% of cellulose and ~78% of hemicellulose losses were registered. The consortium showed stable structure and activity with each of the unpretreated substrates, thus offering a possibility to reduce operational costs of lignocellulose bioconversion. However, this study was directed to anaerobic digestion optimization, and the conditions favored the formation of volatile products such as acetic acid, propionic acid, butanoic acid and glycerin. Nevertheless, a similar approach could be undertaken for EtOH production.

Meanwhile, Ronan *et al.* (2013) enriched and characterised a consortium from household compost, incubated in minimal medium with Whatman Grade 1 Qualitative Filter Paper as the cellulosic substrate at 60°C under static, and initially aerobic conditions. The major fermentation products by the community were acetic acid and ethanol, under both, initial aerobic and anaerobic conditions. The eight dominant and persistent bacterial members of the undefined community after sequential batch transfers were mainly comprised of *Clostridium* species, where at least 3 species were closely related to cellulose-degraders while six were highly similar to known ethanol producers, thus suggesting functional redundancy. At the same time, a member of the *Geobacillus* genus, closely related to facultative anaerobes species was thought to be a key oxygen scavenger, helping to create the anaerobic environment necessary for fermenters, contributing to the versatility observed by the consortium.

Numerous examples of genetically engineered or natural EtOH producing consortia have been described in comprehensive reviews (Lynd 1996; Cheng and Zhu 2012; Zuroff and Curtis 2012) ranging from co-cultures to undefined microbial associations isolated from compost, dung and soil, all degrading diverse lignocellulosic substrates, and thus providing further evidence that supports the advantages of community bioprocessing over the conventional enzyme hydrolysis/ mono-culture fermentation approach.

Although the extremely efficient energy capture is one of the major advantages of consortia over monoculture processes (Zuroff and Curtis 2012), the strength offered by the diversity might be at the same time the main drawback of this approach, as the relationships within the community will become increasingly difficult to predict, and the system naturally, will not tend to EtOH accumulation as it represents an opportunity for an additional consortia member to exploit (see Figure 2.2).

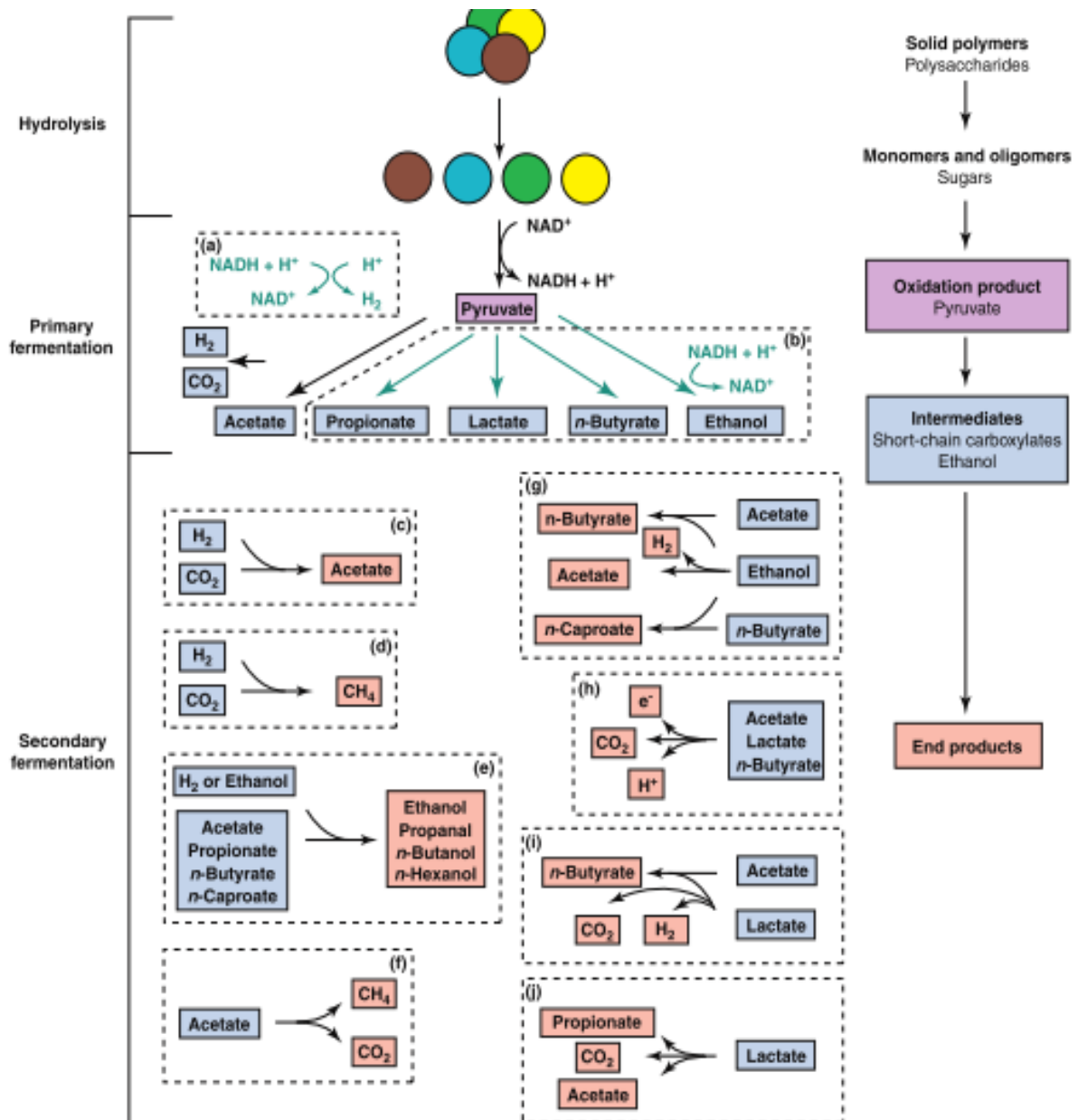


Figure 2.2 MCF possible fermentation pathways, taken from Agler et al. (2011). (a) NADH oxidation; (b) NADH oxidation via reduction of pyruvate to reduced organic products; (c) autotrophic homoacetogenesis; (d) hydrogenotrophic methanogenesis; (e) carboxylate reduction to alcohols with hydrogen or ethanol; (f) aceticlastic methanogenesis; (g) chain elongation of carboxylates with ethanol; (h) electricigenesis (i) lactate oxidation to n-butyrate (acetate and H⁺ as electron acceptor); and (j) lactate reduction to propionate (oxidation to acetate for energy conservation).

Figure 2.2 (Agler et al. 2011) illustrates many of the possible routes sugar fermentation can take in MCF. After conversion to pyruvate and the concomitant production of NADH and H⁺, to maintain the intracellular redox balance, NADH must then be re-oxidized via H⁺ reduction mediated by ferredoxin oxidoreductase or by further pyruvate reduction to fermentation products which require NADH oxidation, depending upon the hydrogen partial pressure (F. Zhang et al. 2012; White 2007; Agler et al. 2011). This is, at high hydrogen partial pressures, electrons from NADH shifts from H₂, acetate and CO₂

production to the generation of increasingly reduced products, such as EtOH (White 2007). Moreover, in MCF, these primary fermentation products can be further utilized as substrates for secondary fermentation reactions, such as autotrophic homoacetogenesis (Köpke et al. 2010), hydrogenotrophic methanogenesis (Crabbe et al. 2016), carboxylate reduction to alcohols with hydrogen or ethanol (Ganigué et al. 2016), among others.

2.4.1 Environmental control of MCF

In MCF, besides genetic modifications, substrate transformation towards a desired fermentation product could potentially be controlled, stabilised and optimised by engineering the physical environment. Studies exploring the effect of different environmental variables such as spatial distribution, pH, temperature, organic load rate (OLR) and H₂ concentration on MCF are briefly described below.

Kim et al. (2008) found that spatial distribution greatly impacted the performance of a cellulose degrading community. They assembled a non-naturally occurring “reciprocal syntrophy” consortium growing in low-nutrient antibiotic medium with carboxymethyl cellulose as a sole carbon source, with no nitrogen source and penicillin G amended incubated at 30 °C. In this three-member consortium each specie performed a function necessary for the survival of the community: *Azotobacter vinelandii* fixed gaseous nitrogen, the only nitrogen source, *Bacillus licheniformis* degraded the penicillin present in the medium and *Paenibacillus curdlanolyticus* hydrolysed cellulose which was the only carbon source. They observed that regardless of their individual characteristics, the community did not thrive under well-mixed conditions. However, when physically separated by culture wells in a microfluidic device, where nanometric pores allowed the diffusion of chemicals and metabolites, but not of cells, the syntrophic interactions were facilitated and the three species grew. This remained true at intermediate separation distances (few hundreds of micrometers), demonstrating that spacial structure was required for the stability of the community. However, the implementation of this approach would be difficult for undefined mixed cultures, and the addition of antibiotics or other additional growth inhibitors would defeat the assumed robustness and flexibility advantages of using a mixed culture over pure culture.

On the basis that temperature and pH play crucial roles on microbial communities structure as they impose selective pressure, Infantes et al. (2011) assessed the influence

of these variables (pH 4, 5 and 6. Temperature 26, 33 and 40 °C) on the H₂ and volatile fatty acids (VFAs) production of a mixed culture enriched from activated sludge fermenting glucose as the only carbon source in anaerobic batch reactors. They observed that at pH 5 and 6, glucose degradation positively increased with temperature. However, at pH 4 the opposite effect was observed as complete glucose utilisation was only achieved at 26 °C. The authors hypothesised that the combined effect of low pH and high temperature increase membrane permeability and the energy required for maintenance, overcoming the benefit of increased metabolic activity caused by higher temperatures. However, pH had a stronger influence on the products obtained (VFAs and H₂ only) than temperature.

No studies have directly assessed temperature-dependent EtOH production by MCF of cellulose or lignocellulosic substrates, however, additional work on pH control was done by Lin et al. (2011). These authors investigated the effect of initial pH (5.5, 7 and 8.5) on ethanol production from cellulose powder (Avicel) under anaerobic thermophilic conditions (60°C) by a 5-member bacterial consortium isolated from an enrichment using napiergrass and sheep dung compost as original inocula, integrated by *Clostridium* strain TCW1, *Bacillus* sp. THLA0409, *Klebsiella pneumoniae*, *Klebsiella oxytoca*, and *Brevibacillus* strain AHPC8120. Additionally, this consortium was augmented with *Clostridium thermocellum*, a cellulolytic bacterium which cannot metabolize pentoses to generate ethanol. They observed simultaneous generation of three dominant fermentation products: acetic acid, butanol and EtOH. Neutral initial pH promoted the highest EtOH yield by the consortium (0.137 L/Kg), being the major fermentation product after 4 days of incubation, while initial acidic pH produced the lowest EtOH yield (0.005 L/Kg). Once the optimal initial pH was determined, they tested EtOH production from acid pre-treated genetically engineered napiergrass, a lignocellulosic non-food crop, obtaining a maximal EtOH yield of (0.05 L/Kg). The authors concluded initial pH could be used to direct the fermentative metabolism of their consortium but did not provide a mechanistic explanation to support this argument.

The latter had been already partially addressed by the work of Temudo et al.(2008), where the effect of pH on the fermentation products generated by an open mixed culture enriched from sludge from a distillery wastewater treatment plant and a potato starch processing acidification tank using glucose as substrate was evaluated. The fermentation was carried out in a chemostat at 30°C, at increasing pH values ranging from 4 to 8.5 under

anaerobic conditions. Although this work was not particularly aimed at EtOH production, its significance regarding the impact of pH on the fermentation profile by a mixed culture, is that they linked the fermentation activity to the changes in the community composition. Four distinctive dominant bacterial communities were identified with different specialised clostridial dominating communities at low (4–5.5) and high (7.5–8 and 8.5) pH, while members of the *Klebsiella* genus were the most abundant at medium pH (6–7). Following the same groupings, at low pH acetate and butyrate were the major fermentation products, shifting to acetate and ethanol under alkaline conditions. However, it must be highlighted that since this experiment was performed in a chemostat and using glucose as the only carbon source, their results might differ and not be comparable with experimental projects using lignocellulosic materials as substrate in batch systems. Nevertheless, from this study it can be assumed that the effect of pH on the product spectrum by mixed cultures is related to the enrichment of specialised microbial sub-communities.

Approaching environmental effects on MFC from a different angle, in their study directed at hydrogen (H_2) production, Zhang et al.(2012) evaluated the metabolic activity of an anaerobic sludge inoculum obtained from a citrate-producing factory wastewater, incubated under anaerobic conditions, at 55°C, constant pH of 5.5, and changing the glucose OLR. from 1.6 to 25 g/L. It was observed that high ORL (24.7g/L) caused higher H_2 concentration in the aqueous phase (H_{2aq}) also known as hydrogen supersaturation (when the H_2 production rate is higher than the H_2 liquid to gas transfer rate), decreased H_2 and biomass yields, while the ethanol/ (acetate+ butyrate) mole ratio increased. They then hypothesised that this could be attributed to the high H_{2aq} as it could cause an increase in the intracellular NADH/NAD⁺ ratio. Since NADH is a key electron donor in fermentative metabolism and it is generated in the oxidation of glucose to pyruvate, a high intracellular concentration of this compound would decrease the organic degradation rate and induce a metabolic shift to more reduced compounds, such as EtOH, helping to restore NAD⁺.

Despite of the insights offered by these studies, there is a clear deficiency on projects investigating environmental factors to direct MCF degrading complex lignocellulose substrates, possibly due to the already complex inocula behavior.

Similarly, even when the coupled study and monitoring of the metabolic products along with the diversity and structure of microbial communities has proved as a valuable tool

in evaluating the effect of environmental factors on MCF, the complex nature of these systems would require deeper analysis and further strategies to achieve a better understanding and consequent control and optimisation.

For instance, to understand the cellulolytic activity and the interactions behind the stable function and structure of their 5-member defined community, Kato et al.(2005) assembled “knockout communities” in which one of the members was eliminated from the consortia aiming to unveil its function and relationship with the other community members. Based on their results after the static incubation at pH 8 and 50°C with filter paper as carbon source of the knockout communities, they developed a conceptual model which involved the synergistic interaction between two aerobic bacterial species with an anaerobic cellulolytic bacterium as it was shown that the aerobes generated anaerobic conditions, while the cellulolytic bacterium supplied acetate and glucose. On the other hand, cellulolytic activity was inhibited by the excessive production of acetate from another community member, while growth suppression was also observed between two members. Since none of the knockout communities showed the stable activity of the original community, the authors concluded that the net balance of positive and negative interactions were essential for the stability of this consortia. This information would then be valuable for direction and optimization of the fermentation activity by this community.

The previous study is an excellent example for the understanding of the interactions within a stable complex mixed culture (more than three species) degrading cellulose. However, as this approach requires intensive work and the availability of detailed information regarding the diversity of inocula, substrates and operational conditions used in MFC, might be restricted to defined communities.

2.5 MCF modelling

EtOH production is the transformation of complex substrates to fuel molecules which can be described by a simple chemical equation $C_6H_{12}O_6 \rightarrow 2CH_3CH_2OH + 2CO_2$. However, the process is characterized by smaller individual substrate transformations e.g. the breakdown of the lignocellulose structure, the subsequent carbohydrate hydrolysis and sugar fermentation.

From this broad perspective, mathematical models have been created based on the stoichiometry and thermodynamics of the individual reactions involved in the main glucose biochemical fermentation pathways to predict the formation of fermentation end-products as function of environmental variables.

Proposing that the products generated in a MCF process are determined by thermodynamics, Rodríguez et al. (2006) constructed a steady-state model where the mixed culture was treated as a single organism able to perform all the major glucose fermentation pathways, considering the free-energy consumed and produced in these reactions. It was assumed that under any given environmental condition, the grouped community would follow the pathway that would allow for a maximum energy yield and the consequent community growth. They used this model to predict the formation of ethanol, acetate, propionate, butyrate, lactate, hydrogen, carbon dioxide, and biomass at different substrate concentration, pH values and hydrogen partial pressure (P_{H_2}). Among their results, they predict that EtOH formation would be favoured at high glucose concentration ($>0.2M$ with a maximum at $0.4M$), pH values < 5.5 regardless of the P_{H_2} , the latter having a more significant effect in acetate and butyrate formation.

Following a similar method of simplification of the MCF to one microbial group ignoring microbial diversity and under the assumption of maximum energy yield as the driving force in fermentation product formation for the construction of their model of glucose fermentation, González-Cabaleiro et al. (2015) also looked at the effect of pH, with the additional mechanistical consideration of changes in the proton motive potential and active transport energy costs caused by pH, to predict the fermentation product spectrum in a continuously stirred reactor. However, the results obtained in this model propose ethanol together with acetate formation at pH values >8 , which although completely opposite from the predictions of Rodríguez et al. (2008), is reported to match the observations of previous experimental work by other authors (Temudo et al. 2007).

The disagreement between the two previous models might arise from the fact that González-Cabaleiro et al. (2015) coupled $FADH_2$ to the reduction of acetaldehyde to ethanol, which in their words, was necessary to ensure the prediction of that observed experimentally, but otherwise, a mechanism without foundation in the literature. On the other hand, Rodríguez et al. (2008) only accounted for $NADH/NAD^+$ in their model.

These are the most relevant examples of thermodynamic modelling for the prediction of fermentation products in MCF that could be found in the literature, however, their

contradictory results raise the question of how reliable the implementation of their predictions would be in systems degrading lignocellulosic substrates. Nevertheless and regardless of their limitations, both have managed to replicate previously done experimental work, which might indicate its value more as a tool for the understanding of specific MCF systems than for general predictions, thus highlight the importance of the inocula microbial diversity in the different results observed experimentally.

2.6 Conclusions

Today, there is ample support for the switch to lignocellulosic substrates for the production of bioethanol, and the existence of commercial-scale facilities using lignocellulosic agricultural waste as feedstock confirms the feasibility of this process. However, the limitations imposed by the composition and structure of these materials remain as a major constraint for their bioconversion and widespread implementation, pushing research towards the exploration of new approaches to achieve competitive ethanol yields. The use of mixed culture fermentation seems particularly promising for the transformation of complex and variable lignocellulosic wastes, such as the organic fraction of municipal solid waste. However, there is a clear lack of experimental research on the utilisation of this substrate in MCF for EtOH production as in general for the direction and optimisation of complex lignocellulosic substrates.

In line with the general aim of this project to develop a multi-species or undefined microbial consortium that will offer robustness and versatility in the bioconversion of OMSW to EtOH and incorporating the findings from the previous studies here reviewed, the following observations can be highlighted as guidelines for the experimental phase of this work:

- Diluted acid /steam pre-treatment was shown to be the most effective method to facilitate OMSW hydrolysis, yielding high amounts of monomers and simple carbohydrates, and subsequent high EtOH titers in yeast fermentation.
- Besides being a more intuitive method for the utilisation and maintenance of mixed cultures, consolidated bioprocessing (co-occurrence of all the EtOH production process steps in the same reactor) would simplify the process and potentially the operational costs.

- Most of the work on lignocellulose transformation has been done under thermophilic conditions ($>40^{\circ}\text{C}$). With only a few examples running at mesophilic conditions ($30\text{-}40^{\circ}\text{C}$) and only one at environmental temperature (26°C). However, lower temperatures could be explored in an attempt to minimise the energy inputs.
- Although constant stirring and chemostat approaches have been presented, many of the studies opted for static batch incubations. This might have had the objective to further simplify the process. However, as a result of this review, is proposed that static conditions could provide the opportunity for the assembly of spatial structure previously described as beneficial for synergy (see section 2.4.1). For instance, motile facultative anaerobes might remain at the top of the liquid phase, utilising the readily available sugars in the medium released after steam pre-treatment and subsequently by the cellulolytic activity of anaerobes, which could remain at the bottom while anaerobic conditions are established while some other organisms might prefer to remain attached to the substrate.
- The manipulation of environmental variables is a promising means to direct MCF towards EtOH production. Among the environmental variables presented, pH appears to have a major effect in the direction of fermentative metabolism. However, the pH range at which EtOH formation is favoured seems to also depend on the type of substrate, its organic load rate, and very likely on the inocula used. Many studies were performed in neutral to alkaline conditions, although a few showed good performance under acidic pH.
- While many of the MCF experimental studies report the dominant species in their consortium, with some monitoring the changes of structure and diversity, and proposing specific species functions, the general application of thermodynamic principles has been underused in their explanations. Here it is proposed that the combination of these information sources into a simple conceptual model could help to the understanding of specific MCF projects, thus avoiding a “black box” approach.
- Therefore, coherent physical environmental control along with conceptual thermodynamic and metabolic models could provide the necessary control conditions to achieve a stable microbial community capable to produce competitive yields of EtOH from OMSW.

Chapter 3. Methods

3.1 Inocula description and sampling

To enrich for bacterial communities with the diverse metabolic capabilities required. to disrupt and transform lignocellulose, five different environments where the degradation of these materials naturally occurs were sampled:

- 1) Compost was taken from the surface layer of a composting pile from Newcastle University's Nafferton Farm, located approximately 19 km west of the city of Newcastle upon Tyne on the north side of the Tyne valley (54°59'08.6"N 1°53'56.2"W).
- 2) Woodland soil was taken near the river Ouseburn at Jesmond Dene from around trees where the leaf-mat was visible. Jesmond Dene is a parkland/woodland located between the areas of South Gosforth and Jesmond Vale in the city of Newcastle upon Tyne (54°59'21.6"N 1°35'26.2"W).
- 3) Manure was collected immediately after excretion by a cow at Newcastle University's Nafferton Farm. The cattle at Nafferton farm are dedicated at dairying, and beef production as a byproduct of the dairying activities.
- 4) Rumen from a male/wether sheep (Suffolk cross breed) provided by Oluwaseun Bolaji from the Department of Agriculture, Food and Rural Development at Newcastle University. Pre-slaughter, the sheep was fed silage-based total mixed ration plus vegetables including turnips.
- 5) Anaerobic digestate granular sludge from a paper industry waste water treatment facility, provided by Dr. Paul Sallis from the Environmental Engineering group at Newcastle University.

The compost, woodland soil, manure and rumen samples were all collected on March 2015, and kept under refrigeration at 4°C until further use. The anaerobic digestate granular sludge had been previously collected by the Environmental Engineering group and kept under refrigeration at 4°C since.

3.2 Organic Municipal Solid Waste (OMSW) analogue composition and preparation

An OMSW analogue was prepared based on the putative biodegradable categories of Mexico City's Municipal Solid Waste (MSW), amounting to 60% of its total composition (Durán et al. 2013). Hence, an adjustment of proportions was calculated by solely considering the organics, paper and cardboard categories as part of the OMSW. As no further information was available regarding Mexico City's organics category composition, this was simplified to food waste for the analogue's preparation. Therefore, the organics category was integrated based on the proportions of food waste in England and Wales (Quested and Johnson 2009). Table 3.1 brings the two data sources together, listing the components and proportions used in this work to prepare the OMSW analogue. All mass values in this study are reported in terms of dry weight mass.

Table 3.1 Composition of the OMSW analogue prepared to be used as substrate for EtOH production throughout this project.

MSW organic fraction category	% OMSW analogue
Organics	
Vegetables (spring greens)	31.3
Fruits (apple cores; banana, oranges and watermelon peelings)	17.6
Bakery (baguette)	13.8
Meals (fried rice)	10.8
Meat (beef meatballs)	9.5
Paper	10
Cardboard	7

To prepare the OMSW analogue, the spring greens, apples, bananas oranges and watermelon were purchased (Hutchinson's Fruit and Veg Ltd., Fenham, Newcastle upon Tyne). The fruits were consumed, keeping the apple cores, banana, oranges and watermelon peelings. The baguette, own brand egg fried rice (Tesco Stores Ltd, UK); and Butcher's Market British meatballs pack (Iceland Foods Ltd, UK) were also purchased locally. Details of the nutritional composition of each of the food items summarised in Table 3.2, were either found in the product labels (fried rice and meatballs) or are reported in the literature (vegetables, fruit peelings and bakery).

Using the National Renewable Energy Laboratory Analytical Procedure (Hames et al. 2008) as a guideline, each of these components were cut into small pieces and individually

dried for two days at $55^{\circ}\text{C} \pm 5^{\circ}\text{C}$. Simultaneously, triplicates of each food component were analysed for water content, total solids and ash composition (A. Sluiter et al. 2008). The dried material of each food category was then individually weighted, blended into a fine powder and sieved through a 1 mm mesh.

The paper category was produced from used office paper, sheets from magazines and newspaper, whereas the cardboard category was formed from thin, lightweight card from breakfast cereal and other packaging along with layers taken from corrugated or fluted packing board from cardboard boxes. These two fractions were also cut into small pieces and blended. Although these materials did not form a powder, their surface was disrupted and softened.

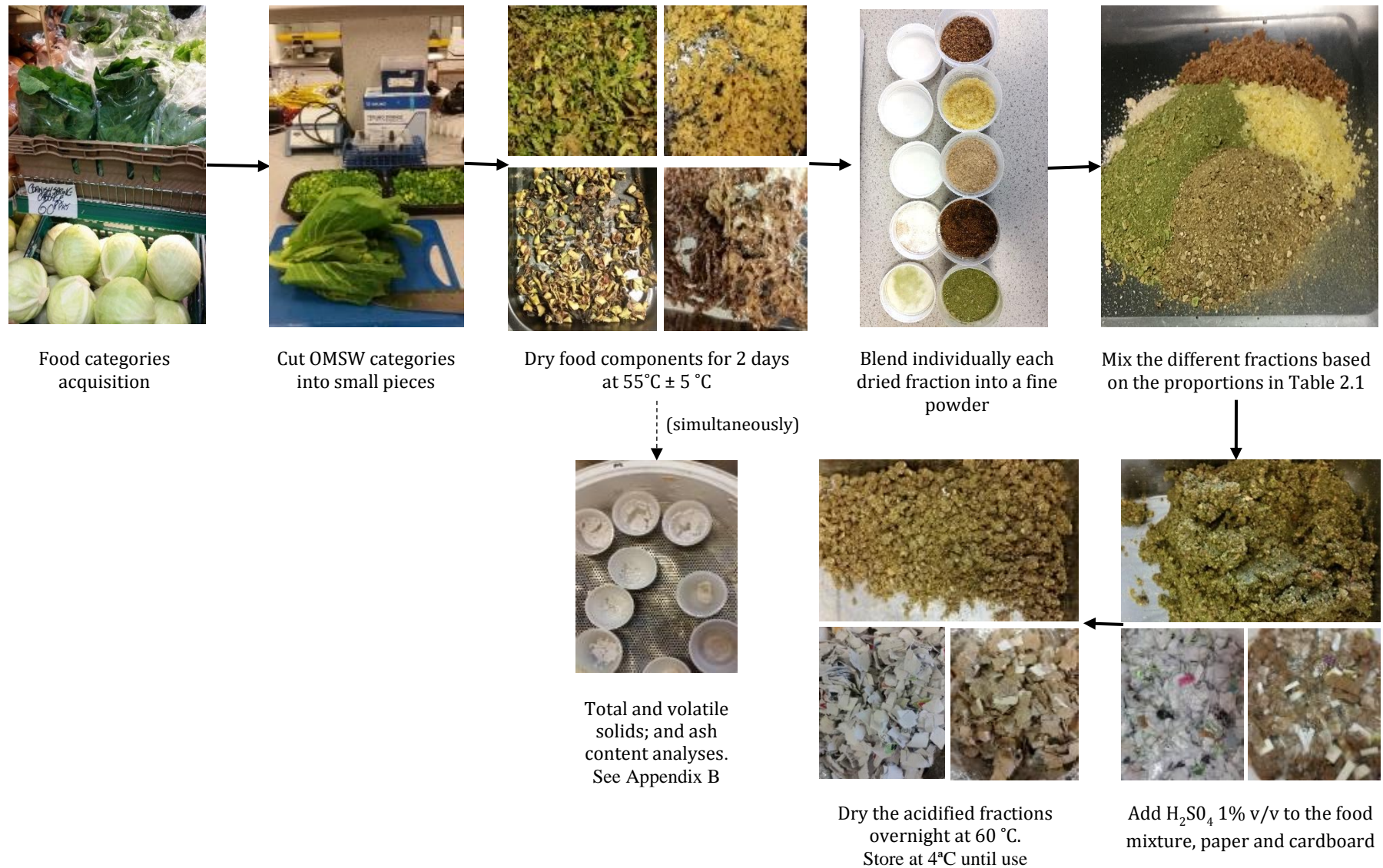
Table 3.2. Nutritional values per 100g reported for the food component used to integrate the organics category of the OMSW analogue.

Food category		Carbohydrates ¹ g	Fibre ² g	Proteins g	Lipids g	Reference
Vegetables	Spring greens	5.42 (0.46)	4.00	3.02	0.61	USDA, 2016
	Apple cores	59.96	13.95	2.80	9.96	Romelle, et al., 2016
Fruit peelings	Bananas	43.40	11.81	10.44	8.40	
	Orange	53.27	14.19	9.73	8.7	
	Watermelon	32.16	26.31	12.42	12.61	ANSES-CIQUAL, 2013
Bakery	Baguette	56.6 (starch 51.8 and 2.12 sugars)	3.02	9.33	1.47	
Meals	Egg fried rice	31.7 (1.3)	1.9	3.9	4.3	Product label
Meat	Beef meatballs	3.8	0	21.1	17.5	Product label

¹ “Carbohydrates” meaning any carbohydrate which is metabolised by humans, including polyols; of which “sugars” means all monosaccharides and disaccharides present in food, excluding polyols, as specified in the EU Regulation No 1169/2011, 2011. Numbers in parenthesis indicate sugar composition or sugar composition and starch by weight (g) ²“Fibre” meaning edible carbohydrate polymers with three or more monomeric units, which are neither digested nor absorbed in the human small intestine as defined by the European Commission Directive 2008/100/EC, 2008.

The dried powdered material obtained from each food category, and the blended paper and cardboard were stored individually in polypropylene containers and kept refrigerated at 4°C until further use. Figure 3.1 summarises the steps performed to prepare the OMSW analogue.

Figure 3.1 OMSW analogue preparation and pre-treatment



3.2.1 OMSW analogue diluted acid pre-treatment

The powder material obtained from each food component was mixed following the proportions specified in Table 3.1 to form the organics fraction of the OMSW analogue.

For the diluted acid pre-treatment (Li et al. 2007), H₂SO₄ 1% v/v was added to the food waste mixture (3mL acid:1g food waste) and in separate containers, to the blended paper and cardboard fractions (4mL acid:1g paper/cardboard). The three individual waste categories were then incubated at 60°C overnight. Figure 3.1 summarises the steps performed to prepare, and acid pre-treat the OMSW analogue.

3.2.2 OMSW medium basic chemical characterisation

The analysis of the OMSW medium was divided into two: A) solid and B) liquid OMSW fractions. The corresponding analyses are described below.

A) Solid OMSW analysis

The components integrating the food fraction of the OMSW analogue were first characterised by evaluating their moisture content (H₂O), total solids (TS), volatile solids (VS) and fixed solids (FS) content. These were conducted in triplicate according to the APHA standard method 2540 for total, fixed and volatile solids and NREL laboratory analytical procedure for moisture content (a Sluiter et al. 2008; APHA 2012). Triplicates of the acid pre-treated OMSW were analysed likewise. The results from these analyses are presented in Appendix B, Table B1.

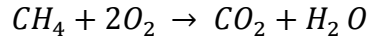
The total Chemical Oxygen Demand (TCOD) of the solid OMSW fraction was estimated using the proportions of the general waste categories in Table 1: 83% food waste, 10% paper and 7% cardboard, with TCOD contents (in gCOD/gmaterial) of 1.10, 0.1 and 0.08 respectively, as reported in the literature (Bayard et al. 2018), giving a TCOD content of 0.128 gCOD/gOMSW (see Appendix B, Table B2).

As the input per bottle was 2.5 gOMSW/50mLmedium (see section 3.3.1), the estimated TCOD content of the medium if all the OMSW dissolved would have been 64 gCOD/L.

Additionally, the Bio Methane Potential (BMP) of the OMSW solid fraction was also estimated using the proportions of the general waste categories in Table 1, with their corresponding BMP contents (in mLCH₄/gmaterial) of 222.44, 19.07 and 15.47, as

reported in the literature (Bayard et al. 2018), giving a BMP content of 256.98 mLCH₄/gOMSW. The COD concentration based on the BMP was determined as follows:

- Based on the stoichiometric reaction for methane oxidation, 4 mol of oxygen are required to oxidise 1 mol of methane to 1 mol of carbon dioxide.



- Therefore, a mol of methane is equivalent to 64gCOD (16g/mol of oxygen*4 mol).
- Using the ideal gas equation for temperature and pressure values of 20° C and 1 atm, 1 mole of gas occupies 24.04 L of volume.

$$V_{(m^3)} = \frac{n_{(mol)} R_{(JK^{-1}mol^{-1})} T_{(K)}}{P_{(Pa)}} ;$$

$$V_{(m^3_{CH_4})} = \frac{1_{(mol_{CH_4})} 8.3144_{(JK^{-1}mol^{-1})} (273 + 20)_{(K)}}{101325_{(Pa)}} * \frac{1000_L}{1_{m^3}}$$

- It then follows that for a mol of methane, there are 344.38mLCH₄ per gCOD (2404mL/mol * 1molCH₄/64gCOD).
- Based on the BMP content estimated for the OMWS analogue, there are 0.75gCOD/gOMSW (256.98mLCH₄/gOMSW / 344.38mLCH₄/gCOD).
- As the input per bottle was 2.5 gOMSW/50mLmedium (see section 3.3.1), the estimated COD content of the medium would have been 37.5 gCOD/L.

Then it can be assumed that 58.59% of the estimated TCOD was biodegradable.

B) Liquid fraction of OMSW medium analysis

Liquid samples taken from serum bottles containing acid and steam pre-treated mineral medium with OMSW (prepared as all microcosms in this project, section 3.3.1) were then used to determine the Chemical Oxygen Demand (COD) according to the APHA method 5220 (Rice et al. 2012), test used to quantify the amount of oxidisable oxygen in liquid media. The average COD of the liquid fraction of the OMSW medium was 19.66 gCOD/L. It can then be assumed that the pre-treatment hydrolysed about 30.72% of the estimated TCOD.

3.2.3 OMSW electron milliequivalents content and electron balances

Electron balances were conducted to broadly evaluate the recovery of electrons from the OMSW medium (electron donor) in the form of soluble fermentation products (electron acceptors). The electron content of the OMSW medium fractions were quantified as COD based on the TCOD and BMP estimates previously described (section 3.2.2) using 8 g COD/e⁻-equivalent (Rittmann and McCarty 2001). In this regard, the electron content (in e-milliequivalents/L) of the OMSW medium were: i) 8000 e-meq./L based on the TCOD estimate, ii) 2450 e-meq./L based on COD quantified in the liquid fraction and iii) 4687.5 e-meq./L based on the BMP estimate derived COD.

For the electron balances, mmol of end-products were converted to electron milliequivalents (e-meq.) using electron equivalents per mole values, obtained using the half-reaction method (Rittmann and McCarty 2001). The recovery of e-meq. to total soluble end-products (quantified in terms of mmol of carbon equivalents) is reported as a percentage of the initial total e-meq. provided as substrate. See Appendix C for the half-reactions used in this project and a demonstration of electron balances calculations.

3.3 Microcosms set up

Different microcosms configurations were set up as small-scale batch fermentation reactors. The following sections describe the routine procedure for the set up. Details of modifications to this procedure can be found in the chapter specific methods sections of Chapter 4, 5 and 6 of this thesis.

3.3.1 Culture medium preparation

It has been shown that RM medium, often used to enrich for cellulolytic bacteria, can be modified using a waste-derived complex nutrient source as a substitute for yeast extract without compromising the cellulolytic activity of the culture, thus making it a cost-effective option for potential industrial applications (Ronan et al. 2013)

In line with the objective of this project of achieving low-input EtOH production, the original RM medium containing urea (2 g/L), KH₂PO₄ (2 g/L), K₂HPO₄ (3 g/L), yeast extract (2 g/L), trace mineral solution 1:100 (v/v), and resazurin (0.002 g/L), was

modified, replacing urea and yeast extract with the acid pre-treated OMSW analogue fractions (80% food waste, 10% paper and 7% cardboard).

The potassium salts and resazurin were mixed and dissolved in distilled water using a magnetic stirrer, and latter integrated with the OMWS analogue (see Figure 3.2).

The trace minerals solution contained $\text{MgCl}_2 \cdot 6\text{H}_2\text{O}$ (20 g/L), $\text{CaCl}_2 \cdot 2\text{H}_2\text{O}$ (5 g/L), and $\text{FeSO}_4 \cdot 7\text{H}_2\text{O}$ (0.25 g/L). This was filter sterilised and 0.5mL added to each of the microcosms after autoclave sterilisation.

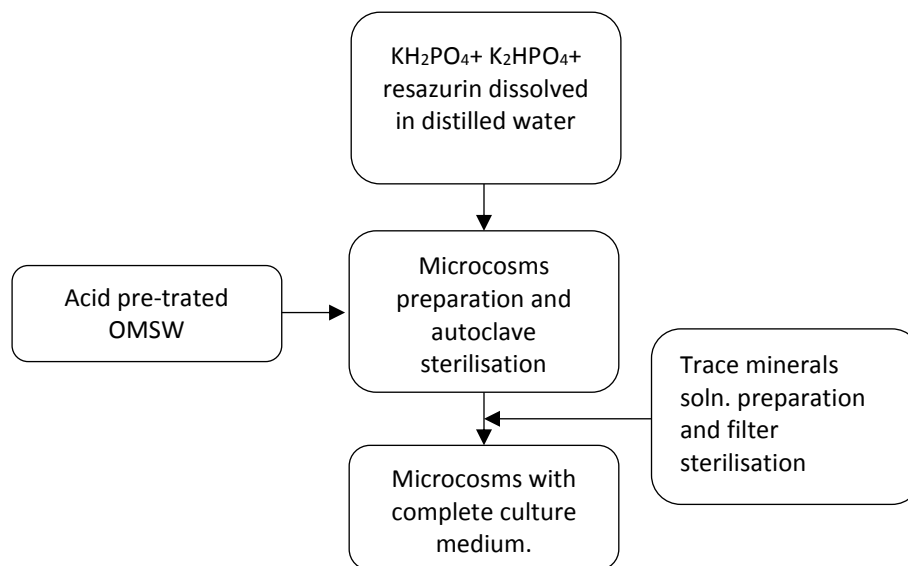


Figure 3.2 Flow diagram of the OMSW analogue culture medium preparation.

Approximately, 2.5g of the acid pre-treated OMSW analogue (2g of food waste, 0.3g paper, 0.2g cardboard) were placed into 120mL serum bottles, after which 49.5mL of the simplified RM media were added to each of these (5% organics medium).

The bottles were autoclaved at 121°C for 15 minutes. This with the double purpose of sterilising the culture media, and completing the OMSW analogue pre-treatment, as it has been shown that the combination of diluted acid and steam pre-treatments is more effective in the disruption of lignocellulosic materials (Li et al. 2007).

During this project the media preparation was done in the evenings, allowing the bottles to cool down overnight, after sterilisation.

3.3.2 Microcosms inoculation

Bottles were opened in the sterile zone generated by a Bunsen burner flame and the pH of the medium was measured on sampled aliquots and adjusted with H₂SO₄ or NaOH, if necessary. Each bottle was then inoculated with 2.5g of the corresponding inoculum, manually agitated and initial samples were taken. The bottles were then sealed with butyl rubber stoppers and aluminium seal crimp caps.

Refer to the methods section at the beginning of Chapters 4, 5 and 6 for details about the experimental design, changes in the culture media composition and pH adjustment. All microcosms configurations in this work were run in triplicate, incubated in the dark, at room temperature (approximately 20°C) under static conditions and sampled as described in the following section.

3.3.3 Microcosms liquid sampling and routine analyses overview

After manual agitation, samples were taken periodically from all microcosms using disposable 3mL plastic syringes, according to the sampling plan specified in the methods section at the beginning of Chapters 4, 5 and 6 and were either stored at -20°C for molecular biology analyses, used for pH measurements or further processed for fermentation products analysis by GC-FID and Ion chromatography.

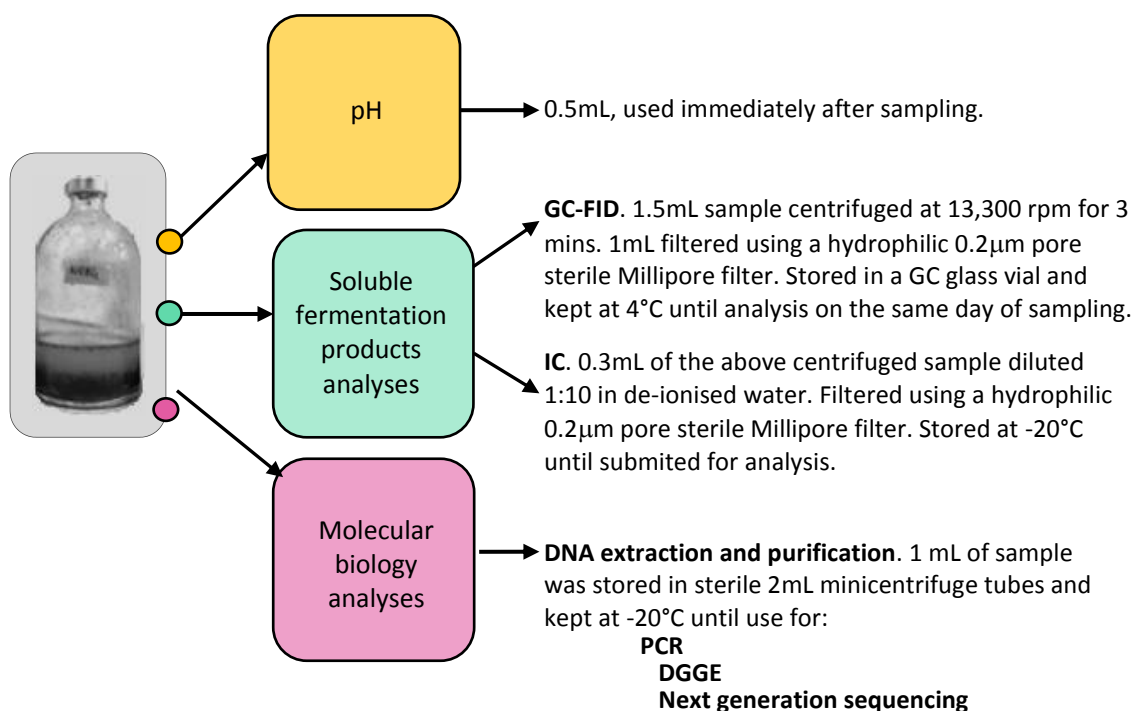


Figure 3.3. General description of the volume of liquid samples and their preparation for the routine analyses performed at different time points for each microcosm.

3.4 Physicochemical analyses of liquid samples

3.4.1 pH measurements

pH is recognised as a key environmental factor for bacterial metabolic activities, with a particular strong effect in the energetics of fermentative processes (Karadag and Puhakka 2010; Rodríguez et al. 2006; Kleerebezem and van Loosdrecht 2007). Thus, its measurement was an integral part of this project.

A Mettler Toledo™ FiveEasy™ Plus FP20 pH meter, fitted with an InLab pH electrode was used to measure the pH of the samples with ± 0.01 accuracy. Standard solutions of pH 4 and 7 were used for calibration at the beginning of each measurement session.

3.4.2 GC-FID

A gas chromatography with flame ionization detection method (GC-FID) was used to quantify the concentration of EtOH and other fermentation products (acetic, propionic and butyric acids, among others). A Trace GC Ultra from Thermo Scientific coupled with an automatic injector was used. The injection volume was 1 μ L, and to prevent contamination of the capillary column the injection port was fitted with a glass liner (5-mm.i.d.), appropriate for split analysis. An Agilent J&W HP-INNOWAX column coated with polyethylene glycol (30mx0.25mmx0.25mm) was used. Hydrogen was the carrier gas at a flow rate of 1.5ml/min at 55kPa, running at 35°C (5min)-150°C/5(0)-250/20(2), for 38 minutes per sample.

ASC reagent grade acetone, ethanol, methanol, butanol, acetic acid, propionic and butyric acid were purchased from Sigma-Aldrich Corporation. Solutions of these reagents were prepared in distilled water at different concentrations for the construction of calibration curves (see the methods sections for chapters 4 and 5). Fresh standard solutions of EtOH and a mixture of volatile fatty acids (VFAs) were prepared and quantified at the start and end of each GC-FID analysis run.

Although the suitability of highly similar methods for the quantification of ethanol, butanol, acetone, acetic and butyric acid has been reported (Lin et al. 2014; Pontes et al. 2009), the repeatability of the VFAs quantification became an issue throughout this project. Diverse strategies were employed to tackle this problem and are described in the appropriate methods section of chapters 5 and 6. However, in the last phases of this project it was decided to perform the VFAs quantification using Ion Chromatography.

3.4.3 VFAs IC

On the day of analysis, the samples were added (1:1v/v) to 0.1M orthosilicic acid, placed in an ultrasonic bath at 30°C and sonicated for 40 minutes for carbonate removal through acidification and CO₂ effervescence, as the presence of this gas can interfere with the IC performance.

Additionally, standard solutions of lactic acid in de-ionised water were freshly prepared on the day of analysis, as the quantification of lactic acid does not form part of the usual VFAs analysis performed by the Environmental Engineering Lab at Newcastle University, where the samples were submitted.

Hence, each VFAs IC analysis included the quantification of acetic, propionic, butyric and lactic acids.

3.5 Statistical analysis of physicochemical data

The R programming language and free software version 3.4.3 (2017-11-30) -- "Kite-Eating Tree" (The R foundation, US) in conjunction with RStudio development environment (RStudio Inc., US) were used to perform the statistical analysis of the physicochemical data obtained.

The specific statistical analyses depended on the nature of the data of which details can be found in the methods section of chapter 4, 5 and 6, along with Appendix A, which shows examples of the statistical analyses workflow.

3.6 Molecular biology analysis

Since this project was focused on the enrichment and selection of a bacterial community able to produce EtOH from OMSW, the analysis of the community composition and function of the bacterial communities present at different time points in the microcosms where EtOH was a major fermentation product, was crucial for the understanding of this process.

The techniques for the molecular biology analysis included Polymerase Chain Reaction (PCR), Agarose Gel Electrophoresis (AGE), Denaturing Gradient Gel Electrophoresis (DGGE) and the Next Generation DNA sequencing (NGS) techniques Ion Torrent Personal Genomic Machine (Ion Torrent PGM) and MiSeq.

3.6.1 DNA extraction and purification

Genomic DNA was isolated from ~0.5mg of samples from each microcosm under study. Due to the heterogeneity of the samples containing a high number of solid particles, soil DNA isolation kits were used for this purpose according to the manufacturer's protocols (Details in the methods section of Chapters 5 and 6). All extractions included procedural blanks.

The PowerSoil® DNA Isolation Kit, originally from Mo Bio Laboratories Inc., UK and later sold as DNeasy PowerSoil Kit by Qiagen N.V., UK along with the FastDNA® SPIN Kit for Soil from MP Biomedicals, LLC, UK were used for the different tests in this project.

These protocols combined mechanical and chemical methods for the isolation of DNA, with the Power soil DNA isolation kit relying on bead beating tubes for sample homogenization and cell lysis, while the FastDNA spin kit used lysing matrix tubes for the same objective. In both cases, cell lysis was followed by a series of chemical purification steps aimed at the removal of non-DNA material, with the implementation of the patented Inhibitor Removal Technology (IRT), which eliminates humic acid and cell debris from samples in the MoBio/Qiagen kits, the main difference between the kits used. Then silica-based membranes were employed in both cases to selectively bind DNA while the remaining contaminants were washed away with EtOH during filtration. Lastly, the purified DNA was eluted with 100µL of DNase/Pyrogen-Free distilled water and stored at -20°C until further use. The success of the DNA isolation was confirmed after PCR amplification and agarose gel electrophoresis.

3.6.2 16s rRNA gene PCR amplification

PCR amplification targeting the variable regions of the highly conserved 16S rRNA gene of the Bacteria and Archaea domains was performed on the DNA extracts to provide the genetic input material for agarose gel electrophoresis, DGGE and NGS.

In general, the PCR master mix was manually prepared using Bioline GmbH reagents. Thus, a 50µL PCR reaction consisted of 5 µL of NH₄ reaction buffer, 2 µL of MgCl₂ (1mM), 2 µL of dNTPs mix (40mM), 0.1 µL of BioTaq DNA polymerase (5u/uL), 2 µL of the appropriate forward and reverse primers pair (10 µM) and 2 µL of DNA extract, all in 36.9 µL of DNase/Pyrogen-Free distilled water.

A Bibby Scientific Techne TC-512 gradient thermal cycler was used for the PCR processing of samples and procedural blanks. The amplification programme for most of the reactions done in this project consisted of 4 min of initial denaturation at 95°C followed by 30 cycles of 1min denaturation at 95°C, 45 s for annealing at 55°C and 1 min of extension at 72°C. The final extension was done for 10 min at 72°C.

Details of the DGGE analysis are provided in section 5.3.6 of Chapter 5, as this technique was only performed for this part of the project and its relevance is limited to the said chapter.

3.6.3 Agarose gel electrophoresis

AGE was used to visually assess the success of the DNA extraction by comparing samples against procedural blanks and by assessment of amplicon size and homogeneity (single, defined band) by comparison with a DNA size marker.

The 1% agarose gels were prepared by dissolving 1g of agarose (Sigma-Aldrich, UK) in 100mL of 1X Tris-Acetate-EDTA (TAE) buffer. 1.6 µL of ethidium bromide (EtBr) were added to the gel solution. The gel was then poured into a casting tray and allowed to cool for 30 minutes. The cast gel was immersed in an electrophoresis chamber containing 1X TAE buffer, after which 8 µL of sample consisting of 5 µL of PCR product previously mixed with 3 µL of DNA loading buffer (Bioline, UK) were loaded into the wells of the gel. The first and last wells of each row of wells was invariably loaded with 2 µL of the reference DNA size marker, Hyperladder II DNA Marker (Bioline, UK).

Electrophoresis was conducted at 100 volts for 45 minutes. The gels were then visualised by UV illumination, using a MultiDoc-It™ Imaging System (UVP, LLC, UK).

3.6.4 Ion-Torrent PGM sequencing pooled library preparation

The procedure to prepare the pooled library for Ion Torrent PGM sequencing involved for each DNA extract, PCR amplification of the targeted region of the 16S rRNA gene with barcoded primers and the purification of the amplified libraries. After which an equimolar pool of the amplicon libraries was prepared. The pooled library was then submitted to the Environmental Engineering research laboratory, Newcastle University for sequencing

with the Ion Personal Genome Machine® (PGM™) System using an Ion 316™ Chip v2 (Life Technologies, UK).

The PCR amplification was performed as described in the section 3.6.2 of this chapter, using the universal primers F515 (5'-GTGNCAGCMGCCGCGGTAA-3') and R926 (5'-CCGYCAATTYMTTTRAGTTT-3') encompassing the V4-V5 region of the 16S rRNA gene, this amplicon is ~400bp in length targeting a fragment between positions 515 to 926, based on *Escherichia coli* numbering (Quince et al. 2011).

Following the manufacturer's guidelines, fusion primers were used. Hence, the F515 primer included an 'A' adaptor (25 bp, 5'-CCATCTCATCCCTGCGTGTCTCCGACTCAG-3') followed by a unique Golay barcode per sample (12 bp) and a key spacer (3bp, 5'-GAT-3') at the 5' end for error correcting (D'Amore et al. 2016). Primer R926 was ligated to a 'B' truncated P1 adaptor (25 bp, 5'-ATCACCGACTGCCCATAGAGAGG-3') attached to the 5' end. Adding up to a 481 bp amplicon size. Details of the Golay barcodes used per sample can be found in Appendix D).

The amplified libraries were then purified using an Agencourt Ampure XP purification Kit (Beckman Coulter Inc., UK), which selectively bonded PCR amplicons to paramagnetic beads, allowing the removal of contaminants by washing steps to finally elute the purified PCR products from the magnetic beads. The manufacturer's protocol was followed and is briefly described below.

49.5µL of Agencourt AMPure Magnetic Particle Solution (mp solution) was added to 45µL of each PCR amplicon (1.1 µL mp solution:1 µL sample), followed by repeated pipette mixing (10x) and 5 min incubation at room temperature. The tubes were then placed on a magnetic rack for 5 min allowing the beads to migrate to the side of the tube in contact with the magnet and the supernatant was aspirated and discarded. 70µL of freshly prepared 70% EtOH solution were added to all the tubes, repeatedly pipette mixed (10x) and incubated for 5 mins at room temperature. The supernatant consisting of EtOH solution and probably, excess oligos, nucleotides and salts was then aspirated and discarded. The tubes were then removed from the magnetic rack and kept opened to air dry any remaining EtOH solution. After this, 20µL of DNase/Pyrogen-Free distilled water was added to the tubes and repeatedly pipette mixed (10x). The tubes were again placed in the magnetic rack for 5 min. Finally, the supernatant containing the purified amplicon was transferred to a clean PCR tube.

To prepare the equimolar pool comprising the purified amplicon libraries, each amplicon was quantified using a benchtop fluorometer Qubit Fluorometer 2.0 in combination with a Qubit® dsDNA HS Assay Kit (Life Technologies, UK). The manufacturer's protocol was followed as described below.

A working solution was prepared by diluting 1:200 v/v of the fluorescent reagent (200X concentrate in dimethyl sulfoxide) in the buffer provided. 2µl of each purified amplicon and 10µL of standards were then diluted into 198 µl or 190µL of working solution, respectively, and incubated for 2 minutes at room temperature. The samples were quantified after calibrating the fluorometer with the standard solutions. The concentration of each sample was reported in ng/mL.

Finally, the equimolar pool of amplicon libraries was assembled by transforming the ng/mL concentration to pM and calculating the dilution factor and volume of the said dilutions of each of these libraries necessary to reach a 1000pM pooled library.

3.6.5 Preparation of samples for MiSeq sequencing

DNA was extracted and purified as described in the section 3.6.1 of this chapter. The purified DNA was diluted 1:10 v/v in 45µL of DNase/Pyrogen-Free distilled water.

To verify the DNA extraction and purification, PCR amplification of the diluted DNA using universal Primer 2 (reverse) and Primer 3 (forward) primers targeting the V3 region of the 16S rRNA gene (Muyzer et al. 1993). Based on *E. coli* 16S ribosomal RNA gene numbering, the annealing positions of these primers are 518-534 and 341 -357 (Brosius et al. 1978). Subsequent Agarose gels of the amplicons were performed, according to the above sections 3.6.2 and 3.6.3, respectively. Procedural blanks were included.

Diluted DNA extracts (40µL of each) were transferred into a 96-well PCR plate (Bio-Rad, UK). The plate was sealed with Microseal® 'B' PCR Plate Sealing Film and stored at -20°C until submission for MiSeq synthesis sequencing (Illumina, UK) at the NU-OMICS research laboratory, Northumbria University, where the 16S rRNA gene V4 primer set (Caporaso et al. 2011) was used for PCR amplification and the library was prepared and validated with the aid of a 2100 Bioanalyzer (Agilent Genomics, UK). After which sequencing following a 2 x 250 bp format with V2 chemistry was performed.

3.7 Next generation sequencing (NGS) data analysis

The sequencing data obtained after NGS were analysed using the open source Mothur software (Schloss et al. 2009), following their 454 standard operating procedure (SOP) (Schloss et al. 2011) and MiSeq SOP (Kozich et al. 2013) as guidelines to quality process (trim, select and screen), align sequences against the reference Silva database release 128 (Quast et al. 2013; Pruesse et al. 2007), and, remove potential chimeras and non-bacterial sequences to then calculate distances; cluster sequences into operational taxonomic units (OTUs) at 97% similarity, classify them using the Silva reference database and to finally, analyse community composition. The community composition analyses were conducted following the workflow diagram below (Figure 3.4).

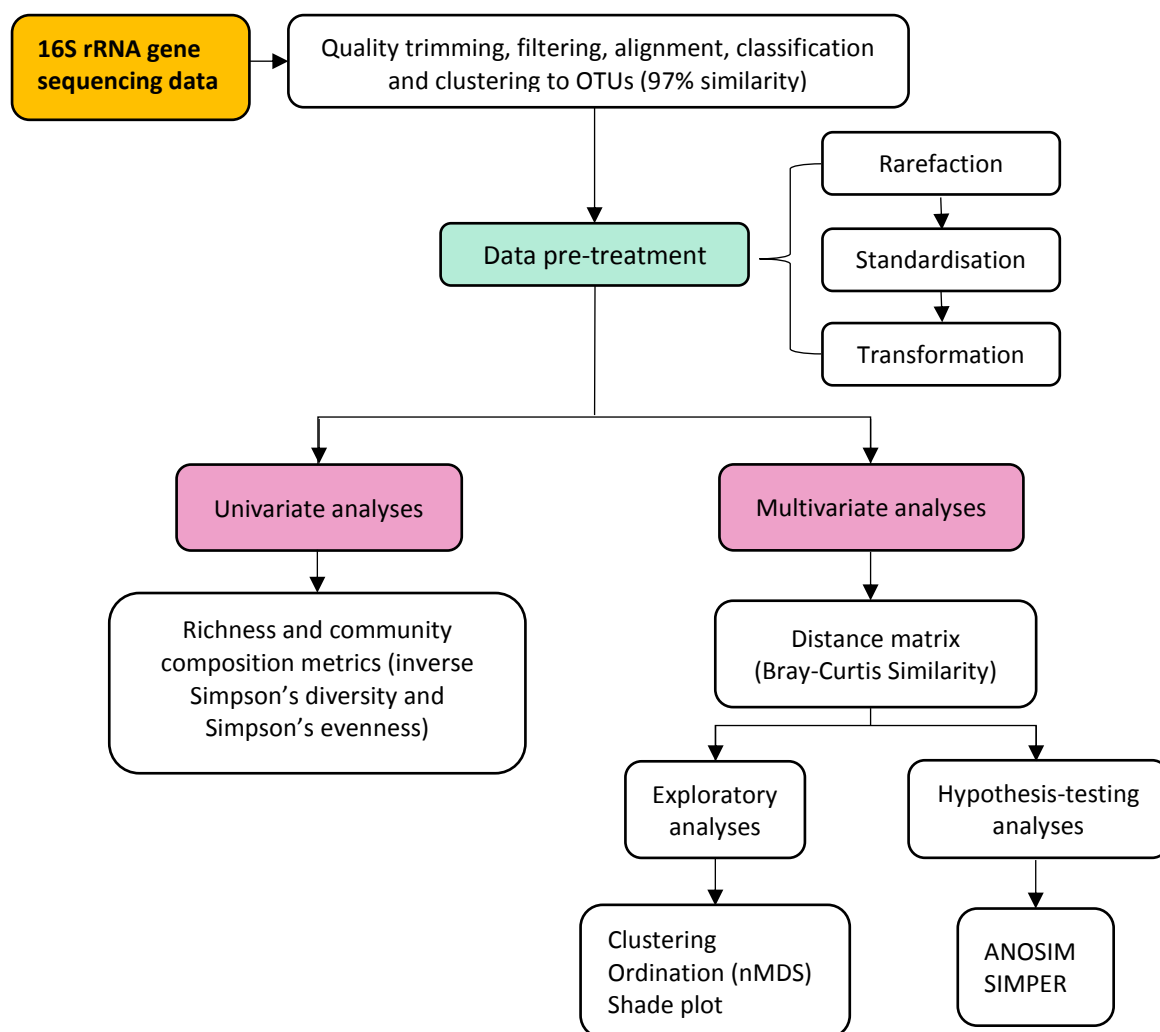


Figure 3.4 Flow diagram of the 16S rRNA gene next generation sequencing data analysis.

Due to the non-continuous nature of sequencing data in addition to the presence of numerous zero values, the sampling bias along with other legacy problems (i.e. PCR bias and OTU definition) all the analyses conducted using this data were non-parametric, thus reducing the effect of the stringent statistical assumptions of parametric methods.

Details of modifications to this procedure and analyses can be found in the methods sections of Chapters 5, 6 and 7.

3.7.1 NGS data pre-treatment

In ecology, it is generally recognised that data without pre-treatment can lead to a poor interpretation of community composition as only the patterns of the most abundant species could be represented (Clarke and Warwick, 2001, Clarke and Gorley, 2006; Ramette, 2007). Particularly, Schloss et al., 2009 report that the number of spurious OTUs (typically chimeras) outputted by Mothur increase as the number of sequences do.

Accordingly, the OTU tables, comprising OTUs and their abundances per sample, generated after quality trimming, filtering, alignment and clustering of the raw DNA sequencing data were randomly subsampled (rarefied, x1000) to the sample with the lowest number of sequences (reads) using the Mothur software (Schloss et al., 2009). In this way, all the samples had the same chance to contain spurious OTUs.

Frequently, the rarefied OTU tables were then standardised by total by expressing the abundances of all individual OTUs as percentage of the total reads in a sample, thus representing OTUs relative abundance (Ramette 2007).

After standardisation, the data was often subjected to square root transformation with the objective to reduce the dominant contribution of the most abundant OTUs (Clarke and Gorley, 2006).

Standardisations and square root transformations were done in R version 3.4.3 (2017-11-30) "Kite-Eating Tree" using the Vegan community ecology package version 2.5-2 (Oksanen et al. 2018).

3.7.2 Univariate analyses

A number of community composition indices were used to broadly compare the different bacterial communities enriched in the different experimental set-ups of this work, as these indices are non-parametric abstractions of the species counts along with their abundances into single coefficients that are often used in ecology to enhance the understanding of communities (Begon et al. 2007; Magurran 2013; Morris et al. 2014).

Below, a brief description of the frequently used multivariate analyses in this thesis is provided.

3.7.3 Species richness (S)

A basic way to characterize a community is to directly count the number of different species comprising it, thus enabling the description and comparison of communities by species richness (S) (Begon et al. 2007).

In this work, operational taxonomic unit (OTU) species richness values were computed in R version 3.4.3 (2017-11-30) "Kite-Eating Tree" using the Vegan community ecology package version 2.5-2 (Oksanen et al. 2018), after rarefaction of the NGS data.

3.7.4 Inverse Simpson's species diversity and evenness indices

Since species richness fails to encompass the abundance of each species in the community ignoring the existence of dominant and rare species and their distribution, which are fundamental parameters to estimate community diversity (Begon et al. 2007), the non-parametric inverse Simpson's diversity coefficient (D) was also computed in this project.

Simpson's index has been recognised as a more robust estimation of community diversity when compared against other commonly used diversity indices (i.e. Shannon's) (Morris et al. 2014; Magurran 2013; Haegeman et al. 2013), since it provides good and consistent estimates of diversity at small sample sizes (Magurran 2013).

Fundamentally, the D index comprises the variance of the species abundance distribution, and it is obtained by calculating the proportion that each species (OTUs, in this case) contributes to the total abundance of individuals in a community (Begon et al. 2007; Simpson 1949).

$$D = \sum_{i=1}^S P_i^2$$

Where: P_i is the proportion for the i th OTU,
 S is the total number of OTUs in the community (richness)
 As D increases, diversity decreases

It must be noted that Simpson's index is often expressed as its complement (1- D) or its reciprocal (1/ D) form, so that its value is directly proportional to the community diversity, this is, the larger the index value, the larger the diversity (Magurran 2013). However, the same character (D) is indistinctly used to represent all the Simpson's index forms (Morris et al. 2014). In this work, the Simpson's inverse diversity coefficient is used and stipulated in the methods sections of the relevant chapters.

$$inv.D = \frac{1}{\sum_{i=1}^S P_i^2}$$

Following the same principles, the evenness or equitability of a community evaluates the distribution of individuals amongst species. It can be determined by expressing Simpson's inverse diversity index as a proportion of the community species richness, which is the maximum possible value $inv.D$ could have if all the OTUs in a community had the same abundance (Begon et al. 2007).

$$E = \frac{1}{\sum_{i=1}^S P_i^2} \times \frac{1}{S}$$

Simpson's inverse diversity and evenness coefficients were computed in R version 3.4.3 (2017-11-30) "Kite-Eating Tree" using the Vegan community ecology package version 2.5-2 (Oksanen et al. 2018) after rarefaction of the NGS data.

3.7.5 Multivariate analyses

Multivariate analyses are required to thoroughly study complex multidimensional data sets (i.e. OTU tables). These methods can provide basic functions such as numeric and graphical summaries of high-dimensional data (i.e. similarity matrices, ordination plots), but also can help to test hypotheses involving multiple variables (i.e. ANOSIM), and to examine relationships between variables (i.e. SIMPER) (Clarke and Warwick, 2001, Clarke and Gorley, 2015; Ramette, 2007; Buttigieg and Ramette, 2014).

Below is provided a brief description of the frequently used multivariate analyses in this thesis.

3.7.6 Bray-Curtis similarity matrix

In general, a resemblance matrix of the data is often required to conduct multivariate analyses, playing an essential role in the ordination and statistical analysis of community composition (Morris et al. 2014; K. R. Clarke 1993).

In this work, the S17 Bray-Curtis resemblance matrix was used as a measure of similarity between samples as it is commonly used and regarded as a robust technique (K. Robert Clarke and Gorley 2006; Morris et al. 2014; Legendre and Legendre 2012). Briefly, this method compares two samples in terms of the minimum abundance of each species (Legendre and Legendre 2012).

PRIMER 7 software (Primer-E Ltd., Plymouth, UK) was used to compute S17 Bray-Curtis resemblance matrices.

3.7.7 Non-parametric multidimensional scaling (nMDS)

The graphical representation of the relative similarity between sample patterns was done through the non-parametric multidimensional scale analysis (nMDS), where the input data was first standardised by total number of reads per sample, transformed by the square root method, and then used to construct a Bray-Curtis similarity matrix. In this method, an iteration is then computed until the distance between the points represent the similarity between samples as close as possible. The closer the points are ordinated in the resulting 2-dimensional plot (2D) the more similar in composition those samples are. Stress values were also included in the nMDS plots as an evaluation of the adequacy of the samples ordination in 2 dimensions, where stress value <0.05 indicates an excellent representation of the data, a value <0.1 is a good representation, <0.2 provides a potentially useful plot, but at stress values >0.3 other exploratory analyses should be considered since the ordination of the points is close to a randomly allocated distribution (Clarke and Warwick, 2001).

PRIMER 7 software (Primer-E Ltd., Plymouth, UK) was used throughout this project to produce nMDS plots.

3.7.8 Analysis of similarities (ANOSIM)

In addition to the graphical representation of the samples as clusters of similar communities, the non-parametric analysis of similarities (ANOSIM) was computed using the PRIMER 7 software (Primer-E Ltd., Plymouth, UK) which utilises the coefficients from the Bray-Curtis similarity matrix, (randomly selected after n number of permutations) to statistically evaluate the dissimilarity between the communities from each experimental set-up (Ramette 2007). The global R-value ranges from 0 to 1, where the closer to 1 the more dissimilar the communities are.

3.7.9 Similarity percentage (SIMPER)

The SIMPER test, part of the PRIMER 7 software (Primer-E Ltd., Plymouth, UK) was also used in each experimental set-up to identify which OTUs contributed to the differences between defined clustered communities previously established by the ANOSIM test.

This analysis first breaks down the average Bray-Curtis similarity within each clustered community into OTUs contributions, defining the most frequent and abundant OTUs for each community, to then compare pairs of different communities at a time, determining the species responsible for sample groupings (discriminating species) between them and their respective contributions to the overall average dissimilarity (Clarke, 1993; Clarke and Gorley, 2015).

Chapter 4. Evaluation of inocula source, pH and environmental oxygen for ethanol production from Organic Municipal Solid Waste

4.1 Introduction

In line with the general aim of this project to develop a multi-species or undefined microbial consortium that will offer robustness and versatility in the bioconversion of the organic municipal solid waste (OMSW) into ethanol (EtOH) and based on the observations from the literature review (see Chapter 2, section 2.6), diverse environments with potential microbial lignocellulose degradation activity were sampled and tested to evaluate their soluble fermentation profiles and thus their capacity to transform OMSW into EtOH under either initial aerobic or anaerobic conditions and at initial neutral or acidic pH. As it has been proposed that mixed cultured fermentation (MCF) under initial aerobic conditions could not only reduce the process operational costs (Ronan et al. 2013), but also provide stability to complex microbial communities (Kato et al. 2005). While pH has a major effect in the direction of fermentative metabolism (Temudo et al. 2007; Rodríguez et al. 2008; González-Cabaleiro et al. 2015). Although many experimental studies have been performed in neutral to alkaline conditions, a few have explored initial acidic pH and showed good performance (Zhang et al. 2012; Ganigué et al. 2016). Nevertheless, fermentation at initial acidic conditions would simplify the production process by skipping the pH conditioning step after acid-pretreatment.

Below, a brief description of the main microbial metabolic activities associated with organic matter degradation occurring in the diverse environments sampled at their normal environmental conditions (pH and oxygen) is presented.

- Compost piles

Compost piles are man-made microbial ecosystem where organic wastes are aerobically degraded to a stable material (Kutzner 2000; Neher et al. 2013). This degradation process has been divided into three successional phases during which different microbial communities get selected by the changes in temperature caused by the metabolic activity in the pile (Kutzner 2000). The first of these phases is characterised by the degradation

of the readily available nutrients by mesophilic bacteria and fungi. The rise in temperature due to this activity leads to the growth of a thermophilic population where more recalcitrant substrates get degraded. When this second phase reaches a plateau less nutrients become available and the thermophilic community activity ultimately declines causing a drop in temperature. In the third phase, the cooling to ambient temperature allows mesophilic organisms to start the degradation cycle again (Kutzner 2000; Neher et al. 2013). Although this process is primarily driven by changes in temperature, notorious changes in pH also occur, typically starting from 4.5 -5.0 increasing to 8.0 -8.1 in the final material (Cekmecelioglu et al. 2005).

It has also been reported that even in thoroughly aerated compost piles, anaerobic micro niches exist, allowing anaerobic microbial metabolism (Kutzner 2000; Atkinson et al. 1996). Thus, making compost a clear source of organic waste degraders and potentially, fermentative microorganisms.

- Woodland soil

A woodland has been defined as a type of forest where there is a sparse density of trees (10%-30%), thus forming areas with limited shade. This is the main difference from forests, which have greater than 30% cover by trees (McElhinny et al. 2005). Nonetheless, the microbial processes in the soils of both environments are highly similar, being responsible for the storage and circulation of carbon by the degradation of recalcitrant biopolymers such as plant litter and woody debris, the incorporation of simpler compounds into the soil, and the mineralization of organic matter (Baldrian 2017; Paul 2006). The abundance of carbon forms in forest soils sustain a complex network of micro niches for organic matter decomposers, specially fungi and bacteria (Paul 2006).

Although fungi seem to dominate the degradation of complex organic matter such as plant biomass, litter and woody debris in these environments due to low nitrogen contents, mykolytic (fungi degraders) bacteria play an important role in early decomposition by degrading fungal mycelia and a high abundance of cellulolytic bacteria has been observed after the initial phase of litter degradation (Baldrian 2017). Bacteria are also crucial for the nitrogen cycle including nitrogen fixation in soils (Paul 2006; Baldrian 2017).

In addition, pH is an important factor to consider, as it affects the organic matter decomposition, solubility and accessibility of nutrients(Lauber et al. 2009). Values of pH

at the surface of forest soils can vary from 6 to 8, being significantly correlated with the bacterial community composition, particularly with changes in the relative abundances of *Acidobacteria*, *Actinobacteria*, and *Bacteroidetes* (Lauber et al. 2009; Fierer and Jackson 2006).

- Rumen

Ruminants depend on the symbiotic interactions with their gut microbiome to obtain energy and nutrients from plant materials. The rumen is an anaerobic microbial environment which represents 64-71% of the volume of the digestive tract in sheep and cattle, sustaining numerous mesophilic bacteria, archaea, protozoa and fungi, which are responsible for the pregastric fermentation of the plant substrates (Flint 1997; McCann et al. 2014). Nevertheless, the rumen microbiome is dominated by bacteria, which provide a large portion of the energy and protein needed by their host through the continuous fermentation of cellulolytic feeds to volatile fatty acids (VFAs) by dividing the task among different functional groups, i.e. cellulolytic, amylolytic, proteolytic, etc., and eventually, being themselves, the source of microbial protein (McCann et al. 2014; Henderson et al. 2015).

It is important to mention that despite being an anaerobic environment, small amounts of oxygen reach the rumen through feed and water, making facultative anaerobic bacteria a normal part of the rumen microbiome (Mann et al. 1954).

As in the case of the previous environments described above, pH is a key factor for the microorganisms in the rumen, optimally ranging from ~7 to 6. The importance of the rumen pH is even more so since its value is used to determine the health status of the animals. For instance, pH above 7.3 strongly suggests a poor-quality diet, typically caused by high supplementation with urea, while a pH value under 6 indicates acidosis, a problem caused by a diet rich in readily available sugars and starch along with a deficiency of long fibre feed, which in the worst case can lead to the animal's death. In both cases, the pH is caused by microbiome structure changes directly influenced by the substrate (McCann et al. 2014).

- Cow faeces

It has been shown that there are significant differences in the bacterial composition between the rumen and the lower intestine of ruminants, with the faecal microbiota being less diverse and notably dominated by obligate anaerobes, particularly by the genera *Clostridium*, *Bacteroides* and *Bifidobacterium* (Liu et al. 2016; Dowd et al. 2008), some of which may improve the digestion of complex cellulosic materials. Nevertheless, as in the case of the rumen, the feces microbiota composition greatly depends on the animal diet.

Due to the pH balance in the ruminants body, cattle faeces tend towards a neutral pH. However, there are few studies reporting the microbial composition of fresh cow faeces as a microbial environment (Dowd et al. 2008; Callaway et al. 2010), as most of the literature investigates the use and microbial composition of manure (faeces mixed with straw typically used for composting) under the light of specific application scopes, for example as inocula for anaerobic digestion (Sun et al. 2015) and its effects on compost of different organic materials (Song et al. 2014).

- Granular anaerobic sludge

As compost, granular anaerobic sludge is a man-made microbial ecosystem, in this case wastewater with high organic matter load gets anaerobically treated to biogas (CH_4 and CO_2). The granules are spherical dense conglomerates of microorganisms self-aggregated through the natural adsorption properties of bacterial extracellular polymers (Schmidt and Ahring 1996).

The transformation of organic matter to biogas requires the interaction of diverse groups of bacteria and archaea in the granules. After bacterial hydrolysis of the complex organic polymers, fermentative bacteria transform the resulting material to VFAs, H_2 and CO_2 . Under methanogenic conditions (20°C - 50°C and pH 6.5 - 8), the VFAs (that are not already acetate) get further oxidised to acetate and H_2 by acetogenic bacteria. After which, the acetate, H_2 and CO_2 are transformed to methane by methanogenic archaea (Schmidt and Ahring 1996; Lim and Kim 2014).

4.2 Objectives

In line with the general aim of this project to simplify bioethanol production from the organic fraction of municipal solid waste, experiments using the previously described inocula sources were conducted to:

- Evaluate the ubiquity of EtOH fermentation, testing the assumption made in the mathematical models described in the literature review (Chapter 2, section 2.5) which propose that the products generated in MCF processes are mostly determined by thermodynamics, despite the microbial community composition.
- Study the fermentation soluble-end products profiles of the individual inocula and determine if initial oxygen presence influences EtOH production.
- Study EtOH production under initial neutral and acidic pH conditions.
- Determine the best combination of inocula/environmental variables (pH/initial O₂) for EtOH production to inform further experimentation.

4.3 Methods

4.3.1 Culture media preparation

The culture medium described in Chapter 3 section 3.3.1 was used for incubation at initial aerobic conditions (non-reduced medium). The same medium was modified by the addition of L-cysteine hydrochloride monohydrate (Sigma-Aldrich, UK) at a concentration of 1 g/L to act as a reducing agent (Ronan et al. 2013). Once sealed, the headspace of the microcosms containing pre-reduced medium was purged for 1 min with oxygen free nitrogen gas (BOC, UK), and this medium was then used for incubations at initial anaerobic conditions.

Microcosms were prepared as described in 3 section 3.3.1 in 120mL serum bottles containing 50mL of either non-reduced or pre-reduced media, plus 2.5g of OMSW analogue.

4.3.2 pH adjustment

As mentioned in section 3.3.2 of Chapter 3, after autoclave sterilisation and before inoculation, the pH of the medium was measured and adjusted according to the experimental design with NaOH 1M or H₂SO₄ 1M. The high concentration of these alkaline and acid solutions was intended to minimize the increment changes in liquid volume in the microcosms. No further pH adjustment was made after inoculation. However, it must be noted that the addition of some of the inocula had an effect on the initial pH of the medium, and that the pH values reported in this chapter for day 0 are those measured after inoculation.

4.3 3 Microcosms inoculation

Individually, bottles were placed on a standard precision balance (0.1g - 0.01g) and inoculated with 2.5g of the corresponding inoculum. In addition to the five individual inocula sources described in section 3.1 of Chapter 3, a set (triplicates) was inoculated with a combination of all of these comprising 0.5g of each adding up to 2.5g. The latter was setup with the objective to explore the possible enrichment of a mixed-source culture ethanologenic community.

4.3.4 Experimental design

To test the ethanologenic capacity of the inocula under initial anaerobic and aerobic conditions the experimental design (EXP 1) considered two factors: A) Inocula source and B) Initial oxygen conditions.

Factor A) had 8 levels, the 5 inocula sources (compost, woodland soil, cow faeces, rumen, sludge), plus microcosms inoculated with a mixture of all original sources (henceforth named "inocula all"), substrate blanks (microcosms with the mixture of all inocula without carbon source, BS) and inocula blanks (microcosms with media and OMSW analogue, without inocula added, BI).

Factor B) had 2 levels, namely, initial anaerobic or aerobic conditions. Giving A*B= 16 possible combinations, which were each tested in triplicate with exception of the inocula blank which was run in duplicate. A total of 46 microcosms were thus prepared. This first test was performed with the substrate and media at an initial neutral pH.

To narrow down the inoculum selection for subsequent analysis, the experiments described above were repeated excluding the two inocula with the lowest EtOH production observed, with $A(6) * B(2) = 12$ possible combinations which were tested in triplicate. Importantly, the microcosms in the second experiment (EXP 2) were incubated under initial acidic pH, the approximate pH of the substrate after pre-treatment (pH~5.5). To evaluate the effect of initial pH in EtOH production, the results of maximal EtOH production by the inocula tested in both experiments were statistically compared as described in this chapter's section 4.3.4.

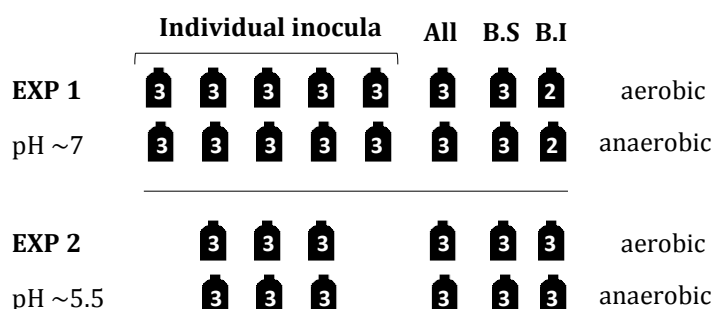


Figure 4.1 Experimental designs (EXP1 and EXP2) to test the effects of inocula source, oxygen presence and pH in EtOH production.

4.3.5 Microcosms incubation and sampling plan

EXP 1 microcosms were incubated in the dark, at room temperature (approximately 20°C) under static conditions for 14 days. Liquid samples were taken every other day for pH measurements and GC-FID soluble fermentation product analyses according to section 3.3.3.

EXP 2 microcosms were incubated under the same conditions as for EXP1 for 30 days. Liquid samples were taken at day 0, 2, 7, 14, 21 and 30 for pH measurements and GC-FID soluble fermentation product analyses according to section 3.3.3 of Chapter 3.

4.3.6 GC-FID quantification of soluble fermentation products

The quantification of soluble fermentation products was done using the GC-FID method described in section 3.4.2 of Chapter 3.

Solutions of ASC reagent grade ethanol, butanol, acetic, propionic and butyric acids were prepared in distilled water at concentrations of 0, 2, 4, 8, 15, 30 and 60mM. These solutions were then analysed in triplicate for the construction of calibration curves at the beginning of each experimental set-up. The following linear equations were obtained from the GC-FID standard curves:

EtOH[mM]=	(Area(mVs)-2.578±2.569mVs)/2.290±0.093 mVs.mM ⁻¹	R ² 0.994
Acetic acid[mM]=	(Area(mVs)-21.228±11.316mVs)/2.700±0.162 mVs.mM ⁻¹	R ² 0.987
Butyric acid[mM]=	(Area(mVs)-2.358±9.443mVs)/5.124±0.302mVs.mM ⁻¹	R ² 0.990
1-Butanol[mM]=	(Area(mVs)-3.867±2.620mVs)/3.105±0.085mVs.mM ⁻¹	R ² 0.997
Propionic acid[mM]=	(Area(mVs)-1.114±13.941mVs)/3.643±0.257mVs.mM ⁻¹	R ² 0.988

Where: ± confidence interval at level 95% (lower 2.5%, upper 97.5%).

For quality control, freshly prepared standard solutions of EtOH and a mixture of volatile fatty acids (VFAs) were prepared and quantified at the start and end of each run of GC-FID analysis.

Samples were processed as described in Chapter 3 section 3.3.3, each of these was analysed 3 times. The calculation for the concentration of soluble fermentation products from the linear regression equation obtained for each calibration curve is illustrated below in Equation 3.1.

$$\text{Eq 3.1} \quad \text{Conc. [mM]} = \frac{\text{Area(mVs)} \pm \text{Intercept (mVs)}}{\text{Gradient (mVs/mM)}}$$

Where: Area (mVs) is the area obtained after GC-FID analysis

Intercept (mVs) the value for intercept from the respective calibration curve

Gradient (mVs/mM) the value for the gradient from the respective calibration curve

4.3.7 Statistical analysis of physicochemical data

The R programming language and free software R version 3.4.3 (2017-11-30) -- "Kite-Eating Tree" was used to conduct statistical analyses of physicochemical data.

The error bars in all the plots presented in this chapter represent the standard error of the mean (SE).

The quantitative comparison of the effects of the different variables tested and their possible interactions on EtOH production was done through 2-way ANOVA analyses. To assess if the data met the 2-way ANOVA test assumptions, the homogeneity of variances and normality of the residuals were examined through the Levene's test for homogeneity of variance and the Shapiro-Wilk normality test.

When the 2-way ANOVA analysis was valid and significant (p -value < 0.05), a Tukey HSD test was then conducted to do multiple pairwise-comparisons between the means of groups and determine which of them were statistically significantly different.

Correlation analyses were also computed to evaluate the relationship between pH and inocula source in EtOH production. To assess the validity of the correlation analyses, the linear relationship of the continuous variables and normal distribution of the data sets were examined through linear regression and the Shapiro-Wilk normality test. If the relationship between the variables was not linear, no correlation analysis was done. Pearson's product-moment correlation was computed when the data set was normally distributed. If the data of one or more variables in each data set was not normally distributed, the non-parametric Kendalls's rank correlation tau was done. The alternative to the null hypothesis in both cases was that true correlation coefficient is not equal to 0 at the 95% confidence level.

A detailed example of the sequence of statistical analyses of physicochemical data can be found in Appendix A.

4.4 Results

4.4.1 EtOH production by different inocula under initial anaerobic conditions at initial neutral pH

After 2 days of incubation, EtOH production was observed in all microcosms incubated under initial anaerobic conditions (Figs. 4.2). However, its dominance in the fermentation products was variable as a function of inocula source.

Rumen inoculated microcosms showed the highest EtOH production which was also the dominant product. At 14 days the average concentration was $26.80\text{mM} \pm 3.18\text{mM}$. Although the sludge inoculated microcosms reached a slightly higher average peak concentration ($29.20\text{mM} \pm 23.82\text{mM}$), this value was due only to one of the replicates (34.35mM), while the other two behaved in a similar way to each other ($4.40\text{mM} \pm 1.62\text{mM}$), hence it was decided to remove this replicate from the subsequent statistical analyses. A closer inspection to the sludge replicates can be found in Fig. 4.6

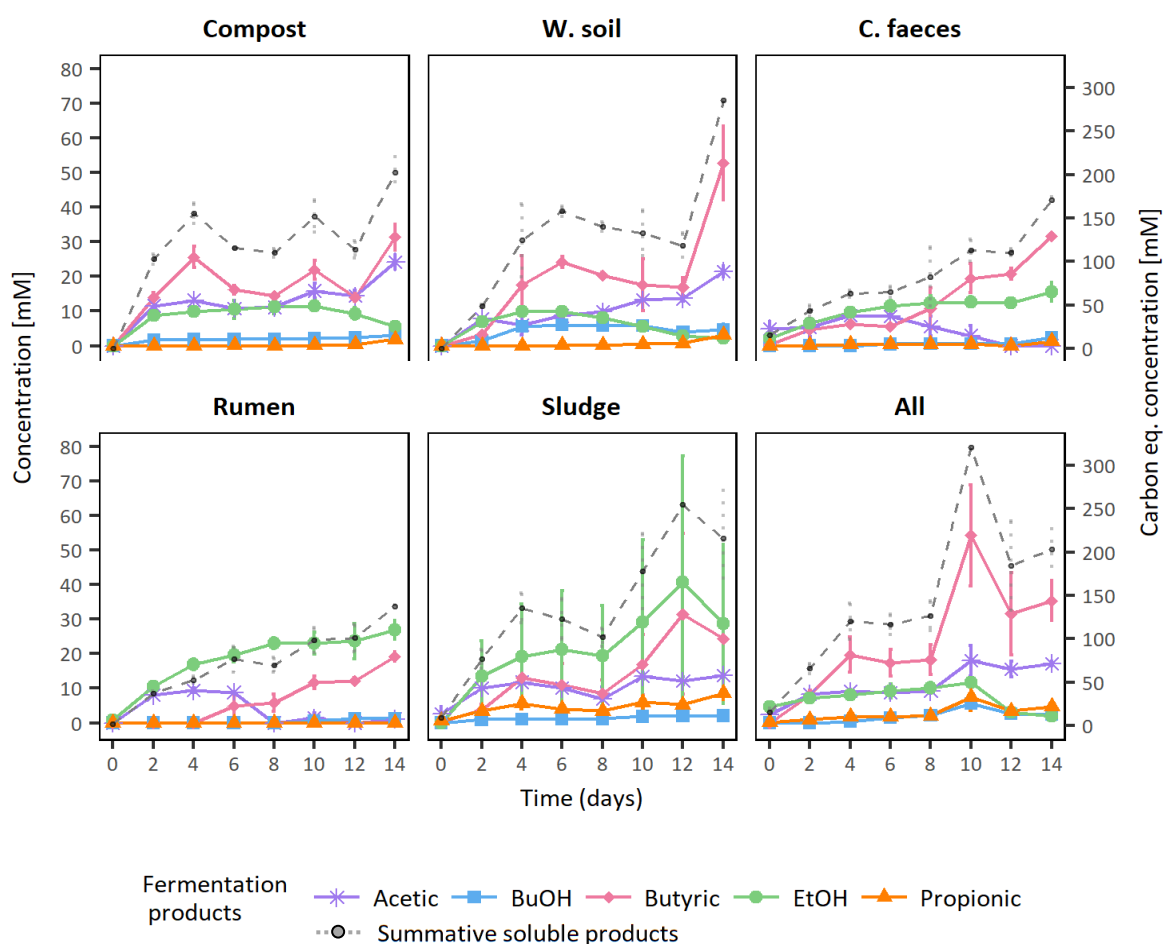


Figure 4.2 Fermentation products by the different inocula tested during 14 days of incubation under initial anaerobic conditions. The summative soluble fermentation products line represents the total equivalents of soluble carbon produced by each inocula.

Meanwhile, c. faeces inoculated microcosms reached a peak EtOH concentration of $15.58 \text{ mM} \pm 3.20 \text{ mM}$ at 14 days of incubation. Compost inoculated microcosms peak EtOH concentration of $11.58 \text{ mM} \pm 1.56 \text{ mM}$ at day 10 was followed by a decrease to $5.67 \text{ mM} \pm 0.87 \text{ mM}$ at 14 days of incubation. Likewise, the combination of all inocula sources produced up to $11.72 \text{ mM} \pm 1.18 \text{ mM}$ at 10 days of incubation after which a decline to $1.84 \text{ mM} \pm 0.38 \text{ mM}$ was observed. W. soil inoculated microcosms produced the lowest concentration of EtOH ($9.98 \text{ mM} \pm 1.32 \text{ mM}$). Apart from rumen, the main soluble fermentation product by the rest of the inocula was butyric acid.

The peak concentration of other fermentation products under initial anaerobic conditions were: $15.88 \text{ mM} \pm 2.24 \text{ mM}$ of acetic acid in compost inoculated microcosms, $5.94 \text{ mM} \pm 1.75 \text{ mM}$ of propionic acid by sludge inoculated microcosms and $23.84 \text{ mM} \pm 1.31 \text{ mM}$ of butyric acid in w. soil inoculated microcosms, all of these were reached at 14 days of incubation. Meanwhile, sludge butanol production maintained a plateau from day 4 to 10 in the range of $5.64 \text{ mM} \pm 0.18 \text{ mM}$ to $5.81 \text{ mM} \pm 0.64$.

4.4.2 EtOH production by different inocula under initial aerobic conditions at initial neutral pH

As for initial anaerobic conditions, EtOH production was observed in all microcosms incubated under initial aerobic conditions after 2 days of incubation (Fig. 4.3). Furthermore, similar variable patterns of product dominance were observed.

More specifically, rumen inoculated microcosms also showed the highest EtOH production under initial aerobic conditions at 14 days with an average concentration of $33.57 \text{ mM} \pm 2.82 \text{ mM}$, furthermore, showing a potential for continued increase after the experimental period.

C. faeces inoculated microcosms peak EtOH production of $18.37 \text{ mM} \pm 2.31 \text{ mM}$ at day 12 showed a decline to $5.75 \text{ mM} \pm 2.78 \text{ mM}$ at 14 days. In a similar fashion, the maximal EtOH production by compost ($9.61 \text{ mM} \pm 1.71 \text{ mM}$, at 2 days) and w. soil ($11.01 \text{ mM} \pm 0.91 \text{ mM}$, at 4 days) was followed by a continuous decrease ($1.79 \text{ mM} \pm 0.11 \text{ mM}$ and $2.26 \text{ mM} \pm 0.59 \text{ mM}$, respectively) until the end of the incubation period. Sludge inoculated microcosms produced up to $6.31 \text{ mM} \pm 1.16 \text{ mM}$ at 10 days of incubation, while the combination of all inocula sources produced the lowest EtOH concentration ($2.20 \text{ mM} \pm 0.59 \text{ mM}$) at 8 days of incubation, followed by a continuous decline.

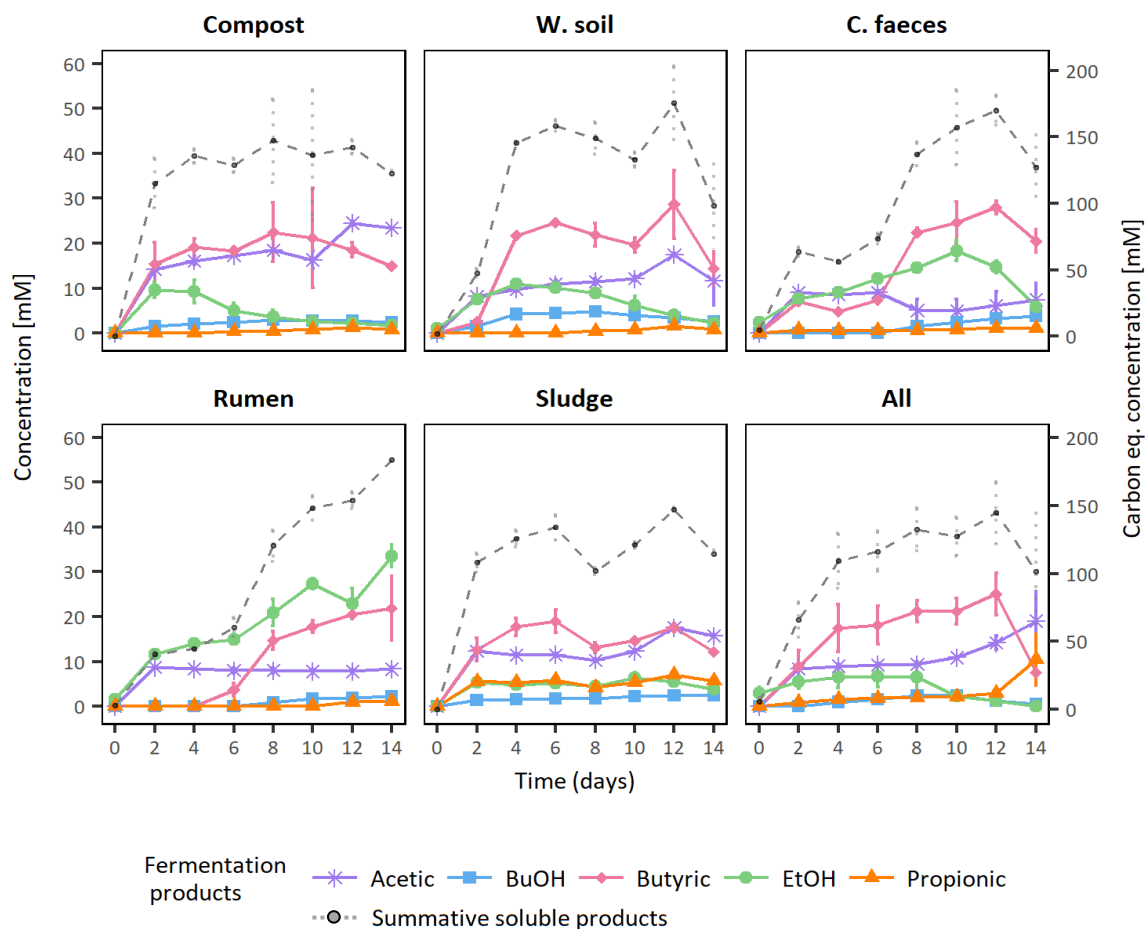


Figure 4.3 Fermentation products by the different inocula tested during 14 days of incubation under initial aerobic conditions. The summative soluble fermentation products line represents the total equivalents of soluble carbon produced by each inocula.

The highest concentrations of other fermentation products were: $24.511 \text{ mM} \pm 0.5202 \text{ mM}$ of acetic acid at 12 days of incubation in compost inoculated microcosms. The highest production of propionic acid ($10.45 \text{ mM} \pm 0.60141 \text{ mM}$) was obtained in the microcosms with all the inocula sources at 14 days, showing a positive exponential trend at the end of the experiment. High concentrations of butyric acid were observed in all the microcosms, rising after 2 days and reaching a plateau-like shape up to 12 days of cultivation, after which a decline was observed in most microcosms except for the inoculated with rumen. The highest concentration of butyric acid ($27.964 \text{ mM} \pm 1.437 \text{ mM}$) was obtained at 12 days in c. faeces inoculated microcosms. Apart from a small concentration of acetic acid in one of the inocula blank replicates, no fermentation activity was observed either in the inocula nor substrate blanks.

4.4.3 Statistical comparison of maximal EtOH production by the different inocula under initial anaerobic and aerobic conditions at initial neutral pH

The maximal values of EtOH production by the various inocula under initial aerobic and anaerobic conditions (Fig. 4.4) were statistically compared to assess whether the differences observed were significant, and if so, which variable was responsible: inocula sources, initial oxygen and/or their interaction.

A 2-way ANOVA analysis was conducted to quantitatively assess these observations. As the data met the homogeneity of variances (Levene's test p -value $0.9205 > 0.05$) and the assumption of a normal distribution (p -value = $0.9869 > 0.05$), the results of this test can be considered valid.

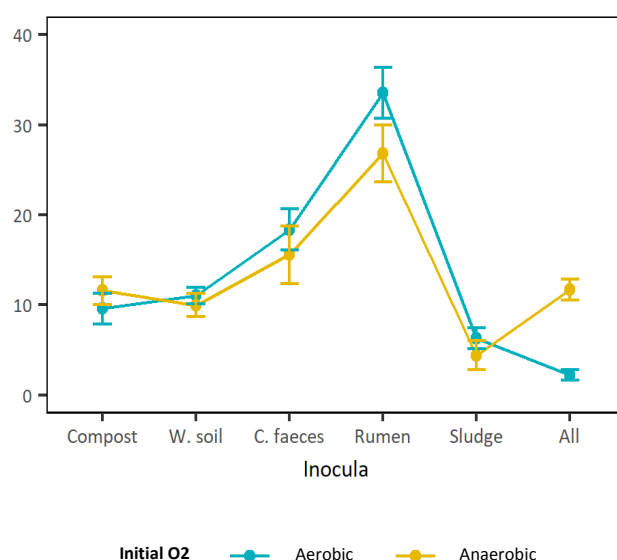


Figure 4.4. Two-way interaction plot of the means of the maxima EtOH concentrations as a response to the combination of the two factors tested: inocula and initial oxygen conditions. Note: these plots and the statistical analyses only considered two sludge replicates.

Based on the p -values and a significance level (signif. codes: 0 '***' 0.001 '**' 0.01 '*' 0.05) from the 2-way-ANOVA results, it was concluded that both factors, inocula (p -value $1.399\text{e-}09$ ***) and initial oxygen (p -value 0.002591 **) as well as their interaction (p -value 0.011391 *) had an statistically significant effect on EtOH production, with inocula being the most significant factor.

A Tukey HDS test was then computed to determine the differences between each of the levels of the two variables as well as their interaction. No significant difference was found between the two levels of initial oxygen (p -value $0.927 > 0.05$). The latter is divergent from

the conclusion reached based on the ANOVA results, as these two tests analyse the data from different perspectives, while the ANOVA assessed the overall relationship between Inocula and Initial O₂, the Tukey test compare the individual levels of these factors.

C. faeces and rumen were significantly different to all the other inocula, however, when considering the interaction of inocula and initial oxygen, as Figure 4.4. suggests, rumen is the only inocula with EtOH production significantly different to the rest, under both, initial aerobic and anaerobic conditions with a *p*-value < 0.05 (Table 4.1).

Importantly, there was no significant difference in EtOH production among any of the same inoculum pairings when comparing their initial incubation in aerobic or anaerobic conditions (i.e. compost-aerobic vs compost-anaerobic *p*>0.05). See Table 4.1 for details on the relevant results of the Tukey HDS test.

Table 4.1. Results of the multiple pairwise-comparison (Tukey HDS test) of the interaction effect of inocula source and initial oxygen conditions on EtOH production at an initial neutral pH.

Inocula*Initial O ₂	diff	lwr	Upr	<i>p</i> -adj
Same inoculum: Aerobic – Anaerobic				
Compost – Compost	1.965	-8.232	12.162	0.999
W. soil – W. soil	-1.025	-11.222	9.172	0.999
<i>C. faeces</i> – <i>C. faeces</i>	-2.794	-12.991	7.403	0.996
Rumen – Rumen	-6.764	-16.961	3.433	0.442
Sludge – Sludge	-1.906	-13.306	9.495	0.999
All – All	9.514	-0.683	19.711	0.083
Rumen/ Initial O₂ vs X inoculum/ Initial O₂				
Aerobic – All/ aerobic	31.364	21.167	41.561	0.000
Anaerobic – All/ anaerobic	15.086	4.889	25.283	0.001
Anaerobic – All/ aerobic	24.600	14.403	34.797	0.000
Aerobic – Compost/ aerobic	23.955	13.758	34.152	0.000
Anaerobic – Compost/ anaerobic	15.226	5.0293	25.423	0.001
Anaerobic – Compost/ aerobic	17.191	6.994	27.388	0.000
Aerobic – W. soil/ aerobic	22.557	12.360	32.754	0.000
Anaerobic – W. soil/ anaerobic	16.818	6.6210	27.015	0.002
Anaerobic – W. soil/ aerobic	15.793	5.596	25.990	0.001
Aerobic – <i>C. faeces</i> / aerobic	15.193	4.996	25.390	0.001
Anaerobic – <i>C. faeces</i> / anaerobic	11.224	1.027	21.420	0.023
Anaerobic – <i>C. faeces</i> / aerobic	8.429	-1.7677	18.626	0.173*
Aerobic – Sludge/ aerobic	-27.26	-37.457	-17.063	0.000
Anaerobic – Sludge/ anaerobic	-22.402	-33.802	-11.001	0.000
Anaerobic – Sludge/ aerobic	20.496	10.299	30.693	0.000

Where diff= difference between means of the two groups, lwr, upr= the lower and the upper values of the confidence interval at 95% and *p* adj= *p*-value after adjustment for the multiple comparisons. X inoculum = any inoculum apart from rumen. All= microcosms inoculated with a mixture of all inocula (see section 4.3.2). *Not significantly different.

In addition, despite of the differences in the soluble products distribution, an overall comparison of the maximal total productivity in terms of carbon equivalents (Figures 4.2 and 4.3, summative soluble products), was done by means of a 2-way ANOVA (95% confidence level), according to which, no statistically significant difference was found in the total productivity of the inocula incubated under initial anaerobic or aerobic conditions (Inocula*O₂ *p*-value 0.710). In average, these systems generated about 183.67±13.10mM of soluble fermentation products.

Based on these analyses it was concluded that rumen inoculum significantly produced higher EtOH concentrations than any of the other inocula tested, under both initial aerobic and anaerobic conditions.

4.4.4 Microcosms at initial neutral pH time profiles

The initial pH of the microcosms sampled in this test ranged from 7.0 to 6.2. As mentioned in section 4.3.2 of this chapter, despite the initial pH adjustment to ~7, the addition of some inocula modified the initial pH of the medium, and the initial pH values reported here are those measured after inoculation. A statistical analysis of the initial pH data can be found in section 4.4.8 of this chapter.

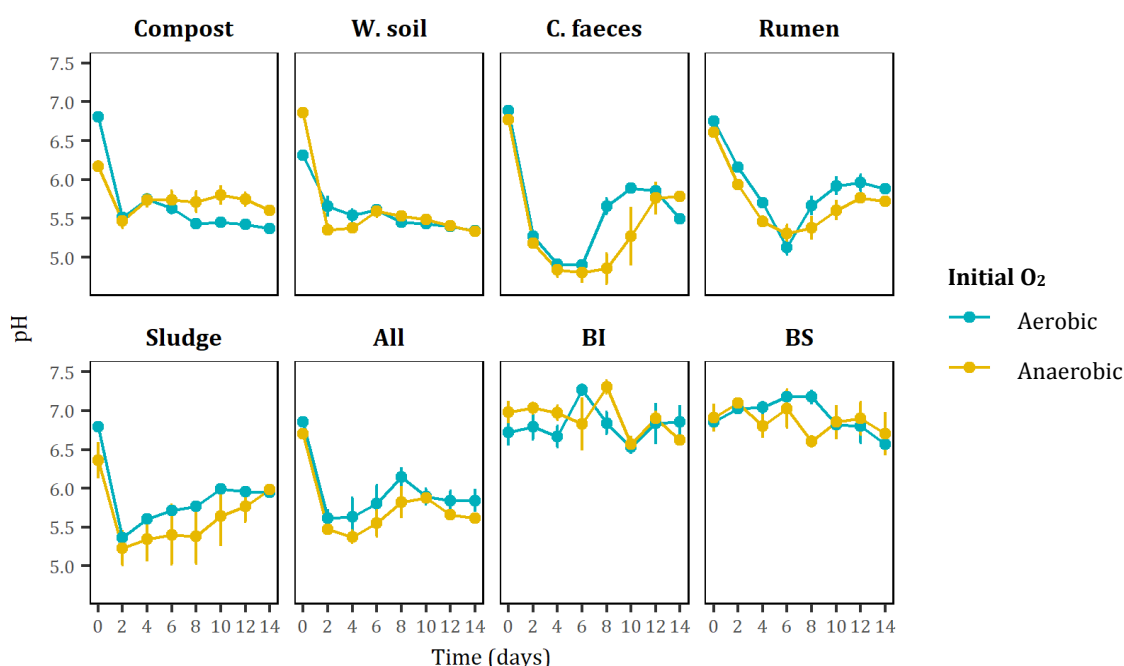


Figure 4.5 pH changes in each inocula configuration and the blanks during the incubation period under initial aerobic and anaerobic conditions. BI= inocula blanks, BS= substrate blanks.

Figure 4.5 shows the pH changes in the different microcosm set-ups during the 14 days of incubation. Most inocula caused a steep drop of pH (~ 1.3 pH units) between days 0 and 2 under both initial oxygen conditions, while rumen showed a gradual pH decrease, reaching a minimum at day 6 (minus ~ 1.5 pH units from the initial value) after which pH was raised up to ~ 0.6 pH units in the final day of incubation. A similar trend was observed in *c. faeces* inoculated microcosms.

In the following section, the effect of inocula and initial oxygen conditions are evaluated when the initial pH of the medium is acidic. The second experimental set up (EXP 2) was informed by the results just presented. Thus, compost and w. soil were not further used as inocula, as they produced the lowest maxima EtOH concentrations, and even though it was shown that there was no significant difference between these inocula, *c. faeces* and sludge, this decision helped to decrease the analyses time and to narrow down the search for an appropriate inocula. Contrarily and despite of its bad performance, it was decided to test EtOH production by sludge at initial acidic pH, due to the observations illustrated in Fig. 4.6, where the fermentation activity of the individual sludge replicates and associated pHs incubated at initial anaerobic conditions are shown to be highly variable.

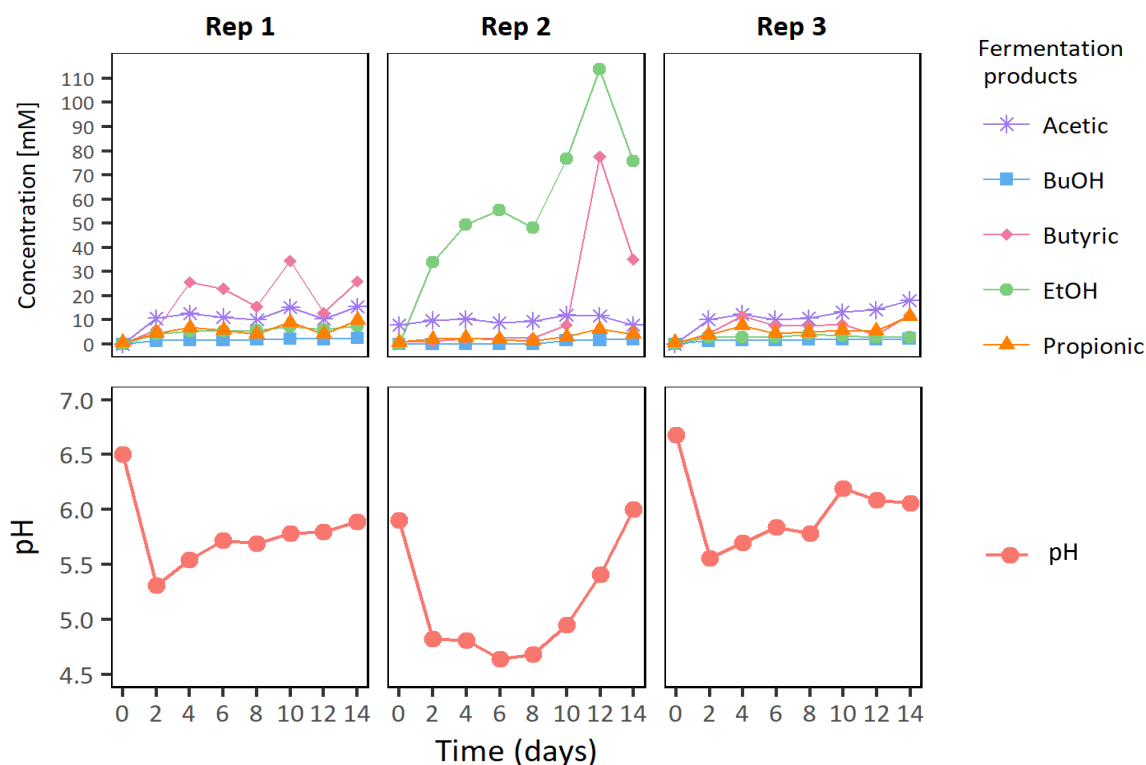


Figure 4.6 Fermentation products and pH curves of the individual sludge inoculated replicates incubated under initial anaerobic conditions.

Specifically, rep 2 produced 34.35mM of EtOH, while the other two produced a noticeably lower concentration ($4.40\text{mM} \pm 1.62\text{mM}$) and intriguingly the initial pH of Rep 2 was 0.5 pH units lower than that of the other two replicates. Whether these two observations were correlated or not, could not be statistically analysed due to the sample size. Therefore, it was decided that the inclusion of sludge in the following test could be relevant to this project.

4.4.5 Effect of inocula under initial aerobic and anaerobic conditions at initial acidic pH

As at initial neutral pH, EtOH production was observed in all microcosms after 2 days of incubation in both the initial oxygen conditions tested (Figs.4.7 and 4.8). Whereas no fermentation activity was quantified either in the inocula or substrate blanks.

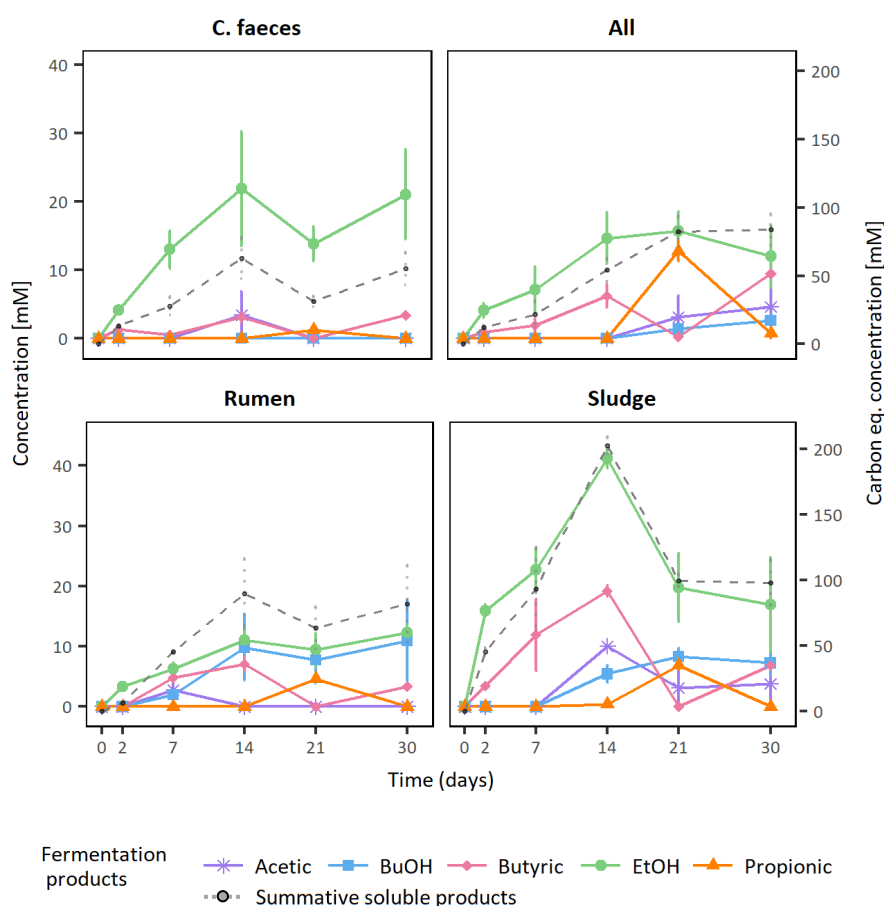


Figure 4.7 Fermentation products by the different inocula tested during 30 days of incubation under initial anaerobic conditions. The summative soluble fermentation products line represents the total equivalents of soluble carbon produced by each inocula.

Remarkably, sludge inoculated microcosms showed the highest EtOH production at 14 days of incubation under both initial anaerobic and aerobic conditions, with average concentrations of $41.18 \text{ mM} \pm 1.61 \text{ mM}$ and $33.33 \text{ mM} \pm 5.58 \text{ mM}$, respectively.

Under initial anaerobic conditions, the combination of *c. faeces*, rumen and sludge inoculated microcosms reached a peak EtOH concentration of $15.74 \text{ mM} \pm 2.79 \text{ mM}$ at 21 days of incubation, while *c. faeces* and rumen inoculated microcosms registered their highest EtOH concentration of $21.00 \text{ mM} \pm 6.53 \text{ mM}$ and $12.28 \text{ mM} \pm 1.23 \text{ mM}$ at day 30. In these incubations the main fermentation product by all the inocula was EtOH.

Regarding other fermentation products under initial anaerobic conditions, the highest concentration of acetic ($10.02 \text{ mM} \pm 0.12 \text{ mM}$) and butyric ($19.20 \text{ mM} \pm 0.93 \text{ mM}$) acids were produced by the sludge inoculated microcosms at 14 days of incubation, while the combination of the inocula sources produced up to $12.78 \text{ mM} \pm 1.44 \text{ mM}$ of propionic acid at 21 days of incubation. The highest production of butanol ($10.93 \text{ mM} \pm 6.74 \text{ mM}$) was registered at day 30 in rumen inoculated microcosms.

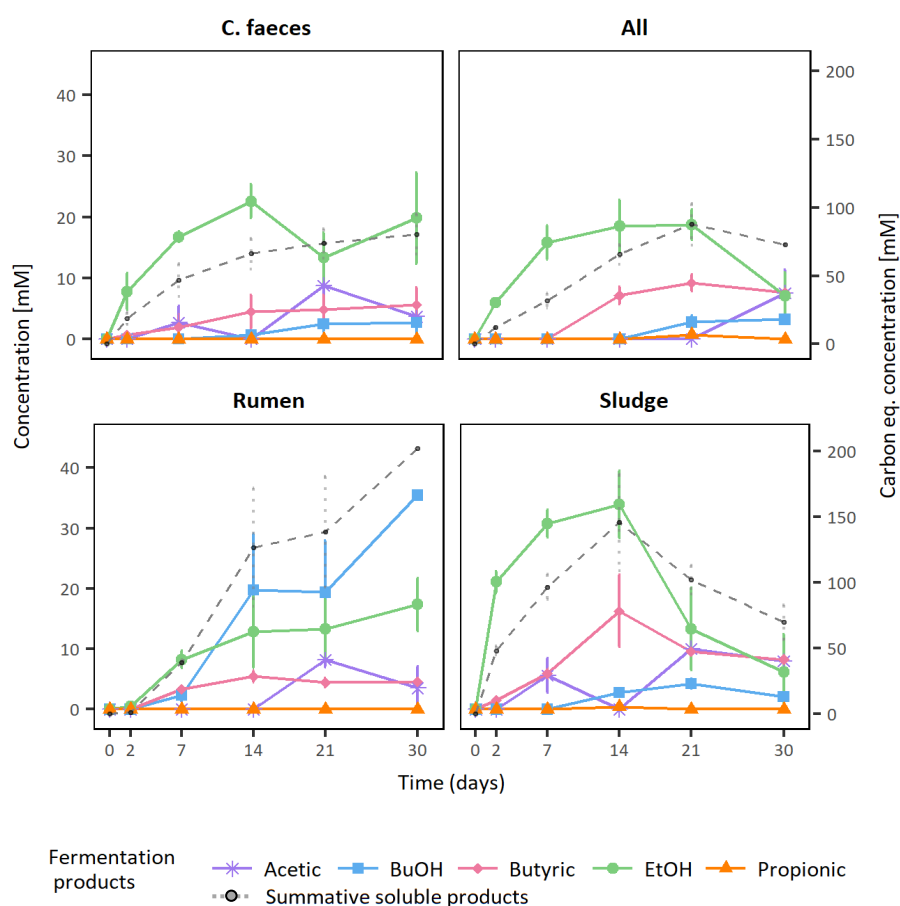


Figure 4.8 Fermentation products by the different inocula tested during 30 days of incubation under initial aerobic conditions. The summative soluble fermentation products line represents the total equivalents of soluble carbon produced by each inocula.

Under initial aerobic conditions, the combination of inocula sources inoculated microcosms reached a peak EtOH concentration of $18.76\text{mM} \pm 2.47\text{mM}$ at 21 days of incubation, while *c. faeces* registered its highest EtOH concentration of $22.60\text{mM} \pm 2.79\text{mM}$ at day 14. The maxima EtOH concentration ($17.33\text{mM} \pm 4.40\text{mM}$) produced by rumen inoculated microcosms was obtained at the end of the incubation period.

Sludge inoculated microcosms also produced the maxima concentrations of acetic and butyric acids of $10.03\text{mM} \pm 1.58 \text{ mM}$ (day 21) and $16.29\text{mM} \pm 5.93\text{mM}$ (day 14), respectively. Although an important high average concentration of butanol ($35.46\text{mM} \pm 20.14\text{mM}$) was achieved by rumen inoculated microcosm on day 30, the high standard error must be noted. No propionic acid production was observed in any of the microcosm set-ups.

4.4.6 Statistical comparison of maxima EtOH production by the different inocula under initial anaerobic and aerobic conditions at initial acidic pH

A statistical analysis like the one presented in section 4.4.3 of this chapter was done to assess the effect of the inocula, initial oxygen conditions and their interaction on EtOH production, at initial acidic conditions of the culture medium (Fig. 4.9).

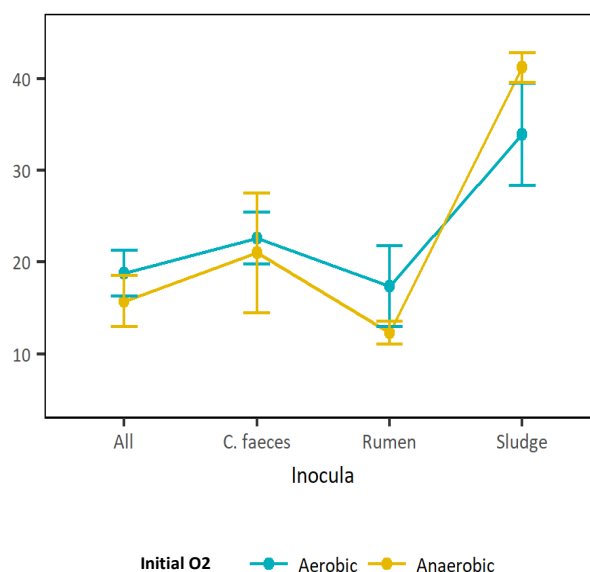


Figure 4.9. Two-way interaction plot of the means of the maxima EtOH concentrations as a response to the combination of the two factors tested: inocula and initial oxygen conditions.

A 2-way ANOVA analysis was done after which its validity was confirmed (Levene's test p -value $0.8838 > 0.05$, Shapiro-Wilk normality test p -value = $0.7952 > 0.05$). The results of this 2-way ANOVA suggested that inocula was the only variable having a significant effect on EtOH production (p -value $9.54e-05^{***}$).

To evaluate the differences between inocula and verify the conclusion regarding initial oxygen concentration, a Tukey HDS test was performed. Effectively, no significant difference was found between the two levels of initial oxygen (p -value $0.827 > 0.05$). Table 4.2 summarises relevant results of the Tukey HDS test. These analyses helped to confirm that sludge inoculated microcosms EtOH production was significantly different from the other treatments.

Table 4.2. Results of the multiple pairwise-comparison (Tukey HDS test) of the interaction effect of inocula source and initial oxygen conditions in EtOH production at initial neutral pH.

Inocula*Initial oxygen	diff	lwr	upr	p adj
Same inoculum: Aerobic - Anaerobic				
C. faeces - C. faeces	-1.608	-20.489	17.273	0.999
Rumen - Rumen	-5.054	-20.771	10.665	0.945
Sludge - Sludge	7.256	-8.462	22.974	0.745
All - All	-3.022	-18.740	12.697	0.997
Sludge: treatment - Inoculum: treatment				
Aerobic – All: Aerobic	15.165	-0.554	30.883	0.063
Anaerobic – All: anaerobic	25.442	9.724	41.161	0.001
Anaerobic – All: aerobic	22.421	6.702	38.139	0.003
Aerobic – C. faeces: aerobic	11.322	-7.559	30.203	0.467*
Anaerobic – C. faeces: anaerobic	20.186	1.305	39.070	0.032
Anaerobic – C. faeces: aerobic	18.578	-0.302	37.459	0.048
Aerobic – Rumen: aerobic	16.591	0.872	32.309	0.035
Anaerobic – Rumen: anaerobic	28.900	13.182	44.618	0.000
Anaerobic – Rumen: aerobic	23.847	8.128	39.565	0.002

Where diff= difference between means of the two groups, lwr, upr= the lower and the upper values of the confidence interval at 95% and p adj= p -value after adjustment for the multiple comparisons.

*Not significantly different.

Additionally, a general comparison of the maximal total productivity by each inocula, in terms of carbon equivalents (Figures 4.7 and 4.8, summative soluble products), was done by means of a 2-way ANOVA (95% confidence level). The total productivity of sludge was overall significantly different to c. faeces (p -value 0.0245), confirming the observations from Figure 4.7, where c. faeces reached a maximal total productivity of 62.817 ± 14.991 mM of carbon equivalents, while sludge produced up to 202.317 ± 6.775 mM.

Excluding *c. faeces*, these systems generated about $135.16 \pm 23.09 \text{ mM}$ of soluble fermentation products.

Based on these statistical analyses it was concluded that sludge inoculum significantly produced higher EtOH concentrations than any of the other inocula tested, under both initial aerobic and anaerobic conditions.

4.4.7 Initial acidic pH time profiles

Figure 4.10 shows the pH changes in the different microcosm set ups during the 30 days of incubation.

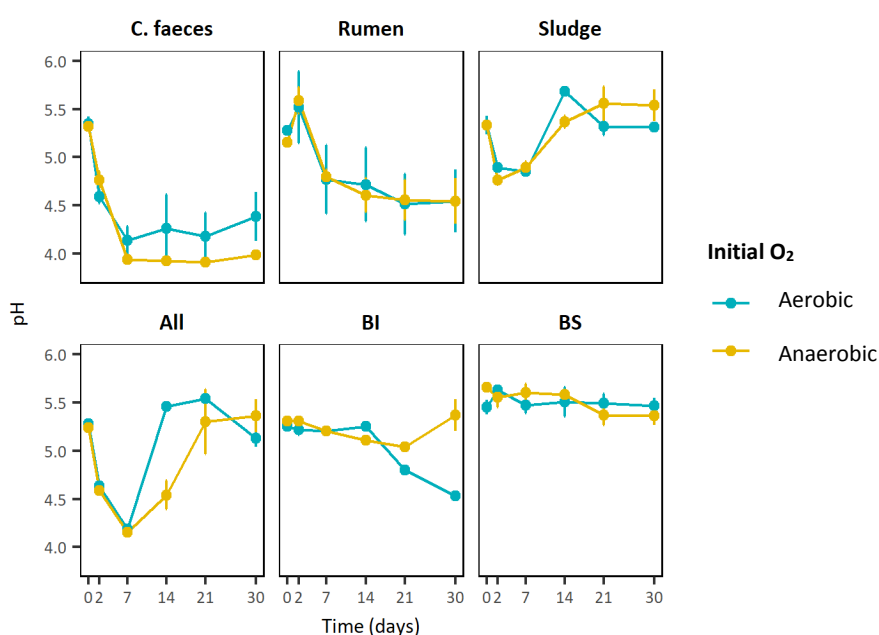


Figure 4.10 pH changes in each inocula configuration and the blanks during the incubation period under initial aerobic and anaerobic conditions.

pH decreased by ~ 1 pH unit between days 0 and 2 under both initial oxygen conditions in *c. faeces*, sludge and the combination of inocula microcosms, while the rumen microcosms experienced a slight rise of pH of about 0.4 pH units, to then follow a gradual decrease until the end of the experiment. In contrast, pH in the sludge inoculated microcosms rose from day 2 to a final a pH value close to the initial one. A similar trend was observed in microcosms containing all the inocula sources. It is important to mention that although a drop in the pH of the inocula blank was observed from day 14, none of the soluble fermentation products quantified in this experiment were detected in the blanks.

4.4.8 Overall comparison of fermentative activity

To broadly compare the maximal total soluble fermentative productivity in terms of carbon equivalents by each inocula, under both variables tested initial O₂ and initial pH, a 2-way ANOVA test was done. Although in average the total productivity of the systems incubated under initial neutral pH (183.67 ± 13.10 soluble carbon meq./L) seemed higher than that of the incubated under initial acidic pH (135.16 ± 23.09 soluble carbon meq./L), the 2-way ANOVA test indicated that the summative fermentative activity of these systems was not significantly different at a 95% confidence level (*p-value* 0.060). Thus, suggesting that the substrate was being degraded to about the same extent in all the microcosms although the product distribution was different.

4.4.9 Correlation analysis between pH and EtOH production.

Figure 4.11 integrates the previous results showing a clear separation between the initial pH of the neutral (pH~6.8) and acidic (pH~5.3) treatments, but a tendency towards pH~6 when the highest EtOH concentration was observed in both treatments.

The results from a 2-way ANOVA and Tukey HDS tests indicated that effectively, maximal EtOH concentrations under initial neutral or acidic conditions were significantly different (*p-value* 0.044). Nevertheless, the maximal EtOH production by rumen at neutral pH was not significantly different to that of sludge under acidic conditions (*p-value* 0.159). Moreover, as Fig. 4.11 suggests, the pH recorded on the day when those maximal EtOH concentrations were reached was not significantly different (*p-value* 0.722).

Thus, to determine whether the differences observed in the performance of the inocula tested in EXP1 and EXP2 were related to the pH of the medium, correlation analyses between maximal EtOH concentration, initial pH and pH at the time point where the maxima EtOH was registered, were computed using the aerobic and anaerobic data sets combined.

As explained in the methods section 4.3.4, the linear relationship of the continuous variables and normal distribution of the data sets were examined to assess if a correlation analysis would be valid. As the data of *c. faeces* didn't follow a linear relationship, no correlation analysis was done for this inocula.

The results of the correlation tests are summarised in Table 4.3. As most of the data sets didn't follow a normal distribution, the non-parametric Kendalls's rank correlation tau (τ) is reported, otherwise, Pearson's correlation coefficient is.

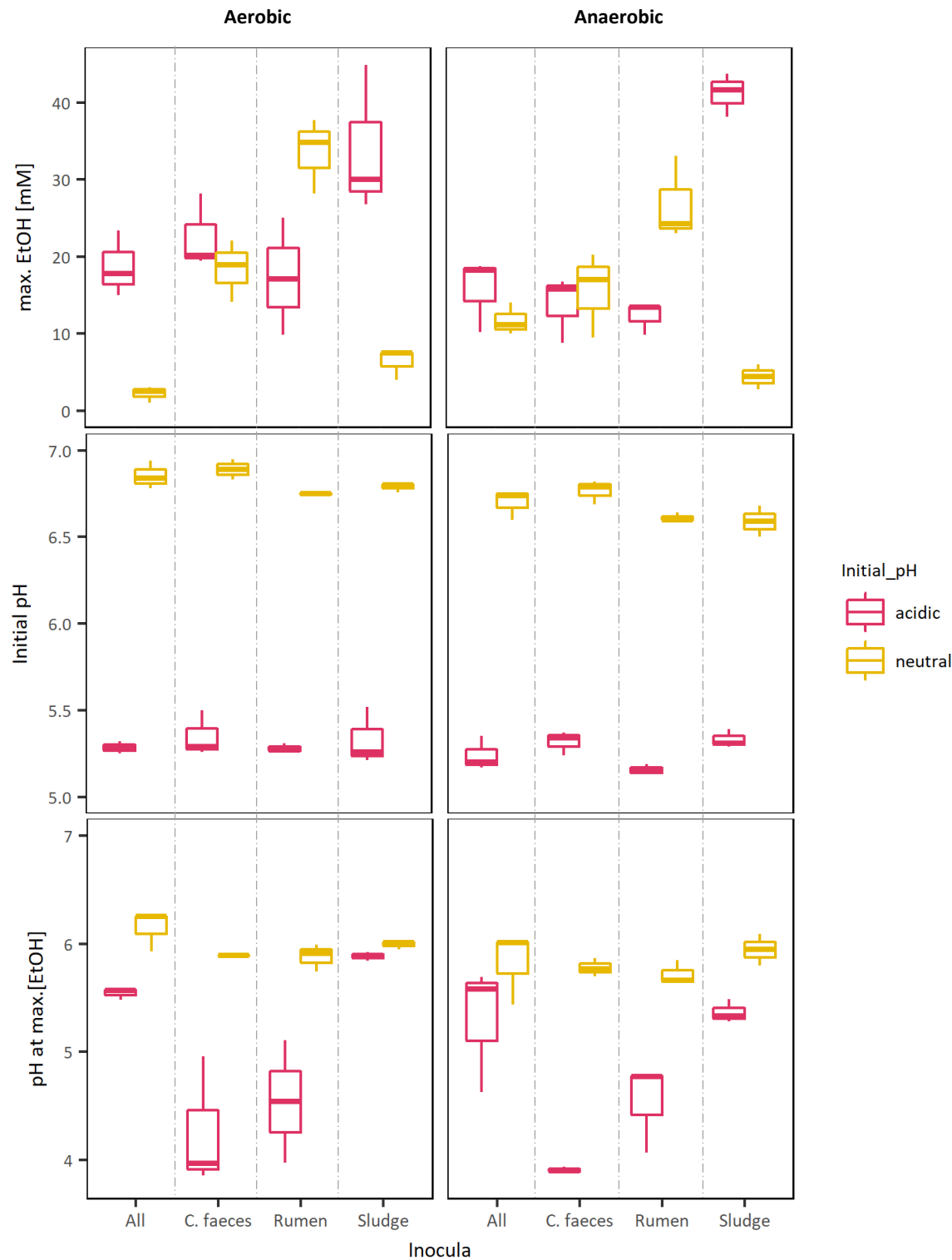


Figure 4.11 Maximal EtOH production by the different inocula and their initial and pH at max. concentration of EtOH in EXP 1 and EXP2.

Table 4.3 Correlation analyses results of maximal EtOH production vs initial pH and pH at maximal EtOH concentration.

Inocula	Initial pH – max [EtOH]		pH at max [EtOH] – max [EtOH]		Initial pH – pH at max[EtOH]	
	Cor. coef.	p-value	Cor. coef.	p-value	Cor. coef.	p-value
All	τ -0.455	0.045	-0.632	0.028	τ 0.565	0.011
Rumen	τ 0.708	0.002	0.807	0.002	τ 0.657	0.003
Sludge	τ -0.600	0.01	τ -0.564	0.017	τ 0.382	0.121*

Cor. coef = Correlation coefficients are either (τ) non-parametric Kendalls's rank correlation tau for data sets that did not follow a normal distribution or Pearson's correlation coefficient.

Colour code : Positive correlation  1  0  -1 Negative correlation.

*Not significant at 95% confidence level.

These results indicate significant correlations between maxima EtOH concentrations and initial pH, but also with the pH of the medium at the day of maxima EtOH production for all the inocula. In agreement with the experimental results, rumen has a positive correlation with both initial and pH at max [EtOH], whereas sludge has a negative correlation with initial pH and pH at max [EtOH]. This is, rumen EtOH production increases at higher pH while sludge does the opposite.

In all cases initial pH and the pH at max EtOH concentration are also correlated. However, although all the coefficients are different to zero and therefore indicative of correlation, the correlation value between these factors for the sludge inocula is low (0.382) and not significant at 95% confidence level. This can be attributed to the observed pH in the pH profiles at day 14 (Figs. 4.5 and 4.10), when the pH of the media was about 5.5 despite of the initial pH treatment, coinciding with the maximal EtOH concentrations produced by sludge.

4.4.10 Rumen and sludge enrichments electron balances

General comparisons of the maximal total productivity (summative soluble end-products) by rumen and sludge were done (2-way ANOVA, 95% confidence level). The total productivity of rumen at neutral pH (185.6 ± 38.9 soluble carbon meq./L, 976.2 ± 197.9 e-meq./L) and sludge at acidic pH (202.3 ± 6.8 soluble carbon meq./L, 711.2 ± 58.79 e-meq./L) in terms of carbon and electron equivalents (see Chapter 3, section 3.2.3) were not significantly different (*p-value* 0.060). However, the proportion of EtOH from these total maximal production values by rumen ($38.5 \pm 4.8\%$ solubleC meq./L, $43.2 \pm 5.0\%$ e-meq./L) were about 10% lower than those of sludge ($48.5 \pm 3.9\%$ solubleC, $58.7 \pm 3.4\%$ e-meq./L). The ratio between carbon and electrons varied slightly between the two different sets, but that might be due to the nature (degree of reduction) of the products generated in each system.

In average, about 10.4% or 20.8% of electrons estimated to be initially fed as OMSW (TCOD or BMP, respectively) were recovered in both systems (rumen and sludge). While 34.4% of electrons in the liquid fraction of the medium (COD) ended up as soluble fermentation products. From these estimates of recovered electrons, EtOH represented 36.9%, 43.3% and 42.7%, respectively (see Appendix C). These results might suggest that hydrolysis of the solid material could have been a bottle-neck of the process and future work should look at the biodegradable methane potential of the OMSW before and after pre-treatment.

4.5 Discussion

From the results presented, the following can be summarised:

- All the tested inocula were capable of ethanogenesis from OMSW, but their performances were different in response to the imposed experimental conditions, thus indicating that the products formed not only depended on the operational conditions, but also in the microbial community composition and dynamics of each system. This observation goes against a common statement in MCF experimental and modelling studies where the product spectrum in a MCF has been considered independent of the inoculum (Temudo et al. 2007; Rodríguez et al. 2006, 2008).

- Despite fermentation being an anaerobic process, no significant differences in EtOH production or the time taken to achieve maximal concentrations was observed when the process was initiated under aerobic conditions.
- EtOH was the main fermentation product of inocula incubated at initially acidic conditions, and at neutral pH for the rumen.

4.5.1 Initial oxygen condition and EtOH production

Research on cellulosic degradation by microbial communities enriched from natural or man-made environments such as soil, compost and manure (Okeke and Lu 2011; Lin et al. 2011; Haruta et al. 2002; Du et al. 2015) has focused on the cellulolytic activity and characterisation of such communities, mostly growing under anaerobic conditions, while few studies have tested enrichment at initial aerobic conditions and closely monitored EtOH production in addition to other fermentation products. Nevertheless, the results presented in this chapter agree with the general observations of the few reports where the cellulolytic (Wongwilaiwalin et al. 2010) or fermentative activity (Kato et al. 2004) of the communities under study was not significantly different to that of anaerobic cultures or showed an even better performance (Ronan et al. 2013). Although these previous studies were done under thermophilic conditions (from 50°C to 60°C), at initial alkaline pH (~8) and were conducted with crystalline cellulose as a carbon source in a yeast extract supplemented media (Wongwilaiwalin et al. 2010; Kato et al. 2004), some of their suggestions could help explain the observations made in this current project.

In summary, 4 possible mechanisms have been proposed in the literature to be linked to the beneficial effect of initial aerobic conditions in community fermentations of cellulolytic substrates:

1. Oxygen consumption by aerobic or facultative anaerobic microorganisms (most likely bacteria) while utilizing readily available substrates (Guo et al. 2010). In the OMSW medium used in this study, these could be mono and disaccharides, peptides and amino acids, thus supplying an anaerobic environment for the growth of the strict anaerobic cellulolytic and/or ethanologenic bacteria likely to be present in rumen and the anaerobic granular sludge. Also, by degrading the readily available compounds, the enrichment of microorganisms able to grow in more complex substrates, such as cellulosic materials could be promoted.

2. pH neutralisation. Kato *et al* (2004) studied the effect of compost derived aerobic isolates in the cellulose degradation by a cellulolytic *Clostridium* strain. During cellulose degradation by the *Clostridium* species pure culture under anaerobic conditions, the pH dropped from 7.5 to 6.0 with no further change, however, when cultivated at initial aerobic conditions together with the aerobic isolates, after experiencing the same pH drop to 6.0, pH then raised to about 7, in a remarkable similar trend to the pH profiles of rumen and sludge presented in this chapter, where pH went from ~7 to 5 and raised to 6 by the end of the experiment with rumen, while sludge inoculated microcosms experienced a drop from pH 5.5 to ~4.6 followed by a raise to pH 5.5 (Figs. 4.5 and 4.10, respectively). This pH recovery effect could be beneficial for mixed cultures as although low pH can trigger solventogenesis (Diender *et al.* 2015; Ganigué *et al.* 2016), pH below the growth pH range of certain community members poses a serious threat to the overall metabolic performance of the mixed culture by inhibiting the degradation activity of cellulolytic organisms (Guo *et al.* 2010).

3. The consumption of metabolites generated during lignocellulose degradation such as organic acids, cellobiose, and glucose by the non-cellulolytic aerobic/facultative anaerobic bacteria, as these could have an inhibitory effect on the cellulolytic activity of other community members (Guo *et al.* 2010). Although this might have occurred here, the quantification of substrate consumption was out of the scope of the present study, besides the culture media used contained diverse potential carbon sources and therefore a direct comparison cannot be made.

4. Aerobes and facultative anaerobes might also stimulate cellulose degradation by excreting low-molecular weight compounds (Guo *et al.* 2010), or even serving as substrate themselves, potentially leading to what has been called “priming-effect” in soil science, this is, the improved rates of mineralization of recalcitrant organic matter when amended with readily available organic matter (Kuzyakov *et al.* 2000). As for the previous argument, due to the complex culture media utilised along with the lack of fermentation activity in the substrate blanks (inocula with no carbon source), the influence of these mechanisms can only be speculated in the present study.

Although the benefits from initial aerobic conditions for cellulose degradation and potentially ethanol production have been described above, fermentation remains an anaerobic process. The fact that among the inocula tested, rumen and anaerobic granular sludge come from mostly anaerobic environments, might help explain the high EtOH

production performance by these inocula, since fermentation is one of their major natural metabolic functions.

4.5.2 EtOH as major fermentation product

In contrast to the EtOH being the main soluble end-product of some single species fermentative metabolism (e.g. *S. cerevisiae*; Madigan, 2015), the inocula tested in this study were expected to yield EtOH at lower concentrations because of their complexity. The likely reasons are twofold:

Energy production in the form of ATP is low in anaerobic fermentative metabolism (as opposed to respiration), and it is generally accepted that microbial populations goal is to grow (biomass production), therefore it can be assumed that under any given environmental condition, microbial metabolism will follow the most energy yielding pathways. As Table 4.4 shows, during substrate level phosphorylation (SLP), ethanol production does not contribute to direct ATP formation, while acetic and butyric acids do (Temudo et al. 2008; Rodríguez et al. 2006; White 2007).

Table 4.4 ATP formation in substrate level phosphorylation.

Product	Y	Y NADH	YATP
Acetate	2	+2	2
Butyrate	1	-2	1
EtOH	2	-2	0

Adapted from Temudo et al. (2007). Y= yield per molecule of glucose oxidised to two pyruvate molecules previously formed by glycolysis through the Embden-Meyerhof-Parnas pathway.

Besides, based on the anaerobic food chain (White 2007), EtOH is a reduced organic compound that once excreted could be further oxidised by some other inoculum member (i.e. acetogens), eventually leading to methane and carbon dioxide as final products (Bertsch et al. 2016). Circumstance that could help explain the observations presented in the metabolic profiles of inocula under initial aerobic/neutral conditions (Fig. 4.4.3) and particularly of sludge under acidic conditions (Figs. 4.4.7 and 4.4.8), where the ethanol peak concentration is followed by a constant decline.

Nonetheless, EtOH was the main soluble fermentation product in rumen inoculated microcosms at initial neutral pH, and in all the microcosms incubated under initial acidic pH and anaerobic conditions.

Other studies working with complex natural inocula degrading cellulose in batch systems, have reported EtOH (Lin et al. 2011) or the product pair EtOH/acetic acid (Ronan et al. 2013) as major fermentation products. However, these results were obtained at an initial pH range of 7-8, with a drop to pH 6 followed by a recovery to neutrality. These studies were done at temperature >50°C, reporting peak EtOH titers of 13.02mM and 12.0mM, respectively, in both cases lower to the ~30mM reported here.

Although it was not possible to find similar results from comparable studies to the presented here in the literature, diverse projects have examined the effect of pH on the MCF of glucose, with the work from Temudo *et al.* (2007) providing a detailed carbon balance analysis of the shifts in the generation of diverse gaseous and soluble fermentation products by a mixture of two sludge sources as inocula growing in a chemostat as a function of pH. However, the results from this study indicated pH higher to 6.5 would favour acetate/EtOH production.

Furthermore, based on the latter study, González-Cabaleiro *et al.* (2015) constructed a metabolic model which largely agreed with those experimental observations, apart from the discrepancy of whether propionate or formate accompany acetate production at high pH values in the switch from butyrate formation, this model predicted EtOH production to be favoured at high pH, particularly at the 8-8.5 pH range (See Fig. 4.12).

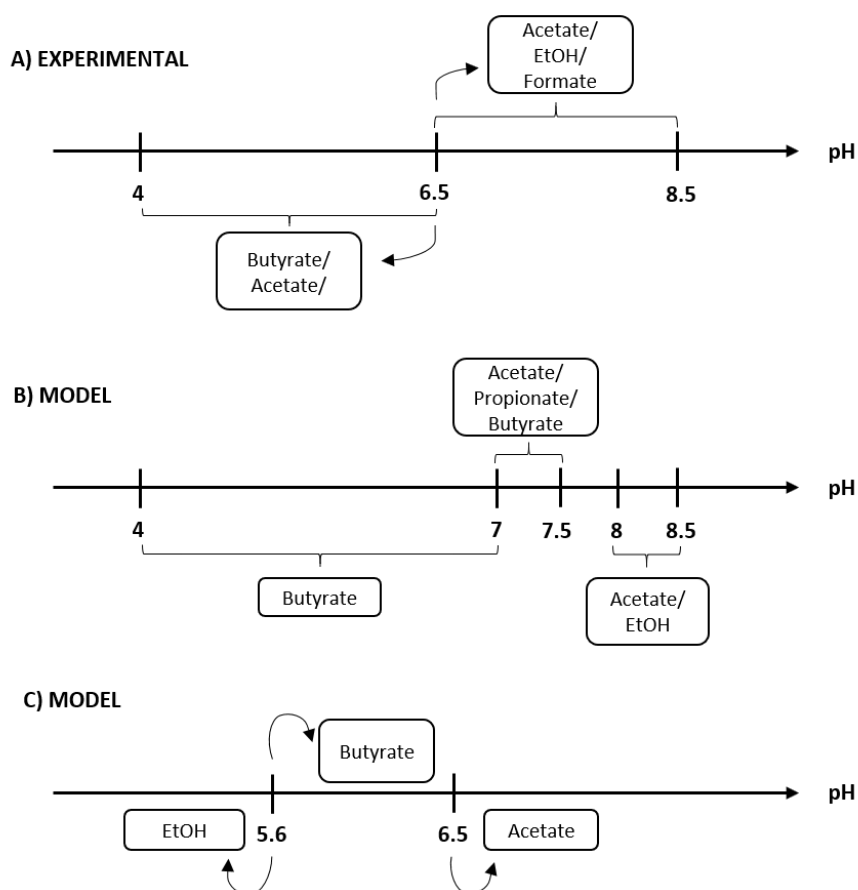


Figure 4.12 Soluble fermentation products as a function of pH in MCF according to the literature. A) Experimental work (Temudo et al. 2007). B) (González-Cabaleiro et al. 2015) and C) (Rodríguez et al. 2006) modelling approaches.

Contrarily, using the model of Rodríguez *et al.* (2006) as reference, EtOH production would be favoured at environmental pH below 5.6, as a low pH would make excretion of acids against the chemical gradient. Additionally, although the ionized form of these products could then be excreted, the negatively charged cell membrane, forces the movement of ionized molecules to be actively mediated (González-Cabaleiro et al. 2015), exceeding the energy benefits of acetic or butyric acid production.

Moreover, the bacterial production of EtOH typically involves the oxidation of 2 molecules of NADH, thus regenerating NAD⁺, a fundamental electron carrier for metabolic redox reactions, including ATP synthesis, ATP hydrolysis and ultimately biomass production.

In agreement with these predictions, almost all the microcosms incubated with initial acidic pH (~5.3) had EtOH as the major soluble end-product. The exception being rumen under initial aerobic conditions, which showed a high, but variable, butanol production.

Another experimental observation that can be linked to external pH driving fermentation products formation as predicted by Rodríguez *et al.* (2006), is the dominance of butyric

acid closely followed by acetic acid in microcosms incubated at initial neutral pH. As the pH of the media moved from ~7 to ~5.5, acetic acid decreased likely due to the active transport energy cost associated with the movement of its ionized form across the membrane, yet butyric acid production, although less efficient in ATP formation than acetic acid, mediates the synthesis of ATP and NAD⁺ regeneration (White 2007).

Interestingly, rumen was the exception in this case, producing EtOH as major fermentation product when starting at pH 6.9 and up to a minimum of pH 5.7, theoretically still favourable for butyrate formation (Rodríguez et al. 2006). Thus agreeing with the predictions of Temudo et al. (2007) and González-Cabaleiro et al. (2015) (see Fig. 4.12).

Although in conjunction, the three studies previously described can provide an overall explanation of what has been experimentally observed, it must be noted that they solely considered the fermentation of glucose as carbon source at 30°C under steady state conditions achieved by means of a chemostat type reactor operation or simulation. In addition, the metabolic models were constructed treating the microbial community as a single organism, neglecting phylogenetic diversity and assuming the environmental conditions direct product formation based on the thermodynamics of maximum energy yield. While the cause for the disagreement between these reports regarding pH and soluble fermentation products formation is not entirely clear, González-Cabaleiro et al. (2015) coupled FADH₂ to the reduction of acetaldehyde to ethanol, which in their words, was necessary to ensure the prediction of the observed experimentally by Temudo *et al.* (2007), but otherwise, a mechanism without foundation in the literature. On the other hand, Rodríguez et al. (2006) only accounted for NADH/NAD⁺ in their model, which could be an over simplification. Also, the works from Temudo *et al.* (2007) and González-Cabaleiro *et al.* (2015) operated under substrate limitation (4 g/L of glucose), whereas Rodríguez et al. (2006) utilised a higher concentration of glucose (10 g/L), and it has been observed that substrate concentration is another environmental factor affecting MCF product spectrum (Temudo et al. 2008; Rodríguez et al. 2008). In the present project, the concentration of OMSW was 50g/L, likely causing further deviation from the glucose-based studies.

The metabolic energetics-based models proved to be useful tools to explain the general patterns observed experimentally, however, one of the most important limitations of their predictions is the neglect of community composition, thus ignoring the potential existence of microbial interactions that would make possible otherwise

thermodynamically unfavourable reactions. Moreover, glucose was considered the only carbon source, which is a valid generalisation as the hydrolysis of cellulose, starch and other simpler carbohydrates would follow glucose metabolism, but under represents the complex composition of OMSW.

The disagreement of the predictions and the lack of further information in the literature regarding direct EtOH production by rumen as inoculum impose a limitation in the explanation of the results observed.

4.6 Conclusions

It was demonstrated that initial oxygen conditions do not play a significant role in EtOH production by the inocula tested, and in general, pH can be considered the driving environmental factor for EtOH production from OMSW in these experiments. However, the inocula source also influenced the formation of this soluble end-product, and their structure and diversity should not be neglected.

Anaerobic granular sludge produced the highest EtOH concentration under initial acidic pH, which would allow the direct fermentation of pre-treated OMSW without previous pH adjustment. While EtOH production by rumen was equally high at initial neutral pH. The EtOH peak production of both inocula (~30mM) was higher than the reported in the literature for similar studies.

It is therefore recommended further experimentation of EtOH production by anaerobic granular sludge and rumen, at initial aerobic conditions and optimisation towards initial acidic pH incubation of both inocula.

Chapter 5. Enrichment and characterisation of ethanogenic communities from different inocula sources degrading the organic fraction of municipal solid waste

5.1 Introduction

Preliminarily in Chapter 4, it was demonstrated that although initial pH can be considered a key environmental factor for ethanol (EtOH) production from the organic fraction of municipal solid waste (OMSW), the inocula source used also plays a significant role in the formation of this soluble end-product. Furthermore, the interaction of both physicochemical and biological factors was shown to drive in opposite directions the ethanogenic activity of rumen and sludge inocula, where maximal EtOH production was achieved at an initial neutral pH or at an initial acidic pH, respectively. It was therefore recognised that further experimentation of EtOH production by anaerobic granular sludge and rumen at initial aerobic conditions should include the study of their microbial community compositions to provide a more holistic understanding of these systems.

Several studies have used a number of sludge sources as inocula for mixed culture fermentation (MCF) (Fang et al. 2002; Wongwilaiwalin et al. 2010; Liang et al. 2014; Liu et al. 2016), while the utilisation of rumen in this type of systems has not been reported. Prior work using sludge, manure, compost and soil as inocula has demonstrated changes in microbial community composition in relation to pH (Temudo et al. 2008; Wu et al. 2017; Infantes et al. 2011; Kim et al. 2011), however the comparison of communities arising from different inocula sources has been sparingly explored (Jimenez et al. 2014; Peacock et al. 2013; Simmons et al. 2014). Even more, although some studies have mixed different inocula sources for the inoculation of MCF reactors (C. W. Lin et al. 2011; Temudo et al. 2008; Du et al. 2015), the determination of whether the enriched community and its function was derived from the combination of this sources has been neglected.

Broadly based on ecology theory (Begon et al. 2007; Fetzer et al. 2015), the combination of inocula with overall similar environmental functions as are rumen and granular anaerobic sludge (anaerobic transformation of organic matter) seems particularly attractive for MCF, as it could provide advantages to the fermentation process by

potentially increasing the richness of the community, and consequently the redundancy of fermentative microorganisms capable of EtOH production under different conditions, thus providing resilience to the system.

5.2 Hypothesis and objectives

The results from Chapter 4 revealed that similar ethanologenic activity could be achieved at initial acidic and neutral pH incubation values when using different inocula sources, namely rumen and sludge. This observation lead to the hypothesis that a novel community enriched by mixing the previous best performing inocula sources could benefit from specialised functional redundancy, allowing the mixed-source community to produce EtOH at a range of pHs.

Accordingly, to test the hypothesis as well as to verify the results from Chapter 4 of high ethanologenic activity of rumen at initial pH 7 and sludge at initial pH 5.5, the experiments presented in this chapter were conducted to:

- Evaluate if a mixed-source community would enhance EtOH production at a range of pH when compared against the ethanologenic activity of the original inocula sources.
- Determine if the enriched community from the combination of rumen and sludge was indeed integrated by retention of members from both original inocula sources.
- Connect the microbial community composition and possible functionality of the enriched communities to the observed ethanol producing activity.

5.3 Methods

5.3.1 Experimental design

To test the hypothesis and evaluate the repeatability of Chapter 4 results, the experimental design considered two factors: A) Inocula source and B) Initial pH. Factor A) had 4 levels, rumen, sludge and the mixture of both (R+S), plus inocula blanks (IB, microcosms with media and OMSW analogue, but without inocula added). Factor B) had 3 levels, initial pH 4.5, 5.5 and 7.0. The inocula blanks (IB) were only done for pH 4.5 and 7, giving $A*B = 11$ possible combinations, each of which were tested in triplicate.

Initial pH	Rumen	Sludge	R+S	IB
~7.0	3	3	3	3
~5.5	3	3	3	
~4.5	3	3	3	3

Figure 5.1 Experimental design to test the effects of inocula source and initial pH in EtOH production.

5.3.2 Microcosms set-up

The methods described in Chapter 3 section 3.3 were followed to conduct the microcosms set-up. In this case, only non-reduced medium was used for incubation under initial aerobic conditions. Sets of microcosms were inoculated individually with 2.5g of rumen, sludge and the combination of these, this is ~1.25g of each individual inocula to add up to 2.5g.

5.3.3 pH adjustment

As previously reported in the Chapter 4 of this thesis, sludge and rumen inocula display opposite ethanologenic activity in response to initial incubation pH values. This is, at low pH (~5.5) sludge produced higher EtOH titers, while rumen did the same at initial pH closer to neutrality. Following the procedure described in section 3.3.2 of Chapter 3, the different initial pH values of the microcosms in this experimental set-up were carefully adjusted after autoclaving and if necessary, slightly after inoculation according to the experimental design, to assure initial comparable conditions for the three inocula tested.

Figure 5.2 shows the distribution of the measured pH values against the targeted value, resulting in 12 microcosms incubated at initial pH 4.49 ± 0.04 , other 9 microcosms at pH

5.47 ± 0.03 and finally, 12 microcosms incubated at initial pH 6.91 ± 0.02 . pH was not adjusted again during the incubation period.

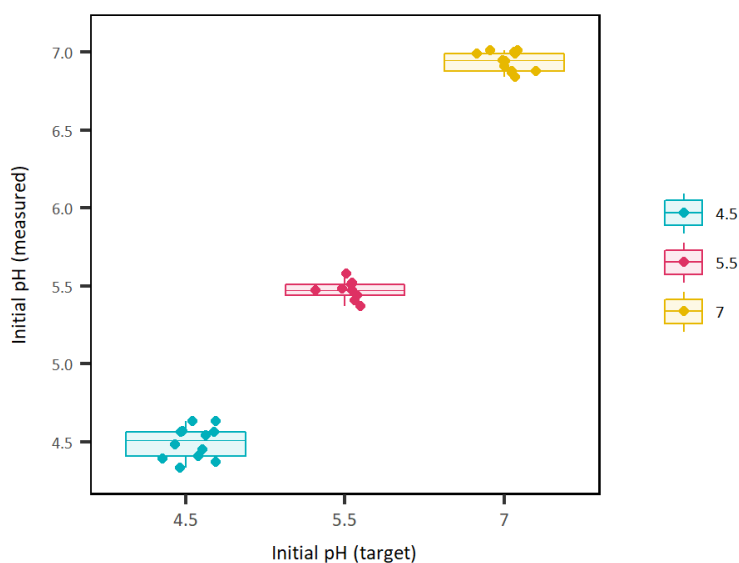


Figure 5.2 Boxplot of the initial pH value groups.

5.3.4 Microcosms incubation and sampling plan

Microcosms were incubated in the dark, at room temperature (approximately 20°C) under static conditions for 25 days. Liquid samples were taken on day 0, 3, 7, 11, 18, 25 for pH measurement and GC-FID EtOH quantification according to section 3.3.3 of Chapter 3. Besides, samples were taken for molecular biology analysis as described in Chapter 3, section 3.6.

5.3.5 GC-FID quantification of soluble ethanol

As mentioned in section 3.4.2 of Chapter 3, although the suitability of highly similar methods for the quantification of alcohols and volatile fatty acids (VFAs) has been reported (X. Lin et al. 2014; Pontes et al. 2009), the detection and repeatability of the GC-FID VFAs quantification became an issue at this stage of this project, despite of the reliable behaviour during the previous tests.

Specifically, during this experimental set-up no VFAs peaks could be detected either on the chromatograms of numerous VFAs standards freshly manually prepared by me or the Geosciences technical staff, as well as on VFAs standards provided by the technical staff of the Environmental Engineering Laboratory of Newcastle University, despite multiple

modifications to the GC programme. However, the quantification of ethanol (EtOH), acetone, and butanol (BuOH) was repeatable and linear. Therefore, due to financial constraints and to avoid further time delays, it was decided to use just GC-FID to quantify alcohols on the samples during this experimental phase.

Based on the soluble fermentation products detected in the previous tests (Chapter4), solutions of ASC reagent grade EtOH, MeOH and BuOH were prepared in distilled water at concentrations of 0, 2, 4, 8, 16, 30 and 60mM. These solutions were then analysed in triplicate for the construction of calibration curves. The following linear equations were obtained from the GC-FID standard curves:

$$\text{EtOH[mM]} = (\text{Area(mVs)} + 2.498 \pm 6.499 \text{ mVs}) / 2.8481 \pm 0.221 \text{ mVs.mM}^{-1} \quad R^2 0.978$$

$$\text{BuOH[mM]} = (\text{Area(mVs)} - 3.524 \pm 1.875 \text{ mVs}) / 2.970 \pm 0.057 \text{ mVs.mM}^{-1} \quad R^2 0.998$$

Where: \pm confidence interval at level 95% (lower 2.5%, upper 97.5%).

For quality control, freshly prepared standard solutions of EtOH were prepared and quantified at the start and end of each GC-FID analysis run.

Samples were processed as described in Chapter 3 section 3.3.3, each of these was analysed 3 times. The calculation for the concentration of ethanol from the linear regression equation obtained is illustrated in section 4.3.3 of Chapter 4.

5.3.6 Statistical analysis of physicochemical data

The method described in Appendix A was followed to conduct the statistical comparison of the EtOH concentrations produced by each inocula under the three different initial pH values.

5.3.7 DNA extraction and purification

The method described in Chapter 3, section 3.6.1 was followed using the PowerSoil® DNA Isolation Kit (MoBio Laboratories, UK) for DNA extraction and purification according to the manufacturer's protocol.

5.3.8 Denaturing Gradient Gel Electrophoresis (DGGE)

DGGE was utilised to visually assess changes in the communities' richness and structure between the different treatments and to determine if a fungal population was present in any of the communities. This method uses a denaturing gradient polyacrylamide gel incubated at high temperatures to separate DNA amplicons based on their nitrogenous bases content, which determines their mobility through the gel. The resulting band pattern provides a qualitative overview of the microbial community composition that can be further analysed in a semiquantitative manner (Muyzer et al. 1993).

PCR was conducted targeting the V3 region of the 16S rRNA gene. Primer 2 (reverse, 5'-ATT ACC GCG GCT GCT GG-3') and Primer 3 (forward, with a GC clamp on the 5'end, 5'-CGC CCG CCG CGC GCG GCG GGC GGG GCG GGG GCA CGG GGG GCC TAC GGG AGG CAG CAG-3') were used as explained in the pioneering work of Muyzer *et al.* (1993). Based on *E. coli* 16S ribosomal RNA gene numbering, the annealing positions of these primers are 518-534 and 341 -357 (Brosius et al. 1978).

The 50 µL PCR master mix preparation of samples and procedural blanks along with the amplification programme were done as described in section 3.6.2 of Chapter 3.

Fungal DDGE analysis was done using the primer pair ITS3 (forward, 5'- GCA TCG ATG AAG AAC GCA GC-3') and ITS4 (reverse with a GC clamp on the 5'end, 5'- CGC CCG CCG CGC CCC GCG CCC GGC CCG CCG CCC CCG CCC CTC CTC CGC TTA TTG ATA TGC), targeting the internal transcribed spacer region (ITS) in the fungal ribosomal RNA (rRNA) operon (White et al. 1990; Op De Beeck et al. 2014).

For the fungal analysis, the 50 µL PCR master mix preparation of samples and procedural blanks was done as described on section 3.6.2 of Chapter 3. however, the amplification programme consisted of 5 min of initial denaturation at 94°C followed by 25 cycles of 30s denaturation at 94°C, 30 s for annealing at 55°C and 30s of extension at 72°C. The final extension was done for 5 min at 72°C.

To conduct bacterial and fungal DGGE, a BioRad DCode™ system integrated by a buffer tank, a gradient maker and an electrophoresis cassette, was employed. 10% polyacrylamide gradient gels were prepared with a mixture of 30% and 60% denaturing solutions (see Table 5.1). The denaturing solutions were filtered using a 0.45µm hydrophilic Millipore filter (Fisher Scientific, UK) before pouring into the gradient maker-peristaltic pump system container, where the solidifying agents APS (160µl of 0.1g

APS/mL distilled water) and TEMED (16 μ L) were added just before dispensing the mixture into the electrophoresis cassette (capacity for 2 gels) by running the Watson and Marlow 520U peristaltic pump (Watson and Marlow, UK) at 4 rpm. A 20 well comb was inserted at the top of the gel which was then allowed to set for 2h.

Table 5.1 Reagents for the preparation of DGGE denaturing solutions.

Reagent	30% denaturing soln.	60% denaturing soln.
Acrylamide	10 mL	10 mL
TAE 50x	0.8 mL	0.8 mL
Deionised formamide	4.8 mL	9.6 mL
Urea	5.04 g	10.08 g
Distilled water	24.4 mL	19.6 mL

Total volume of 40mL for the simultaneous preparation of 2 gels (20 mL each).

27 μ L aliquotes consisting of 20 μ L of PCR product previously mixed with 7 μ L of DNA loading buffer (Bioline GmbH, UK) were loaded into individual wells of the cast gel, except for the first and last wells which were loaded with 10 μ L of the reference DNA size marker, Hyperladder II DNA Marker (Bioline, GmbH, UK). The gel was then placed in the preheated BioRad DCode™ buffer tank (60°C) containing 1X TAE. Electrophoresis was run at 50V for 17 hours.

A solution of 0.02% v/v SyBr gold (Invitrogen Life Science Technologies, UK) was used to stain the gels for 30 minutes, after which a MultiDoc-It™ Imaging System (UVP LLC, UK) was used to carry out visualisation.

5.3.9 DGGE gels statistical analysis

The BioNumerics software (Applied Math, Belgium) was used to analyse the band patterns obtained from the DGGE gels images. The banding patterns in all gels were normalised using the DNA size marker profile and the bands belonging to each sample were automatically detected. After which manual verification and if necessary, correction was done. Quantification of band patterns were computed to generate comparisons within and between gels through the presence/absence Jaccard similarity coefficient. The

output from BioNumerics was then exported for further analyses in the PRIMER 7 software (Primer-E Ltd., Plymouth, UK).

Similarly to the approach described in section 3.7 of Chapter 3, the graphical representation of the relative similarities between sample patterns was done through non-parametric multidimensional scaling analysis (nMDS), using a Bray-Curtis similarity matrix (Clarke and Warwick, 2001).

The samples were also clustered in groups of similarity using the software's cluster analysis, which is displayed on plots as contour overlays.

Finally, the non-parametric analysis of similarities (ANOSIM) was computed using the Bray-Curtis similarity matrix (after 999 permutations of the data) to statistically evaluate (0.1% significance level) the dissimilarity between the communities from each initial pH treatment for the individual inocula used (Ramette 2007). The global R-value ranges from 0 to 1 indicate similarity or dissimilarity, where values closer to 1 are more dissimilar.

5.3.10 Ion Torrent PGM sequencing pooled library preparation

As described in Section 3.6.4 of Chapter 3, for bacterial community analyses DNA extracts from each of the samples under analysis were subjected to PCR amplification of the V4-V5 region of the 16SrRNA gene using individual Golay barcodes attached to the F515 forward primer. Ion Torrent technology was then used to sequence the replicates of rumen, sludge, R+S and inocula blanks. As the chip for sequencing was shared with other projects, only samples taken straight after inoculation (t0) and after 11 days from enrichments in the initial pH incubation at which each inocula produced the highest amount of EtOH were sequenced. This was done to gain a deeper understanding of the change in community composition and the microorganisms responsible for EtOH fermentation under these conditions. Table C1 in Appendix C lists the samples sent for amplification and the corresponding sequence of barcodes used. Apart from the samples on Table C1, a procedural blank was included for sequencing.

5.3.11 16S rRNA sequencing processing and community composition analyses

The Mothur v.1.39.5 software (Schloss et al. 2009) was used to quality filter, remove potential chimeras and non-bacterial or archaeal sequences, and cluster into OTUs

sequences with a minimum length of 275nt (from 696397 high quality reads) through a distance matrix where any pairwise distance larger than 0.15 was eliminated, after which the rarefaction of all the libraries to the smallest library count (8987 reads) was then performed following the 454 standard operational procedure (SOP) of the software creators (Schloss et al. 2011). The OTUs (selected at 97% similarity) and associated files generated were then used to conduct ecological and ordination analyses following the workflow described in section 3.7 in Chapter 3.

The OTUs/abundance rarefied data was imported into PRIMER 7 software (Primer-E Ltd., Plymouth, UK) to compute the Bray Curtis similarity matrix between each rarefied sample. The Bray-Curtis similarities were then used within PRIMER 7 to produce an nMDS ordination plot and sample cluster tree graph integrated into a shade plot. A non-parametric ANOSIM test was used to evaluate the statistical significance (0.1% significance level of sample statistic) of community composition differences between groups of samples. For groups that were found to be significantly different, SIMPER analysis was conducted to identify both, the most abundant OTUs integrating each sample, as well as the discriminatory OTUs between the sample groups, accumulative contributing to 70% of the total similarity or dissimilarity between groups, respectively

Additional to the taxonomy assignments (up to genus level) for the OTUs made by Mothur (using Silva database release 128), the most abundant representative sequence within each OTU was aligned against the 16S rRNA sequences (Bacteria and Archaea) GenBank database using the megablast algorithm (Boratyn et al. 2012).

5.4 Results

5.4.1 Ethanologenic activity of the different inocula tested at an initial pH range

After 2 days of incubation, EtOH production was observed in all microcosms inoculated with sludge and the mix of rumen and sludge (R+S). However, the microcosms inoculated with rumen only showed ethanologenic activity when incubated under initial pH 5.5 and 7, displaying a complete lack of activity at initial pH 4.5 (Fig. 5.3). In general, the concentration of EtOH produced was variable as a function of inocula source and initial pH.

In agreement with the results discussed in Chapter 4, rumen inoculated microcosms showed the highest EtOH production ($17.39\text{mM} \pm 1.18\text{mM}$) after 25 days of incubation at initial pH 7. Sludge inoculated microcosms displayed the lowest maximal EtOH concentration ($6.51\text{mM} \pm 2.31\text{mM}$) after 3 days of incubation at this initial pH. Meanwhile, R+S maximal EtOH concentration ($13.81\text{mM} \pm 1.33\text{mM}$) under initial neutral conditions was reached at 11 days of incubation. It must be noted that EtOH production was observed in the inocula blanks incubated under these conditions, reaching a peak concentration ($2.36\text{mM} \pm 0.5\text{mM}$) at the end of the experiment.

Also similar to Chapter's 4 results, after 7 days of incubation under initial pH 5.5, sludge inoculated microcosms showed the highest EtOH production ($18.10\text{mM} \pm 1.40\text{mM}$), and rumen inoculated microcosms displayed the lowest maximal EtOH concentration ($4.40\text{mM} \pm 1.90\text{mM}$) at the end of the incubation period. Under this initial pH, R+S reached a maximal EtOH concentration of $17.19\text{mM} \pm 1.82\text{mM}$ at 11 days of incubation.

At pH 4.5, the lowest initial pH tested, all treatments showed their lowest maximal EtOH production. Sludge inoculated microcosms reached an average peak concentration of $12.32\text{mM} \pm 0.96\text{mM}$ after 18 days of incubation, while R+S maximal EtOH production ($8.99\text{mM} \pm 2.14\text{mM}$) was achieved after 7 days of incubation. Inocula blanks and rumen inoculated microcosms did not show EtOH generation.

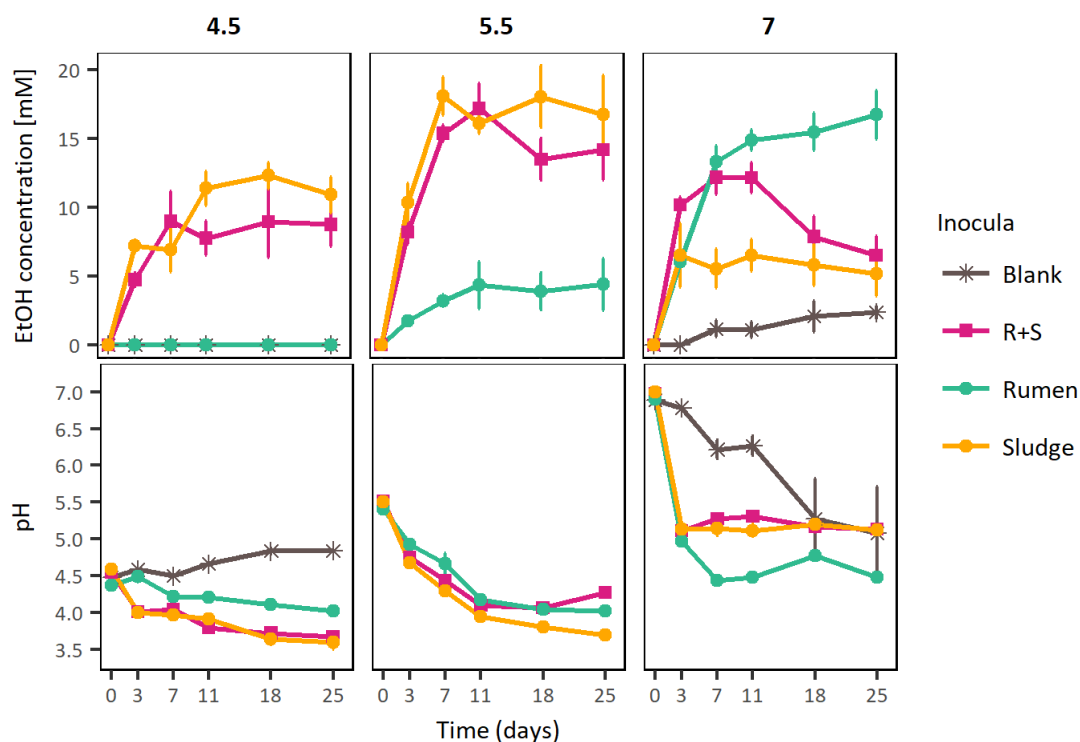


Figure 5.3 EtOH production profiles and pH curves of the different inocula incubated at a range of initial pH. The error bars represent the standard error of the mean (SE).

Figure 5.3 also shows the pH changes in the different microcosm set-ups during the 25 days of incubation. Under initial pH 5.5 all microcosmos displayed a uniform decreasing tendency, reaching minimal values between 4.5 (R+S) to 3.6 (sludge) by the end of the experiment. Contrarily, in microcosms incubated at initial pH values 4.5 and 7, pH behaviour was variable across inocula. Nevertheless, at the lowest and highest initial pH values tested, sludge and R+S pH profiles followed a similar drop from 4.5 to 3.5, and from 7 to 5, respectively. Meanwhile, rumen inoculated microcosms showed a small reduction of pH when inoculated at initial pH 4.5 (~0.5 pH units), and the largest drop observed in the experiment when inoculated at initial neutral conditions (~2.5 pH units). The inocula blanks incubated at initial acidic pH remained stable, while a distinctive drop (~1.5 pH units) was observed in blanks incubated at initial neutral conditions from day 7 until the end of the experiment.

Although these results generally confirmed the observations from the previous chapter by showing how initial pH seems to play a major role in EtOH production by the two original inocula sources in an opposite direction, it must be noted that apart from the ethanologenic activity at pH 7, the EtOH production and pH profiles of sludge and R+S were highly similar, inducing to question whether R+S was enriched from both original inocula sources, or dominated by the sludge microbiota.

5.4.2 Statistical comparison of maximal EtOH production by the different inocula at an initial pH range

The maximal values of EtOH production by the various inocula under initial aerobic and anaerobic conditions (Fig. 5.4) were statistically compared to assess whether the differences observed were significant, and if so, which variable was responsible for the variations: inocula sources and/or initial pH, and most importantly, whether the interaction of both factors significantly influenced EtOH production.

As the data met the homogeneity of variances (Levene's test p -value $0.9300 > 0.05$) and the assumption of a normal distribution (p -value = $0.1807 > 0.05$), a 2-way ANOVA analysis was conducted to quantitatively assess these observations.

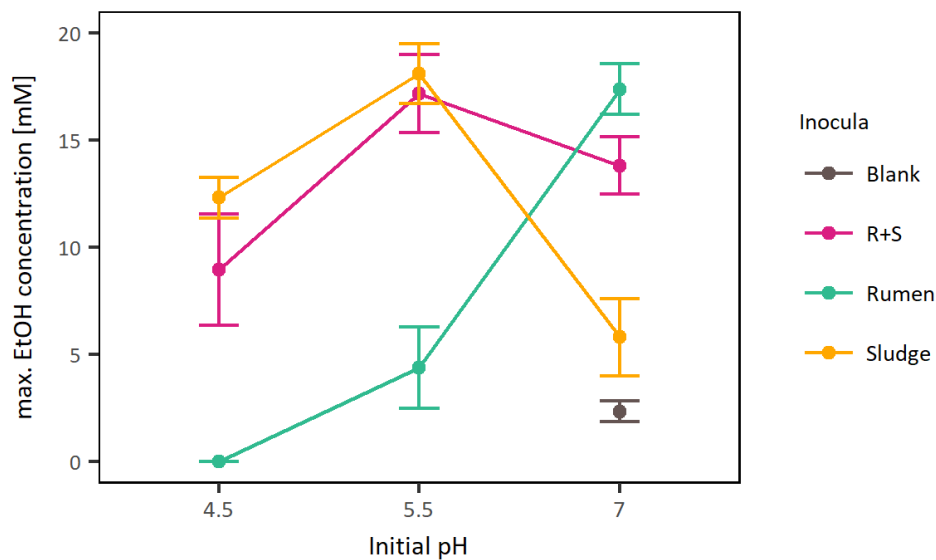


Figure 5.4. Two-way interaction plot of the means of the maxima EtOH concentrations as a response to the combination of the two factors tested: inocula and initial pH conditions. Rumen EtOH maximal production increases with initial pH, while sludge and R+S ethanologenic activity increase between 4.5 and 5.5, to drop between 5.5 and 7 initial pH.

Based on the p -values and a significance level (signif. codes: 0 '***' 0.001 '**' 0.01 '*' 0.05) from the 2-way-ANOVA results, it was concluded that both factors, inocula (p -value $3.65e-09$ ***) and initial pH (p -value 0.000339 ***) as well as their interaction (p -value $3.86e-07$ ***) had an statistically significant effect on EtOH production, with the interaction potentially being the most significant factor.

A Tukey HDS test was then computed to determine pairwise differences between each of the levels of the two variables as well as their interaction. See Table 5.2 for details on the relevant results of the Tukey HDS test.

As suggested by the EtOH production profiles and pH curves (Fig. 5.4), the ethanologenic activity of sludge and R+S was not significantly different when incubated under initial pH values 4.5 and 5.5. However, they were significantly different at initial pH 7, where notably, R+S EtOH production was not significantly different to that of rumen, while sludge inoculated microcosms EtOH productivity was similar to that of the inocula blanks (Table 5.2).

Table 5.2. Results of the multiple pairwise-comparison (Tukey HDS test) of the interaction effect of inocula source and initial pH conditions on EtOH production.

Treatment	diff	lwr	Upr	<i>p</i> .adj
Initial pH 4.5				
Sludge - Rumen	12.317	4.399	20.236	0.001
Rumen - R+S	-8.953	-16.872	-1.035	0.018
Sludge - R+S	3.364	-4.555	11.282	0.904*
Initial pH 5.5				
Sludge - Rumen	13.705	5.787	21.624	0.000
Rumen - R+S	-12.795	-20.713	-4.876	0.000
Sludge - R+S	0.910	-7.008	8.829	1.000*
Initial pH 7				
Sludge - Rumen	-11.564	-19.482	-3.645	0.001
Rumen - R+S	3.575	-4.344	11.493	0.866*
Sludge - R+S	-7.989	-15.908	-0.071	0.047
Rumen-Blank	15.026	7.108	22.945	0.000
Sludge - Blank	3.462	-4.456	11.381	0.887*
R+S - Blank	11.452	3.533	19.370	0.002
Initial pH at maximal [EtOH]				
5.5:Sludge - 7:Rumen	0.712	-7.206	8.631	1.000*
7:Rumen - 5.5:R+S	0.198	-7.721	8.116	1.000*
Initial pH at maximal [EtOH] vs Initial pH minimal [EtOH]: same inocula				
7:Rumen - 4.5:Rumen	17.388	9.469	25.306	0.000
5.5:Sludge - 7:Sludge	-12.276	-20.195	-4.358	0.001
5.5:R+S - 4.5:R+S	8.236	0.318	16.155	0.037

Where diff= difference between means of [EtOH] between two groups, lwr, upr= the lower and upper values for 95% confidence intervals and *p* adj= *p*-value after adjustment for the multiple comparisons. [EtOH] = EtOH concentration. *Not significantly different.

Remarkably, there was no significant difference in the maximal EtOH production between any of the inocula, this is, rumen ethanogenic activity at pH 7 was not significantly different to that of sludge or R+S at pH 5.5. Additionally, EtOH production by R+S under initial pH 5.5 and 7 was also not significantly different (*p* adj = 0.902)

Although the mixed-source (R+S) inoculated microcosms showed a behaviour similar to the sludge inoculated ones when incubated under an initial acidic pH, the ethanogenic activity of R+S was also similar to that of rumen at neutral pH, supporting the hypothesis that a combination of rumen and sludge microbial communities could lead to a robust

community able to produce EtOH at a range of pH values. Therefore, to further understand and support these observations, a series of molecular biology analyses were performed and are presented down below.

5.4.3 DGGE fungal and bacterial analysis

Although DGGE is limited in the resolution and information it can provide at a molecular biology level, in the context of this experiment, DGGE gels helped to readily determine bacterial composition variation between replicates, and whether the enriched communities after 11 days of incubation under the initial pH at which their maximal EtOH production was observed were different to those at the beginning of the experiment. Additionally, DGGE was also used to indicate significant variation between treatments, thus informing the selection of samples for next generation sequencing analysis.

Furthermore, as the literature review (Chapter 3) revealed, most of the microbial communities enriched in mixed culture fermentation (MCF) studies were bacterial, nevertheless, it was considered sensible to inspect, through DGGE, if the communities enriched in this study had a rich fungal community, since diverse yeasts are well known ethanologenic organisms (Morales et al. 2014; Mohd Azhar et al. 2017).

In this regard, a few pale bands can be observed in the fungal DGGE fingerprint (Fig. 5.5) of the replicates of most inocula at time 0, while an intense band appeared in two of the rumen replicates. One of the sludge replicates also showed a highly intense band. Apart from a couple of pale bands, R+S did not seem to have an appreciable fungal community. It must be noted that despite of the presence of these intense bands, EtOH production in the different replicates of rumen and sludge did not vary notably ($\pm 1.18\text{mM}$ and $\pm 1.40\text{mM}$, respectively).

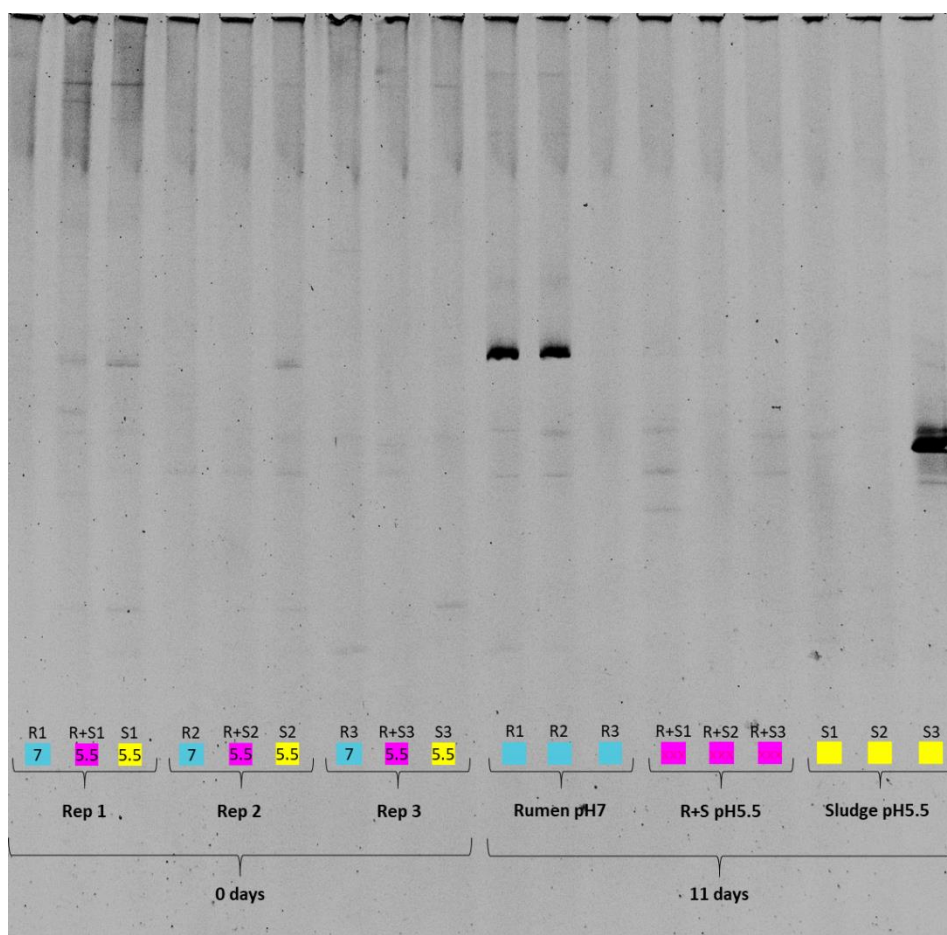


Figure 5.5. DGGE fingerprints of fungal ITS region in the rRNA gene fragments amplified from the different inocula under study at the initial pH where their maximal EtOH production was achieved. Blue markers indicate rumen replicates, pink markers indicate R+S replicates and yellow markers indicate sludge replicates.

These results are in agreement to the descriptions provided at the beginning of Chapter 4 (section 4.1), where rumen and anaerobic granular sludge microbial environments were found to be dominated by prokaryotes. Based on this results, it was decided to focus on the analysis of the bacterial composition of these communities henceforth.

On this subject, the individual DGGE bacterial fingerprints of the diverse treatments under study showed a rich bacterial composition (see Fig. 5.6). Overall, highly similar band patterns are observed at time 0 (first 9 lanes) on the fingerprints of A) rumen, B) sludge and C) R+S, followed by a clear change after 11 days of incubation, where the banding pattern of the replicates at initial pH 4.5 within each of these treatments are clearly variable across all fingerprints, as opposed to the pattern observed for replicates within each treatment at pH 5.5 and pH 7, where they appear to be highly similar.

Additionally, a clear reduction in the number of bands from t0 to 11 days of incubation for all fingerprints suggest a reduction in their richness, while the appearance (i.e. rumen)

and switch (i.e. sludge) of highly intense bands indicates a change on the most abundant community members. Nevertheless, numerous bands repeat between initial pH 5.5 and 7 within each treatment, with only a few bands being exclusive or particularly intense in the three replicates of the maximal EtOH production initial pH for each inocula (marked in green Fig. 5.6), bringing into question if only few community members were directly involved in EtOH production of OMSW in these systems.

16S rRNA amplicons extracted directly from rumen and sludge (by triplicate) were also inspected through DGGE (Fig. 5.6 D) as an overview of these source communities. A rich bacterial composition is observed in both cases, with numerous faint bands spanning through the gel gradient, particularly in the case of rumen, suggesting an even community. Next to the original inocula, the banding patterns of the inocula blanks are displayed. While not evident bands could be observed at time 0 at any of the initial pH incubations, two of the blank replicates incubated under initial neutral pH displayed clear varying banding patterns after 11 days, with two of those bands repeating in these replicates (Fig. 5.6, D), repeated bands marked in green). Notably, this agrees with the EtOH concentration quantification results for the inocula blanks after 11 days of incubation, where EtOH production was only detected on these two replicates (1.25mM and 2.05mM, respectively).

nMDS plots of the DGGE fingerprints of the treatments where the different inocula showed maximal EtOH production (see Fig. 5.7) were conducted using the Bionumerics and Primer 7 software, as explained in section 5.3.7 of this chapter. It is important to notice that in all the nMDS plots, the samples at time 0 clustered together, whereas after 11 days, each set of replicates for initial pH 5.5 and 7 moved similarly, creating distinctive groups that share 60% similarity (based on Bray-Curtis similarity matrix). The behaviour of the replicates of initial pH 4.5 varied greatly across all inocula, with the replicates of R+S shown to be completely independent from each other.

To assess if the clusters in the nMDS plots, were based significantly on initial pH treatment, ANOSIM tests were conducted, confirming the observation that each initial pH generated significantly different banding patterns, and thus likely enriched different bacterial communities. Each nMDS plot displays a box in the lower left corner with the R values derived from their individual ANOSIM tests.

Additionally, an nMDS plot was made to compare the banding patterns of the three inocula at 11 days of incubation under the different initial pH tested accompanied with an

ANOSIM calculation (Figure 5.7, D). Importantly, the different inocula formed significantly different distinctive clusters.

These results reinforced the observations made on section 5.4.2, where the statistical analyses results showed that the R+S inocula could behave as sludge or rumen, depending on the initial pH, by suggesting that the community enriched from R+S might indeed have a different bacterial composition to that of the original inocula (Fig. 5.7 -D). Thus, DGGE fingerprints reinforced the decision to conduct NGS analysis to investigate the different bacterial communities in more detail.

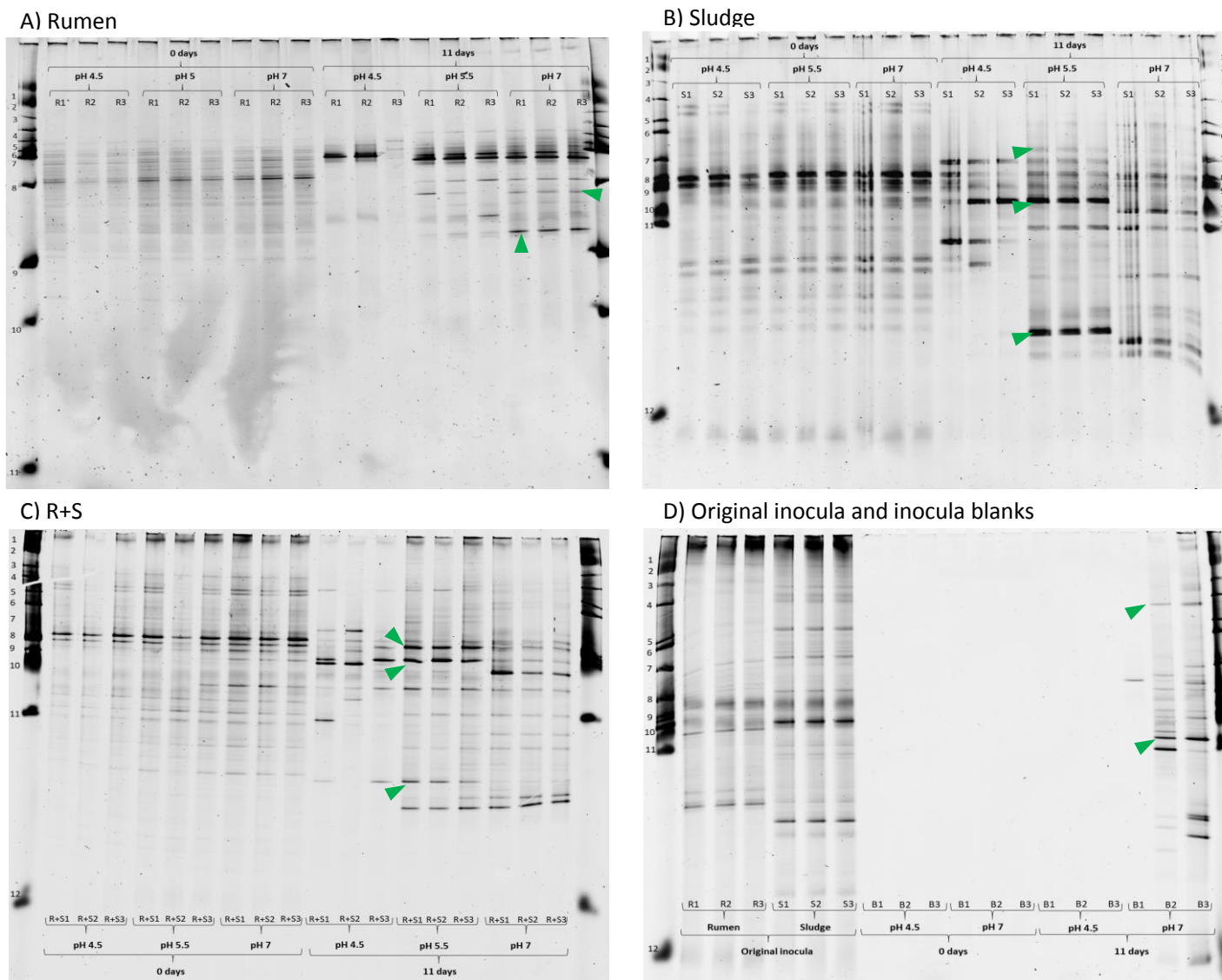


Figure 5.6. DGGE fingerprints of the different inocula under study. In gels A), B) and C) the first 9 lanes of each gel represent time 0 of the replicates growing at pH 4.5, pH 5.5 and pH 7 respectively, whereas the following 9 lanes were loaded with samples of those same replicates after 11 days of incubation. D) Original rumen and sludge replicates followed by t0 samples from the inocula blanks and their respective samples after 11 days of incubation. Notably, B2 and B3 replicates produced EtOH, but B1 did not. The green markers point at bands that are uniquely found or particularly intense in the three replicates of the maximal EtOH production initial pH for each inocula.

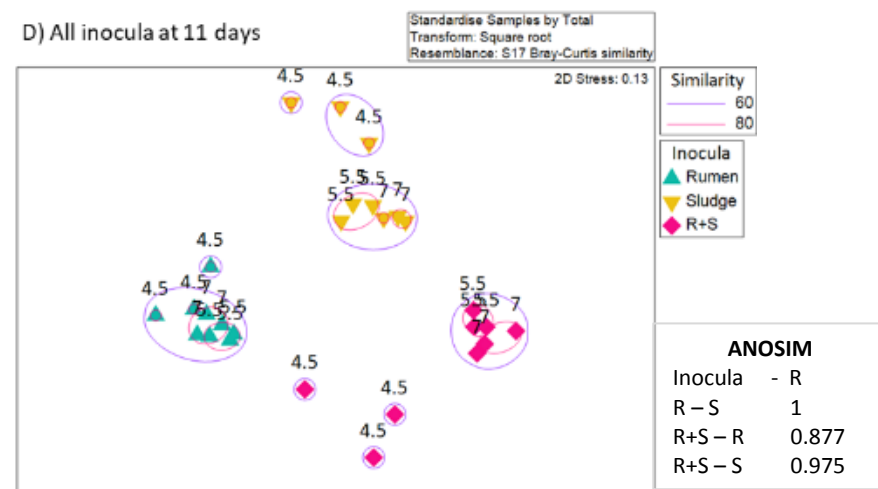
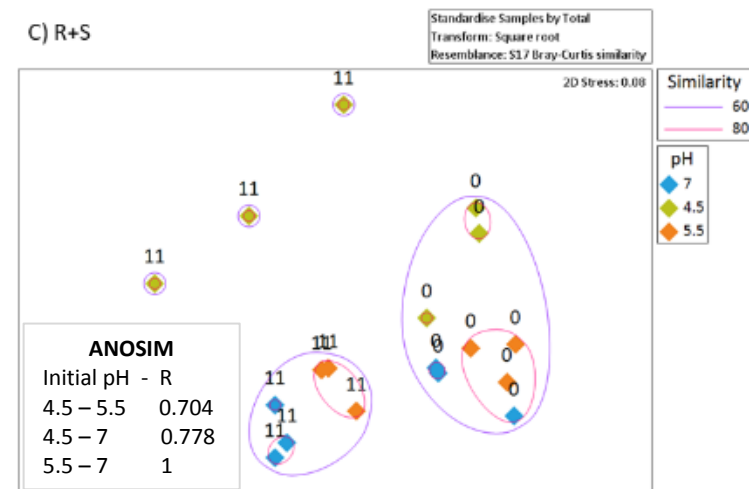
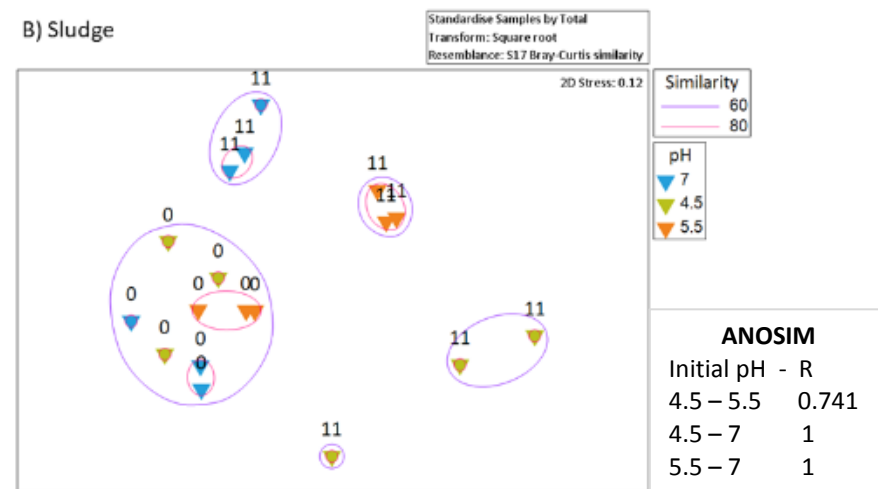
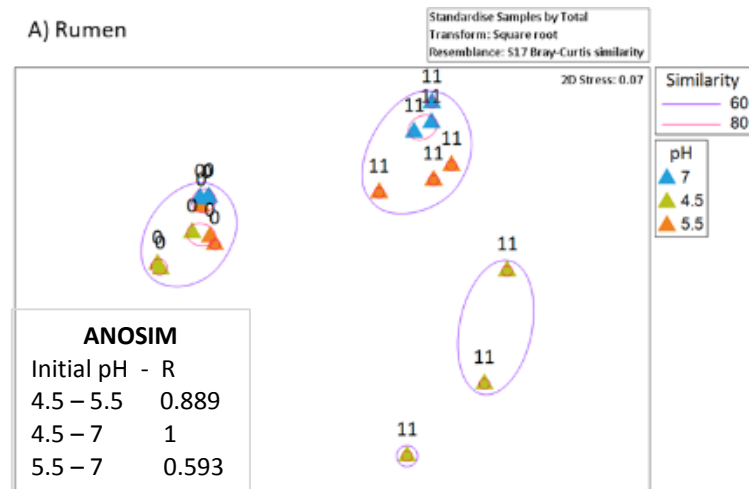


Figure 5.7 A), B), C) nMDS ordination plots of the respective individual DGGE fingerprints in Figure 5.6. The 0 and 11 labels on top of the keys indicate the days of incubation at which the samples were taken. D) nMDS plot of all the inocula at the different initial pH tested after 11 days of incubation, the labels on top of the keys indicate the initial pH. In all plots, samples with 60% and 80% similarity are encircled by a purple or pink line, respectively. ANOSIM R values expand from 0 to 1, where 1 indicates high separation or dissimilarity between clusters. 2D stress values indicate good representation of the data on these 2D nMDS plot

5.4.4 Community composition indices

The sequence libraries obtained after 16s rRNA NGS of the samples taken at the beginning of the experiment (day 0) and after enrichment (day 11) from the replicates of rumen and inocula blanks incubated at initial pH 7 along with sludge and R+S incubated at initial pH 5.5 (conditions at which maximal EtOH production was observed) were quality processed as described in sections 3.7 and 5.39 of this thesis to obtain the operational taxonomic units (OTUs) integrating the different inocula under study. 31356 OTUs were identified among all samples and inocula blanks, 37079 of which were found cummulatively in the inoculated microcosms samples and 8272 of which were found in the inocula blanks. However, it must be noted that numerous OTUs were identified only once in one of the samples, with several zero values comprising the OTU/abundance table.

Nevertheless, to obtain an overview of the microbial communities composition enriched from the different inocula at the pH where their maximal EtOH production was observed, these OTUs and their abundances were used to compute richness (S), diversity (Simpson's inverse diversity, D) and evenness (Simpson's evenness, E) indices (Fig. 5.8). The differentiation between shared and unique OTUs across samples is presented in section 5.4.6.

At the beginning of the experiment rumen had the richest (3190 ± 37 OTUs), most diverse (159 ± 10) and most even ($0.05 \pm 2.59e-3$) bacterial community among the inocula, while the sludge richness (2022 ± 58 OTUs), diversity (12 ± 1.4) and evenness ($5.73e-3 \pm 5.36e-4$) were the lowest. Initially, R+S showed high richness (2673 ± 146 OTUs), but low diversity (34.2 ± 12) and evenness ($1.24e-2 \pm 3.61e-3$). The inocula blanks had a poorly rich (1810 ± 15 OTUs), but highly diverse (207 ± 13) and even bacterial composition ($1.14 \pm 7.93e-3$).

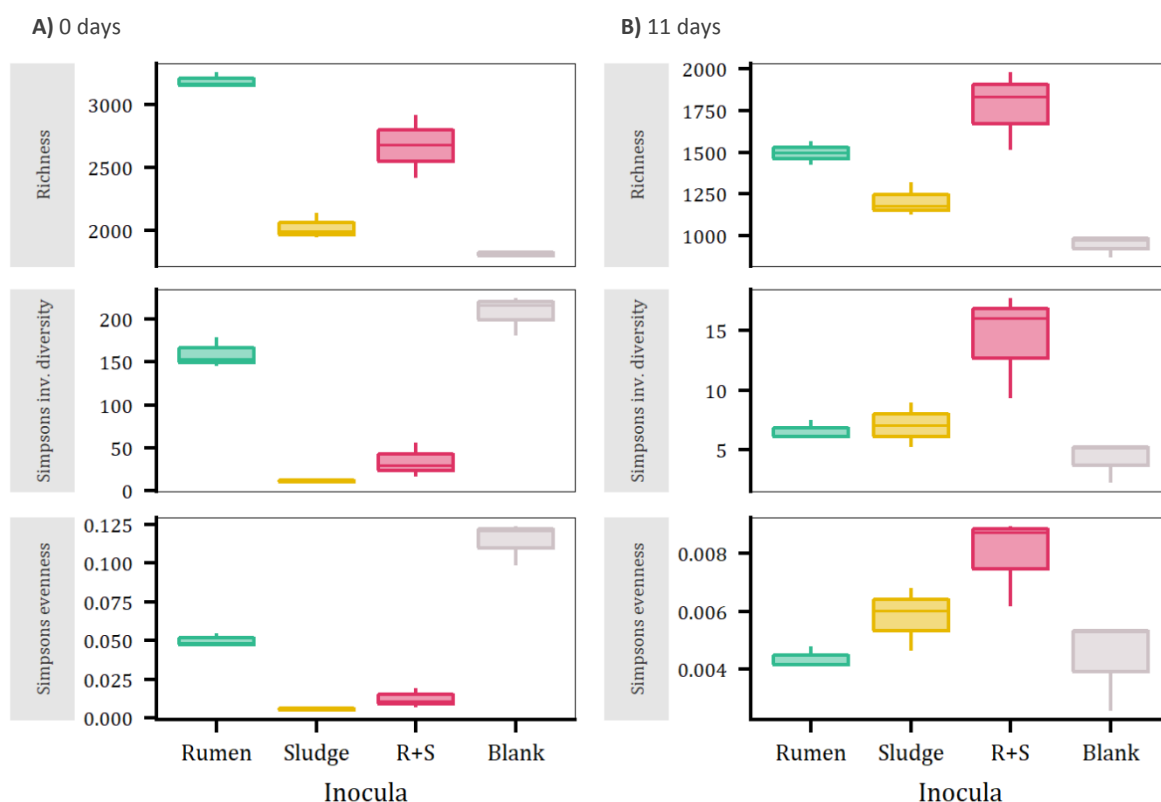


Figure 5.8 A) Richness, Simpson's inverse diversity and Simpson's evenness indices of the communities at time 0, represented as boxplots. B) The same microbial composition indices are displayed for the communities enriched after 11 days of incubation. The error bars represent the standard error of the mean (SE).

After 11 days of incubation the richness of all the communities dramatically decreased (53% for rumen, 40% for sludge and 34% for R+S) as well as their diversity and evenness. Rumen had the least diverse (6.55 ± 0.48) and least even ($4.37e-3 \pm 2.12e-4$) bacterial composition, while R+S richness (1775 ± 138 OTUs), diversity (14.35 ± 2.55) and evenness ($7.95e-3 \pm 8.91e-3$) although variable, were the highest among the inocula. Sludge remained the least rich (1207 ± 58 OTUs) community, but showed higher diversity (7.09 ± 1.09) and evenness ($5.82e-3 \pm 6.35e-4$) than rumen, with values that remained relatively constant to the obtained for t0. The inocula blanks bacterial composition indices also decreased notably (48%). The decrease in richness and diversity suggests the enrichment of OTUs fitted to grow under the specific initial pH conditions and utilise OMSW as substrate.

To confirm the loss of richness was due to enrichment rather than to the absence of growth, the quantification of 16sRNA amplicons for each inocula was compared between day 0 and 11. Post-incubation DNA average concentrations (ng/mL) for the inoculated microcosms samples were higher or similar compared to day 0, indicating growth under the said conditions.

5.4.5 Ordination and statistical comparison of the different inocula before and after enrichment

nMDS ordination plots of the day 0 inoculated microcosms and after 11 days enrichment revealed distinct community compositions across the different inocula, as well as between day 0 and enrichment samples (B, Fig. 5.9). However, the samples at time 0 clustered together, whereas after 11 days of enrichment, each set of replicates for the individual inocula formed separate groups that shared at least 30% similarity.

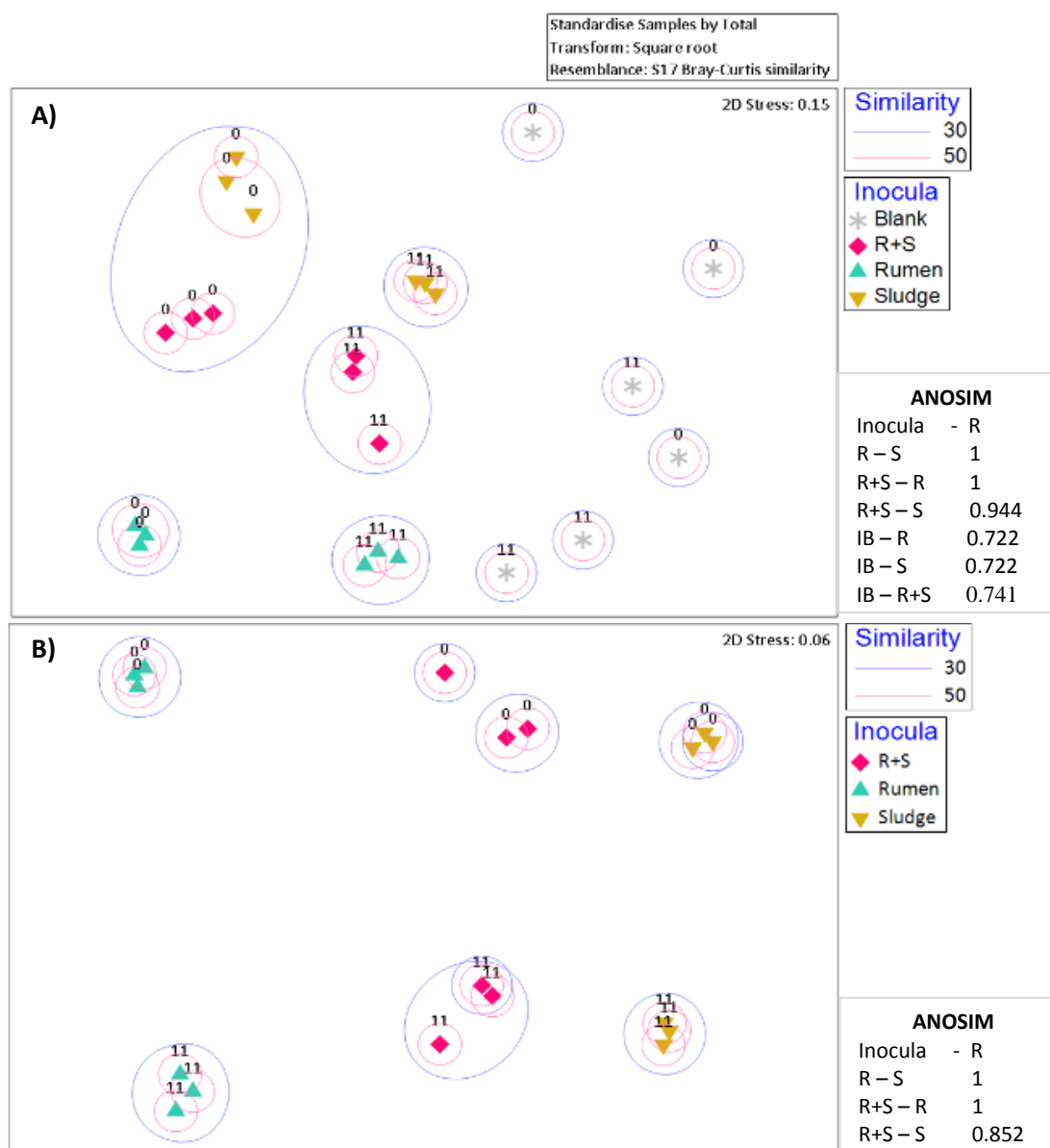


Figure 5.9 A) nMDS of all the inocula at the time of their maximal EtOH production including inocula blanks. B) nMDS of only the inoculated microcosms samples. In all plots, the 0 and 11 labels on top of the keys indicate the days of incubation at which the samples were taken. Samples with 30% and 50% similarity are encircled by a blue or pink line, respectively. 2D stress values indicate good representation of the data on these 2D nMDS plots. ANOSIM R values (0.1% significance level) expand from 0 to 1, where 1 indicates high separation or dissimilarity between clusters.

However, when the inocula blanks community composition is considered, sludge and R+S communities share 30% similarity, but cluster separately after enrichment. This might be due to the effect of the variability between the inocula blanks composition replicates on the data set, which showed to be completely independent from each other at both sampling times, suggesting the original presence, and posterior enrichment of bacterial communities randomly derived from the OMSW waste, able to survive the autoclaving pre-treatment (i.e. spore forming). See below section for more information.

ANOSIM tests were then conducted to assess if the clusters in the nMDS plots were statistically different, confirming the observation that the community composition of each inocula at both sampling times was significantly different. Each nMDS plot displays a box in the lower left corner with the R values derived from their individual ANOSIM tests.

As the clear separation of samples based on the resemblance of their community composition was statistically significant (ANOSIM test), further analysis of the samples in terms of individual OTUs was conducted.

5.4.6 Specific bacterial OTUs typical of the inocula groups before and after enrichment

The most frequent and abundant OTUs for each group of samples defined by the ANOSIM test, which agreed with the different treatments replicates (inocula x sampling day), were determined using the similarity percentages (SIMPER) test on the Bray-Curtis similarity matrix indices. Before the resemblance matrix computation, the data set was standardised, and square root transformed, as previously described in sections 5.3.9 and 3.7.9 of this thesis. Additionally, under the assumption that the most abundant OTUs are the most active within a community, the transformed data set was filtered (Clarke and Gorley, 2015) to only consider OTUs accounting for >1% percent of the total number of individuals in each sample.

A preliminary SIMPER test (data not shown), revealed the inocula blanks initial average similarity (43.97%) mostly due to five OTUs, three of which were uncultured bacteria, decreased (32.29%) after 11 days of enrichment, when three *Leuconostoc* species, all of them closely related to *Leuconostoc mesenteroides* (>97% similarity), a facultative anaerobe typically found on the skin of fruits and vegetables (Lampert et al. 2017) and two *Pseudomonas* species, *P. proteolytica* and *P. weihenstephanensis* (99% similarity),

both isolated from raw milk and dairy products (Stoeckel et al. 2016; von Neubeck et al. 2016), accounted for up to 73.87% of the cumulative similarity of these replicates.

Although all of the aforementioned OTUs were also found in some of the inoculated enrichments, after considering the low similarity between inocula blank replicates, the high variations demonstrated in the nMSD plot, the high presence of numerous zero values and OTUs only found once in one of these replicates after inspection of the OTU/abundance table, in addition to the low EtOH concentration produced by them (<3mM) in comparison to the inoculated microcosms, it was decided to conduct the SIMPER test only with the data from the inoculated samples in order to denoise the analysis. Nevertheless, the significant enrichment of OTUs in the inoculated samples that were also found in the blanks, is highlighted in the results below.

Table 5.3 presents a list of the OTUs that contributed the most to the average composition of each inocula/sampling day group in descending order (Con.%), as well as the ratio of the average contribution divided by the standard deviation of those contributions across all sample pairs in each group (Sim/SD). The latter allowed the identification of OTUs that contributed consistently to the average bacterial composition of each group of replicates. The identity of each OTU is based on the closest similar species (>97% sequence identity match, when possible) found after the individual sequences were megablasted in the GenBank database (Boratyn et al. 2012) as described in section 5.3.9. The average similarity of each group along with the cut-off cumulative similarity (>70%) of the OTUs listed is also presented.

Table 5.3. Most frequent and abundant OTUs found in each inocula group at the beginning of the experiment and after 11 days of enrichment as determined by SIMPER test

Rumen day 0 Average similarity: 83.62 Cumulative similarity: 74.75				Rumen 11 days Average similarity: 84.48 Cumulative similarity: 71.35			
OTU	Identity	Sim/SD	Con.%	OTU	Identity	Sim/SD	Con%
13	<i>Ruminococcus a.</i> ^a	17.95	11.78	2	<i>Pseudomonas w.</i>	21.74	31.92
14	<i>Millionella m.</i> ^b	8.08	10.37	4	<i>Aeromonas r.</i>	11.06	20.66
19	<i>Lutispora t.</i> ^a	20	9.63	12	<i>Carnobacterium</i>	44.07	6.9
23	<i>Prevotella r.</i>	17.35	8.61	10	<i>Enterococcus</i>	8.7	6.37
20	<i>Succiniclasicum r.</i>	21.75	8.61	5	<i>Leuconostoc m.</i>	7.05	5.5
34	<i>Holdemania m.</i> ^b	17.7	7.14	-	-	-	-
41	<i>Victivallis v.</i> ^b	8.73	6.7	-	-	-	-
37	<i>Spiroplasma v.</i> ^b	7.95	6.36	-	-	-	-
65	<i>Paraprevotella c.</i> ^b	6.58	5.57	-	-	-	-

Sludge day 0 Average similarity: 86.29 Cumulative similarity: 70.65				Sludge 11 days Average similarity: 88.04 Cumulative similarity: 72.44			
OTU	Identity	Sim/SD	Con.%	OTU	Identity	Sim/SD	Con%
1	<i>Pseudomonas c.</i>	23.69	31.02	3	<i>Clostridium</i>	38.07	21.85
7	<i>Lentimicrobium s.^b</i>	12.37	17.7	9	<i>Pseudomonas p.</i>	35.25	15.7
6	<i>Proteiniphilum s.^a</i>	21.67	11.11	5	<i>Leuconostoc m.</i>	41.32	14.01
16	<i>Clostridium p.^a</i>	19.89	5.61	1	<i>Pseudomonas c.</i>	7.5	10.81
8	<i>Acinetobacter e.</i>	3.53	5.21	11	<i>Macellibacteroides</i>	10.62	10.06
R+S day 0 Average similarity: 77.03 Cumulative similarity: 71.67				R+S 11 days Average similarity: 81.93 Cumulative similarity: 71.89			
OTU	Identity	Sim/SD	Con.%	OTU	Identity	Sim/SD	Con%
1	<i>Pseudomonas c.</i>	3.53	17.82	3	<i>Clostridium</i>	57.48	14.66
6	<i>Proteiniphilum s.^a</i>	4.22	12.51	10	<i>Enterococcus</i>	146.71	11.62
13	<i>Ruminococcus a.^a</i>	34.51	7.68	8	<i>Acinetobacter e.</i>	52.91	9.55
7	<i>Lentimicrobium s.^b</i>	5.91	7.58	12	<i>Carnobacterium</i>	12.88	8.91
21	<i>Leptolinea t.^a</i>	9.82	4.93	1	<i>Pseudomonas c.</i>	14.91	7.1
15	<i>Paludibacter p.^a</i>	50.93	4.84	2	<i>Pseudomonas w.</i>	3.48	6.85
14	<i>Millionella m.^b</i>	10.88	4.68	5	<i>Leuconostoc m.</i>	2.37	6.67
24	<i>Mucinivorans h.^b</i>	65.25	4.68	4	<i>Aeromonas r.</i>	18.41	6.53
16	<i>Clostridium p.^a</i>	6.36	3.84	-	-	-	-
11	<i>Macellibacteroides f.</i>	2.35	3.12	-	-	-	-

^a 97-90% sequence identity match, ^b90>-85 sequence identity match, ^c 85-80 sequence identity match. No species was assigned when multiple hits at the same maximal identity percentage occurred. The letters next to the genus indicate the species name when the OTU was >97% similar to the said species in multiple hits. Although this is not the canonical way to write taxonomy, it was used on this table to visually simplify comparisons, or when multiple species of the same genus corresponded to different OTUs. Details of the closest related species are given below.

In agreement with the richness indices reported before, the different inocula communities were less rich after 11 day of incubation, this being particularly noticeable for the rumen inoculated microcosms. However, the average similarity within each group of replicates showed a slight increase, confirming a conserved pattern of enrichment occurring in the individual microcosms of each inocula group.

Straight after inoculation the rumen inoculated microcosms community composition was comprised by OTUs closely related (>97%) to two of the dominant bacteria found in the rumen environment i.e. *Prevotella* and *Ruminococcus*, as well as by other bacterial genera typically found in the rumen, namely *Succinivibrionaceae*, *Mollicutes* and *Paraprevotella*, and members of the *Erysipelotrichaceae* and *Victivallaceae* families. Although less specifically, *Lutispora* and *Millionella* also belong to the commonly found rumen orders *Bacteroidales* and *Clostridia*, respectively (Henderson *et al.*, 2015 study of the rumen microbial

community composition determined in >700 samples from 32 animal species and 35 countries).

However, after 11 days of enrichment, a complete shift in the community was observed, now comprised by *Leuconostoc*, a common rumen member, and the non-prevalent, but known to occur in the rumen *Carnobacterium* and *Enterococcus*. *Pseudomonas* and *Aeromonas* are not considered part of the rumen bacterial composition. It must be noted that the same OTUs similar to both *Leuconostoc mesenteroides* and *Pseudomonas weihenstephanensis* were also enriched in at least one of the inocula blanks.

Meanwhile, the sludge inoculated microcosms showed an initial bacterial composition mostly comprised by OTUs highly similar to the species in the GenBank database *Pseudomonas caeni* (99%), isolated from the sludge of an anaerobic ammonium-oxidizing bioreactor (Xiao et al. 2009) and *Proteiniphilum saccharofermentans* (96%), isolated from mesophilic laboratory-scale biogas reactors, as well as a member of the genus *Clostridium* (*C. papyrosolvans*, 91% similarity) and of the phylum bacteroidetes (*Lentimicrobium saccharophilum*, 87%, novel species from a novel family) isolated from the effluent of a paper-mill and methanogenic granular sludge, respectively (Madden et al. 1989; Liwei Sun et al. 2016). While most *Acinetobacter* species (98% similarity) are typical members of aerobic granular sludge (Adav et al. 2009)

After 11 days of enrichment only *Pseudomonas caeni* remained as part of the most abundant OTUs in sludge inoculated microcosms but was replaced as the most abundant OTU by a *Clostridium* species (99% similarity) a commonly reported member of anerobic sludge bacterial communities (Fang et al. 2002), also *Macellibacteroides fermentans* (98% similarity), an obligate anaerobe isolated from an anaerobic filter treating wastewater from an abattoir (Jabari et al. 2012) was enriched. Finally, *L. mesenteroides* and *P. proteolytica* (both 99% similarity) could probably have emerged from the substrate, as found in at least one of the inocula blanks and the rumen inoculated microcosms.

The most frequent and abundant OTUs initially comprising the R+S inoculated microcosms were mostly derived from sludge (*P. caeni*, *P. saccharofermentans*, *M. fermentans*, *Lentimicrobium s.*, and *C. papyrosolvans* along with *Leptolinea tardivalis*, which has been isolated from mesophilic anaerobic granular sludge (Yamada et al. 2006) accounting for about 50% of the community composition. Since the SIMPER analysis was cut off at 70% cumulative composition, the contribution of abundant rumen derived bacteria (*Ruminococcus* and *Paludibacter*, common ruminal members (Henderson et al.

2015), along with *Millionella* and *Mucinivorans*-like OTUs, species isolated from the gut of different animals (Nelson et al. 2015) only amounted to 22%.

However, after 11 days of incubation, the community was comprised by a balanced enrichment of bacteria also observed in sludge inoculated microcosms (*Clostridium*, *P. caeni* and *Acinetobacter*) and in rumen inoculated microcosms (*Enterococcus*, *Carnobacterium* and *Aeromonas*). The presence of *P. weihenstephanensis* and *L. mesenteroides* support the idea of these OTUs being part of the OMSW.

Additionally, also in agreement with the evenness indices, these results for the SIMPER analysis corroborated the fact that although initially rumen had the most even community composition, this decreased after enrichment, while the sludge and particularly R+S evenness increased with enrichment (See contribution percentages in Table 5.3). This event could provide stability to the sludge and R+S enriched communities (Begon et al. 2007).

The initial composition and enrichment of different OTUs closely related to bacteria known to be found in the original inocula sources, rumen and sludge, validates the enrichment from these inocula despite of the growth of bacteria that might derive directly from the substrate. Further analysis as to which might be the roles and environmental factors selecting for these microorganisms is discussed in section 5.5 of this chapter.

5.4.7 Specific discriminating bacterial OTUs before and after enrichment within single inocula and between the enriched communities from different inocula

Section 5.4.5 described the characteristic OTUs comprising each bacterial community, without a direct comparison of the contribution percentage trend of these OTUs between groups. However, SIMPER also allowed the identification of the OTUs which contributed the most to differences in community composition within and between the inocula replicates groups, comparing pairs of groups at a time.

Table 5.4 presents a list of the OTUs that contributed the most to the average dissimilarity within community compositions at the start of incubation and after enrichment within each inocula in descending order (Contrib.%). The identity of each OTU is the closest similar species (>97% sequence identity match, when possible) found after the individual sequences were megablasted in the GenBank database (Boratyn et al. 2012) as described

in section 5.3.9. The average dissimilarity (Av. Diss) in the contribution to the communities' compositions of each OTU denotes the increment (+) or decrease of that particular OTU after enrichment. The total average dissimilarity between the initial community and the enrichment along with the cut-off cumulative dissimilarity (>70%) of the OTUs listed is also included.

Table 5.4. Discriminating OTUs between initial inocula community composition and after 11 days of enrichment as determined by SIMPER test

Groups R0 & R11				
Average dissimilarity = 81.47 Cumulative dissimilarity = 71.98%				
OTU	Identity	Av.Diss	Diss/SD	Contrib%
2	<i>Pseudomonas w.</i>	+15.29	14.57	18.77
4	<i>Aeromonas r.</i>	+10.64	12.3	13.06
12	<i>Carnobacterium</i>	+4.12	4.16	5.05
10	<i>Enterococcus</i>	+4.07	3.33	4.99
5	<i>Macellibacteroides</i>	+3.69	2.83	4.53
19	<i>Lutispora t.^a</i>	-3.52	6.37	4.32
14	<i>Millionella m.^b</i>	-3.19	3.73	3.92
13	<i>Ruminococcus a.^a</i>	-3.01	11.18	3.7
22	<i>Serratia l.</i>	+2.91	3.83	3.57
23	<i>Prevotella r.</i>	-2.82	3.91	3.46
32	<i>Pseudomonas l.</i>	+2.79	4.61	3.43
20	<i>Succiniclasicum r.</i>	-2.6	5.23	3.19
Groups S0 & S11				
Average dissimilarity = 60.28 Cumulative dissimilarity = 70.65%				
OTU	Identity	Av.Diss	Diss/SD	Contrib%
3	<i>Clostridium</i>	+11.12	8.87	18.45
9	<i>Pseudomonas p.</i>	+7.59	21.92	12.6
1	<i>Pseudomonas c.</i>	-6.92	6.23	11.48
5	<i>Leuconostoc m.</i>	+6.86	17.78	11.38
7	<i>Lentimicrobium s.</i>	-6.35	8.5	10.53
11	<i>Macellibacteroides</i>	+3.75	3.58	6.22
Groups RS0 & RS11				
Average dissimilarity = 63.72 Cumulative dissimilarity = 70.9%				
OTU	Identity	Av.Diss	Diss/SD	Contrib%
3	<i>Clostridium</i>	+6.76	28.06	10.61
10	<i>Enterococcus</i>	+5.5	32.07	8.64
2	<i>Pseudomonas w.</i>	+4.61	2.05	7.23
12	<i>Carnobacterium</i>	+4.23	11.31	6.64
1	<i>Pseudomonas c.</i>	-4.06	1.9	6.37
5	<i>Leuconostoc m.</i>	+3.74	3.25	5.87
4	<i>Aeromonas r.</i>	+3.24	10.79	5.09
6	<i>Proteiniphilum s.^a</i>	-3.23	2.82	5.07
8	<i>Acinetobacter e.</i>	+2.93	2.87	4.61

OTU	Identity	Av.Diss	Diss/SD	Contrib%
7	<i>Lentimicrobium s.^b</i>	-2	4.9	3.14
15	<i>Paludibacter p.</i>	-1.73	2.29	2.71
13	<i>Ruminococcus a.</i>	-1.61	2.77	2.52
24	<i>Mucinivorans h.^b</i>	-1.54	10.21	2.42

^a <97>90% sequence identity match, ^b<90>85 sequence identity match, ^c<85>80 sequence identity match. No species was assigned when multiple hits at the same maximal identity percentage occurred. The letters next to the genus indicate the species name when the OTU was >97% similar to the said species in multiple hits. Although this is not the canonical way to write taxonomy, it was used on this table to visually simplify comparisons, or when multiple species of the same genus corresponded to different OTUs. Details of the closest related species are given below.

The enrichment of *P. weihenstephanensis*, *Aeromonas*, *Carnobacterium*, *Enterococcus* and *Macellibacteroides* (all found as typical from rumen after 11 days of incubation), along with *Serratia* (99% similarity) and *Pseudomonas lundensis* (97% similarity) -like OTUs, drove the differentiation between the initial and enriched ruminal communities. Generally, shifting the community from *Bacteroidales* and *Clostridiales* as dominant orders (33% and 22%, respectively), to a community dominated by members of the *Lactobacillales* (60%).

Whereas the increment in the contribution or enrichment of *Clostridium*, *Pseudomonas proteolytica*, *Leuconostoc mesenteroides* and the *Macellibacteroides*-like OTU, had a major effect in the differentiation within the initial and enriched bacterial communities derived from sludge, where the community shift between bacterial orders was rather subtle, as members from the *Pseudomonadales*, *Bacteroidales*, and *Clostridiales* orders just changed in relative abundance respect to the others, with a member of the *Porphyromonadaceae* being replaced by a *Lactobacillales* as part of the most abundant OTUs.

Similar to the pattern observed for the typical bacterial composition of R+S (see Table 5.4), most of the OTUs enriched in rumen and sludge inoculated microcosms were also enriched in the R+S community, causing the differentiation between the 0 and 11-days communities of this treatment. In this regard, there was a clear shift from the moment of inoculation, where the community was comprised mostly of members of the *Bacteroidales* (44%) and *Clostridiales* (33%) orders, to a community dominated by *Pseudomonadales* (37.5%) and *Lactobacillales* (37.5%), in addition to members of the *Clostridiales* and *Aeromonadales* orders after 11 days of incubation.

Also, aiming to compare the bacterial communities enriched from the different inocula, SIMPER analysis was used to determine which OTUs along with their average abundances

(Av. Abund) were primarily responsible for differences between these groups in a pair-wise fashion (Table 5.5).

Table 5.5. Discriminating OTUs between the enriched communities from the different inocula as determined by SIMPER test

Groups R11 & S11					
Average dissimilarity = 92.11 Cumulative dissimilarity = 71.26%					
OTU	Identity	R11 Av.Abund	S11 Av.Abund	Diss/SD	Contrib%
2	<i>Pseudomonas w.</i>	6.09	0	16.21	14.5
3	<i>Clostridium</i>	0	5.04	8.95	11.77
4	<i>Aeromonas r.</i>	4.01	0	13.8	9.55
9	<i>Pseudomonas p.</i>	0.07	3.46	16.94	8.07
1	<i>Pseudomonas c.</i>	0	2.58	7.98	6.13
11	<i>Macellibacteroides</i>	0.18	2.52	5.17	5.55
8	<i>Acinetobacter e.</i>	0	2.23	4.94	5.32
5	<i>Leuconostoc m.</i>	1.4	3.13	3.16	4.13
12	<i>Carnobacterium</i>	1.56	0	4.18	3.7
10	<i>Enterococcus</i>	1.54	0.05	3.19	3.54
Groups RS11 & R11					
Average dissimilarity = 52.26 Cumulative dissimilarity = 72.1%					
OTU	Identity	RS11 Av.Abund	R11 Av.Abund	Diss/SD	Contrib%
3	<i>Clostridium</i>	3.69	0	39.14	13.2
2	<i>Pseudomonas w.</i>	2.57	6.09	2.98	12.93
8	<i>Acinetobacter e.</i>	2.43	0	26.61	8.95
4	<i>Aeromonas r.</i>	1.74	4.01	6.49	8.35
1	<i>Pseudomonas c.</i>	1.93	0	9.39	7.1
10	<i>Enterococcus</i>	2.96	1.54	2.73	5.24
11	<i>Macellibacteroides</i>	1.39	0.18	1.49	4.41
6	<i>Proteiniphilum s.</i>	0.91	0	2.93	3.32
5	<i>Leuconostoc m.</i>	2.06	1.4	1.45	3.12
12	<i>Carnobacterium</i>	2.32	1.56	1.73	2.84
36	<i>Pseudomonas l.</i>	0.24	0.96	5.25	2.64
Groups RS11 & S11					
Average dissimilarity = 45.03 Cumulative dissimilarity = 72.54%					
OTU	Identity	RS11 Av.Abund	S11 Av.Abund	Diss/SD	Contrib%
9	<i>Pseudomonas p.</i>	0.39	3.46	9.9	12.52
10	<i>Enterococcus</i>	2.96	0.05	29.24	11.86
2	<i>Pseudomonas w.</i>	2.57	0	2.15	10.5
12	<i>Carnobacterium</i>	2.32	0	12.54	9.47
4	<i>Millionella m.b</i>	1.74	0	10.81	7.1
3	<i>Clostridium</i>	3.69	5.04	2.64	5.53

OTU	Identity	RS11 Av.Abund	S11 Av.Abund	Diss/SD	Contrib%
11	<i>Macellibacteroides</i>	1.39	2.52	1.43	4.89
5	<i>Leuconostoc m.</i>	2.06	3.13	1.69	4.35
17	<i>Macellibacteroides s.</i>	0.42	1.24	1.59	3.33
13	<i>Ruminococcus a.</i>	0.74	0	11.04	3

^a <97>90% sequence identity match, ^b<90>85 sequence identity match, ^c<85>80 sequence identity match. No species was assigned when multiple hits at the same maximal identity percentage occurred. The letters next to the genus indicate the species name when the OTU was >97% similar to the said species in multiple hits. Although this is not the canonical way to write taxonomy, it was used on this table to visually simplify comparisons, or when multiple species of the same genus corresponded to different OTUs. Details of the closest related species are given below.

The above results show that the evident presence/absence of OTUs closely related to species commonly found either in rumen or sludge caused the differences between these two enriched communities. However, OTUs highly similar to different *Pseudomonas* species also contributed greatly to this differentiation, with *P. weihenstephanensis* and *P. proteolytica*, both potentially derived from the substrate, contributing to 14.5% and 8.07% of the total difference, respectively.

The differences between R+S against the original inocula sources community compositions were also clearly determined by the presence/absence of OTUs shown to be associated to each of the alternative inocula, e.g. R+S differences against sludge were caused by the enrichment of rumen derived OTUs. However, the individual contributions of OTUs thought to be enriched from OMSW also played an important role in the overall average dissimilarity, as *P. weihenstephanensis* seems to be preferentially enriched in rumen and R+S, while *P. proteolytica* is mostly abundant in sludge. *Leuconostoc mesenteroides* showed similar average abundances in all enrichments. Further information regarding the habitats and putative functions of the organisms closely similar to the OTUs presented in Tables 5.4, 5.5 and 5.6 is provided in the discussion.

5.5 Discussion

The results presented in this chapter confirmed the observation from previous experimental set-ups (Chapter 4), where rumen produced higher EtOH concentrations when inoculated at initial neutral pH, while sludge showed the best ethanologenic performance at initial acidic pH. Additionally, microcosms inoculated with a mixture 1:1

(w/w) of these inocula (R+S) significantly produced the same EtOH concentrations than the original inocula sources at both of the initial pH incubation conditions (pH 7 and 5.5).

However, significantly lower maximal concentrations were reached by all inocula during this experimental set-up in comparison with previous results (drop by ~10mM). This difference could be simply attributed to the problems with the GC-FID performance reported in section 5.3.4, therefore further technical assistance, examination and validation of the instrument and quantification method should be deployed before conducting further quantification of soluble fermentation products.

Independently, 16S rRNA gene sequencing data analysis of samples taken from the best performing inocula/initial pH treatments revealed significant shifts in microbial community composition after 11 days of enrichment, showing that despite the initial richness of the inocula sources, the communities enriched from OMSW incubation were predominantly dominated by a reduced number of OTUs, most of which were found only in low abundances in the corresponding original inocula. This decrease in richness agrees with that reported in other fermentation enrichment studies (Temudo et al. 2008; Ye et al. 2007; Peacock et al. 2013).

Here, presumably the high nutrient availability provided by a complex substrate as is OMSW which could have otherwise led to high rates of diverse populations growth, was constrained by environmental factors (20°C, initial pH) eventually increasing the opportunity for the best fitted community members to dominate and possibly completely outgrow others (Begon, 2007). Although this is a plausible explanation for the overall loss of richness observed, the enrichment of particular genera and specific species can be attributed to both, the original inocula source and the initial pH used for their incubation. These observations are further discussed in the following section.

5.5.1 Putative functions of the enriched communities' members

Rumen and anaerobic granular sludge are specialised anaerobic environments where organic matter fermentation is a major community function (Flint 1997; Schmidt and Ahring 1996). However, inherent differences in their natural microbial composition and commonly degraded carbon sources were expected to select for different bacteria in the OMSW enrichments. Additionally, since the initial pH of these inocula sources before incubation was in both cases close to neutrality (7.14 ± 0.02 , 6.91 ± 0.02 , rumen and

sludge, respectively), their opposite behaviour regarding EtOH production when incubated at an initial pH range was then expected to be linked to their bacterial communities' composition.

Broadly, the enriched communities (considering OTUs decreasingly contributing to the 70% of the total relative abundance) from both inocula as well as from their mixture (R+S), were essentially dominated after 11 days by members of the phyla *Firmicutes*, *Proteobacteria*, and *Bacteroidetes*, the latter of particular predominance in R+S. While all the abundant *Proteobacteria* enriched belonged to the gamma class, specifically to the *Pseudomonas*, *Aeromonas* and *Acinetobacter* genera, the *Firmicutes* enriched in the rumen community were all members from the *Bacilli* class, while sludge enrichment comprised both *Clostridia* and *Bacilli* members, as well as R+S, and although the latter had a higher variety of *Bacilli* than sludge, its *Clostridia* dominant member was the most abundant OTU in this enriched community.

From this simple characterisation it can be inferred that all communities displayed linked trophic interactions, where the aerobic (*Pseudomonas* and *Aeromonas*) and facultative anaerobes (some *Bacilli* members) might have initiated the OMSW consumption of the readily available sugars dissolved, causing CO₂ accumulation and O₂ consumption, thus providing an appropriate environment for the growth of obligate anaerobes (*Clostridia* and some *Bacilli* members) capable of fermentation and degradation of more complex organic matter (cellulose), possibly releasing more simple organic compounds into the media, as previously proposed in other studies of MCF initially incubated under aerobic conditions degrading and fermenting cellulosic substrates (Kato et al. 2005; Guo et al. 2010).

However, to elucidate how this seemingly straight forward mechanism led to different ethanologenic activity by the inocula tested here in response to the initial pH of the media, a closer inspection to the OTUs found to be typical in each enrichment as well as to the OTUs mainly responsible for the differentiation between these communities (Tables 5.4 and 5.6) was conducted and compared against the literature.

The dominance of the genus *Clostridium* at acidic pH (5.5) in sludge and R+S enriched communities was also observed in the bacterial community composition of a mixed-source community enriched from two sludge sources, namely, a distillery wastewater treatment plant and a potato starch processing acidification tank, incubated in a mesophilic (30°C) continuously stirred reactor with constant pH control and provided

with glucose as only carbon source (Temudo et al. 2008). However, the main fermentation product under these conditions was butyrate. Nevertheless, this same study found that at pH between 6.25 and 7, the community was dominated by the facultative anaerobic bacteria *Klebsiella* and ethanol and acetate were the main fermentation products. The authors attributed the production of butyrate as a main fermentation product at low pH to the bioenergetic consideration of higher ATP yield through butyrate formation from the fermentation of glucose and NAD⁺ regeneration. Nevertheless, they argued that at neutral pH the bioenergetics are equally favourable for the dominant production of the EtOH/acetate pair or butyrate (ΔG^0 -258.3/2.0 ATP, ΔG^0 -259.3/2.4 ATP), and therefore the community composition selection could be caused by other environmental factors.

The proposal of bioenergetics selecting for butyrate production at controlled low pH cannot be fully compared to the experimental observations of this work as the initial aerobic conditions in addition to the presence of multiple possible carbon sources in the OMSW, such as simple and complex carbohydrates, proteins and lipids, obscures which would be the most energetically favourable fermentation end-product, even more so as apart from the initial pH, the environmental pH was allowed to be self-regulated by the bacterial community. Additionally, this argument overlooks the metabolism specific to the dominant bacteria enriched.

Thus, it is proposed that a broader thermodynamic outlook would better help explain the production of EtOH as a main fermentation product at low pH. For instance, while the production of both butyrate and EtOH regenerates NAD⁺, the generation of the former, being a charged molecule, could require active membrane transport in order to be exported from the cell, which is likely coupled to a proton translocation into the cell, increasing internal pH maintenance requirements, hence overcoming the benefit of ATP production by butyrate production (Rodríguez et al. 2006; Hoelzle et al. 2014), as discussed in section 2.5 of Chapter 2.

For instance, while several cellulolytic *Clostridium* members (e.g. ruminal) cannot grow at pH values lower than 6 (M. Desvaux et al. 2001; Mickaël Desvaux 2006), other members of this genus change their metabolism from acidogenic to solventogenic when pH decreases. The dominant OTU closely related to *Clostridium* in the sludge and R+S enriched communities, was highly similar uniquely to species belonging to the second group (99% similarity to *C. beijerinckii*, *C. acetobutylicum*, *C. saccharoperbutylacetonicum*), which produce butanol, and acetone at pH ~ <5.1, while

ethanol is formed in both phases (Amador-Noguez et al. 2011; Millat et al. 2013; Poehlein et al. 2017), thus rejecting the generalist hypothesis that butyrate formation is favoured at low pH (4.5-5.5).

It is also worthy of note that *C. acetobutylicum* preserves a constant proton gradient across the membrane as its only mechanism to maintain a constant intracellular pH, causing the intracellular pH of this species to follow the external pH within a $\Delta p \sim 1$. In consequence, environmental pH directly influences changes of cellular physiology such as the synthesis of solvent producing enzymes by this bacterium (Millat et al. 2013).

Alternatively and supporting the necessity to inspect the metabolism of the dominant community members, EtOH along with acetic acid have been reported as major fermentation products from the degradation of vegetable wastes after 10 days of operation of initially aerobic mesophilic (30°C) batch reactors at (controlled) pH 5 inoculated with anaerobic sludge from an anaerobic digestion tank (Ye et al. 2007). The particularly high EtOH proportion detected at this pH in comparison to other pH values tested, was attributed by the authors to the abundant presence of a bacterium relatively closely related (93% similarity) to *Clostridium ljungdahlii*, an heterotroph and autotroph able to produce (or consume) EtOH and acetic acid from syngas (CO, CO₂ and H₂) through the Entner–Doudoroff and the Wood–Ljungdahl pathways, respectively, in a pH range of 4–6 (Tanner et al. 1993; Köpke et al. 2010). Interestingly, during autotrophic growth, *C. ljungdahlii* is thought to conserve energy by coupling reduced ferredoxin to generate a proton gradient along with NADH, which is then utilised to reduce CO₂ and produce EtOH (Köpke et al. 2010). This example emphasises the benefits of the study of highly abundant community members coupled to their metabolism for the understanding of fermentation products formation in MCF. Meanwhile, butyric acid was the major fermentation product at pH 7, while *Clostridium acidisoli* along with *Lactobacillus* species were the dominant community members (Ye et al. 2007). The latter finding also partially agrees with the observed in the rumen enrichment, where the community was mostly dominated by members of the *Lactobacillales* family after 11 days.

Another potential EtOH producer in the sludge inoculated microcosms was the OTU closely related to *Macellibacteroides* (100% similarity), as this anaerobic bacterium isolated from an upflow anaerobic filter treating abattoir wastewaters, has not only shown cellobiose consumption, which would be abundant in the pre-treated OMSW

media, but also lactate, acetate, butyrate and EtOH production (Jabari et al. 2012; B. Zhang et al. 2017).

Oppositely, the community enriched from rumen at initial pH 7 in this project produced a substantial EtOH concentration likely produced by its three dominant OTUs closely related (97% similarity) to members of the *Lactobacillales* family, namely *Carnobacterium* (98% similarity with four *Carnobacterium* species), *Enterococcus* (99% similarity with six *Enterococcus* species), and *Leuconostoc mesenteroides* (100% similarity), all tolerant to high CO₂ concentrations, heterolactic facultative anaerobes (H. Zhang and Cai 2014), and all able to produce lactic acid, CO₂, ethanol, and/or acetic acid among other products (Hammes and Hertel 2006). All these genera are known to occur in the rumen, albeit not abundantly, being associated with acidosis problems (Henderson et al. 2015). However, it is unlikely that the OTU similar *L. mesenteroides* greatly contributed to EtOH formation since this bacterium was also enriched in the inocula blanks where EtOH production was relatively low in comparison to the other treatments.

In this regard, *L. mesenteroides* (optimal growth pH 6.7), has been reported to have a higher affinity for sucrose and fructose over glucose degradation, while the latter sugar as well as citrate and pyruvate, potential electron acceptors for regeneration of NAD⁺/NADH (Elshaghabee et al. 2016), have shown to direct the metabolism of this bacterium towards acetate (in the presence of O₂), or mannitol (in anaerobiosis) at the expense of EtOH (Dols et al. 1997). Therefore, it can be inferred that *L. mesenteroides* probably flourished in all the enriched communities due to the high content of vegetable and fruit matter present in OMSW, rich in fructose, with little contribution to the overall EtOH formation.

However, it has been shown that co-cultures of *Leuconostoc* and *Carnobacterium* species along with another arbitrary bacterium, produced lactic acid and ethanol as main fermentation products from the degradation of ham when incubated at initial pH 6.5 (Vasilopoulos et al. 2010). Suggesting that *L. mesenteroides* EtOH production could have been higher in the inoculated microcosms than in the inocula blanks due to its co-occurrence with other bacteria such as *Carnobacterium*. An additional trait favouring the growth of these bacteria over others is their production of bacteriocins (Lampert et al. 2017; Hammes and Hertel 2006), proteinaceous antibacterial compounds (Ogunbanwo et al. 2003).

At the same time, *Enterococcus* has shown biphasic fermentation, switching from homolactic to heterolactic fermentation, in the degradation of whey when inoculated at initial neutral conditions. This phenomenon can be triggered by carbon-excess conditions, leading to increase in pyruvate formation and over production of NADH, consequently directing the metabolism towards EtOH generation (Guerra et al. 2010). Additionally, *Enterococcus* species isolated from the gastrointestinal tract of animals has also shown high cellulolytic activity, (Li et al. 2016; Wang et al. 2009).

Therefore, it is suggested that the OTUs highly similar to lactic acid bacteria were responsible for EtOH production in rumen inoculated microcosms, and their heterolactic functional redundancy was potentially disregarded by their other specific traits.

Although the role of the *Pseudomonas* members in all the enriched communities could be mostly attributed to the ubiquity of this genus, its ample metabolic spectrum and the initial aerobic conditions of the incubation (Madigan 2015), other general and particular characteristics of the dominant *Pseudomonas* enriched in this work potentially contributed to their growth under the conditions tested.

For instance, biofilms comprising *Pseudomonas* strains have been used for the detoxification of pre-treated feedstocks solutions for ethanol production due to their ability to degrade aromatic compounds and their organic-solvent tolerance, the latter attributed to the presence of outer membranes typical for Gram-negative bacteria and the production of biofilm specific compounds i.e. exopolysaccharide, which impede the solvent diffusion into the cell (Khiyami et al. 2005). Hence, this feature could have protected *Pseudomonas* members from the build-up of EtOH toxicity (from 6% to 18% by volume, depending on the bacteria), i.e. increase in membrane permeability (Haft et al. 2014), while benefiting the community by degrading inhibitors derived from the substrate pre-treatment, such as lignin-related phenolic compounds. Additionally in this regard, *Aeromonas* and *Pseudomonas* species have been reported to degrade lignin under mesophilic neutral incubation conditions (Deschamps et al. 1980; Rashid et al. 2017), while a dominant cellulolytic *Aeromonas* species has also been isolated from the gastrointestinal tract of animals (Li et al. 2016). Hence, the abundant enrichment of an *Aeromonas* species in rumen inoculated microcosms could also be linked to cellulose and lignin degradation.

Pseudomonas species were also abundantly enriched in an MCF system inoculated with cow dung for the production of hydrogen and EtOH from cellulose, xylose and glucose (C.

Y. Lin and Hung 2008). In this study, different unspecified *Pseudomonas* species grew at a pH range from 5.5 to 9.5, with the species growing at lower pH mostly enriched with xylose as carbon source, while a member of the *Enterobacteriaceae* family *Klebsiella* dominated the cellulolytic enrichment at pH 5.5. The authors suggested *Pseudomonas* having a possible beneficial effect in the aggregation of fermentative bacteria, without further discussion in this respect. Nevertheless, *Pseudomonas* have been found as some of the key responsible bacteria for the aggregation of granular sludge (Adav et al. 2009). Besides, they are well known pentose oxidisers (Fuente-Hernández et al. 2013), which could explain their dominance in their xylose enrichment, as well as the presence of *P. proteolytica* and *P. weihenstephanensis* in the highly rich OMSW enrichments of the current work.

Appart from conducting glucose, xylose and trehalose oxidation (among other sugars), *P. proteolytica* and *P. weihenstephanensis* are both psychrotolerant (4-33°C) extracellular peptidase producers at a pH range 5-11 (Stoeckel et al. 2016; von Neubeck et al. 2016; Jain et al. 2017), a trait which could have allowed them to degrade the meat-derived peptides present in OMSW media.

However, *P. caeni* a *Pseudomonas* isolated from the sludge of an anaerobic ammonium-oxidizing bioreactor, able to grow at a pH range 5-11, does not seem to use single sugars as sole carbon sources but has shown utilisation of malic and capryl fatty acids as sole carbon sources. Moreover, this species is capable of nitrate and nitrite reduction under anaerobic conditions (Xiao et al. 2009). Although *P. proteolytica* and *P. weihenstephanensis* have been both associated with milk proteolysis (Stoeckel et al. 2016) and were enriched in the inocula blanks of this work, it is speculated that the particular prevalence of *P. proteolytica* over *P. weihenstephanensis* in the sludge enriched community incubated under initial pH 5.5, might be linked to its high extracellular lipase activity, reportedly enhanced at low pH (Jain et al. 2017), which could be coupled to some of the fatty acids consumption by *P. caeni*, further stimulating lipase activity.

Most of the OTUs enriched in either rumen or sludge communities were also highly enriched in R+S, except for *P. proteolytica* and *Macellibacteroides*. Instead, an *Acinetobacter*, OTU derived from sludge, that a close relative has previously demonstrated its ability to deplete lignocellulose-derived toxic compounds as sole carbon source (Parawira and Tekere 2011), as well as proteolytic activity (Adav et al. 2010), was enriched. Additionally, this genus has been extensively deployed in aerobic wastewater

treatment due to its phosphorus removal capacity through poly-phosphate formation (Ghigliazza et al. 1998). A trait triggered by high organic contents under aerobic conditions, also causing phosphorous release as energy generation mechanism under low oxygen levels (Ghigliazza et al. 1998; Auling et al. 1991). Thus, the possibility of phosphorus sequestration/secretion by this bacterium in the R+S community was not unlikely to occur.

In summary, based on the general metabolic activities of the dominant OTUs, the MCF process could be simply divided in two major metabolic functions: organic carbon oxidation under aerobic conditions, followed by fermentation by facultative anaerobes/obligate anaerobes once most of the oxygen had been consumed with subsequent carbon dioxide accumulation and pH drop (Fig. 5.10). Since this work is focused on EtOH production, a third metabolic distinction could be proposed between general fermenters and those with potentially higher EtOH production (numbered in hierarchical order for each community under the assumption of higher metabolic activity by the most abundant organism).

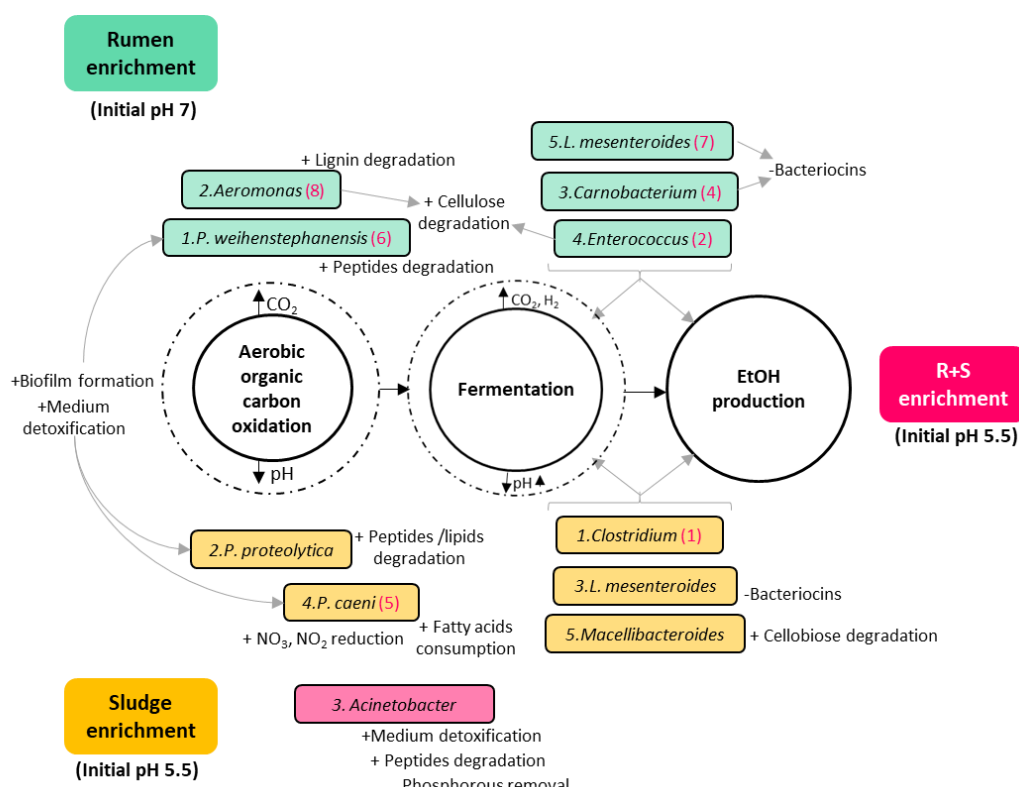


Figure 5.10 Diagram of the putative functionalities of the dominant OTUs enriched from the different inocula under study. Turquoise rectangles: rumen enriched. Yellow rectangles: sludge enriched. Pink rectangle: R+S enriched. The numbers before the species name indicate in hierarchical order their contribution to the total relative abundance of their community. Numbers in brackets after the species name, signal OTUs also enriched in the R+S community in hierarchical order of contribution to the total relative abundance for this community. +/- symbols before specific OTUs putative functions indicate an activity possibly benefiting (+) or damaging (-) the community.

As expected, functional redundancy occurred not only between but within communities, and it was not exclusive of the general divisions among aerobic oxidation and fermentation of organic matter, but also of the particular traits that could benefit or damage the communities. It is worth highlighting here the abundant enrichment of bacteria able to degrade aromatic compounds and detoxify the medium, indicating that the *in-situ* acid pre-treatment without further conditioning played an additional constraint for the enrichment.

Another important finding is the co-enrichment of rumen and sludge-derived OTUs in the R+S community. As these OTUs were not present or highly abundant directly after inoculation in the R+S microcosms, it is safe to assume their actual enrichment, which provided the R+S community with further functional redundancy and indicates *Clostridium* and *Enterococcus* might be the major EtOH producers in the original inocula enrichments. This result also demonstrated that most of the OTU enriched were capable of function and even to produce EtOH under acidic conditions (pH > 4.5, see Fig. 5.2), questioning which mechanisms occurring in R+S allowed the enrichment of ruminal-derived bacteria under initial pH 5.5, when it was previously shown (Fig. 5.2) the low ethanol production by this inocula when incubated at initial acidic pH.

Additionally, the high functional redundancy also brings into question whether these OTUs are interacting in a symbiotic/detrimental way or can co-exist independently. Unfortunately, the existence of interactions (competition or symbiosis) between the communities' members cannot be fully determined from community composition analyses based on 16S rRNA sequences and were further limited in this study since only two data points of the best performing communities (initial pH at maximal EtOH concentration microcosms) enriched from each inocula were compared between each other. Moreover, only EtOH production could be linked to the communities' bacterial composition, missing information of further soluble fermentation products for a more complete analysis.

5.5.2 Enrichment of a mixed-source novel community

Nevertheless, EtOH production profiles along with 16S rRNA sequencing analyses demonstrated the successful enrichment of a novel mixed-source community, whereby bacteria derived from both original inocula seemed to equally contribute to the total relative abundance, with the additional enrichment of bacteria probably derived from the substrate itself.

Although it is not uncommon to inoculate MCF systems with a mixture of inocula sources (Temudo et al. 2008; Guo et al. 2010; Jimenez et al. 2014; C. W. Lin et al. 2011; Du et al. 2015), at the moment of writing it was not possible to find another study investigating whether the community enriched was derived from the combination of those inocula or not. This could be due to the usual enrichment approaches used of sequential transfers until stable degradation/fermentation activity is reached in batch reactors (Kato et al. 2004; Haruta et al. 2002; Ronan et al. 2013; Guo et al. 2010), or until steady state conditions are established in continuous reactors (Temudo et al. 2008; Li Sun et al. 2015; Wu et al. 2017), where the bacterial community composition is only determined at this stage for potential isolation of the most abundant members (Kato et al. 2005; Wahyudi et al. 2010; Zhou et al. 2015), or for the general characterisation of the system (Temudo et al. 2008; Ronan et al. 2013; C. W. Lin et al. 2011). Although this is understandable, since the final community would be the one used for further production, elucidating the mechanisms of enrichment, adaptation and potential enhanced capabilities could also provide more efficient identification of promising communities/species for the transformation of specific lignocellulosic substrates into the desired metabolic product (Garcia et al. 2011; Peacock et al. 2013; Jimenez et al. 2014). Additionally, the initial study of community composition is particularly relevant for mixed-source inocula projects, since the combination of inocula could be not even necessary, thus simplifying the process for future reproducibility.

In this case, although only the R+S community enriched at initial pH 5.5 was analysed, functional redundancy can be assumed from the presence of ruminal and sludge derived OTUs in this enriched community, in addition to the fact that EtOH production by this community was not significantly different to the its maximal and that of rumen when inoculated at initial pH 7.

5.6 Conclusions

The results presented in this chapter confirmed the previous observations of high ethanologenic activity of rumen at initial pH 7 and sludge at initial pH 5.5, revealing that the opposite behaviour in terms of ethanologenic activity as a function of initial pH displayed by these communities was coupled to differences in their bacterial community composition, thus contradicting the proposal that the community composition of MCF can be generally neglected, since soluble end-products formation is mostly driven by the operational environmental conditions.

As expected, the enriched communities' members showed similar functionalities involved in aerobic and anaerobic organic matter degradation. However, the enrichment of OTUs closely related to aerobic species able to detoxify the medium by degrading lignocellulose-derived organic compounds, provides a further explanation for the beneficial effect of initial aerobic conditions in MCF systems.

Thus, it can be concluded that not only the inocula source and initial pH influenced the enrichment of the particular OTUs described, but also the unconditioned pre-treated substrate, due to both, its nutrients composition and the toxic compounds derived from it, Reinforcing the reasons for the dramatic loss of richness observed in all the communities.

Additionally, the statistical analysis from the physicochemical results along with the 16S rRNA gene sequencing analyses, supported the initial hypothesis of this work, as a novel community (R+S) was enriched from the combination of OTUs derived from both original inocula sources, rumen and sludge, showing similar ethanologenic performance under initial acidic and neutral conditions.

The analysis of this results and their comparison against the literature further revealed the presence of putative functional redundancy in all the enriched communities, this was particularly clear in the R+S enrichment, where the ethanologenic activity maintenance at a range of pH (5.5-7), can be attributed to this redundancy.

Although this is a promising result, the usefulness of this community for EtOH production in MCF will depend on the demonstration of its stable ethanologenic activity across transfers. The presence of functional redundancy might provide community composition stability, therefore aiding to this purpose.

It is therefore recommended the utilisation of R+S in following ethanol production studies from OMSW. Based on the results presented in Chapter 4 and here, the best operational conditions for batch reactors inoculated with this community are initial aerobic conditions and initial pH 5.5.

Finally, the quantification of EtOH should be accompanied by that of other soluble fermentation products, most importantly of butyric, acetic and lactic acids, since these seem to be the major fermentation products of the OTUs integrating R+S.

Chapter 6. Transition of microbial communities during the adaptation to fermentation of OMSW at low pH.

6.1 Introduction

In mixed-culture fermentation (MCF) the enrichment of a community with the desired activity through sequential transfers is a common practice as this selective process (Jimenez et al. 2014; D. J. Lee et al. 2013; Varrone et al. 2015), is thought to enrich microorganisms that thrive under the operational conditions while generating the desired product. Transfer times range from hours to days (Varrone et al. 2015; Kato et al. 2004; Ronan et al. 2013; Ganigué et al. 2016). However, few have studied the activity and transformation of the microbial community across transfers (Jimenez et al. 2014; D. J. Lee et al. 2013; Garcia et al. 2011).

Therefore, the work presented in this chapter was carried out to evaluate if the community shown to be enriched from two different inocula sources, namely rumen and anaerobic sludge (R+S), and able to grow in the organic fraction of municipal solid waste as the only carbon and energy source while generating ethanol as its main soluble fermentation product (see previous chapter) is functionally stable through successive transfers. Critically, this community was monitored for changes in its composition to assess which organisms are important in this fermentation system to be able to understand and optimise EtOH production.

6.2 Objectives

- To enrich an efficient and stable ethanologenic bacterial community through successive inocula transfers.
- To monitor the soluble fermentative activity and community composition of the enriched communities within inoculation batches and between transfers.
- To determine the optimal inocula transfer time to maintain high ethanologenic activity.

- To determine the putative functions of individual microorganisms enriched in the successful (in terms of EtOH production and stability) communities.

6.3 Methods

6.3.1 Experimental set-ups

Three independent experiments were carried out to test the stability of the R+S community ethanologenic activity by performing successive inocula transfers (Trⁿ) after initial inoculation (Inoc.) from the seed environments as illustrated by Fig. 6.1.

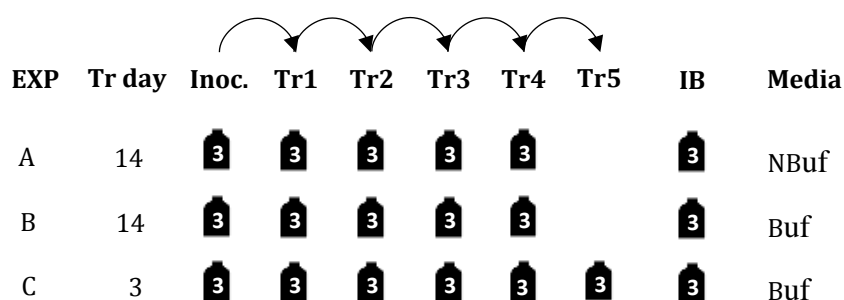


Figure 6.1 Experimental set-up of the different transfer configurations to test the stability of EtOH production by the R+S community. “Tr day” indicates the length of time in days between transfers. The number “3” on top of the bottles indicates the number of replicates (x3). “IB” Inocula blanks”, “NBuf” Non-buffered, “Buf” Buffered.

The transfer time for experimental set-ups A and B was decided based on observations from the experiments described in previous chapters where peak EtOH production occurred at 14 days. Whereas the results from EXPs A and B informed the shorter transfer time used in EXP C. In a similar manner, based on the experimental results from these experimental set-ups, non-buffered and buffered media were tested (see section 6.3.2). All inoculated microcosms, subsequent transfers and inocula blanks for each experiment were conducted in triplicate. Inocula blanks (IB) were microcosms with media and OMSW analogue, but without inocula added.

6.3.2 Microcosms preparation

The methods described in Chapter 3 section 3.3 were followed for microcosms preparation, however, in this case, only non-reduced medium was used for incubation under initial aerobic conditions. Additionally, a filter-sterilised 0.1M bicarbonate-

carbonate buffer (PROMEGA 2012) was used at the beginning of the incubation period in all microcosms for experiments B and C with the aim of adjusting the initial pH of the media to 5.5. In all cases pH was not adjusted again during the incubation period.

The initially inoculated replicates from each experimental set-up were inoculated individually with 2.5g of rumen and sludge, this is ~1.25g of each individual inocula to add up to 2.5g. Successive transfers were then inoculated with 2.5g from their corresponding previous microcosm at the appropriate transfer time (Fig 6.1).

6.3.3 Microcosms incubation and sampling

Microcosms were incubated in the dark, at room temperature (approximately 20°C) under static conditions for 14 days, except for the initial inoculated set of replicates from EXP C, which were incubated for 21 days. Liquid samples were taken on day 0, 7 and 14 from EXPs A and B, and on day 0, 3, 7, 10 and 14 from EXP C for pH measurement and GC-FID EtOH quantification according to section 3.3.3 of Chapter 3. In addition, samples were taken for IC VFAs and molecular biology analyses as described in Chapter 3, sections 3.4.3 and 3.6, respectively.

6.3.4 GC-FID quantification of soluble ethanol

As reported in section 5.3.4 of Chapter 5, although the suitability of highly similar methods for the quantification of alcohols and volatile fatty acids (VFAs) has been reported (X. Lin et al. 2014; Pontes et al. 2009), the detection and repeatability of the GC-FID VFAs quantification became an issue at this stage of this project. However, the quantification of ethanol (EtOH) and butanol (BuOH) was found to be repeatable and linear. Therefore, it was decided to use GC-FID just to quantify alcohols in all the samples.

For quality control, freshly prepared standard solutions of EtOH were quantified at the start and end of each GC-FID analysis run. Furthermore, a 0.8mM solution of 4-methylpentan-2-one puris. p.a., ACS reagent, ≥99.5% (GC) (Sigma-Aldrich, UK) was used as an internal standard added to both, samples and EtOH standards. Otherwise, samples were processed as described in Chapter 3 section 3.3.3.

Although calibration curves were prepared to verify the linearity of the quantification method as previously described in the methods sections of Chapters 4 and 5, the

calculation for EtOH concentration from the experiments described in the present chapter relied on the use of the internal standard (Magee and Herd, 1999) as follows:

- i. Reference standard solutions of internal standard (RIS) and EtOH (RES) were analysed before and after each GC-FID run and their response (r) calculated ($r = \text{Area(mVs)} / \text{Concentration [mM]}$).
- ii. The EtOH relative response was then obtained ($r_{re} = r_{RES} / r_{RIS}$).
- iii. Experimental samples (ex) containing a set volume of internal standard of known concentration (is) were then analysed and their EtOH response determined ($r_{ex} = r_{is} * r_{re}$).
- iv. Finally, EtOH concentrations were calculated ($\text{exEtOH conc. [mM]} = \text{Area} / r_{ex}$).

6.3.5 Statistical analysis of physicochemical data

The method described in Appendix A was followed to conduct the statistical comparison of the EtOH concentration produced across all the successive transfers of the R+S community.

6.3.6 DNA extraction and purification

The method described in Chapter 3, section 3.6.1 was followed using the FastDNA® SPIN Kit for Soil¹ (MP Biomedicals LLC, UK) and DNeasy PowerSoil Kit² (Qiagen, UK) for DNA extraction and purification from samples taken from EXPs A¹ and B¹, as well as EXP C², according to the manufacturers' protocols.

6.3.7 Ion Torrent PGM sequencing pooled library preparation

As described in Section 3.6.4 of Chapter 3, for bacterial community analyses DNA extracts from the samples under analysis from EXPs A and B were subjected to PCR amplification of the V4-V5 region of the 16SrRNA gene using individual Golay barcodes attached to the F515 forward primer. Ion Torrent technology was then used to sequence the samples from replicates of initially inoculated, transfer 1 and transfer 4 at 0, 7 and 14 days from EXPs A and B. This was done to gain a deeper understanding of the change in community composition and the microorganisms responsible for EtOH fermentation across transfers. Table C2 in Appendix C lists the samples from EXPs A and B sent for amplification and the

corresponding sequence of barcodes used. Apart from the samples on Table C2, a procedural blank from each experimental set-up was included for sequencing.

6.3.8 Preparation of samples for MiSeq sequencing

MiSeq synthesis sequencing (Illumina, UK) technology was then used to sequence the samples from EXP C replicates of initially inoculated microcosms at days 0, 3, 7, 10, 14 and 21, as well as of Transfers 1, 3 and 5 at 0, 3, 7 and 14 days (day 3 samples were not taken from Transfer 5 replicates). A procedural blank was included for sequencing. These samples were prepared before submission for analysis according to the method described in Chapter 3 section 3.6.5.

6.3.9 16S rRNA sequencing processing and community composition analyses

The Mothur v.1.39.5 software (Schloss et al. 2009) was used to quality filter, remove potential chimeras and non-bacterial or archaeal sequences, and cluster into OTUs the sequences of the individual set-ups through a distance matrix where any pairwise distance larger than 0.15 was eliminated, after which the rarefaction of all the libraries to the smallest library count was then performed following the 454 or Miseq standard operational procedures (SOP) for Ion Torrent or Miseq sequencing data of the software creators (Schloss et al. 2011; Kozich et al. 2013). The OTUs (selected at 97% similarity) and associated files generated were then used to conduct ecological and ordination analyses following the workflow described in section 3.7 in Chapter 3.

The individual OTUs/abundance rarefied data sets were imported into PRIMER 7 software (Primer-E Ltd., Plymouth, UK) to compute the Bray Curtis similarity matrix between each rarefied sample. The Bray-Curtis similarities were then used within PRIMER 7 to produce an nMDs ordination plot and sample cluster tree graph integrated into a shade plot. A non-parametric ANOSIM test was used to evaluate the statistical significance ($\geq 0.1\%$ significance level of sample statistic) of community composition differences between groups of samples. For groups that were found to be significantly different, SIMPER analysis was conducted to identify both, the most abundant OTUs integrating each sample, as well as the discriminatory OTUs between the sample groups,

accumulatively contributing to 70% of the total similarity or dissimilarity between groups, respectively.

Additional to the taxonomy assignments (up to genus level) for the OTUs made by Mothur (using the Silva database release 128), the most abundant representative sequence within each OTU was aligned against the 16S rRNA sequences (Bacteria and Archaea) GenBank database using the megablast algorithm (Boratyn et al. 2012).

6.3.10 Preparation of samples for Thermogravimetry-Differential Scanning Calorimetry-Quadrupole Mass Spectrometry (TG-DSC-QMS) of Exp B

To broadly assess organic matter degradation by the R+S community, TG-DSC-QMS was conducted to characterise carbon composition of the OMSW after incubation of Exp B microcosms as this technique has been shown to be adequate to differentiate between cellulose-like and lignin-like organic carbon components in soils and organic waste (Lopez-Capel et al. 2005; Blake et al. 2017; Pietro and Paola 2004).

For preparation, samples taken after the incubation period from the replicates of initially inoculated microcosms and from the inocula blanks from EXP B were freeze dried for 24h followed by cryogenic grinding for 3 min at 10rps in a Spex mill 6750 freezer mill (Thermo Fischer, UK) after prior emersion in liquid nitrogen (1 min). Samples (1g) were then submitted for TG-DSC-QMS analysis at the Geochemistry Laboratory, Newcastle University, where a Netzsch JupiterSTA 449C instrument with helium/oxygen (80%/20%) as the carrier gas mix flowing at 30 ml/min for a heating cycle from 25 to 900 °C at a ramping rate of 10 °C/min, was employed to conduct this analysis.

See Appendix D for details of the analysis of these results.

6.4 Results

6.4.1 Soluble fermentation products across 14-days transfers (Exp A)

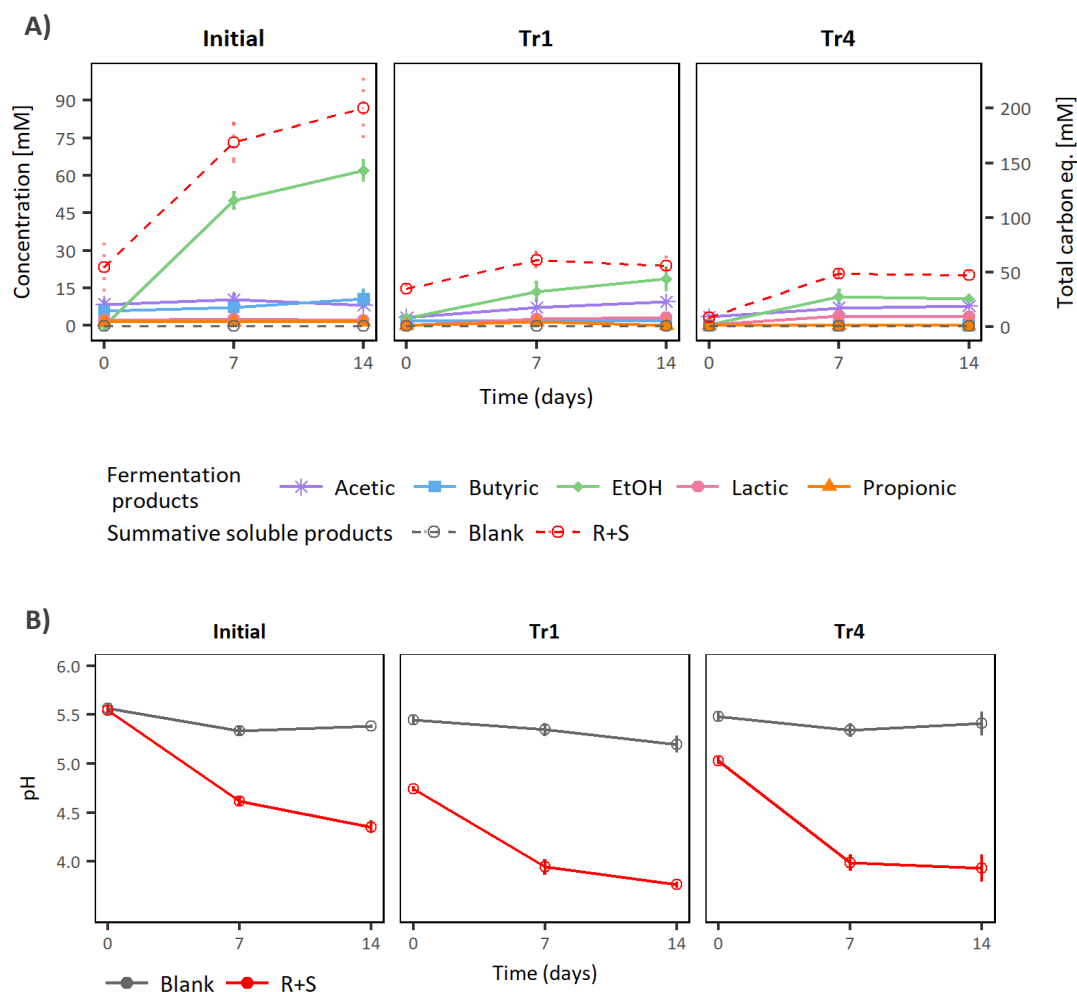


Figure 6.2 Exp A. A) Fermentation products by the R+S community across transfers tested during 14 days of incubation with no carbonate buffer addition. The summative measured soluble fermentation products line represents the total milliequivalents of soluble carbon produced in each transfer. B) pH profiles from the R+S inoculated microcosms and the inocula blanks across the different transfers.

After 14 days, the initially inoculated microcosms reached a peak EtOH concentration of $62.05\text{mM} \pm 4.55\text{mM}$, with EtOH being the major fermentation soluble product generated. However, the high ethanologenic activity decreased dramatically across transfers (Fig. 6.2), peaking at $18.63\text{mM} \pm 4.99\text{mM}$ after 14 days in Tr1 and $11.61\text{mM} \pm 2.49\text{mM}$ in Tr4. This is only 30.02% and 18.71% of the EtOH production observed in the initial inoculation, respectively.

From the other soluble fermentation products quantified, acetic acid reached peak concentrations of $7.42\text{mM} \pm 1.99\text{mM}$ (in. inoc at 7 days), $6.28\text{mM} \pm 0.69\text{mM}$ (Tr1) and $4.80\text{mM} \pm 0.78\text{mM}$ (Tr4). While butyric acid was only produced in the initial inoculated

microcosms and the first transfer, with maximal production of $10.63\text{mM} \pm 3.94\text{mM}$ and $2.17\text{mM} \pm 0.21\text{mM}$, respectively. Lactic acid production behaved similarly across transfers, with peak concentrations of $2.60\text{mM} \pm 0.84\text{mM}$, $3.39\text{mM} \pm 0.44\text{mM}$ and $3.55\text{mM} \pm 0.29\text{mM}$. Propionic acid was only detected in the initially inoculated and Tr1 microcosms generating low maximal concentrations of $1.47\text{mM} \pm 0.06\text{mM}$ and $1.43\text{mM} \pm 0.31\text{mM}$, respectively.

Importantly, the maximal total productivity in terms of carbon milliequivalents (Fig. 6.2, A: summative soluble products) decreased in the same fashion as EtOH production decline across transfers, going from $200.36\text{mM} \pm 27.64\text{mM}$ during the initial inoculation to $49.10\text{mM} \pm 27.64\text{mM}$ in the last transfer, losing up to 75.49% of total productivity.

Similarly, estimations of maximal total productivity in terms of electron milliequivalents showed a decreasing trend across transfers, going from initial $1101.39 \pm 144.86 \text{ e}^- \text{ meq./L}$ to $383.16 \pm 63.44 \text{ e}^- \text{ meq./L}$ after 14 days in Tr1 and $232.99 \pm 26.08 \text{ e}^- \text{ meq./L}$ in the last transfer. Nevertheless, the proportion of electrons used to produce EtOH did not varied drastically ($68.70 \pm 4.17\%$, $56.43 \pm 6.23\%$, $54.04 \pm 4.38\%$, respectively), thus suggesting a general loss of metabolic activity as opposed to a change of fermentative pathways.

However, testing the latter hypothesis would require further experimentation, for instance, measurements of other fermentation products such as gas production (e.g. CO_2 , H_2), bacterial growth (e.g. cell numbers determination via flow cytometry) and substrate degradation (e.g via BMP), which were not conducted during this project, but would highly improve the understanding of these observations through a more complete mass balance analysis of the system.

Although the initial pH of all the microcosms was adjusted to 5.5 before inoculation, the addition of inocula to the transfers caused a drop in the initial pH of about ~ 0.5 pH units (Fig 6.2 B: Tr1 and Tr4). A 2-way-ANOVA followed by A Tukey HDS test were computed, confirming the significant difference not only between the originally inoculated microcosms and the transfers (In. inoc-Tr1 p -value $2.4\text{e-}5$, In. inoc-Tr4 p -value $3.1\text{e-}4$), but also between the Tr1 and Tr4 (p -value 0.007).

The significant difference between transfers and the originally inoculated microcosms (2-way ANOVA followed by TukeyHSD test p -value <0.05) could be caused by the type of inocula used, this was sludge and rumen which both had close to neutral pH values,

probably therefore not altering that of the initial culture media. The transfers, however, were inoculated with growth media with a pH of about 4.5.

The inocula blanks maintained a pH close to 5.5 across all transfers. In agreement, their maximal productivity in terms of soluble carbon milliequivalents reached about 1mM in all stages of this experimental set-up.

Based on these observations, it was hypothesised that the general loss of fermentative activity could have been caused by the significantly lower initial pH of the transfers and that further pH adjustment after inoculation would improve the production of soluble fermentation products.

This hypothesis was therefore tested in a similar (x3) experimental set-up (Exp B), where transfer media initial pH was adjusted after inoculation using a carbonate buffer (pH range 9.2-10.8) (PROMEGA 2012). This buffer was chosen for pH adjustment over a strong base (e.g. NaOH) to avoid affecting the microorganisms recently inoculated and because there was a low chance of its components being used as carbon or energy source (Ghafari et al. 2009).

6.4.2 Soluble fermentation products across 14-days transfers with initial pH amended after inoculation (Exp B)

As for Exp A, in this experimental set-up, where the transfer microcosms initial pH was adjusted to 5.5 after inoculation, EtOH production was dominant in the initial inoculation, however, a similar pattern of fermentative activity loss was observed across transfers (Fig. 6.3).

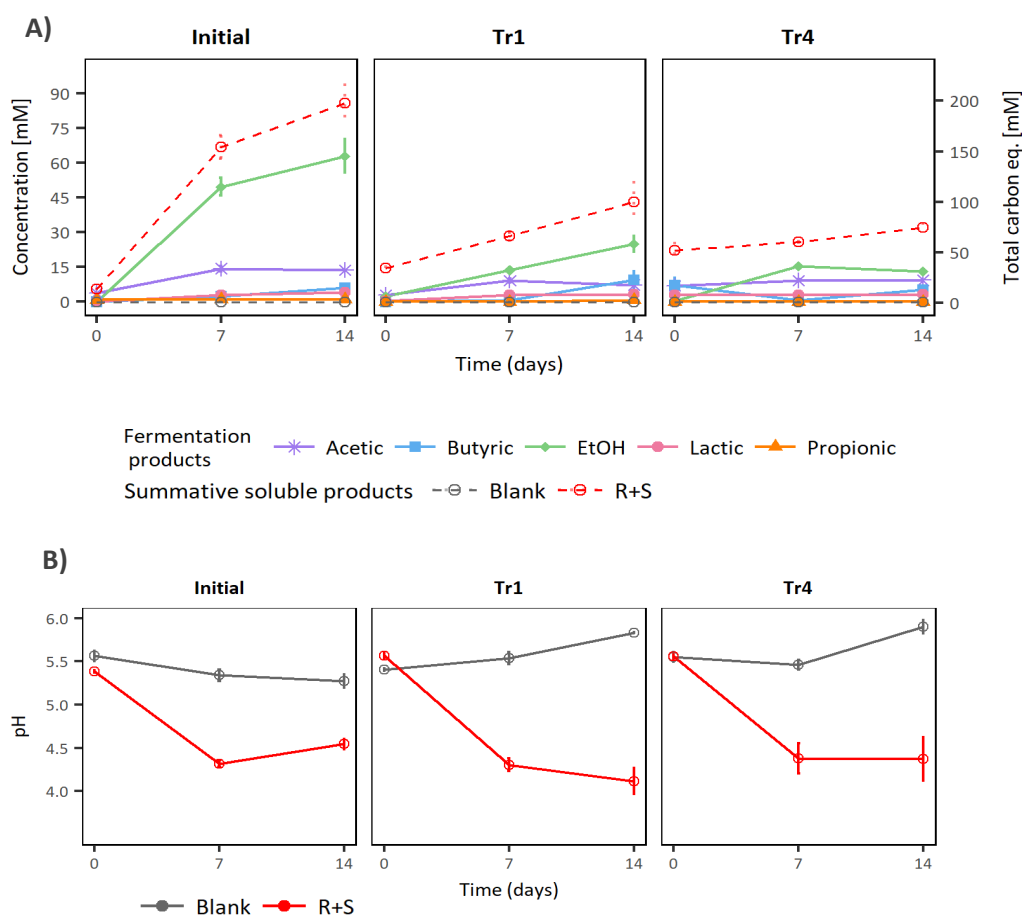


Figure 6.3 Exp B. A) Fermentation products by the R+S community across transfers tested during 14 days of incubation and initial carbonates buffer addition. The summative measured soluble fermentation products line represents the total milliequivalents of soluble carbon produced in each transfer. B) pH profiles from the R+S inoculated microcosms and the inocula blanks across the different transfers.

More specifically, the initially inoculated microcosms reached a peak EtOH concentration after 14 days of incubation of $62.96\text{mM} \pm 7.77\text{mM}$, with EtOH also being the major fermentation soluble product generated. However, the high ethanologenic activity also decreased dramatically across transfers, peaking at $25.02\text{mM} \pm 4.03\text{mM}$ after 14 days in Tr1 and $15.34\text{mM} \pm 1.95\text{mM}$ in Tr4 after 7 days, this is only 39.74% and 24.36% of the production observed in the initial inoculation, respectively.

Acetic acid was the second major soluble fermentation product with peak concentrations of $10.75\text{mM} \pm 0.41\text{mM}$ (in. inoc), $4.32\text{mM} \pm 1.41\text{mM}$ (Tr1) and $6.34\text{mM} \pm 0.35\text{mM}$ (Tr4). While butyric acid maximal production in each transfer was $5.98\text{mM} \pm 0.76\text{mM}$, $9.49\text{mM} \pm 4.18\text{mM}$ and $5.14\text{mM} \pm 2.01\text{mM}$. Lactic acid production remained relatively stable across transfers, with peak concentrations of $4.1\text{mM} \pm 0.38\text{mM}$, $3.23\text{mM} \pm 1.07\text{mM}$ and $3.11\text{mM} \pm 0.95\text{mM}$. Propionic acid was only detected in the initially inoculated and Tr1

microcosms, generating low maximal concentrations of $1.05\text{mM}\pm0.06\text{mM}$ and $0.67\text{mM}\pm0.33\text{mM}$, respectively.

The maximal total productivity in terms of carbon milliequivalents (Fig. 6.3, A: summative measured soluble products) decreased across transfers, going from $197.26\text{mM}\pm19.98\text{mM}$ during the initial inoculation to $99.71\text{mM}\pm20.78\text{mM}$ in the first transfer and then to $74.83\text{mM}\pm4.75\text{mM}$ in the last transfer, losing first 49.45% to up to 60.03% of total productivity, showing a slight improvement from Exp A results.

Estimations of maximal total productivity in terms of electron milliequivalents also showed a decreasing trend across transfers, going from initial $1071.41 \pm 114.21 \text{ e}^- \text{ meq./L}$ to $596.76 \pm 104.06 \text{ e}^- \text{ meq./L}$ after 14 days in Tr1 and $372.36 \pm 24.04 \text{ e}^- \text{ meq./L}$ in the last transfer. Similar to Exp A results, the proportion of electrons used to produce EtOH ($70.24 \pm 1.37\%$, $51.20 \pm 4.47\%$, $42.91 \pm 4.88\%$, respectively), suggested a general loss of metabolic activity as opposed to a change of fermentative pathways.

A 2-way-ANOVA (p -value 0.06) confirmed, albeit with borderline significance, that the initial pH values across transfers were not significantly different as suggested in Fig. 6.3 B.

6.4.3 TG-DSC analysis of OMSW after initial inoculation in Exp B

The organic carbon decomposition process in the TG-DSC analyses of the OMSW remaining after incubation for 14 days as part of either initially inoculated and Tr₄ microcosms, as well as of the initial and Tr₄ inocula blanks in Exp B, occurred mainly in four stages: $\sim 200\text{-}390^\circ\text{C}$, $\sim 390 - 480^\circ\text{C}$, $\sim 480 - 520^\circ\text{C}$, and $\sim 520 - 610^\circ\text{C}$. Modest but clear differences in these temperature ranges were only observed for the OMSW from initially inoculated microcosms mostly from the second stage onwards, with ranges of $389\text{-}470^\circ\text{C}$, $470\text{-}506^\circ\text{C}$ and $506\text{-}583^\circ\text{C}$, possibly indicating smaller fractions of organic matter to be combusted at these ranges, in comparison to that of the other treatments. In all cases, the fixed solids content (residual mass) was obtained after combustion at 397°C .

Each of these temperature ranges can be associated to the loss of certain category of organic carbon compounds (Lopez-Capel et al. 2005; Pietro and Paola 2004; Blake et al. 2017), where the first of these corresponds to labile matter mostly comprised by compounds like aliphatic and carboxylic groups (Lopez-Capel et al. 2005; Blake et al. 2017). The second and third temperature ranges are associated to the loss of refractory hemicellulose-like and cellulose-like

organic carbon fractions, respectively (Pietro and Paola 2004; Lopez-Capel et al. 2005). The fourth temperature range represents the mass loss of refractory organic matter, such as lignin-like compounds (Lopez-Capel et al. 2005; Pietro and Paola 2004; F. Guo et al. 2016).

Modest differences in the percentage of mass loss were observed between treatments, where OMSW from initial inocula blanks, Tr₄ inocula blanks as well as Tr₄ microcosms all had 58% of labile organic content losses against the 55% found for OMSW in initially inoculated microcosms. Regarding the hemicellulose-like fraction, OMSW from both, initially and Tr₄ inoculated microcosms had a mass loss of 12%, whereas their corresponding inocula blanks lost 14% and 15% of mass respectively. All treatments had a cellulose-like mass loss of 3.4%. The lignin-like fraction mass loss of initial and Tr₄ inoculated microcosms was of 5.9%, while that of the corresponding blanks was of 6.3% and 7.3% respectively.

The OMSW from initially inoculated microcosms showed slightly but distinctively smaller mass losses of labile, hemicellulose-like and lignin-like compounds, and the highest fixed solids content (15.6 %) among the different treatments, suggesting the active degradation of solid OMSW. However, the apparently modest consumption of the solid OMSW could also be due to the liable organic content present in the liquid medium released from the solid substrate after the steam pre-treatment (7857mg_{Carbon_eq}/L COD).

Since the OMSW from Tr₄ microcosms had a closer TG-QMS profile to that of the inocula blanks, than to the initially inoculated microcosms, these results further support the previously stated hypothesis of loss of activity by the end of the 14-days transfer process.

See Appendix D, Table D1 for the detailed results of TG-DSC analysis.

6.4.4 Statistical comparison of maximal fermentative production at the different transfers in Exps A and B

The maximal values of EtOH production during the different transfers in Exps A and B were statistically compared to assess whether the initial pH adjustment had indeed caused an improvement in the ethanologenic or total fermentative productivity. 2-way ANOVA analyses was conducted to quantitatively assess these observations.

Regarding maximal EtOH production across experimental set-ups and transfers, it was concluded that in general the maximal EtOH concentrations between experimental set-

ups were not significantly different (p -value 0.403), however, significant differences were caused by the transfers (p -value $2.84\text{e-}07$ ***).

A Tukey HDS test was then computed to determine the differences in maximal EtOH concentration between corresponding transfers from the two experimental set-ups, with no significant difference found between any of these pairs (A:Initial-B:Initial, A:Tr1-B:Tr1, A:Tr4-B:Tr4 p -value >0.9).

A similar statistical analysis was then conducted to compare maximal total productivity in terms of carbon milliequivalents between experimental set-ups. The 2-way-ANOVA results showed no statistical difference between both experiments (p -value 0.128), but differences at transfer level were found (p -value $5.51\text{e-}06$ ***). The subsequent Tukey HDS test between corresponding transfers from the two experimental set-ups also revealed no significant difference in the maximal total fermentative productivity obtained in Exps A and B (A:Initial-B:Initial p -value 0.99, A:Tr1-B:Tr1 p -value 0.49, A:Tr4-B:Tr4 p -value 0.86).

Based on these results the hypothesis of initial pH differences driving the loss of ethanologenic or fermentative activity was rejected.

Additional experimental set-ups testing the addition of trace minerals and abiotic inocula matrix (autoclaved original inocula sources) were conducted without a successful maintenance of fermentative activity after the first transfer. As the physicochemical variables tested did not contribute to an advancement in the results, it was decided to analyse the microbial community composition of Exps A and B and determine if changes in the communities from the different transfers could help in the understanding of the activity loss observed.

6.4.5 Community composition indices of 14-day transfers

The libraries obtained after 16S rRNA NGS sequencing of samples taken at the beginning of each transfer(day 0), and after 7 and 14 days of incubation from the replicates of both experimental set-ups (A and B) were quality processed as described in sections 3.7 and 5.39 of this thesis to obtain the relative abundances and distributions of identified operational taxonomic units (OTUs) across the different microbial communities enriched in these systems.

To obtain an overview of the microbial communities composition enriched, these OTUs and their abundances were used to compute some general diversity metrics, namely, richness (S), diversity (Simpson's inverse diversity, D) and evenness (Simpson's evenness, E) indices (Fig. 6.4).

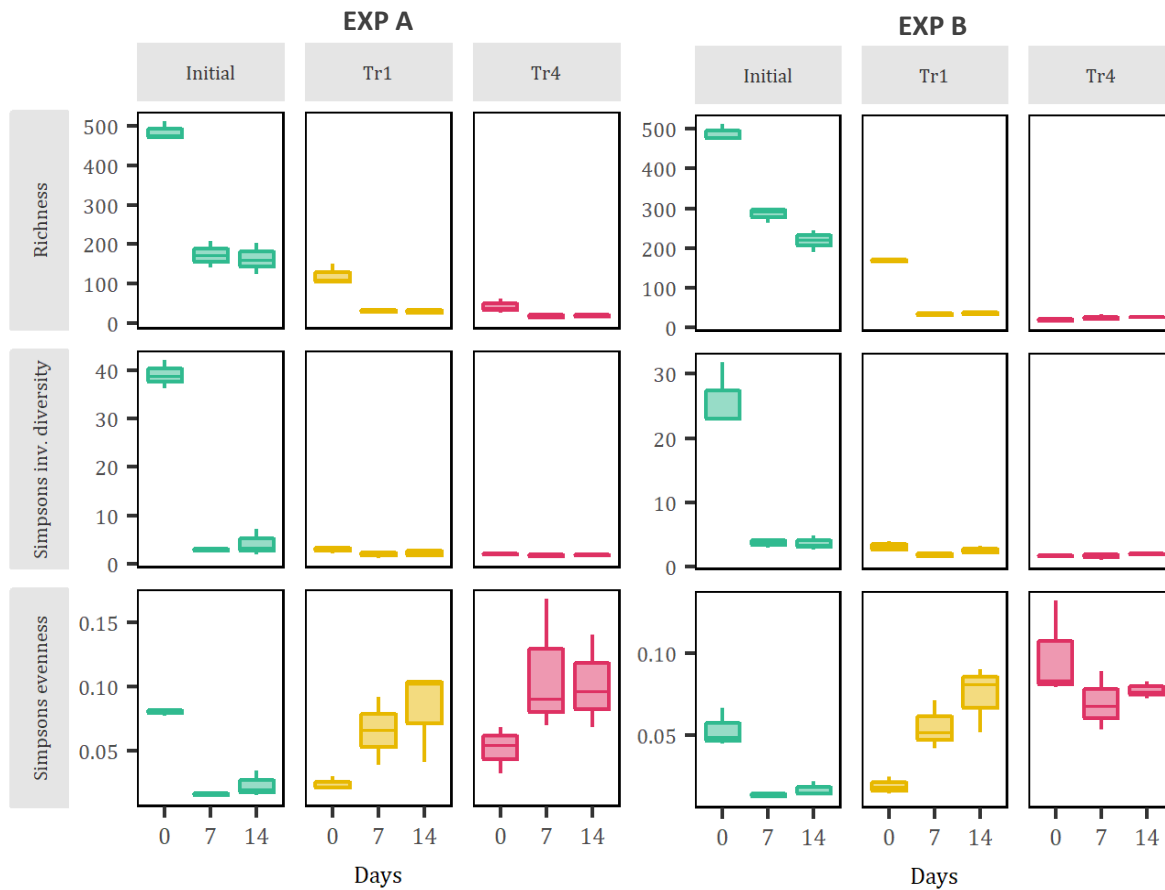


Figure 6.4 A) ExpA richness, Simpson's inverse diversity and Simpson's evenness indices of the communities at the different sampling days across transfers represented as boxplots. B) The same microbial composition indices are displayed for the communities enriched in ExpB.

In both experimental set-ups a loss of richness and diversity was observed over time (principally in the first 7 days) and between the initially inoculated microcosms and the first transfer. Regarding richness, specifically, from the original 486 ± 13 OTUs present in the initially inoculated microcosms in EXP A, only 163 ± 22 OTUs were abundant at 14 days. From these, an average of 120 ± 15 OTUs were transferred into Tr1 in which only 28 ± 4 OTUs were found to be abundant by the end of its incubation period. Tr4 was only inoculated with 43 ± 1 OTUs and finished with only 19 ± 4 OTUs.

Similarly, for the initially inoculated Exp B microcosms, richness notably decreased after 14 days of incubation (by about 270 OTUs), with most of the loss occurring in the first 7

days. The first transfer experienced an average loss of about 133 ± 14 OTUs after 14 days of incubation. Tr4 richness slightly increased with time to 26 ± 10 OTUs by the end of its incubation period after being only inoculated with 19 ± 2 OTUs.

Likewise, the diversity in ExpA dramatically decreased from an initial inoculation with 40 different and abundant OTUs to a community seemingly comprised of only 2 OTUs by the end of Tr4. While ExpB initial inoculation with 26 different OTUs concluded with a 2 member community as well. In the light of these results, the apparent evenness increase tendency observed in both experimental set-ups (Fig. 6.4) can be attributed to the probable dominance by 2 OTUs by the end of the transfers incubation.

Although the decrease in richness and diversity could suggest the enrichment of OTUs fitted to grow under the specific initial conditions and utilise OMSW as substrate. These results along with those of loss of fermentative activity (Figs. 6.2 and 6.3) probably indicate the absence of growth, particularly after transfer from the initially more active inoculated microcosms in both experimental set-ups.

To broadly evaluate whether the loss of richness and diversity was mostly due to the absence of growth rather than dramatic enrichment of particular taxa, the quantities of 16sRNA amplicons for each time point across transfers in both experimental set-ups was compared. Post-incubation DNA average concentrations (ng/mL) in Tr4 was found to be about 10% of that from the initially inoculated microcosms. Nevertheless, DNA average concentrations were overall higher in ExpB (~60%) possibly indicating a positive effect in growth by the initial pH adjustment performed post-inoculation in these microcosms.

6.4.6 Ordination and statistical comparison of the communities in 14-days transfers

nMDS ordination plots of EXPs A and B were computed to evaluate if the replicates clustering would reveal distinct community compositions across transfers (Fig. 6.5).

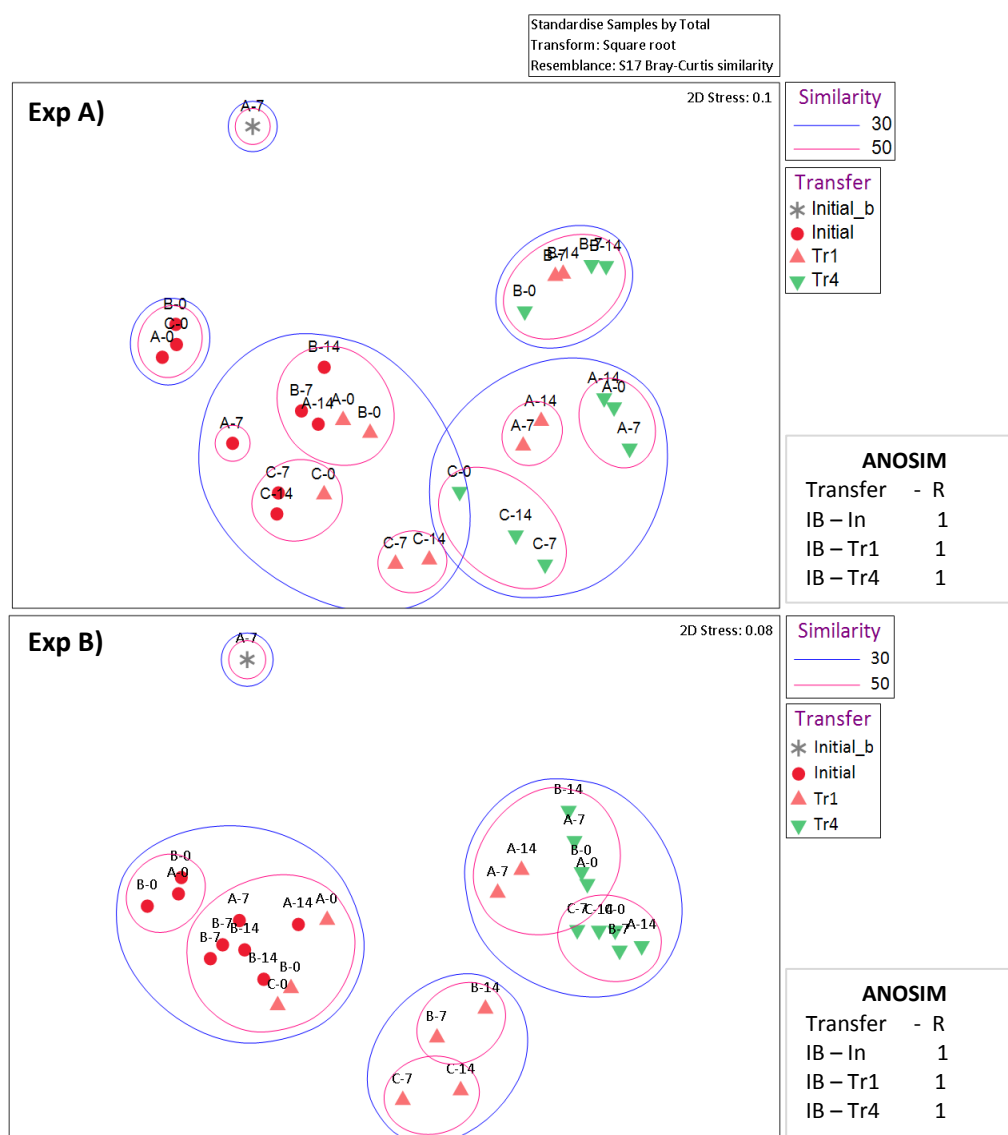


Figure 6.5 A) and B) nMDS representation of the relatedness of microbial communities in Exp A and Exp B replicates including an inocula blank. In all plots, the letters on top of the keys (A,B, C) are used to differentiate individual replicates, they are followed by numbers (0,7,14) indicating the days of incubation at which the samples were taken. Samples with 30% and 50% similarity are encircled by a purple or pink line, respectively. 2D stress values indicate good representation of the data on these 2D nMDS plots. ANOSIM R values (0.1% significance level) shown to the right of the plots correspond to pairwise comparison of the inocula blank (IB) vs the individual transfers, where 1 indicates high separation or dissimilarity between clusters.

Most of the sets of replicates for the transfer groups from Exp A did not cluster in clear separate groups relating to either transfer or sampling day (Fig 6.5-A). Nevertheless, a distinct cluster was formed by the replicates of the initially inoculated microcosms at day

0, sharing at least 50% community composition similarity. The replicates from this initial inoculation at both following sampling days clustered with the day 0 samples from Tr1, sharing at least 30% community composition similarity, which could be expected as the community members of Tr1 proceeded directly from them, however, while one of Tr1 replicates (“c”) was part of this cluster, the other two formed separate clusters with Tr4 samples, sharing at least 30% similarity. This ordination indicates that divergence between replicates directed the clustering of samples rather than transfer number or sampling day.

Meanwhile, a distinct cluster was formed by the replicates of the initially inoculated microcosms from Exp B at day 0, sharing at least 50% similarity (Fig 6.5-B). The replicates from this initial inoculation at both following sampling days clustered with the day 0 samples from Tr1, sharing at least 50% community composition similarity. Two of Tr1 replicates from the subsequent sampling days formed a separate cluster sharing at least 30% similarity, while the third of these replicates clustered with Tr4 samples, sharing at least 30% similarity.

In both ordination plots the inocula blank was confined to its own region of the plot indicating its marked different composition from the rest of the samples as confirmed by the ANOSIM test (Fig 6.5).

ANOSIM tests were then conducted to assess if the clusters in the nMDS plots were statistically different, thus indicating if the community composition of each transfer varied significantly. Details of the relevant results can be found in (Table 6.1).

Table 6.1. Exps A and B pairwise comparisons of sampling points within and between transfers of each experimental set-up as determined by ANOSIM test

EXP A. Pairwise comparisons	ANOSIM R	EXP B. Pairwise comparisons	ANOSIM R
Within transfers sampling points			
Initial 0 – Initial 7	1	Initial 0 – Initial 7	1
Initial 0 – Initial 14	1	Initial 0 – Initial 14	1
Initial 7 – Initial 14	-0.037	Initial 7 – Initial 14	0.815
Tr1 0 – Tr1 7	0.370	Tr1 0 – Tr1 7	0.667
Tr1 0 – Tr1 14	0.444	Tr1 0 – Tr1 14	0.963
Tr1 7 – Tr1 14	-0.296	Tr1 7 – Tr1 14	-0.296
Tr4 0 – Tr4 7	-0.296	Tr4 0 – Tr4 7	-0.074
Tr4 0 – Tr4 14	-0.407	Tr4 0 – Tr4 14	-0.111
Tr4 7 – Tr4 14	-0.37	Tr4 7 – Tr4 14	-0.259

Between transfers at the same time points			
Initial 0 – Tr1 0	1	Initial 0 – Tr1 0	1
Initial 0 – Tr4 0	1	Initial 0 – Tr4 0	1
Tr1 0 – Tr4 0	0.889	Tr1 0 – Tr4 0	1
Initial 7 – Tr1 7	0.704	Initial 7 – Tr1 7	1
Initial 7 – Tr4 7	0.815	Initial 7 – Tr4 7	1
Tr1 7 – Tr4 7	0.037	Tr1 7 – Tr4 7	0.556
Initial 14 – Tr1 14	0.63	Initial 14 – Tr1 14	1
Initial 14 – Tr4 14	0.778	Initial 14 – Tr4 14	1
Tr1 14 – Tr4 14	-0.037	Tr1 14 – Tr4 14	0.148
Initial 14 – Tr1 0 ^a	0.148	Initial 14 – Tr1 0 ^a	-0.074

ANOSIM R values ($\geq 0.1\%$ significance level) range from 0 to 1, where 1 indicates high separation or dissimilarity between clusters. ^aPairwise comparisons between initially inoculated microcosms at 14 days and Tr1 at inoculation day.

ANOSIM values for both experimental set-ups showed a clear dissimilarity between transfers at day 0 as well as between the initially inoculated microcosms and the initial and last transfer after 7 days of incubation. However, the separation is vague within transfers and their different sampling points, with a number of them obtaining negative ANOSIM *p*-values, which have been reported to be indicative of the high variability of the data and possibly the irrelevance of the factor being investigated as a driver of dissimilarity (Chapman and Underwood 1999). In this case, the said irrelevance can be attributed to the nature of the experiments, whereby the community composition of the transfer was conditional being directly dependent on a previous one (e.g. Tr1 depended from initially inoculated), therefore some degree of similarity was to be expected. Nevertheless, the high variability observed from day 7 to day 14 for Tr1 and within all the sampling points of Tr4 of both experimental set-ups remained unclear. Accordingly, further analysis of the samples in terms of their individual OTUs was conducted.

6.4.7 Specific bacterial OTUs typical of the different 14-days transfers

The most frequent and abundant OTUs for each group of replicates (transfer x sampling day) were determined using the similarity percentages (SIMPER) test on the Bray-Curtis similarity matrix indices. Before the resemblance matrix computation, the data set was standardised, and square root transformed, as previously described in sections 5.3.9 and 3.7.9 of this thesis. Additionally, under the assumption that the most abundant OTUs are the most active within a community, the transformed data set was filtered (Clarke and Gorley, 2015) to only consider OTUs accounting for $>1\%$ percent of the total number of

individuals in each sample. Figure 6.6 offers a simple visualisation of the results from this test.

Based on the physicochemical results as well as the nMSD plots and ANOSIM results, the inocula blank was not included in the SIMPER analysis to simplify the interpretation of these analyses, as only one of the replicates had a sequence library large enough in comparison to the others (above 1000 reads) to be accounted for in the libraries normalisation.

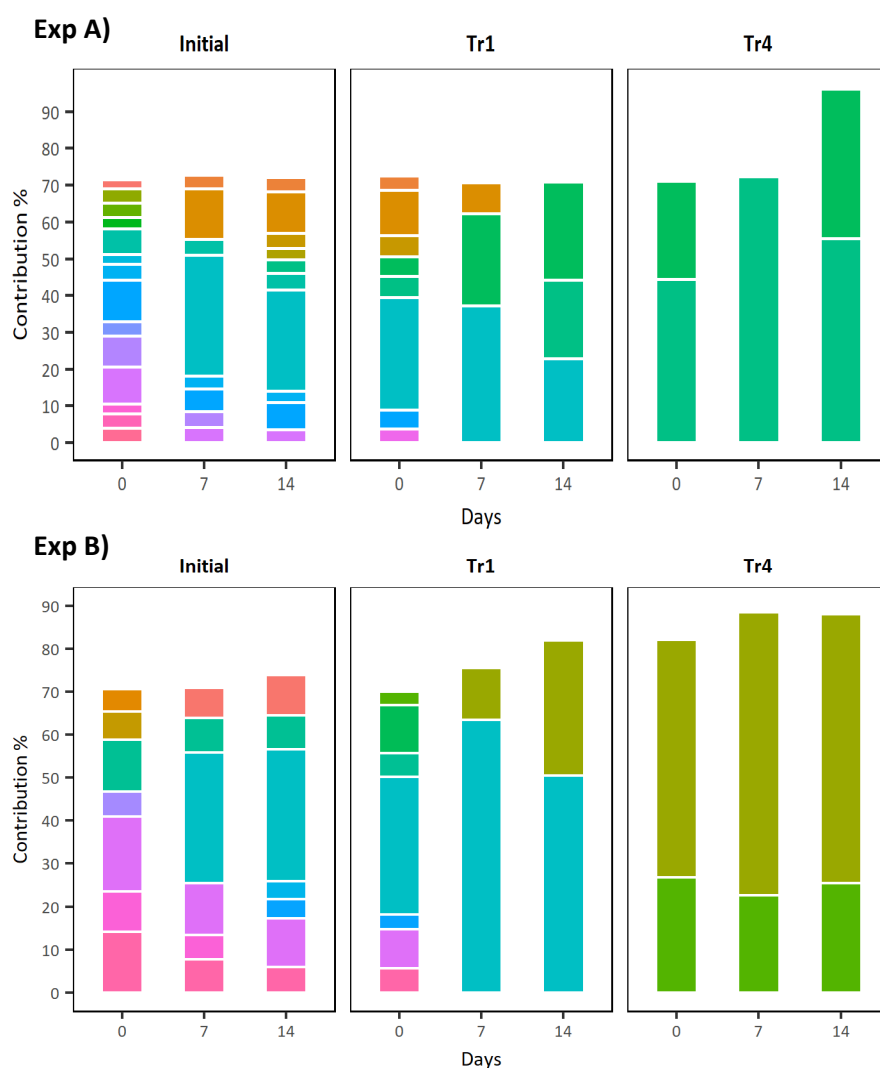


Figure 6.6 Stacked bar plots with different colours representing the average number of individual OTUs accounting for at least 70% of the cumulative similarity in each transfer/sampling day group from Exp A and Exp B. No taxa assignments are included in this graphic representation of abundance.

In agreement with the richness and diversity indices reported before, the successive transfers communities were less rich over time, this being particularly clear for the last transfer, where effectively 2 OTUs represented more than 90% of the cumulative

similarity by the end of both experimental set-ups. It is also worth noticing that despite the higher number of OTUs contributing to the total community similarity in the initial inoculated microcosms from Exp A (14 OTUs) compared against those of Exp B (7 OTUs), the ethanologenic activity by the enriched communities after 7 and 14 days was not significantly different, suggesting not all OTUs present in the initial inoculation of Exp A were crucial for the high EtOH production observed in these systems.

Tables 6.2 and 6.3 present a detailed list of the OTUs that contributed the most to the average composition of each sampling day group in the initially inoculated microcosms and transfers from both experimental set-ups in descending order (Con.%), as well as the ratio of the average contribution divided by the standard deviation of those contributions across all sample pairs in each group (Sim/SD). The latter allowed the identification of OTUs that contributed consistently to the average bacterial composition of each group of replicates. The identity of each OTU is the closest similar species (>97% sequence identity match, where possible) found after the individual sequences were megablasted in the GenBank database (Boratyn et al. 2012) as described in section 5.3.9. The average similarity of each group along with the cut-off cumulative similarity (>70%) of the OTUs listed is also presented.

Table 6.2. Most frequent and abundant OTUs found in each sampling point from the initially inoculated microcosms from experimental set-ups A and B as determined by SIMPER test

Exp A - Initial com. - 0 days Average similarity: 87.61 Cumulative similarity: 71.54				Exp B - Initial com. - 0 days Average similarity: 90.43 Cumulative similarity: 70.63			
OTU	Identity	Sim/SD	Con.%	OTU	Identity	Sim/SD	Con%
7	<i>Petrimonas</i>	14.84	11.34	5	<i>Petrimonas</i>	9.57	17.55
9	<i>Ruminococcus</i>	127.83	10.12	10	<i>Ruminococcus</i>	319.76	14.18
11	<i>Pseudomonas c.</i>	8.15	8.52	8	<i>Leptolinea</i>	28.23	11.98
10	<i>Leptolinea</i>	26.67	6.96	12	<i>Pseudomonas c.</i>	5.4	9.26
15	<i>Methanobacterium</i>	38.98	4.29	14	<i>Ignisphaera</i>	75.37	6.67
22	<i>Turicibacter</i>	34.69	3.95	18	<i>Paludibacter</i>	20.5	5.85
27	<i>Syntrophomonas</i>	36.9	3.95	23	<i>Flintibacter</i>	21.19	5.14
23	<i>Flintibacter</i>	26	3.89				
20	<i>Gracilibacter</i>	136.71	3.88				
26	<i>Prevotella</i>	11.04	3.82				
18	<i>Ignisphaera</i>	4.29	3.09				
48	<i>Aminivibrio</i>	10.21	2.64				
16	<i>Levilinea</i>	13.85	2.59				
38	<i>Syntrophobotulus</i>	51.9	2.51				

Exp A – Initial com. – 7- days Average similarity: 78.57 Cumulative similarity: 72.61				Exp B – Initial com. - 7 days Average similarity: 89.16 Cumulative similarity: 70.97			
OTU	Identity	Sim/SD	Con.%	OTU	Identity	Sim/SD	Con%
1	<i>Leuconostoc m.</i> ▲+7.2	40.83	32.79	2	<i>Leuconostoc m</i> ▲+7	29.69	30.54
6	<i>Clostridium s.</i> ▲+3.3	29.13	13.62	5	<i>Petrimonas</i> ▼-0.9	26.16	11.95
7	<i>Petrimonas</i> ▼-1.3	4.57	6.33	8	<i>Leptolinea</i>	9.19	7.96
10	<i>Leptolinea</i> ▼-0.6	4.36	4.43	10	<i>Ruminococcus</i> ▼-1	8.18	7.75
11	<i>Pseudomonas c.</i> ▼-1.5	12.26	4.21	7	<i>Clostridium s.</i> ▲+1.7	9.82	7.08
9	<i>Ruminococcus</i> ▼-1.7	33.13	4.16	12	<i>Pseudomonas c.</i> ▼-0.8	21.15	5.68
13	<i>Clostridium b.</i> ▲+1.3	1.43	3.69				
15	<i>Methanobacterium</i>	3.44	3.38				
Exp A – Initial com. - 14 days Average similarity: 69.20 Cumulative similarity: 72.05				Exp B – Initial com. - 14 days Average similarity: 76.57 Cumulative similarity: 73.96			
OTU	Identity	Sim/SD	Con.%	OTU	Identity	Sim/SD	Con%
1	<i>Leuconostoc m.</i> ▼-0.6	4.14	27.47	2	<i>Leuconostoc m.</i> ▼-0.1	9.58	30.81
6	<i>Clostridium s.</i> ▼-0.7	11.27	11.37	5	<i>Petrimonas</i> ▼-0.3	65.88	11.33
7	<i>Petrimonas</i> ▼-0.1	23.63	7.38	7	<i>Clostridium s.</i> ▲+0.6	7.97	9.47
10	<i>Leptolinea</i> ▼-0.2	26.12	4.6	8	<i>Leptolinea</i>	10.43	7.8
12	<i>Clostridium t.</i> ▲+1.3	1.36	4.06	10	<i>Ruminococcus</i> ▼-0.6	46.88	5.9
13	<i>Clostridium b.</i> ▼-0.1	4.14	3.79	13	<i>Methanobacterium</i>	10.99	4.53
5	<i>Lactobacillus c.</i> ▲+1.5	0.58	3.59	11	<i>Levilinea</i> ▲+0.4	2.42	4.11
9	<i>Ruminococcus</i> ▼-0.1	4.87	3.52				
19	<i>Enterococcus</i>	11.86	3.14				
15	<i>Methanobacterium</i>	8.92	3.13				

The letters next to the genus indicate the species name when the OTU was >98% similar to the said species in multiple hits. Although this is not the canonical way to write taxonomy, it was used on this table to visually simplify comparisons, or when multiple species of the same genus corresponded to different OTUs. Details of the closest related species are given below. The symbols next to the OTU closest relative genus indicate if this OTU increased ▲ or decreased ▼ compared to the previous sampling point. Numbers next to OTUs names indicate the amount of this increment (+) or reduction (-).

Notably, the initially inoculated microcosms from both experimental set-ups shared six OTUs members of the genera *Petrimonas*, *Ruminococcus*, *Leptolinea*, *Pseudomonas*, *Flintibacter* and *Ignisphaera* straight after inoculation, three of which were also part of the R+S initial community presented in chapter 5 (section 5.4.6), namely *Ruminococcus albus*, *Leptolinea tardivitalis* and *Pseudomonas caeni*. From the common OTUs in initial inoculated microcosms, *R. albus* derives from rumen (Henderson et al. 2015) and possibly the *Flintibacter* species too (98% similarity), as it is a recognised member of the mouse gut microbiome (Lagkouvardos et al. 2016), while *Petrimonas*, *L. tardivitalis* and *P. caeni* have all been reported as members of anaerobic sludge (Hahnke et al. 2016; Yamada et al. 2006; Xiao et al. 2009). The *Ignisphaera*-like archaeon (84% similarity) has been found in

an enrichment of cellulolytic and hemicellulolytic organisms from a hot spring (Peacock et al. 2013).

Other members from the Exp A initial community were also strongly associated to either the rumen environment (*Prevotella* and *Turicibacter* (Bekele et al. 2010; J. H. Liu et al. 2016)), or anaerobic sludge (*Methanobacterium beijingense*, 100% similarity, isolated from sludge granules (Liu et al., 2016); *Syntrophomonas wolfei*, 98% identity, isolated from an anaerobic digester sludge (DOE Joint Genome Institute 2006); *Gracilibacter*, 86% similarity, an strict anaerobic fermentative bacterium isolated from a constructed wetland system receiving acid sulphate water (Y. J. Lee et al. 2006) and *Syntrophobotulus*, 89% similarity, originally isolated from anaerobic sewage sludge (Friedrich et al. 1996)). However, the member of the *Aminivibrio* genus closest relative, 98% similarity, was a species isolated from soil (Honda et al. 2013). Nevertheless, this genus, comprised of amino-acid fermenting bacteria is part of the family *Synergistaceae*, which can inhabit anaerobic environments including animal gastrointestinal tracts and wastewater treatment plants (Vartoukian et al. 2007). Therefore, this OTU could have proceeded from either inocula source.

Leuconostoc mesenteroides (100% similarity) was enriched after 7 days of incubation, contributing to at least 30% to the total composition of the communities in both experimental set-ups, supporting the idea of this OTU being part of the OMSW, as previously discussed in Chapter 5, section 5.5. The other OTU enriched after 7 days in both communities from Exps A and B was *Clostridium saccharoperbutylacetonicum* ($\geq 99\%$ similarity), however, while *C. saccharoperbutylacetonicum* contributed with 13.6% to the average Exp A community composition, it only accounted for 7% of Exp B composition.

The Exp A, 7-day community was also enriched for *Clostridium beijerinckii* (99% similarity), a solvent-producing clostridial species as is *C. saccharoperbutylacetonicum* (Keis et al. 2001). Apart from these new OTUs, both communities were still mostly composed of OTUs from their initial communities, such as *P. caeni* and the OTUs belonging to the genera *Petrimonas*, and *Ruminococcus*; all of which slightly decreased from their initial average abundance. Some OTUs, namely *M. beijingense* in ExpA and the *Leptolinea*-like OTU (91% similarity) in ExpB remained stable, as they did not contribute to the dissimilarity between initial and 7-days communities. The later were then 53.26% (ExpA) and 35.64% (ExpB) dissimilar to their corresponding initial “parents”.

By the end of the incubation period both communities were mostly comprised of their 7-days members, with *L. mesenteroides* dominating both experiments, but in general showing a slight decrease in their contribution to the total composition of their communities. *Clostridium tyrobutyricum* (100% similarity) another solventogenic clostridial species, and *Lactobacillus casei* (99% similarity), a species commonly found in intestinal tracts of animals with optimal growth pH of 5.5 (Cai et al. 2007), were enriched in ExpA community. Meanwhile, ExpB, registered a slight increase in the average abundance of *C. saccharoperbutylacetonicum*, while a member of the *Anaerolineaceae* family with *Levilinea saccharolytica* as its closest relative (87% similarity) was enriched. The later has been isolated from anaerobic sludge granules (Yamada et al. 2006). Once more *M. beijigense* did not contribute to the dissimilarity between the 7 and 14-days communities.

As described above, inocula transfers were then conducted from the 14-days communities into fresh culture media, with the adjustment of pH to 5.5 after inoculation in ExpB microcosms as the only difference in the procedure. Table 6.3 presents the members of inoculated and enriched communities in the first and last (4th) transfers in both experimental set-ups.

Table 6.3. Most frequent and abundant OTUs found in each sampling point from the first (Tr1) and last (Tr4) transfers from experimental set-ups A and B as determined by SIMPER test

Exp A - Tr1 - 0 days Average similarity: 76.67 Cumulative similarity: 72.48				Exp B - Tr1 - 0 days Average similarity: 73.89 Cumulative similarity: 70.06			
OTU	Identity	Sim/SD	Con.%	OTU	Identity	Sim/SD	Con%
1	<i>Leuconostoc m.</i>	18.26	30.58	2	<i>Leuconostoc m.</i>	9.74	31.97
6	<i>Clostridium s.</i>	17.15	12.28	7	<i>Clostridium s.</i>	78.64	11.18
12	<i>Clostridium t.</i>	9.21	5.85	5	<i>Petrimonas</i>	16.59	9.17
5	<i>Lactobacillus c.</i>	1.13	5.69	10	<i>Ruminococcus</i>	18.85	5.55
2	<i>Lactobacillus b.</i>	1.13	5.32	8	<i>Leptolinea</i>	7.94	5.51
7	<i>Petrimonas</i>	19.18	5.21	13	<i>Methanobacterium</i>	8.68	3.47
13	<i>Clostridium b.</i>	4.34	3.83	6	<i>Lactobacillus c.</i>	0.58	3.22
17	<i>Sporolactobacillus</i>	11.27	3.71				
Exp A - Tr1 - 7 days Average similarity: 26.21 Cumulative similarity: 70.56				Exp B - Tr1 - 7 days Average similarity: 38.36 Cumulative similarity: 75.6			
OTU	Identity	Sim/SD	Con.%	OTU	Identity	Sim/SD	Con%
1	<i>Leuconostoc m.</i>	1.41	37.26	2	<i>Leuconostoc m.</i>	2.14	63.51
2	<i>Lactobacillus b.</i>	0.69	25.07	1	<i>Lactobacillus b.</i>	9.85	12.09
6	<i>Clostridium s.</i>	43.14	8.23				

Exp A – Tr1 - 14 days Average similarity: 26.50 Cumulative similarity: 70.76				Exp B – Tr4 - 14 days Average similarity: 34.93 Cumulative similarity: 81.96			
OTU	Identity	Sim/SD	Con.%	OTU	Identity	Sim/SD	Con%
2	<i>Lactobacillus b.</i>	0.58	26.68	2	<i>Leuconostoc m.</i>	2.84	50.53
1	<i>Leuconostoc m.</i>	1.02	22.76	1	<i>Lactobacillus b.</i>	5.69	31.42
3	<i>Lactobacillus c.</i>	0.71	21.32				
Exp A – Tr4 - 0 days Average similarity: 39.94 Cumulative similarity: 70.98				Exp B – Tr4 - 0 days Average similarity: 68.58 Cumulative similarity: 51.53			
OTU	Identity	Sim/SD	Con.%	OTU	Identity	Sim/SD	Con%
3	<i>Lactobacillus c.</i>	1.14	44.39	1	<i>Lactobacillus b.</i>	7.03	55.37
2	<i>Lactobacillus b.</i>	0.89	26.59	3	<i>Lactobacillus c.</i>	13.26	26.79
Exp A – Tr4 - 7 days Average similarity: 29.00 Cumulative similarity: 72.36				Exp B – Tr4 - 7 days Average similarity: 46.27 Cumulative similarity: 96.35			
OTU	Identity	Sim/SD	Con.%	OTU	Identity	Sim/SD	Con%
3	<i>Lactobacillus c.</i>	0.8	72.36	1	<i>Lactobacillus b.</i>	5.5	65.94
				3	<i>Lactobacillus c.</i>	0.58	22.61
Exp A – Tr4 - 14 days Average similarity: 31.80 Cumulative similarity: 95.99				Exp B – Tr4 - 14 days Average similarity: 26.50 Cumulative similarity: 70.76			
OTU	Identity	Sim/SD	Con.%	OTU	Identity	Sim/SD	Con%
3	<i>Lactobacillus c.</i>	0.99	55.37	1	<i>Lactobacillus b.</i>	69.77	69.77
2	<i>Lactobacillus b.</i>	0.7	40.63	3	<i>Lactobacillus c.</i>	26.59	96.35

The letters next to the genus indicate the species name when the OTU was >98% similar to the said species in multiple hits. Although this is not the canonical way to write taxonomy, it was used on this table to visually simplify comparisons, or when multiple species of the same genus corresponded to different OTUs. Details of the closest related species are given below.

The initial transferred communities were also dominated by *L. mesenteroides* (>30% contribution). However, the first transfer of ExpA at day 0 contained an important proportion of solventogenic clostridia, with these three OTUs cumulatively contributing with 21.96% to the total community composition. While two *Lactobacillus* species contributed in total to 11% to the initial ExpA Tr1 composition. *Petrimonas* was also part of the inoculum along with *Sporolactobacillus nakayamae* (100% similarity) a spore-forming, homofermentative lactic acid bacteria primarily described as member of fermentation starters of alcoholic beverages and also found in soil samples (Yanagida et al. 1997).

The ExpB Tr1 initial community was mostly comprised by the OTUs present in the 14-days community it came from, except for the *Levilinea*-like OTU which did not contributed to the cumulative 70% cut-off of most abundant members in the transfer. Instead, *L. casei* represented 3.22% of the total community composition.

Then, as Fig. 6.6 and Table 6.3 show, from day 7 onwards after the first transfer, *Lactobacillus* species, mainly *L. brevis* (99% similarity) and *L. casei* dominated the enriched communities until the end of both experimental set-ups.

6.4.8 Preliminary conclusions leading to the design of Experiment C

In agreement with the physicochemical results, it was concluded the addition of carbonates buffer did not make a significant difference in the community composition of the enriched communities after the initial transfer to fresh media. However, the dominant species at the end of these experimental set-ups have optimal acidic pH for growth (Xu et al. 2017; Cai et al. 2007).

The maximal EtOH concentrations generated by the initially inoculated microcosms in both experimental set-ups were reached at 14 days of incubation, and although the ethanologenic activity showed an increasing tendency, which could suggest the presence of ethanologenic and ethanol-tolerant bacteria, the steepest part of the exponential phase occurred before 7 days of incubation, a time point at which both communities were comprised by different proportions of *L. mesenteroides*, *C. saccharoperbutylacetonicum* and *P. caeni* as well as members of the genera *Petrimonas*, *Ruminococcus* and *Leptolinea*, from which only *L. mesenteroides*, *C. saccharoperbutylacetonicum* and *Petrimonas* were transferred into fresh media. As at 14 days EtOH production in the starting microcosms was still increasing, it would be safe to assume that the ethanologenic bacteria were still viable, with *C. saccharoperbutylacetonicum* being likely responsible for EtOH production. This observation of viability therefore indicates problems in the transfers themselves.

As discussed in chapter 5, although they do not participate directly in EtOH production, the role of aerobic bacteria such as *P. caeni* could be crucial for the establishment of the right environmental conditions for fermentative microorganisms to thrive. Despite *Lactobacillus* being facultative anaerobes, their activity does not seem to be enough to provide such conditions.

Based on the physicochemical results along with the dramatic loss of richness and diversity over time observed at 7 days of the first transfer it was hypothesised that an earlier transfer time would allow the systems to retain the different metabolic activities required for the R+S community to maintain its high ethanogenic activity. Two alternative mechanisms for how this might be achieved could be considered. The first is that an earlier transfer time would simply maintain a high level of the diversity present in the original inoculate and hence the desired ethanogenic activity. Alternatively, early transfer may still engender diversity loss, but impose different selection pressures (i.e. resource availability) resulting in different communities with different functions. The results from the tests conducted to evaluate this hypothesis are presented below.

6.4.9. Soluble fermentation products across 3-days transfers (Exp C)

The soluble fermentative activity of the R+S community was monitored for 21 days during the initial inoculation incubation, and for 14 days for the subsequent sequential transfers. However, in all cases, transfers were made after 3-days (Fig. 6.1). Consistent with the previous experimental set-ups, EtOH was the main soluble fermentation product with a maximal concentration of $56.85\text{mM} \pm 2.6\text{mM}$ reached in the initially inoculated microcosms after 14 days of incubation, followed by a slight decrease to $50.96\text{mM} \pm 8.12\text{mM}$ at 21 days (Fig. 6.7). The latter could be attributed to the variability between replicates at the end of the incubation period as suggested by the standard error, but also to the utilisation of EtOH as substrate (Müller and Frerichs 2013).

Although EtOH maximal productivity decreased to an average of $30.5\text{mM} \pm 1.3\text{mM}$ in the subsequent transfers (about 56.2% of the initial production), EtOH remained the major soluble fermentation product and a more stable soluble fermentative activity was apparently achieved by conducting a 3-days transfers regime (Fig. 6.7).

More specifically, Tr1 microcosms reached a peak EtOH concentration after 14 days of incubation of $33.89\text{mM} \pm 5.20\text{mM}$, while Tr3 production peaked with $29.66\text{mM} \pm 3.75\text{mM}$. By the fifth transfer EtOH maximal concentration was maintained at $29.90\text{mM} \pm 3.75\text{mM}$. Exps A and B maximal EtOH concentrations in the last transfers (4th) were $11.61\text{mM} \pm 2.49\text{mM}$ and $15.34\text{mM} \pm 1.95\text{mM}$, respectively.

In all cases, butyric acid was the second major soluble fermentation product with a peak concentration of $20.10\text{mM}\pm0.91\text{mM}$ in the initially inoculated microcosms at 21 days, reaching similar maximal concentrations at 14 days in Tr1 and Tr5 of $23.14\text{mM}\pm5.13\text{mM}$ and $19.74\text{mM}\pm4.80\text{mM}$, respectively. Tr3 peak butyric acid production was of $10.39\text{mM}\pm1.00\text{mM}$.

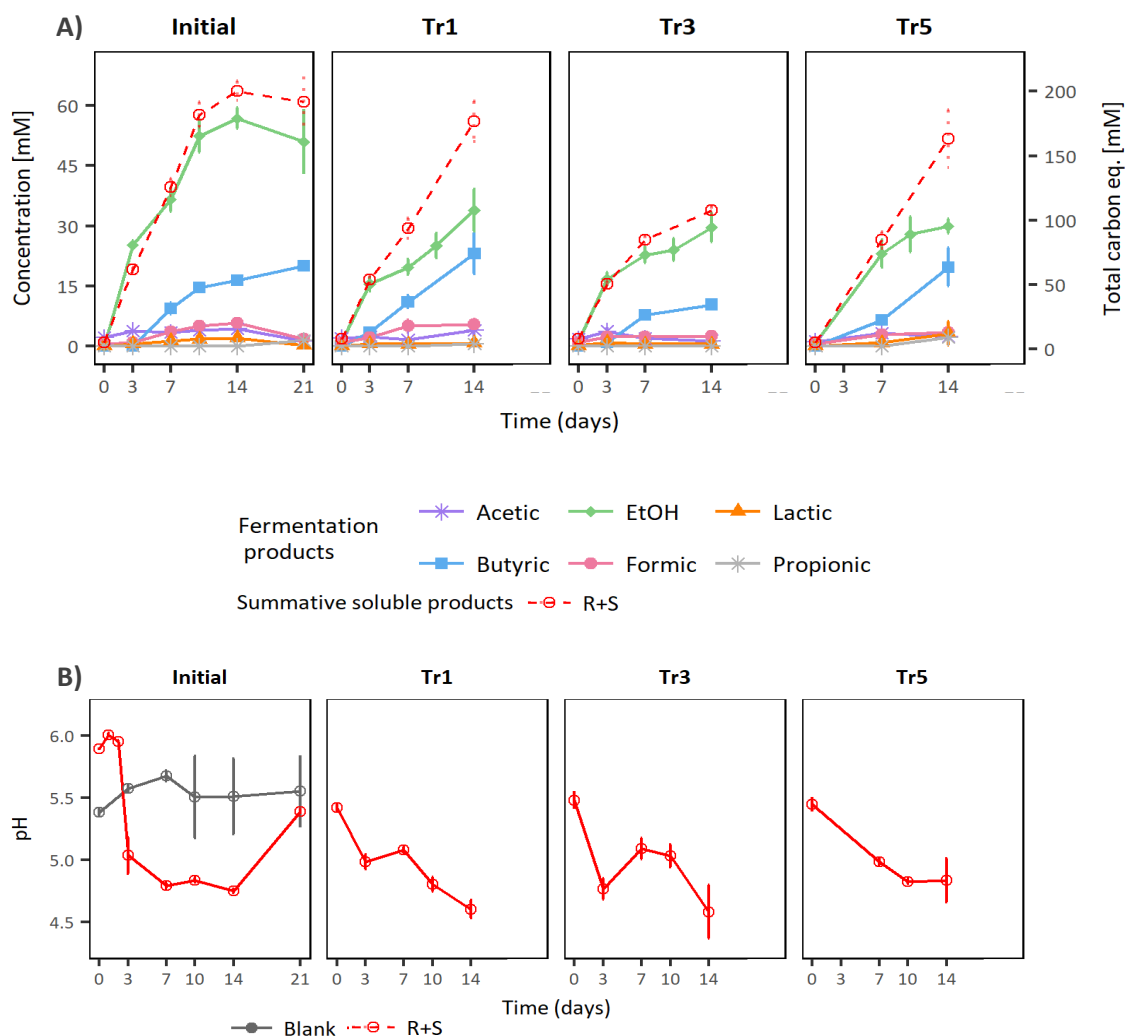


Figure 6.7 Exp C. A) Fermentation products by the R+S community across transfers tested across 3-days transfers incubations with initial carbonates buffer addition. The summative measured soluble fermentation products line represents the total milliequivalents of soluble carbon produced in each transfer. B) pH profiles from the R+S inoculated microcosms across the different transfers. Inocula blanks were only conducted during the first transfer.

While although acetic acid maximal production was low, it remained relatively stable across transfers, reaching up to $4.33\text{mM}\pm0.57\text{mM}$ (In. inoc, 14 days), $3.96\text{mM}\pm1.52\text{mM}$ (Tr1, 14 days), $3.72\text{mM}\pm0.99\text{mM}$ (Tr3, 3 days) and $3.32\text{mM}\pm0.22\text{mM}$ (Tr5, 7 days). In a more variable fashion, lactic acid production was also low, but with peak concentrations of $2.06\text{mM}\pm0.04\text{mM}$, $0.77\text{mM}\pm0.10\text{mM}$, $1.011\text{mM}\pm0.10\text{mM}$ and $3.19\text{mM}\pm2.99\text{mM}$, in

subsequent transfer order. Propionic acid was only detected in the initially inoculated microcosms, with a maximal concentration at 21 days of $1.47\text{mM} \pm 0.23\text{mM}$.

The use of IC for the quantification of VFAs allowed for the monitoring of formic acid as well, reaching up to $5.88\text{mM} \pm 0.133\text{mM}$ in the initially inoculated microcosms after 14 days and $5.45\text{mM} \pm 1.26\text{mM}$, $2.60\text{mM} \pm 0.28\text{mM}$, $3.44\text{mM} \pm 0.49\text{mM}$ in the sequential transfers.

The maximal total productivity in terms of carbon milliequivalents (Fig. 6.7, A: summative measured soluble products) from the initially inoculated microcosms was $200.30\text{mM} \pm 7.47\text{mM}$ slightly decreasing by about 11.8% to $176.61\text{mM} \pm 15.83\text{mM}$ in the first transfer and more noticeably by 46.1% in Tr3 ($107.92\text{mM} \pm 3.04\text{mM}$), to then reach $163.21\text{mM} \pm 22.59\text{mM}$ by the end of the last transfer (-18.5% from the initial), showing a clear improvement in terms of total soluble fermentation productivity from the 14-days transfers experimental set-ups.

Estimates of maximal total productivity in terms of electron milliequivalents supported those observations, going from initial $1082.73 \pm 43.56 \text{ e}^- \text{ meq./L}$ to $923.30 \pm 71.30 \text{ e}^- \text{ meq./L}$ and $586.69 \pm 23.35 \text{ e}^- \text{ meq./L}$ after 14 days in Tr1 and Tr3, to $848.96 \pm 111.11 \text{ e}^- \text{ meq./L}$ in the last transfer. Similarly, the proportion of electrons used to produce EtOH did not varied drastically across transfers ($62.98 \pm 0.49\%$, $44.91 \pm 8.78\%$, $60.27 \pm 5.07\%$ and $43.16 \pm 3.43\%$, respectively). These estimates would signify that 23.1%, 13.53% and 44.16% of electrons were recovered in the initial inoculation incubations (based on TCOD, BMP or COD estimates, respectively. See appendix C), and 8.53%, 14.55% or 27.84% of the electrons fed into the system ended up as EtOH. While in the last transfer 4.49%, 7.36% or 14.64% of electrons from the OMSW (based on TCOD, BMP or COD estimates, respectively) were recovered as EtOH.

Although the pH profiles from the different transfers varied in trajectory, apart from the initially inoculated microcosms, all transitioned from about 5.5 to pH 4.7 at the end of their incubation periods (Fig. 6.7 B). The increase in pH observed in the initially inoculated group at the beginning of the incubation in comparison to that of the inocula blanks might have been caused by the inocula sources, nevertheless, by day 3, it had decreased to pH 5 remaining at about 4.8 until day 14 and increasing to 5.4 by the end of the incubation period. Noticeably, this pH increment coincided with the EtOH peak concentration, followed by its slight drop along with other VFAs, while butyric acid seemed to increase slightly.

6.4.10 Statistical comparison of maximal fermentative production at the different transfers in Exp C

A 2-way-ANOVA followed by a Tukey HDS test were computed to evaluate whether the ethanol maximal production across transfers as well as their maximal total productivity in terms of carbon milliequivalents was statistically different.

Differences in the maximal EtOH production across transfers were found (p -value 0.00183, significance level 0.001). However, in agreement with the observations made in the previous section, the Tukey HDS results demonstrate that although all transfers produced significantly different maximal concentrations to the initial one (p -values <0.008), their production did not differ among themselves (p -values >0.8). From which it can be concluded that a stable ethanologenic activity was achieved.

A similar statistical analysis was then conducted to compare maximal total productivity in terms of carbon milliequivalents between transfers. The 2-way-ANOVA results showed statistical difference between transfers (p -value 0.0106, significance level of 0.01). While the subsequent Tukey HDS test showed differences in Tr3 maximal productivity when compared to that of the initially inoculated microcosms (p -value 0.008) and the first transfer (p -value 0.039), it was found that Tr1 and Tr5 maximal productivities were not different between themselves (p -value 0.91) as well as to that of the initial inoculated microcosms (p -values >0.3).

Although these results demonstrate that fermentative activity stability was achieved, the significant loss of EtOH production between the initially inoculated microcosms and the first transfer suggest changes in the microbial community composition that were not addressed by an earlier transfer time and that strongly influence the ethanologenic activity of R+S. Additional experiments testing the addition of trace minerals and abiotic inocula matrix (autoclaved inocula sources) in a sequential 3-day transfer could provide further insight.

The following sections then analyse the microbial community composition of Exp C transfers aiming to determine if changes in these communities could help in the understanding of the activity loss observed, and in conjunction with Exps A and B results, shed light into the ethanologenic members of the system.

6.4.11 Community composition indices

The OTUs obtained after the quality processing of the 16s rRNA NGS sequence libraries as described in section 6.4.5 of this chapter, were used along with their relative abundances to compute richness (S), diversity (Simpson's inverse diversity, D) and evenness (Simpson's evenness, E) indices of the different sampling points across the 3-day transfers (Fig. 6.8).

As expected, the initially inoculated microcosms had richer and more diverse average communities at day 0, but also throughout the duration of their incubation period, where the initial 283 ± 6 OTUs decreased to about 139 ± 4 OTUs by day 21. Tr1 was then inoculated with 119 ± 16 OTUs, however this number decreased to only 37 ± 3 OTUs at 14 days.

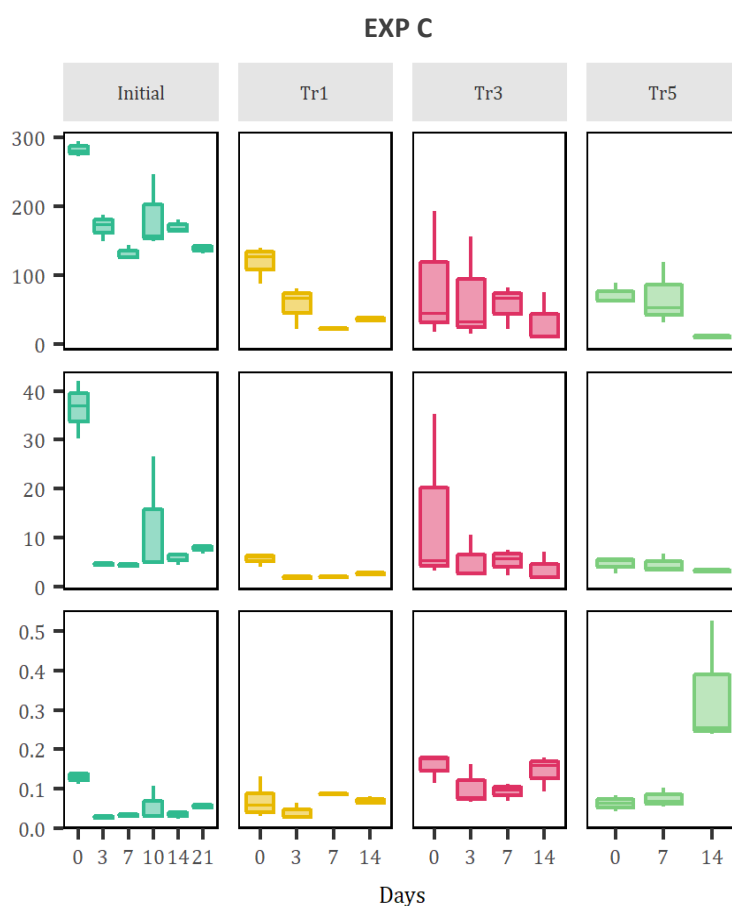


Figure 6.8 ExpC richness, Simpson's inverse diversity and Simpson's evenness indices of the communities at the different sampling days across transfers represented as boxplots.

Meanwhile, Tr3 microcosms showed high variability, with an average richness of 86 ± 54 OTUs at the beginning of the incubation and 33 ± 22 OTUs at the end of it. Tr5 was inoculated with 72 ± 9 OTUs declining to 11 ± 2 OTUs after 14 days. Although the richness

of these communities was generally higher than that of the 14-days transfers, the diversity levels after day 0 remained similarly low in all transfers, suggesting the community compositions were dominated by a small number of OTUs. While overall modestly higher levels of evenness were achieved, which were particularly notable in Tr3 and Tr5.

The decrease in richness and diversity along with the fermentative activity results previously presented in section 6.4.9 indicated the enrichment of OTUs fitted to grow under the specific conditions, produce EtOH and utilise OMSW as substrate. It could be then inferred that at 3 days, the ethanologenic microorganisms are actively growing (exponential phase) and survive the transfer process better than other organisms already in stationary phase or which grow later in the succession occurring in these batch experiments.

6.4.12 Ordination and statistical comparison of the communities in the 3-days transfers

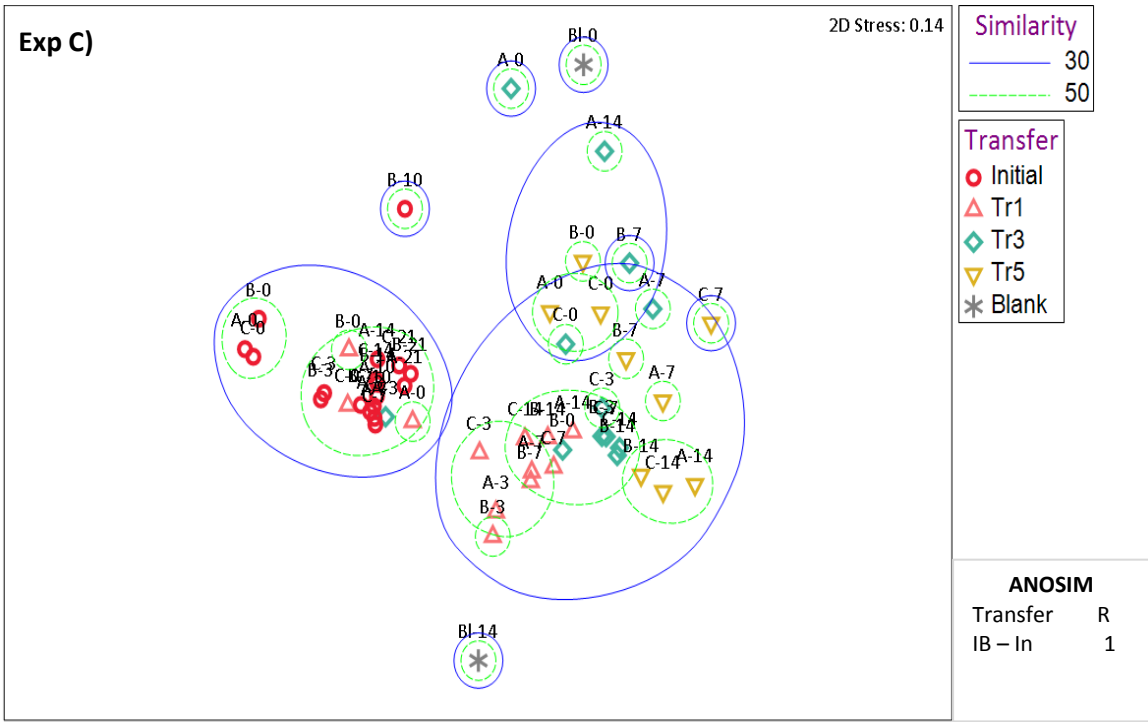


Figure 6.9 nMDS of Exp C replicates including inocula blanks at days 0 and 14 of the initially inoculated microcosm batch. In all plots, the letters (A, B, C) on top of the keys are used to differentiate replicates, they are followed by numbers (0,3,7,14,21) indicating the days of incubation at which the samples were taken. Samples with 30% and 50% similarity are encircled by a purple or green line, respectively. The 2D stress value indicates a good representation of the data on these 2D nMDS plots. ANOSIM R values (0.1% significance level) shown to the right of the plots correspond to pairwise comparison of the inocula blank (IB) vs the individual transfers, where 1 indicates high separation or dissimilarity between clusters.

In agreement with the similar fermentative activity previously demonstrated, most of the sets of replicates for the transfer groups from Exp C did not cluster in clear separate groups relating to either transfer or sampling day (Fig 6.9), suggesting the enrichment of microbial communities comprised of similar members. Nevertheless, a distinct cluster was formed by the replicates of the initially inoculated microcosms at day 0, sharing at least 50% community composition similarity. These replicates clustered further with the rest of the initially inoculated microcosms samples (except for the 10-day “B” replicate, which did not cluster with any other sample) along with the replicates from Tr1 at day 0, sharing at least 30% similarity among them. Most of Tr1, Tr3 and Tr5 samples shared at least 30% similarity, apart from the replicates of Tr3 and Tr5 at the day of inoculation. These samples, which clustered together at 30% similarity, partially intersected the rest of the samples. The inocula blank at both sampling points remained distinct from any of the other samples.

ANOSIM tests were then conducted to statistically determine if some of the communities in Exp C were different, or if indeed they were mostly similar. Details of the relevant results can be found in (Table 6.4).

These results show that apart from Tr3, communities at days 0 and 14 within transfer groups were significantly different (R value 1), while vague at the days in between the distinction was vague. Equally distinctive from each other were the communities of transfers at time 0 when compared against the initially inoculated microcosms, as well as those from Tr1 and Tr5 at this sampling time. The differentiation between transfers communities at other time points were less clear, with the pairs Tr1 at 14 days and Tr3 at 0 days (R value 0.111), as well as Tr3 at 14 days and Tr5 at 0 days (R value 0.333) being rather similar, indicating the probable maintenance of certain OTUs between successive transfers.

Table 6.4. Exp C pairwise comparisons of sampling points within and between transfers as determined by ANOSIM test.

EXP C	ANOSIM	EXP C.	ANOSIM
Pairwise comparisons	R	Pairwise comparisons	R
Within transfers time points		Between transfers at the same time points	
Initial 0 – Initial 3	0.963	Initial 0 – Tr1 0	0.963
Initial 0 – Initial 7	1	Initial 0 – Tr3 0	1
Initial 0 – Initial 10	0.556	Initial 0 – Tr5 0	1
Initial 0 – Initial 14	1	Tr1 0– Tr3 0	0.519
Initial 0 – Initial 21	1	Tr1 0– Tr5 0	1
Initial 3 – Initial 7	0.259	Tr3 0– Tr5 0	0.444
Initial 3 – Initial 10	0.37	Initial 3 – Tr1 3	1
Initial 3 – Initial 14	1	Initial 3 – Tr3 3	0.481
Initial 3 – Initial 21	1	Tr1 3– Tr3 3	0.333
Initial 7 – Initial 10	0.074	Initial 7 – Tr1 7	1
Initial 7 – Initial 14	0.815	Initial 7 – Tr3 7	1
Initial 7 – Initial 21	1	Initial 7 – Tr5 7	1
Initial 14 – Initial 21	0.815	Tr1 7– Tr3 7	0.667
Tr1 0 – Tr1 3	1	Tr1 7– Tr5 7	0.556
Tr1 0 – Tr1 7	1	Tr3 7– Tr5 7	-0.074
Tr1 0 – Tr1 14	1	Initial 14 – Tr1 14	1
Tr1 3 – Tr1 7	0.185	Initial 14 – Tr3 14	0.519
Tr1 3 – Tr1 14	0.519	Initial 14 – Tr5 14	1
Tr1 7 – Tr1 14	0.37	Tr1 14– Tr3 14	-0.037
Tr3 0 – Tr3 3	-0.111	Tr1 14– Tr5 14	0.963
Tr3 0 – Tr3 7	0.222	Tr3 14– Tr5 14	0.481
Tr3 0 – Tr3 14	-0.111	Initial 14 – Tr1 0 ^a	0.704
Tr3 3 – Tr3 7	0.222	Tr1 14 – Tr3 0 ^a	0.111
Tr3 3 – Tr3 14	-0.037	Tr3 14 – Tr5 0 ^a	0.333
Tr3 7 – Tr3 14	0		
Tr5 0 – Tr5 7	0.444		
Tr5 0 – Tr5 14	1		
Tr5 7 – Tr5 14	0.481		

ANOSIM R values ($\geq 0.1\%$ significance level) expand from 0 to 1, where 1 indicates high separation or dissimilarity between clusters. ^aPairwise comparisons between day 14 microcosms and the subsequent transfer at the time of inoculation.

SIMPER analysis was then conducted to determine which OTUs contributed to either the similarity or dissimilarity among the different communities according to transfers and sampling days, to possibly elucidate the fermentative activity observed.

6.4.13 Specific bacterial OTUs typical from the different 3-days transfers

The most frequent and abundant OTUs for each group of replicates (transfer/ sampling day) were determined using the similarity percentages (SIMPER) test based on Bray-Curtis similarity indices, as previously explained in section 6.4.7 of this chapter. Figure 6.10 offers a visual summary of the results from this test.

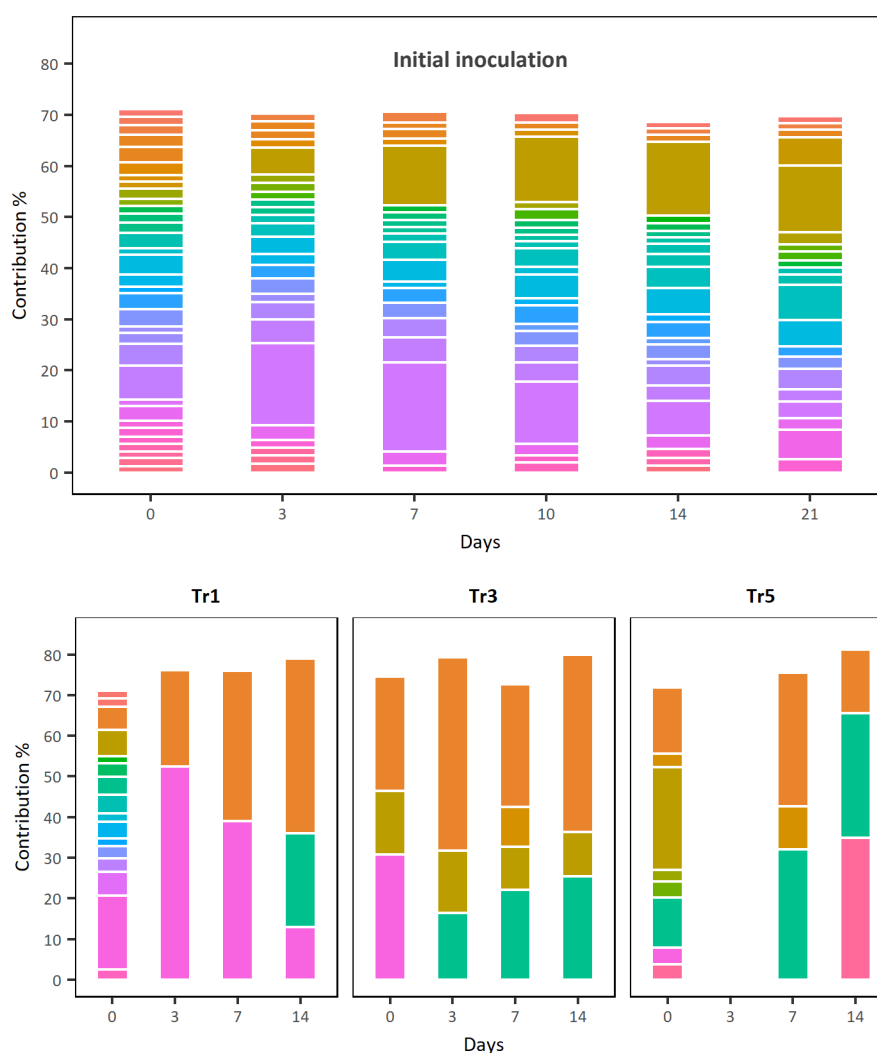


Figure 6.10 Stacked bar plots with different colours representing the average number of OTUs accounting for at least 70% of the cumulative similarity in each transfer/sampling day group from Exp C.

In agreement with the richness indices, the communities in the initially inoculated microcosms were notably rich when compared to those observed in the initial incubations of Exps A and B, more importantly, this richness was to some degree maintained over the 21 days of the incubation period. This clear divergence from the other two initially inoculated communities' behaviour (see Fig. 6.6) could however, be due to the different methods used for sequencing. While Exps A and B were analysed using the Ion Torrent

sequencing platform, using barcoded primers expanding the V4-V5 hypervariable region, Exp C DNA samples were processed with the MiSeq, Illumina technology, employing barcoded primers targeting the V4 hypervariable region, as explained in Chapter 3 section 3.6.5. Although a deep analysis of the differences between these strategies is well out of the scope of this thesis, the use of primers targeting multiple regions, as is the V4-V5 pair has been shown to produce reads that do not fully overlap, thus generating assembled reads with higher error rates (Kozich et al. 2013; Schloss 2016). The misrepresentation of Exps A and B could have been possible, however, the similar pattern of few OTUs dominating the transferred communities in all experimental set-ups (Figs. 6.6 and 6.10) would make this issue even more debatable.

Tables 6.5 and 6.6 present a detailed list of the OTUs that contributed the most to the average composition of each sampling day group in the initially inoculated microcosms and transfers from this experimental set-up in descending order (Con.%), as well as the ratio of the average contribution divided by the standard deviation of those contributions across all sample pairs in each group (Sim/SD). The latter allowed the identification of OTUs that contributed consistently to the average bacterial composition of each group of replicates. The identity of each OTU is the closest similar species (>97% sequence identity match, when possible) found after the individual sequences were megablasted in the GenBank database (Boratyn et al. 2012) as described in section 5.3.9. The average similarity of each group along with the cut-off cumulative similarity (>70%) of the OTUs listed is also presented.

Table 6.5. Most frequent and abundant OTUs found in each sampling point from the initially inoculated microcosms from experimental set-ups C as determined by SIMPER test

Exp C – Initial com. 0 days Average similarity: 76.51 Cumulative similarity: 71.13				Exp C – Initial com. 3 days Average similarity: 77.52 Cumulative similarity: 70.24			
OTU	Identity	Sim/SD	Con.%	OTU	Identity	Sim/SD	Con%
7	<i>Pseudomonas c.</i>	21.68	6.65	2	<i>Pseudomonas w.</i> ▲	21.36	16.15
9	<i>Proteiniphilum</i>	8.59	4.22	1	<i>Clostridium b.</i> ▲	12.23	5.25
8	<i>Methanobacterium</i>	14.92	3.89	7	<i>Pseudomonas c.</i> ▼	42.26	4.6
13	<i>Petrimonas</i>	25.86	3.35	9	<i>Proteiniphilum</i> ▼	7.11	3.42
12	<i>Parapusillimonas</i>	25.12	3.13	8	<i>Methanobacterium</i> ▼	116.22	3.38

OTU	Identity	Sim/SD	Con.%	OTU	Identity	Sim/SD	Con.%
18	<i>Leptolinea</i>	36.71	2.99	13	<i>Petrimonas</i> ▼	7.42	3.09
21	<i>Aminomonas</i>	13.19	2.96	16	<i>Ruminococcus</i> ▼	8.58	2.83
16	<i>Ruminococcus</i>	10.92	2.9	3	<i>Leuconostoc m.</i> ▲	11.67	2.66
27	<i>Bathyarchaeota</i>	37.54	2.56	12	<i>Parapusillimonas</i> ▼	8.65	2.64
43	<i>Aminomonas</i>	27.78	2.42	29	<i>Methanosaeta</i> ▼	7.8	2.06
29	<i>Methanosaeta</i>	7.84	2.39	21	<i>Aminomonas</i> ▼	3.92	1.83
35	<i>Prevotella</i>	17.16	2.13	80	<i>Endomicrobium</i> ▲	14.75	1.77
34	<i>Cryptanaerobacter</i>	17.45	2.07	25	<i>Victivallis</i>	42.99	1.72
47	<i>Gracilibacter</i>	13.99	2.03	34	<i>Cryptanaerobacter</i> ▼	10.41	1.65
37	<i>Aminivibrio</i>	6.41	1.85	43	<i>Aminomonas</i> ▼	10.41	1.65
17	<i>Succiniclasticum</i>	7.74	1.82	18	<i>Leptolinea</i> ▼	24.11	1.6
46	<i>Verrucomicrobiaceae</i>	27.78	1.71	27	<i>Bathyarchaeota</i> ▼	24.11	1.6
62	<i>Gelidibacter</i>	12.94	1.7	37	<i>Aminivibrio</i> ▼	24.11	1.6
68	<i>Alkalitalea</i>	5.49	1.66	46	<i>Verrucomicrobiaceae</i> ▼	24.11	1.6
67	<i>Flintibacter</i>	3.29	1.61	35	<i>Prevotella</i> ▼	4.29	1.56
45	<i>Actinomyces</i>	4.7	1.51	10	<i>Escherichia</i>	42.99	1.54
53	<i>Treponema</i>	6.83	1.5	47	<i>Gracilibacter</i> ▼	42.99	1.54
63	<i>Subsaxibacter</i>	4.79	1.38	17	<i>Succiniclasticum</i>	4.46	1.52
61	<i>Carboxydotherrmus</i>	5.59	1.37	72	<i>Gracilibacter</i>	6.02	1.46
22	<i>Prevotella</i>	27.78	1.35				
100	<i>Syntrophobacter</i>	5.96	1.34				
39	<i>Leptolinea</i>	6.41	1.31				
96	<i>Desulfovibrio</i>	6.41	1.31				
50	<i>Ruminococcaceae</i>	27.78	1.21				
25	<i>Victivallis</i>	4.06	1.2				
38	<i>Oribacterium</i>	4.06	1.2				
82	<i>Brevundimonas</i>	4.79	1.19				
Exp C – Initial com. 7 days Average similarity: 78.31 Cumulative similarity: 70.56				Exp C – Initial com. 10 days Average similarity: 54.80 Cumulative similarity: 70.27			
OTU	Identity	Sim/SD	Con.%	OTU	Identity	Sim/SD	Con.%
2	<i>Pseudomonas w.</i> ▼	76	17.39	1	<i>Clostridium b.</i> ▲	3.59	12.8
1	<i>Clostridium b.</i> ▲	19.79	11.61	2	<i>Pseudomonas w.</i> ▼	2.76	12.08
7	<i>Pseudomonas c.</i> ▼	14.57	4.87	8	<i>Methanobacterium</i>	3.55	4.66
8	<i>Methanobacterium</i> ▲	10.89	4.24	7	<i>Pseudomonas c.</i> ▼	4.11	3.81
9	<i>Proteiniphilum</i>	26.43	3.84	3	<i>Leuconostoc m.</i>	5.78	3.64
3	<i>Leuconostoc m.</i> ▲	33.24	3.54	12	<i>Parapusillimonas</i> ▲	4.56	3.59
13	<i>Petrimonas</i> ▼	6.19	3	9	<i>Proteiniphilum</i> ▼	4.11	3.3
12	<i>Parapusillimonas</i> ▼	8.29	2.93	13	<i>Petrimonas</i> ▼	3.32	2.81
16	<i>Ruminococcus</i> ▼	81.4	2.72	16	<i>Ruminococcus</i> ▼	3.32	2.29
37	<i>Aminivibrio</i>	13.14	2.11	10	<i>Escherichia</i> ▲	10.56	2.13
21	<i>Aminomonas</i> ▼	15.24	1.89	49	<i>Tissierella</i> ▲	11.79	1.99
18	<i>Leptolinea</i>	6.65	1.56	45	<i>Actinomyces</i>	5.78	1.82
62	<i>Gelidibacter</i>	10.28	1.49	87	<i>Marinilabiliaceae</i> ▲	4.77	1.52
17	<i>Succiniclasticum</i> ▼	81.4	1.42	34	<i>Pelotomaculum</i> ▼	11.79	1.41

OTU	Identity	Sim/SD	Con.%	OTU	Identity	Sim/SD	Con%
42	<i>Fermentimonas</i>	81.4	1.42	47	<i>Gracilibacter</i>	11.79	1.41
47	<i>Gracilibacter</i>	81.4	1.42	70	<i>Mucilaginibacter</i>	11.79	1.41
27	<i>Bathyarchaeota</i>	3.6	1.38	82	<i>Brevundimonas</i> ▲	11.79	1.41
43	<i>Aminomonas</i> ▼	7.51	1.25	92	<i>Frisingicoccus</i> ▲	11.79	1.41
29	<i>Methanosaeta</i> ▼	8.46	1.24	100	<i>Syntrophobacter</i> ▲	11.79	1.41
50	<i>Intestinimonas</i> ▼	8.46	1.24	111	<i>Corynebacterium</i> ▲	11.79	1.41
Exp C – Initial com. 14 days Average similarity: 76.64 Cumulative similarity: 70.39				Exp C – Initial com. 21 days Average similarity: 75.28 Cumulative similarity: 70.34			
OTU	Identity	Sim/SD	Con.%	OTU	Identity	Sim/SD	Con%
1	<i>Clostridium b.</i> ▲	123.5	14.44	1	<i>Clostridium b.</i> ▼	19.26	13.07
2	<i>Pseudomonas w.</i> ▼	37.64	6.85	3	<i>Leuconostoc m</i> ▼	191.79	6.78
8	<i>Methanobacterium</i> ▲	31.61	5.06	4	<i>Sporolactobacillus</i> ▲	3.83	5.82
3	<i>Leuconostoc m.</i> ▼	36.8	4.14	14	<i>Clostridium a.</i> ▲	20.81	5.54
9	<i>Proteiniphilum</i> ▲	79.08	3.91	8	<i>Methanobacterium</i>	29.59	5.2
12	<i>Parapusillimonas</i> ▲	39.07	3.14	9	<i>Proteiniphilum</i>	16.71	4.02
7	<i>Pseudomonas c.</i> ▲	6.02	2.95	2	<i>Pseudomonas w.</i> ▼	7.14	3.33
13	<i>Petrimonas</i> ▲	16.86	2.85	7	<i>Pseudomonas c.</i> ▼	17.13	2.4
18	<i>Leptolinea</i> ▲	53.74	2.57	23	<i>Clostridium t.</i> ▲	104.51	2.33
16	<i>Ruminococcus</i> ▲	12.31	2.57	13	<i>Petrimonas</i> ▼	54.31	2.29
39	<i>Leptolinea</i> ▲	11.16	1.97	16	<i>Ruminococcus</i> ▼	13.31	2.17
49	<i>Tissierella</i>	53.74	1.75	18	<i>Leptolinea</i> ▼	54.31	2.05
42	<i>Fermentimona</i>	7.99	1.54	12	<i>Parapusillimonas</i> ▼	8.76	2.05
67	<i>Flintibacter</i>	14.08	1.48	10	<i>Escherichia</i> ▲	54.31	1.78
27	<i>Nitrososphaera</i> ▲	20.87	1.48	17	<i>Succinoclasticum</i> ▲	54.31	1.62
53	<i>Treponema</i> ▲	20.87	1.48	21	<i>Aminomonas</i>	13.43	1.51
25	<i>Victivallis</i> ▲	4.67	1.41	42	<i>Fermentimonas</i>	4.49	1.43
37	<i>Aminivibrio</i> ▲	2.54	1.3	45	<i>Actinomyces</i>	4.58	1.43
22	<i>Prevotella</i> ▲	11.12	1.3	39	<i>Leptolinea</i> ▼	6.03	1.38
34	<i>Pelotomaculum</i> ▼	11.12	1.3	5	<i>Enterococcus</i> ▲	10.23	1.32
45	<i>Actinomyces</i>	11.12	1.3	37	<i>Aminivibrio</i> ▼	54.31	1.26
47	<i>Gracilibacter</i> ▲	11.12	1.3				
21	<i>Aminomonas</i>	14.93	1.3				
20	<i>Lentimicrobium</i>	53.74	1.24				

The letters next to the genus indicate the species name when the OTU was >98% similar to the said species in multiple hits. Although this is not the canonical way to write taxonomy, it was used on this table to visually simplify comparisons, or when multiple species of the same genus corresponded to different OTUs. Details of the closest related species are given below. The symbols next to the OTU closest relative genus indicate if this OTU increased ▲ or decreased ▼ compared to the previous sampling point.

At time 0, the community was evenly comprised of more than 30 OTUs, with *P. caeni* having the highest contribution (6.65%). Other OTUs, such as members of the genera *Proteiniphilum*, *Methanobacterium*, *Petrimonas*, *Leptolinea*, *Aminomonas*, *Ruminococcus*, *Prevotella*, and *Gracilibacter* which were previously detected in Exps A and B, as well as in the communities studied in Chapter 5, represented each, at least 1% of the total initial community composition.

After 3 days, although most of these OTUs remained as part of the community, their contribution to the total composition decreased, while *P. weihenstephanensis* (100% similarity), *C. beijerinckii* (100% similarity), *L. mesenteroides* (100% similarity), and a member of the *Endomicrobiaceae* family, with *Endomicrobium proavitum*, a symbiotic bacterium isolated from termites' gut, as its closest relative (91% similarity) were enriched.

Since the EtOH concentration at day 3 of the initial incubation ($25.32\text{mM} \pm 1.06\text{mM}$) was almost equivalent to the total maximal concentration reached in the subsequent transfers, the community enriched at this time point played an important role for the achievement of the total ethanologenic activity observed in these microcosms, which, based on the SIMPER results, was only 38.87% dissimilar to that from day 0, with the enrichment of *P. weihenstephanensis* (14.7%), *C. beijerinckii* (6.46%), *L. mesenteroides* (2.53%) and decrease in the community composition contribution from *P. caeni* (3.24%), members from the *Leptolinea* (2.04%), *Aminomonas* (1.73%) and *Proteiniphilum* (1.62%) genera, a member from the *Thaumarchaeota* phylum (1.57%) and *Prevotella copri* (1.54%) adding the most to the average dissimilarity between these two communities.

After 7 days of incubation, *P. weihenstephanensis* was still the most abundant OTU, although its contribution decreased as well as that of *P. caeni* and other members of the initial community such as the members of the *Petrimonas*, *Ruminococcus* and *Aminomonas* genera. While the contribution to the total community composition of *C. beijerinckii*, *M. beijingense* and *L. mesenteroides* increased.

By day 10, *C. beijerinckii* was the most abundant OTU, being closely followed by *P. weihenstephanensis*, while the *L. mesenteroides* abundance remained relatively stable. Although numerous OTUs showed an increase in their contribution to the community composition, the decreasing abundance of *P. weihenstephanensis* (5.12%) and incremental in *C. beijerinckii* (3.07%) contributed the most to the 34.77% dissimilarity between the 7 and 10-days communities.

The maximal EtOH production was reached at 14 days, time point at which *C. beijerinckii* was the most abundant OTU (14.44%), with *P. weihenstephanensis*, *M. beijingense*, *L. mesenteroides*, *Parapusillimonas granuli* (98% similarity), a bacterium isolated from granules from a wastewater-treatment bioreactor, along with a member of the *Proteiniphilum* genus also greatly contributing to the total community composition.

By the end of the incubation period *C. beijerinckii* had still the highest contribution, followed by *L. mesenteroides*. While *Sporolactobacillus putidus* (100% similarity), *Clostridium acetobutylicum* (99% similarity), *Clostridium tyrobutyricum* (100% similarity), as well as members of the *Escherichia* (100% similarity), *Enterococcus* (100% similarity).and *Succiniclasicum* (96% similarity) genera were enriched. From which the enrichment of *C. acetobutylicum* (7.09%), *S. putidus* (6.17%) and *C. tyrobutyricum* (2.65%), along with the relative decrease of *P. weihenstephanensis* (4.27%), *L. mesenteroides* (2.97%), and *C. beijerinckii* (2.08%) contributed the most to the 30.84% dissimilarity between this and the previous community compositions. In section 6.5 of this chapter, the possible consequences of the community changes just described as well as the proposal for putative functions for the most abundant OTUs is presented.

Inocula transfers were then conducted from the 3-days communities into fresh culture media, with the adjustment of pH to 5.5 after inoculation. Table 6.6 presents the members of inoculated and enriched communities in the first and last (5th) transfers in this experimental set-up.

Table 6.6. Most frequent and abundant OTUs found in each sampling point from transfers 1,3 and 5 from experimental set-up C as determined by SIMPER test.

Exp C				Tr1- 0 days				Exp				Tr1- 3 days			
Average similarity: 64.16								Average similarity: 60.88							
Cumulative similarity: 71.11								Cumulative similarity: 76.08							
OTU	Identity	Sim/SD	Con%	OTU	Identity	Sim/SD	Con%	OTU	Identity	Sim/SD	Con%	OTU	Identity	Sim/SD	Con%
2	<i>Pseudomonas w.</i>	22.97	18.13	2	<i>Pseudomonas w.</i> ▲	6.24	52.45	2	<i>Pseudomonas w.</i> ▼	3.34	39.05	1	<i>Clostridium b.</i> ▲	38.17	36.93
10	<i>Escherichia</i>	10.59	6.54	1	<i>Clostridium b.</i> ▲	9.45	23.63								
7	<i>Pseudomonas c.</i>	51.11	5.77					Exp				Tr1- 7 days			
1	<i>Clostridium b.</i>	13.3	5.67					Average similarity: 65.03							
8	<i>Methanobacterium</i>	7.72	4.48					Cumulative similarity: 75.98							
3	<i>Leuconostoc m</i>	9.22	4.42					OTU	Identity	Sim/SD	Con%				
12	<i>Parapusillimonas</i>	19.68	4.02					2	<i>Pseudomonas w.</i> ▼	3.34	39.05				
9	<i>Proteiniphilum</i>	9.22	3.34					1	<i>Clostridium b.</i> ▲	38.17	36.93				
18	<i>Leptolinea</i>	44.39	3.3												

13	<i>Petrimonas</i>	4.24	3.02	Exp Tr1- 14 days Average similarity: 56.82 Cumulative similarity: 79.02			
16	<i>Ruminococcus</i>	10.44	2.58				
29	<i>Methanosaeta</i>	4.25	2.13				
21	<i>Aminomonas</i>	13.06	2.12				
34	<i>Pelotomaculum</i>	3.05	1.97	OTU	Identity	Sim/SD	Con%
43	<i>Aminomonas</i>	3.52	1.87	1	<i>Clostridium b.</i> ▲	191.98	43.02
47	<i>Gracilibacter</i>	5.64	1.75	3	<i>Leuconostoc</i> ▲	13.76	23.06
				2	<i>Pseudomonas w.</i> ▼	1.38	12.95
Exp C Tr3- 0 days Average similarity: 33.56 Cumulative similarity: 74.61				Exp - Tr3 - 3 days Average similarity: 37.22 Cumulative similarity: 79.37			
OTU	Identity	Sim/SD	Con%	OTU	Identity	Sim/SD	Con%
2	<i>Pseudomonas w.</i>	2.33	30.79	1	<i>Clostridium b.</i> ▲	2.74	47.6
1	<i>Clostridium b</i>	1.39	28.24	3	<i>Leuconostoc m</i> ▲	1.26	16.36
10	<i>Escherichia</i>	1.4	15.58	10	<i>Escherichia</i> ▼	2.05	15.41
Exp - Tr3 - 7 days Average similarity: 42.66 Cumulative similarity: 72.6				Exp Tr3- 14 days Average similarity: 36.00 Cumulative similarity: 79.94			
OTU	Identity	Sim/SD	Con%	OTU	Identity	Sim/SD	Con%
1	<i>Clostridium b.</i> ▼	6.04	30.19	1	<i>Clostridium b</i> ▼	43.68	43.68
3	<i>Leuconostoc m</i> ▲	6.46	22.1	3	<i>Leuconostoc</i> ▼	25.41	25.41
10	<i>Escherichia</i> ▼	4.8	10.64	10	<i>Escherichia</i> ▲	10.86	10.86
5	<i>Enterococcus</i> ▲	1	9.67				
Exp Tr5- 0 days Average similarity: 51.75 Cumulative similarity: 71.94				Exp Tr5- 7 days Average similarity: 40.16 Cumulative similarity: 75.52			
OTU	Identity	Sim/SD	Con%	OTU	Identity	Sim/SD	Con%
10	<i>Escherichia</i>	10.25	25.31	1	<i>Clostridium b.</i> ▲	12.77	32.87
1	<i>Clostridium b.</i>	51.46	16.33	3	<i>Leuconostoc</i> ▲	3.4	32.08
3	<i>Leuconostoc</i>	3.05	12.37	5	<i>Enterococcus</i> ▲	2.8	10.57
2	<i>Pseudomonas w.</i>	65.46	4.06	Exp Tr5- 14 days Average similarity: 62.98 Cumulative similarity: 81.27			
448	<i>Fermentibacillus</i>	11.21	4				
4	<i>Sporolactobacillus</i>	12.43	3.75	OTU	Identity	Sim/SD	Con%
5	<i>Enterococcus</i>	1.01	3.35	4	<i>Sporolactobacillus</i> ▲	4.97	34.9
11	<i>Faecalibacterium</i>	16.25	2.77	3	<i>Leuconostoc</i> ▼	15.63	30.63
				1	<i>Clostridium b.</i> ▼	2.09	15.74

Despite the inoculation of the first transfer with apparently a rich community of 16 OTUs, after 3 days of incubation, *P. weihenstephanensis* represented more than 50% of the total community composition, followed by *C. beijerinckii* with an average contribution of 23.63%, thus reaching the 70% similarity cut-off.

After 7 days the contribution of both OTUs was almost equivalent, with the two of them accounting for 76% of the total community composition. By the end of the incubation period, *C. beijerinckii* was the most abundant OTU, while *L. mesenteroides* was significantly enriched and the *P. weihenstephanensis* contribution diminished. The third transfer was mostly dominated by *C. beijerinckii*, *L. mesenteroides* and an *Escherichia* genus member, despite *P. weihenstephanensis* being the dominant OTU at the time of inoculation. By the end of the experimental set-up, *C. beijerinckii*, *L. mesenteroides*, *S. putidus* and an *Enterococcus* genus member had contributed in different proportions to the total community composition in transfer 5.

Importantly, despite the richness observed throughout the incubation period of the initially inoculated microcosms, the successive transfers were still dominated by few OTUs. However, the ethanologenic activity of these earlier transfers was notably higher than that of the Exps A and B experimental set-ups, with the continued enrichment in Exp C of *C. beijerinckii*, a solventogenic clostridial member, as opposed of the *Lactobacillus* species dominating the 14-days transfers, as a clear drive for the differences in EtOH production observed, providing a candidate for the organism principally generating EtOH from the OMSW. This, as well as the possible causes for the overall reduction in ethanologenic activity after the initial inoculation across transfers is discussed in the following section.

6.5 Discussion

In all experiments, the batch of microcosms directly inoculated with the combination of rumen and sludge produced about 60mM of EtOH by the 14 of incubation and reached an average total productivity of soluble fermentation products in terms of carbon and electron milliequivalents of about 200mM and 1085.18 e⁻ meq. /L, respectively. Hypothetically recovering about 13.56%, 23.15% or 44.28% of electrons from the OMSW, based on TCOD, BMP or COD estimates, respectively. Based on those estimates, about 10%, 15% or 30% of the electrons initially provided by the substrate were used for EtOH production (see Appendix C), As the BMP estimate represents the concentration of biodegradable carbon, and therefore of electrons, present in a substrate, it is a better indicator of the substrate's matter and energy fate in fermentation studies than TCOD and COD estimates. Consequently, it is safe to assume that about 15% of the electrons

originally estimated to be part of the OMSW ended up as EtOH in these systems. These results were observed regardless of the time which had elapsed in-between experimental set-ups, i.e., 3 months between Exps A and B, and 12 months between Exps B and C. This consistency lead to the conclusion that the ethanologenic activity after initial inoculation with the combination of these inocula sources under the environmental conditions tested is a reproducible and repeatable process.

Clear similarities were also found in the microbial composition of these initial communities, where based on 16S rRNA gene sequences, it was possible to elucidate their most abundant microorganisms.

6.5.1 Putative functions of the most abundant members enriched across transfer experiments

Considering that equivalent maximal EtOH concentrations were reached in these three experiments at 14 days of incubation and under the assumption that abundance reflects activity, it is deduced that the smallest communities (Exp B-7days: 6 OTUs, Exp B-14 days: 7 OTUs) comprised all the functional capabilities required to achieve such ethanologenic activity.

During the exponential phase of ethanologenic activity (0 to 7 days), the community enriched in Exp B was comprised of *L. mesenteroides*, *C. saccharoperbutylacetonicum*, *P. caeni* and the OTUs members from the *Petrimonas*, *Ruminococcus* and *Leptolinea* genera, with these 6 OTUs accounting for at least 70% of the total community composition. In agreement, Exp A 7-days community, mostly comprised *L. mesenteroides*, *C. saccharoperbutylacetonicum*, *P. caeni*, and OTUs belonging to *Petrimonas*, *Ruminococcus* and *Leptolinea* genera, additionally *C. beijerinckii* was enriched. Of these organisms, the Exp C 7-days community coincidentally had high abundance of *L. mesenteroides*, *P. caeni*, and the *Petrimonas*, *Leptolinea* and *Ruminococcus*-like OTUs, among others, with the difference of having *C. beijerinckii* and *P. weihenstephanensis* as its most abundant members.

The possible functions of some of these OTUs have already been discussed in Chapter 5 section 5.5.1, where it was proposed that initial high abundance of *Pseudomonas* might be responsible to depletion of oxygen in the headspace and the liquid media, creating the necessary conditions for strict anaerobes, such as *Clostridium*, to grow. Besides, although

Pseudomonas is traditionally classified as an “aerobic” genus, its members have been found in diverse anaerobic environments (Hall-Stoodley et al. 2004; Sun Yoon et al. 2002; Alvarez-Ortega and Harwood 2007), thus explaining its prevalence or at least persistence even after the first days of incubation in this study. Additionally, the capability of this genera to form exopolysaccharides makes them likely responsible for the aggregation of granular sludge (Adav et al. 2009), besides of providing them with organic-solvent tolerance and protection in their ability to degrade aromatic compounds to the extent that they have been used for the detoxification of pre-treated feedstocks solutions for ethanol production (Khiyami et al. 2005). Particularly, *P. weihenstephanensis* is a psychrotolerant (4-33°C) extracellular peptidase producer at a pH range 5-11 (Stoeckel et al. 2016; von Neubeck et al. 2016; Jain et al. 2017), a trait which could have allowed it to degrade the meat-derived peptides present in OMSW media, apart from being a well-known pentose oxidiser (Fuente-Hernández et al. 2013). Similarly, *P. caeni* can grow at a pH range 5-11 and does not seem to use single sugars as sole carbon sources but has shown utilisation of malic and capryl fatty acids as sole carbon sources. Moreover, this species is capable of nitrate and nitrite reduction under anaerobic conditions (Xiao et al. 2009). Therefore, having a broad spectrum of carbon sources in the media used in this study, it can be speculated that it can be speculated that the pseudomonads, avoided strong competition with other members of the community for resources for growth.

With respect to EtOH production itself, the ability of change their metabolism from acid to solvent formation in response to low pH (Amador-Noguez et al. 2011), might have provided an ecological advantage to the solventogenic clostridial species (*C. beijerinckii* and *C. saccharoperbutylacetonicum*,) to thrive under the incubation conditions tested in this study. These OTUs were, therefore, likely the main organisms responsible for the high EtOH production in the initial group of microcosms, as although they are known to produce butanol and acetone at pH ~ <5.1, ethanol is formed by them at both lower and higher pH values, when the acidogenic phase its taking place (Amador-Noguez et al. 2011; Millat et al. 2013; Poehlein et al. 2017).

The fact that the OTU enriched in Exps A and B was mostly similar to *C. saccharoperbutylacetonicum* (99% similarity) while the one in Exp B was identified mainly as *C. beijerinckii* (100% similarity) could almost be deemed as inconsequential in terms of this work, as a thorough study comparing the metagenomes of several solventogenic clostridial species strains (Poehlein et al. 2017) grouped these two into a

phylogenetic clade where, among other sequence similarities, its members encode a protein complex able to reduced ferredoxin to NADH, generating an ion gradient across the cytoplasmic membrane that can be used for additional ATP synthesis via the ATPase. No members of the other major clade (i.e. *C. acetobutylicum*) possess these genes. Nevertheless, under the incubation condition in the present project, it is unlikely further NADH production would have been favoured in these species, as the high proton concentration due to the low environmental pH would require NAD⁺ restoration, a condition that can be met by EtOH production.

Additionally, both clostridial species have shown tolerance to ferulic acid, a phenolic compound found in lignin hydrolysates, which was probably present in the acid and steam pre-treated OMSW culture medium, thus counting on further ecological advantage over other species (S. Lee et al. 2015; Yao et al. 2017). Further research has also shown solventogenic *Clostridia* can co-metabolise sugars (e.g. glucose and cellobiose) along with acetic and butyric acid for solvent formation at low pH (<5.5) (Wen et al. 2014; Maddox et al. 2000), thereby allowing sufficient time for spore formation and thus long-time survival (Poehlein et al. 2017). This phenomenon can lead to a gradual pH increase, as that observed in Fig. 6.7 of Exp C.

One of the differences reported between these two species is the inefficient pentose utilization of *C. beijerincki*, while *C. saccharoperbutylacetonicum* has shown xylose and arabinose degradation levels similar to glucose degradation (Wen et al. 2014; Yao et al. 2017).

Another recurrent OTU that has been enriched in all these experimental set-ups as well as in the community described in Chapter 5 is *L. mesenteroides*, which likely proceeded from the substrate itself. This organism has been reported to have a higher affinity for sucrose and fructose over glucose degradation, while the latter sugar as well as citrate and pyruvate, have been shown to direct the metabolism of this bacterium towards acetate (aerobically) or mannitol (in anaerobiosis) at the expense of EtOH production (Dols et al. 1997). Therefore, it can be induced that *L. mesenteroides* flourished in all the enriched communities due to the high content of vegetable and fruit matter present in OMSW, rich in fructose, but with little contribution to the overall EtOH formation. The reduced input by this bacterium to the total EtOH production in the initial inoculations is further supported by the Exp C longer incubation periods and sampling monitoring, where *L. mesenteroides* contribution to the total community composition was relatively

low, although in apparent growth, as it kept increasing until day 21, when it was the second most abundant community member.

Although cellulolytic *Ruminococcus*-like OTUs (*R. albus*, *R. champanellensis* and *Ruminococcus flavefaciens* >90% similarity) were present from the moment of inoculation, and showed a decreasing tendency in the enriched communities, their prevalence as one of the most abundant contributors to the total community composition through the initially inoculated microcosms, unlike numerous other OTUs that were “washed” away. This persistence indicates their probable participation within the communities enriched. One of their clear metabolic advantages over other organisms is their ability to use cellulose as a substrate (Suen et al. 2011; Chassard et al. 2011), therefore avoiding substrate competition, however, their growth ceases at pH values under 5.8 (Desvaux 2006), which would explain their decreasing abundance overtime.

Interestingly though, *Ruminococcus albus* can use the glycolytic pathway to ferment one mole of glucose to one mole of ethanol, one mole of acetate, two moles of H₂, and two moles of CO₂, yielding, three ATPs, *R. albus* does this through a hydrogenase that transfers electrons from NADH to H⁺ to produce H₂. When this gas accumulates in the medium, the hydrogenase does not oxidize NADH because the equilibrium favours NAD⁺ reduction. Two molecules of NADH are then used to reduced acetyl-CoA to ethanol (White 2007). Thereby, *Ruminococcus*-like OTUs could have actively participated in EtOH production, mostly at the beginning of the incubation, when the pH was not increasingly acidic, and they had substrate availability advantage, but only after the environment was sufficiently anaerobic, thereby leaving a narrow time frame for this OTU to contribute to EtOH formation in these systems.

There were two other OTUs abundantly found in all these experimental set-ups, but not in the previous chapter, namely the *Petrimonas*-like OTU (95% similarity) and *Leptolinea*-like OTU (90% similarity). The *Petrimonas* genus is comprised by two facultatively anaerobic bacteria of the family *Porphyromonadaceae* (phylum *Bacteroidetes*), isolated from mesophilic biogas reactors. These bacteria can ferment carbohydrates, some organic acids and casamino acids, but not amino acids. Additionally, one of its members, *P. sulfuriphila* can reduce nitrate and sulphur to ammonium and sulphide, respectively (Hahnke et al. 2016; McIlroy et al. 2017).

Similarly, the genus *Leptolinea* has been isolated from sludge in a mesophilic UASB reactor (Yamada et al. 2006), and is a member of the *Anaerolineae* family, one of the prevalent

groups found in anaerobic digesters (Xia et al. 2016; B. Zhang et al. 2017), where it is hypothesised it does not participate in cellulose degradation or anaerobic symbiotic interactions, but mostly provides adhesive properties to sludge granules and contributes as a carbohydrates and peptides fermenter (Xia et al. 2016; Kirkegaard et al. 2017).

At 14 days, time point at which the maximal EtOH production was reached in all the initial systems, most of these bacteria were still among the most abundant members of the enriched communities in different proportions, with the overall higher contribution of *Clostridium* and *L. mesenteroides*, and the decreasing presence of the rest, particularly evident for *Pseudomonas*, likely resulting from oxygen depletion. This is further supported by the presence of *Methanobacterium beijingense* ($\geq 99\%$ similarity), an archaeon isolated from anaerobic sludge granules, in all these communities at 14 days, where it could have been producing methane from H_2/CO_2 or formate. However, the level at which this organism was active should have been low as its pH range for growth and methane production is 6.5-8.0 (Ma et al. 2005). Besides, its H_2 utilisation would have triggered hydrogenic bacteria (i.e. *Ruminococcus*) to produce high levels of H_2 directing their metabolism towards acetic acid formation instead of EtOH (White 2007), but as the fermentation profiles show, acetic acid was produced rather modestly in all systems. Nevertheless, a *Methanobacterium* isolated from an acidic wetland with a constant temperature of 15°C at the depth of sampling, has shown, despite its very slow growth rate (on the order of days), to conduct hydrogenotrophic methanogenesis over a range of low pH values (3.8 to 6.0) and temperatures (5 to 30°C), with maximal rates at pH 5.0 to 5.5 and 25 to 30°C (Kotsyurbenko et al. 2007).

Although the potential function of the different members can be estimated from their reported physiological activities, it remains unclear whether these organisms were interacting with each other or were able to survive individually. Moreover, accounting only for the low pH registered at days 7 and 14 (~ 4.6), and that from the OTUs in the average enriched community, only the clostridial species, *L. mesenteroides* and *P. saccharoperbutylacetonicum* are reported to grow under acidic conditions (S. Lee et al. 2015; Maddox et al. 2000; McDonald et al. 1990; von Neubeck et al. 2016), while *P. caeni* and the members of the *Ruminococcus*, *Petrimonas* and *Leptolinea* grow closer to neutrality, with pH 6 being reported as their lower limit (Suen et al. 2011; Hahnke et al. 2016; Yamada et al. 2006; Xiao et al. 2009). The active contribution to the community functionality as well as its composition by the latter OTUs is, therefore, speculative.

Thereby and based on the conceptual model proposed in Chapter 5, the average R+S community comprised by the OTUs described above would function as follows (Fig. 6.11).

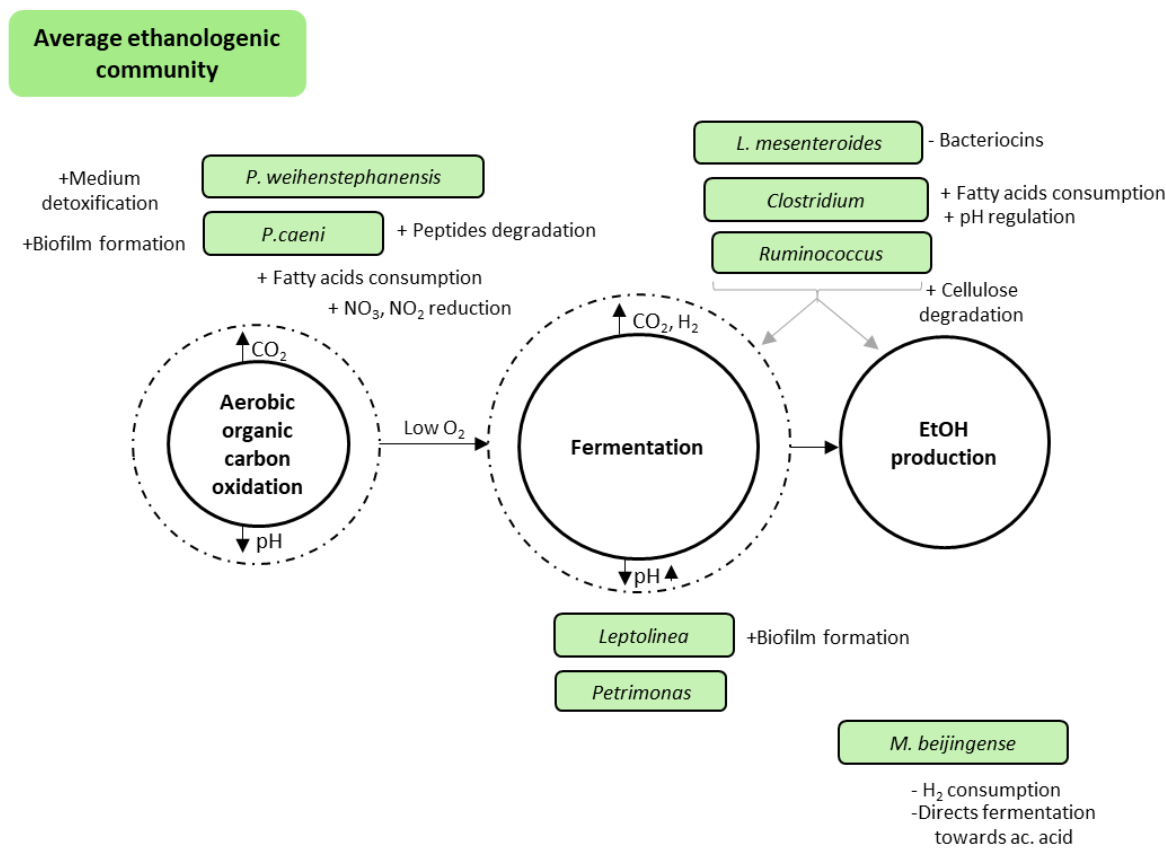


Figure 6.11 Diagram of the putative functionalities of the dominant OTUs. +/- symbols before specific OTUs putative functions indicate an activity possibly benefiting (+) or damaging (-) the community.

However, it is hypothesised that a form of biofilm was generated by *Pseudomonas* and *Leptolinea* action, creating microenvironments where the community members could perform their metabolic activities protected from low pH and other growth inhibitors (Khiyami et al. 2005; L. Zhou et al. 2014; Lund et al. 2014). In this regard, *Pseudomonas* biofilms have been shown to be capable of providing shelter to other bacteria in multi-species biofilms formed in industrial settings (Coughlan et al. 2016), where the non or poor biofilm formers (e.g lactic acid producers) as well as the pseudomonads species benefited from environmental protection and nutrients exchange (Marchand et al. 2012). Furthermore, an enriched cellulolytic microbial community growing in static batch reactors incubated under mesophilic conditions degraded up to 80% of crystalline cellulose after 20 days of incubation was shown to grow as a thin bacterial biofilm, where the authors concluded cellulose solubilisation rates depended on the amount of biofilm formation and architecture (O'Sullivan et al. 2005). Therefore, biofilm formation would have also been supported by the static incubation conditions of the present work.

Under this hypothesis, *Ruminococcus* cellulolytic activity would have benefited the carbohydrates oxidisers (*P. caeni*) and fermenters (*Clostridium*, *Petrimonas* and *Leptolinea*), while actively contributing to EtOH production. Nevertheless, it is also possible that the cellulolytic fraction of the OMSW was not consumed, as many of these OTUs could grow on fatty acids, peptides and the simpler carbohydrates likely to be in solution due to the *in-situ* substrate pre-treatment.

Additionally, a study of EtOH production from unwashed rice bran hydrolysate (pH 6) by the biofilm producing bacterium *Zymomonas mobilis* found that the biofilm had served to preserve ethanologenic activity by providing a protective niche for growth in the presence of toxic inhibitors caused by acid pre-treatment (Todhanakasem et al. 2014)

Although more studies such as micrographies and fluorescence *in situ* hybridization (FISH) would be required to demonstrate this hypothesis (Todhanakasem et al. 2014; O'Sullivan et al. 2005; L. Zhou et al. 2014), a thin layer was observed to develop at the top of the substrate in inoculated microcosms which was clearly different to the state of inocula blanks (Fig. 6.12). Thereby, the possibility of biofilm formation aiding the activity of the described community is not unlikely.

Under the assumption of these functions, the dramatic loss of ethanologenic and general fermentative activity in Exps A and B after transfers could be mostly attributed to the absence of *Pseudomonas* and *Clostridial* species, where *Lactobacillus casei* and *Lactobacillus brevis* dominated in different proportions in the transferred communities.

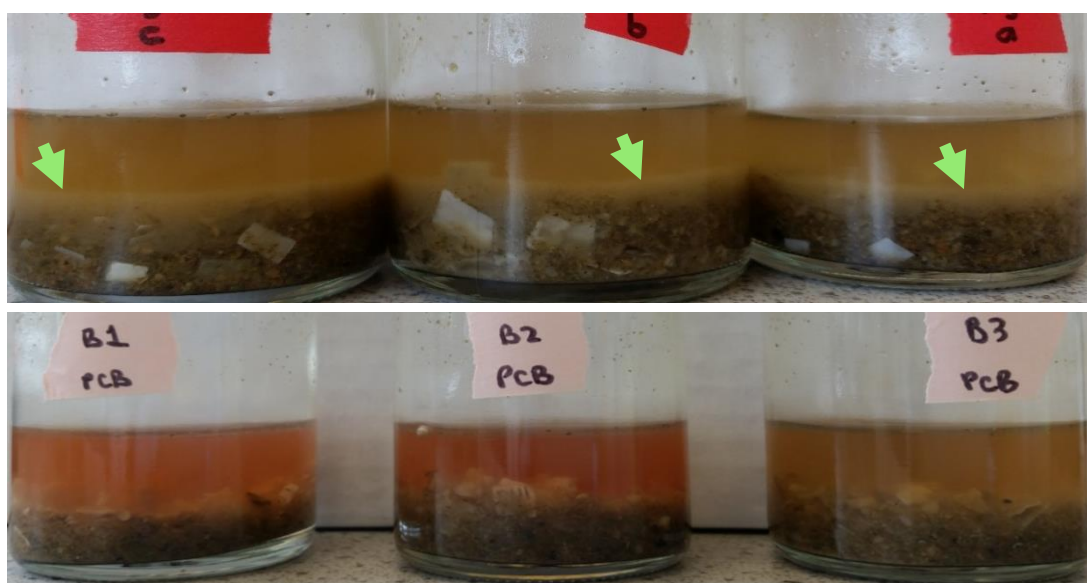


Figure 6.12. A) Inoculated microcosms at 7 days of incubation. B) Inocula blanks at 7 days of incubation. Images from Exp C. Green arrows in the image signal the biofilm-like membrane.

Although both lactic acid bacteria are facultatively anaerobic acid resistant organisms commonly found in the gastrointestinal tracts of animals as well as in fermented plant material, a difference in energy generation exists between them (H. Zhang and Cai 2014; Cai et al. 2007). Being obligate heterofermentative species, *L. brevis*, as well as *L. mesenteroides*, are restricted to follow the pentose phosphoketolase (PPK) pathway, while *L. casei* can utilise both, the glycolytic and PPK pathway (Poolman 1993). Using the PPK pathway, lactic acid bacteria produce equimolar amounts of CO₂, lactate and ethanol or acetate from one mole of glucose. Since the first steps of this pathway follow the pentose phosphate pathway until glucose is converted into xylulose-5-phosphate, bacteria like *L. brevis* and *L. mesenteroides* prefer pentoses over hexoses (Olsson and Hahn-Hägerdal 1996; Dols et al. 1997) and whether they produce EtOH or acetate depends on the environmental conditions (Spector 2009). EtOH production is preferred when the redox balance of the cell requires maintenance, as is low pH, since EtOH formation regenerates two NAD⁺ molecules. Alternatively, under conditions where NAD⁺ can be regenerated without ethanol formation, acetate is produced, with the concomitant ATP generation. Thus, while acetate formation provides the cell with 2 ATP, the path to EtOH production only yields one ATP molecule (Spector 2009; White 2007). In Exps A and B transfers the pH decreased after inoculation to values below 4.5 and above 4.0, which favour EtOH formation (McDonald et al. 1990) as reflected in the corresponding fermentation profiles. However, very low pH affects energy production, eventually leading to a stop in growth. The pH value at which this occurs depends on in the individual lactobacillus species, since their internal pH lowers as function of that of the external and they have developed different resistance levels, i.e. *L. mesenteroides* stops growing when its internal pH drops below 5.4, which is caused by an external pH close to 4.5 (McDonald et al. 1990).

In disagreement with the previous discussion, lactic acid production in those experimental set-ups was low (~3.5mM) although relatively stable across transfers, while maximal acetic acid production was about 8mM, suggesting that the growth of these bacteria was not fully supported and that the microorganisms in the remaining 30% of the total community composition were contributing to the production of this organic acid. The apparent modest growth by these lactic acid bacteria could have also been further affected by bacteriocin production by these bacteria, as previously described in Chapter 5, bacteriocins are proteinaceous antibacterial compounds against species closely related to the producer strain (Ogunbanwo et al. 2003) and their production has been shown to

be triggered by low pH (Lund et al. 2014), so it could have been possible that both species were affecting i.e. limiting each other's growth and overall fermentative productivity.

Nevertheless, their ability to grow in presence of oxygen, acid resistance and bacteriocin production likely provided these OTUs with certain advantages over other organisms directly after inoculum transfers, where it was likely that most OTUs would have entered a stationary or death phase of growth and would have required of a longer time to adapt to the new environmental conditions of the transfer (S. Lee et al. 2015).

In contrast, the more successful (from an ethanologenic standpoint) transfer case was at 3 days after inoculation, where *Pseudomonas* and *Clostridium* remained being enriched throughout the study, and although this discussion has stressed their putative crucial functions for the high ethanologenic activity observed, their maintained transfer and important contribution to the total composition of at least the communities inoculated in Tr1, Tr3 and Tr5 (day 0), was clearly not enough to maintain EtOH production at the high initial levels, since this decreased to almost 50% of the original.

At 7 and 14 days of incubation in Tr3 and Tr5 *L. mesenteroides* surpassed *P. weihenstephanensis* as a main contributor to the total community composition, where facultative anaerobes *Escherichia* and *Enterococcus* genera members were enriched, representing at last 10% each to the total community composition. Both genera could have been enriched from the rumen where they participate as fermenters (Mann et al. 1954; Henderson et al. 2015).

However, as described in section 6.4.10 the total fermentative activity of these transfers was equivalent to that of the initially inoculated microcosms, with butyric acid being produced to about 20mM, indicating these communities were not only viable, but active, despite the pH in these systems being around 4.7.

Unfortunately, it was not possible to find similar results from comparable studies to those presented here in the literature as most work on mixed culture fermentations reporting the use of sequential transfers for enrichment/selection of a community with desired traits, determine the bacterial community composition once a stable degradation/fermentation activity is reached in batch reactors (Kato et al. 2004; Haruta et al. 2002; Ronan et al. 2013; P. Guo et al. 2010), or until steady state conditions are established in continuous reactors (Temudo et al. 2008; Sun et al. 2015; Wu et al. 2017), for potential isolation of the most abundant members (Kato et al. 2005; Wahyudi et al.

2010; K. Zhou et al. 2015), or for the general characterisation of the system (Temudo et al. 2008; Ronan et al. 2013; C. W. Lin et al. 2011), but fail to track the changes in community composition to get there.

Nevertheless, there have been studies evaluating the adaptation of microbial communities from their source until the desired activity is observed (Jimenez et al. 2014; Garcia et al. 2011; Varrone et al. 2015). For instance, a study aiming to enrich a microbial community from subsurface lake sediments and rumen combined 1:1 v/v for anaerobic digestion of carrot pomace, also monitored community changes using pyrosequencing of the 16S rRNA gene, doing so during three consecutive transfers, where the inocula transfer into fresh medium was conducted when methane production ceased. A drastic loss of diversity was also observed in this study, with the enrichment of the bacterial groups *Bacilli*, *Porphyromonadaceae* and *Spirochaetes* while *Methanosarcina mazei* represented up to 99% of the archaeal population in the stable community. The failure of this community to maintain high methane yields at the last transfer was attributed to the low ratio of archaea against bacteria, although successful substrate utilisation (near 100%) was observed (Garcia et al. 2011).

In that study as well as in the present Exps A and B, transfer timing could have played a critical role to maintain organisms with the desired activity before they passed into non-viability (i.e. were sufficiently senescent as to be alive and metabolically active, but no longer capable of growth or doing so in a very slow rate (Bisson 1999)), thus having a competitive disadvantage against other more viable bacteria at the time of transfer.

In a different work comparing glycerol degradation by activated sludge and anaerobic sludge across transfers, employing different transfer techniques, it was found that while activated sludge was successfully transferred (reaching almost 100% substrate degradation) between batches every 72h, time at which gas production stop; the anaerobic sludge was inactive after a few transfers. The latter problem was circumvented by the authors by trying a fed-batch mode and continuous culture as alternative adaptation strategies, with continuous culture allowing effective substrate degradation by a stable community mostly comprised of *Clostridium*, *Klebsiella*, and *Escherichia* related bacteria (Varrone et al. 2015).

However, by aiming at methane production, these studies were inherently different to the system presented here, since the operational conditions involved 37°C incubations and neutral pH. Thereby, different metabolic and thermodynamic principles would have

dictated the failure/success of the transfers performance, notwithstanding that methane is an irreversible produced catabolic endpoint, whereas EtOH can also be a substrate (Bertsch et al. 2016; Agler et al. 2011).

Finally, research where clostridial species were the most relatively abundant organisms enriched from anaerobic sludge to ferment syngas, showed that acidic conditions were necessary to trigger solventogenesis in these bacteria, but pH under 4.5 was detrimental to their growth and recovery, concluding that a minimum pH value of 4.8-4.7 during any stage of the incubation could allow solvent production and *C. kluyveri* growth. In this study a maximum of 1.7g/L (36.9mM) EtOH was produced along with butanol, hexanol and their corresponding VFAs in minor amounts (Ganigué et al. 2016).

As discussed in Chapter 4 section 4.5.2, metabolic energetics-based models proved to be useful tools to explain the general fermentation patterns observed experimentally, in this case, the fermentation model proposed by Ramírez *et al*, (2006) is still the most successful explaining the fermentative profiles seen in Exp C, where stable ethanologenic activity was achieved.

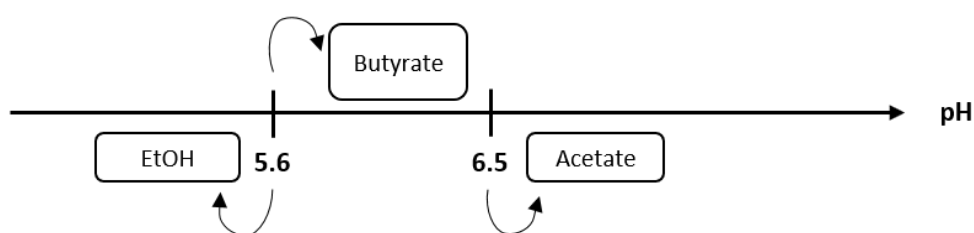


Figure 6.13 Soluble fermentation products as a function of pH in MCF according (Rodríguez et al. 2006) modelling approach.

However, this as other similar models, have limitations in their predictive and explanatory power by neglecting community composition, ignoring the potential existence of microbial interactions that would make possible otherwise thermodynamically unfavourable reactions or the timing of events in relation to individual cell growth, viability and death. Moreover, since glucose is often considered the only carbon source, such models would under represents the complex composition of OMSW, where, based on the putative functions derived from the community analysis, peptides and lipids could have been used as substrates.

Thus, combining this model with the putative functionalities of the average community described in Fig. 6.11 along with the transfer results of Exp C, it is proposed that *C. beijerincki* was the main organism responsible for EtOH production (2 EtOH+2NAD⁺/glucose,) and pH maintenance in these systems by benefiting from *P. weihenstephanensis* consumption of oxygen and possible biofilm formation to be able to produce butyric acid (1 BTA+2NAD⁺/glucose), therefore gaining energy while restoring redox balance that kept this microorganism viable and active for the successive transfers, as the regeneration of NAD⁺ is for metabolic redox reactions, including ATP synthesis, ATP hydrolysis and ultimately biomass production (White 2007). *L. mesenteroides* could have contributed to EtOH generation to maintain its Δp gradient functional (McDonald et al. 1990; Dols et al. 1997).

While the decrease in EtOH production after the initial inoculation could have been due to the loss of the other members of the so-called average community, as for example it has been shown that the biofilm formed by multi-species was stronger and stable than when produced by a single species, and therefore the absence of *P. caeni* and the *Leptolinea* member in the enrichments could have been detrimental. Additionally, extra EtOH production could have been achieved by *Ruminococcus* growth, which also failed to be enriched in the transfers, besides, this OTU could have released simple carbohydrates by degrading cellulose. Nevertheless, this is all speculative and further work would be required to elucidate the difference in functionality between the initially inoculated microcosms and the successive transfers.

6.5.2 Known and unknown selective pressures influencing the bacterial communities enriched

Although pH and inoculum source seem to have directed fermentation towards EtOH production, other factors could have exerted selective pressure in these systems. As previously suggested, the presence of lignin-derived compounds, which the enrichment of bacteria able to degrade aromatic compounds supports (e.g. *Pseudomonas*), is likely to have negatively affected the growth of other inoculum members, including potential ethanologenic bacteria (Parawira and Tekere 2011; Y. Zhang and Ezeji 2014; S. Lee et al. 2015).

Another factor that was not tested in the present study and which probably influenced the results observed is the inoculum to substrate ratio (I/S) in terms of its volatile solids content. While I/S ratios in terms of VSS content are regularly conducted in studies evaluating anaerobic digestion, most studies dedicated to ethanol production report the inoculum concentrations in terms of mass of inoculum per volume of liquid medium, inoculum volume/ medium volume ratios or percentages (Varrone et al. 2015; Ronan et al. 2013; Kato et al. 2004).

Although, at the time of writing, it was not possible to find studies on I/S ratios evaluation regarding EtOH production from lignocellulosic substrates by mixed cultures, it has been observed (F. Zhang et al. 2012) that a high glucose loading rate (24.7g/L) increased the ethanol/ acetate + butyrate mole ratio produced by an anaerobic sludge obtained from a citrate-producing factory wastewater, however substrate accumulated notably in effluent at higher substrate loading rates. Additionally, it has been shown that the hydrolysis of municipal solid waste and subsequent methanogenesis by sludge inoculated reactors at I/S ratios under 0.12 is limited by the inoculum concentration (Boulanger et al. 2012). Contrarily, H₂ production yields were improved by an I/S of 0.07 in microcosms inoculated with sludge degrading a reconstructed OMSW, when compared to lower and higher I/S ratios (Florio et al. 2017). Thus, no direct conclusion could be derived from the literature, as optimal I/S ratios not only depend on the inoculum and substrate concentrations, but also seem to vary in relation to the desired end-product. For instance, while methane production seems to be improved by higher I/S ratios due to the potential increase in the number of methanogens in the system (Boulanger et al. 2012; Silva Lopes et al. 2004), the opposite was observed for hydrogen production. The previous examples strongly indicate the determination of optimal I/S should be performed for each study. In the present work, the I/S ratio of R+S inoculated microcosms was 0.064 (see Appendix G). However, it is highly recommended to conduct experiments to evaluate the effect of different I/S ratios in order to select the most appropriate for EtOH production from the OMSW analogue used here.

The substrate used itself could have also played a significant role in the selection of the enriched communities, as there is evidence that differences in OMSW composition (e.g. carbohydrates, protein, fat proportions) can lead to different fermentation profiles (Alibardi and Cossu 2015) due to the enrichment of different functional microbial populations (Lü et al. 2009).

Regarding the transfer times evaluated, the initial presence of oxygen in the medium at the beginning of each transfer could have also imposed a two-fold limitation in the growth of anaerobic bacteria (i.e. *Clostridium*) due to i) anaerobes inability to growth under initially aerobic conditions and ii) as the diversity of aerobic organisms originally present in the inoculum was clearly reduced across transfers, oxygen depletion was likely prolonged, potentially favouring the growth of facultative organisms (Tang et al. 2004). The latter factor seems to have played an important role during the 14-day transfers, where acidophilic, specialised decaying-plant material degraders *Lactobacilli* dominated transfers enrichments, potentially further limiting the growth of slow-growing competitors by further decreasing the medium pH (De Vos et al. 2009). Similarly, the kinetic growth of the most abundant OTUs enriched in the original inoculation could have also strongly influenced the results observed. For instance, despite the successful retention of pseudomonads and clostridial species during the 3-day transfers, EtOH production diminished without a clear switch in the soluble end-products generated, suggesting, as previously discussed, an overall reduction of fermentative activity. However, the lack of gases measurements, cell counts and relevant bacterial groups monitoring limits the understanding of these observations. CO₂, H₂ and CH₄ measurements coupled with cell and spore counts and qPCR could have helped elucidate if the aerobic/ facultative anaerobic members activity and growth was higher than that of the putative ethanologenic spore-forming *Clostridium* species. Evaluation of these parameters would provide a deeper characterisation and understanding of these systems.

4.6 Conclusions

A stable ethanologenic bacterial community able to produce an average EtOH concentration of 30mM as its main soluble fermentation product was reproducibly enriched through 3-days successive inocula transfers. The enriched communities seemed to rely on the presence of *C. beijerincki* and *P. weihenstephanensis*, as dominant members for at least the beginning of the incubations, after which other fermentative microorganisms where also enriched.

However, it is recommended that further work aiming to optimise this stable, but less productive, community, should test the addition of trace minerals and abiotic inocula matrix (autoclaved inocula sources) across successive transfers, as previously, but unsuccessfully done in Exp B of the present study. Since 3-days transfers have been shown

to maintain ethanologenic activity, albeit at lower concentration, it would be possible to assess, for instance, if the absence of some chemical factor which was diluted from the original inocula, could enhance EtOH productivity.

Importantly, the batch of replicate microcosms directly inoculated with the combination of rumen and sludge produced about 60mM of EtOH in three individual experimental set-ups conducted with 12 months in between indicating that the ethanologenic activity after initial inoculation with the combination of these inocula sources under the environmental conditions tested is a reproducible and repeatable process.

The present study along with the few currently found in the literature demonstrates that successive inocula transfer is not a straight forward process as commonly depicted by MCF batch studies, where the activity of the original inocula source is either qualitatively reported (i.e. filter paper disappearance) or not specified. In this work the significantly higher ethanologenic activity of the initial inocula would support the need to investigate further means to maintain the functional useful enriched community and the interactions between its members and the physical environment leading to high EtOH production.

Chapter 7. Modelling the metabolic interactions within ethanol producing bacterial communities degrading the organic fraction of municipal solid waste

7.1 Introduction

Experimentally, a mixed-source community able to generate $59.76 \text{ mM} \pm 2.77 \text{ mM}$ of EtOH in batch microcosms has been reproducibly enriched at room temperature under initial aerobic conditions and without further conditioning of the acid pre-treated organic municipal solid waste (OMSW) used as substrate. Additionally, enrichments after successive transfers of this community, reproducibly generated $30.5 \text{ mM} \pm 1.3 \text{ mM}$, with the advantage of activity and community composition stability over time (see chapter 6). The minimal input required by these communities makes them good candidates for implementation in biorefinery projects in both developed and developing countries. Nevertheless, optimisation and control of EtOH production by these communities remains a challenge.

The study of the interactions within ethanologenic microbial communities has been recognized as a necessity to accomplish a reliable system (Zuroff and Curtis, 2012). Indeed, mathematical and conceptual models of the relationships within ethanologenic co-cultures and defined multispecies communities have been used as tools to establish a rational basis for improvement and optimisation (Kato et al. 2005; Shou et al. 2007).

Numerous modelling approaches aimed at unravelling the function and structure of microbial communities have been reported (Smolders et al. 1995; Hanly and Henson 2013; Grimm et al. 2010; Zomorodi and Maranas 2012; Huston et al. 1988). However many of these approaches require detailed metabolic information as inputs or ignore mass balances and growth constraints (Kato et al. 2005; Janssen 2010). In contrast, a “species metabolic interaction analysis” (SMETANA) is a modelling approach that can predict metabolic exchanges and networks within a bacterial community under nutritionally challenging conditions, starting with as little information as 16S ribosomal RNA sequences (Zelezniak et al. 2015).

SMETANA relies on a Flux Balance Analysis (FBA) from genome-scale metabolic network reconstructions (GEMs), which contain all the known metabolic reactions in an organism and the genes encoding for each enzyme (Babaei et al. 2014; Wang et al. 2011). The models reconstructed for individual bacteria are then integrated by the SMETANA pipeline, which uses the FBA to compute the flow of metabolites through the metabolic networks, predicting the growth rate of an organism or the rate of production of an important metabolite (Babaei et al. 2014; Orth et al. 2010). From this information, SMETANA then calculates: the Metabolic Resource Overlap (MRO, the maximum possible overlap between the minimal nutritional requirements of all member species), the Metabolic Interaction Potential (MIP, the maximum number of essential nutritional components that a community can provide for itself through interspecies metabolic exchanges) and, the SEMETANA score (the sum of all interspecies dependencies under a specified nutritional environment) for a given community (Zelezniak et al. 2015).

FBA is an important tool to make use of the knowledge contained in annotated genomes, while SMETANA is a significant development to create bacterial community models.

7.2 Aim and objectives

The aim at this stage in the PhD project was to develop bacterial community metabolic models capable of explaining the experimentally observed data by completing the following objectives:

- The reconstruction and manual curation of multiple species models based on 16S RNA experimental data.
- To obtain representations of the metabolic interactions capable of explaining observed fermentation products by the initially inoculated batch microcosms and by the community enriched across transfers.
- To compare the models of these different scenarios through the Metabolic Resource Overlap (MRO), Metabolic Interaction Potential (MIP) and SEMETANA score calculations.

7.3 Methods

7.3.1 Identification of the closest species to experimentally determined OTUs

Using MEGA X (Kumar et al. 2018), the representative sequences of the most abundant OTUs in the average and transferred communities described in Chapter 6 were aligned against highly similar sequences in the nucleotide 16S ribosomal RNA sequences (Bacteria and Archaea) NCBI database (Altschul et al. 1990; Zhang et al. 2000; Boratyn et al. 2012). The closest related species to each OTU was then selected based on the queries' output (% query cover and % identity) and its NCBI taxonomy ID (NCBI:txid) recorded. Additionally, to validate the results from the queries, phylogenetic trees were constructed using the neighbour joining method and clustering through 500 bootstrap test replicates.

7.3.2 Representative genomes retrieval

Annotated whole genomes (finished, fasta format) of the closest similar species to the highest relatively abundant OTUs were retrieved by searching for their NCBI:txids in the EnsemblBacteria genome database, release 38 (Paul Julian Kersey et al. 2018; P. J. Kersey et al. 2009).

7.3.3 Species-Level genome-scale metabolic model reconstruction

Drafts of the genome-scale metabolic models (GEMs) for the individual species were built using CarveMe 1.1.0 (Machado et al. 2018). To do so, this programme utilises the annotated genomes fasta files as input to then compute the stoichiometric matrix for a particular organism, where cellular metabolites are accounted as rows, metabolic reactions as columns, and the elements of the matrix are the stoichiometric coefficients of the metabolites involved in each reaction, considering positive values for products and negative values for reactants. A metabolic network model is then created in an iterative process (Orth et al. 2010; Machado et al. 2018).

To run CarveMe, the Anaconda distribution of Python 2.7 was used along with the IBM CPLEX solver. Additionally, a file listing in detail the experimental culture media components and their corresponding BiGG IDs (Hyduke et al. 2011; King et al. 2016) was

created and used to gap-fill the models with CarveMe, this was done to guarantee that the model could reproduce growth in the experimentally verified OMSW medium.

7.3.4 Draft GEMs curation and simulation

The draft GEMs produced by CarveMe were then subject to manual curation, where the presence and directionality of the exchange reactions (cell \leftrightarrow environment / secretion \leftrightarrow uptake) of well documented exchange metabolites relevant to this study, such as carbohydrates and fermentation products, were inspected and compared against the fermentation profiles obtained experimentally through this project as well as with the literature for each of the individual species. When needed, these or specific transport reactions (from the cytosolic to the “exchange” compartments) were constrained to correct reaction directionality and nutrient transport information.

To evaluate the feasibility of the curated models, FBA simulations were carried out iteratively with the biomass production reaction (growth) as the objective function to solve the stoichiometric matrix (Orth et al. 2010). These cycles of *in silico* experiments were conducted until the FBA demonstrated that growth for each individual GEM was possible under the set constraints.

The individual model curations and FBA simulations were done using openCOBRA v3.0 (Hyduke et al. 2011) in MatLab (release 2018a), where the functions “addReaction” and “changeRxnBounds” were the main COBRA toolbox functions employed to curate individual models (Hyduke et al. 2011).

7.3.5 Community metabolic modelling simulation

The construction of the communities’ models, their simulation and the calculation of the MIP, MRO and SMETANA score were conducted through the SMETANA pipeline, a submodule of the Framed Python package (version 0.4.0) for analysis and simulation of metabolic models (Machado et al. 2017; Zelezniak et al. 2015).

Figure 7.1 summarises the strategy developed to obtain the metabolic model of the bacterial communities under study.

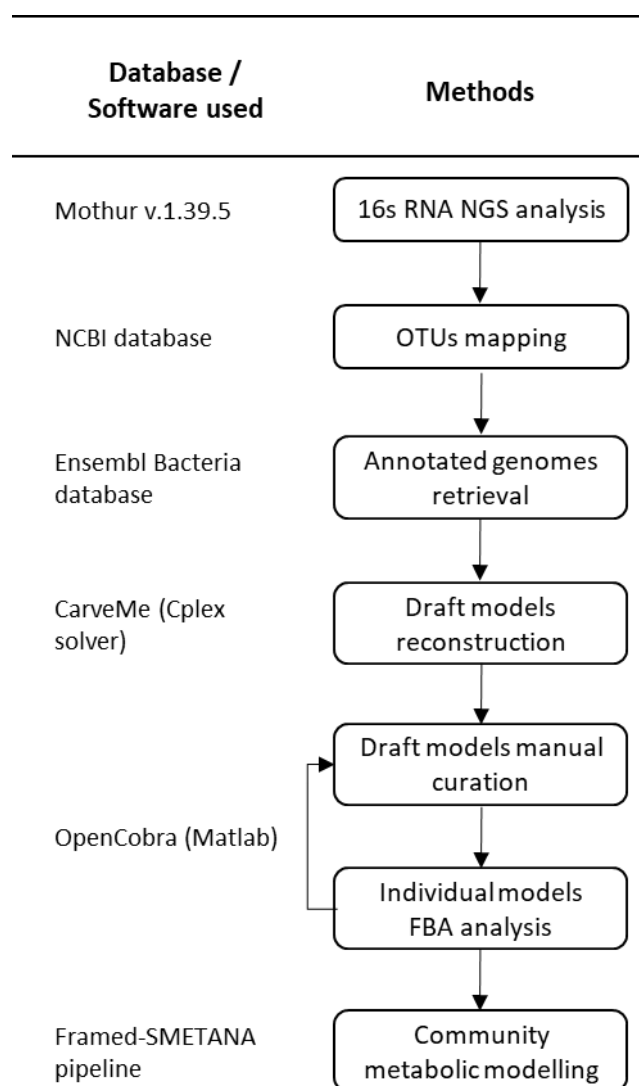


Figure 7.1 Workflow diagram of the steps and computational biology/bioinformatic tools employed to construct the metabolic model of the bacterial community starting from 16S ribosomal RNA sequences.

7.4 Results

7.4.1 Closest species annotated genomes retrieval to experimentally determined OTUs

The individual species to which each of the most abundant OTUs in the enriched communities were mapped based on their sequence identity match within the BLAST database and the corresponding phylogenetic trees generated in MEGA X (see Appendix E) are presented in Table 7.1. The NCBI:ID presented corresponds to the specific strain for which an annotated whole genome sequence was available in the Ensembl Bacteria database.

Table 7.1. Experimental OTUs phylogenetic alignment results.

OTUs closest related species	Q.C. (%)	Identity (%)	NCBI: txid	EtOH
<i>Clostridium saccharoperbutylacetonicum</i>	100	100	931276	+
<i>Clostridium beijerinckii</i>	100	100	290402	+
<i>Leptolinia tardivitalis</i>	99	91	229920	NA
<i>Leuconostoc mesenteroides</i>	100	100	33966	+
<i>Proteiniphilum saccharofermentans</i>	100	95	1642647	NA
<i>Pseudomonas caeni</i>	100	100	521719	-
<i>Pseudomonas weihenstephanensis</i>	100	100	1608994	-
<i>Ruminococcus albus</i>	100	93	697329	+

Percentages of Query Cover (Q.C.) and Identity, their corresponding NCBI taxonomy ID used to retrieve their genomes, and the ability of this species to produce EtOH. NA, no experimental evidence in the literature, but theoretically possible.

Proteiniphilum saccharofermentans, a facultatively anaerobic bacteria of the family *Porphyromonadaceae* isolated from mesophilic laboratory-scale biogas reactors (Hahnke et al. 2016), was used instead of *Petrimonas* (a close relative from the same family) as none of the annotated whole genome sequences from the species comprising the latter genus was available. Additionally, and supporting this decision, the phylogenetic tree of the respective OTUs related to these species (see Chapter 6), shows an equally closer match identity to *Proteiniphilum* than to *Petrimonas* (see Appendix E).

Although the percentage of BLAST sequence identity for the OTUs related to *R. albus*, *P. saccharofermentans* and *L. tardivitalis* was $\leq 95\%$, the reported environmental sources from which the sequences in the NCBI database were obtained (Yamada et al., 2006; Suen et al., 2011; Hahnke et al., 2016) agree with the experimental inocula sources of this study (rumen and anaerobic sludge).

7.4.2 Draft GEMs manual curation and simulation

After the draft GEMs of the annotated whole genome sequences were constructed via CarveMe, their manual curation involved inspection and adjustment of stoichiometric and reversibility constraints on exchange reactions based on a comprehensive literature

search for previous works containing biochemically distinguishable traits over these species (Keis et al. 2001; Kim et al. 2008; Ward et al. 2015; Dols et al. 1997; Hahnke et al. 2016; Xiao et al. 2009; Stoeckel et al. 2016; Thurston and Dawson 1993). For instance, the members of the community are mesophilic, facultative anaerobes, apart from *Clostridium beijerinckii*, *C. saccharoperbutylacetonicum* and *R. albus* which are obligate anaerobes. Most of these bacteria are fermentative except for the *Pseudomonads* species. In optimal growth conditions, *C. saccharoperbutylacetonicum*, *P. saccharofermentans* and *R. albus* can ferment cellulose, while *Clostridium beijerinckii*, *C. saccharoperbutylacetonicum*, *L. mesenteroides* and *R. albus* have shown EtOH production. None of the members of the community grows on EtOH as sole carbon source (Dols et al., 1997; Keis et al., 2001; Yamada et al., 2006; Xiao et al., 2009; Suen et al., 2011; Hahnke et al., 2016).

Incorporating this information along with the experimental results, the exchange reactions (cell \leftrightarrow environment / secretion \leftrightarrow uptake) of the individual draft models were constrained. For example, in all models EtOH exchange was bound to be irreversible based on lack of growth on EtOH reported in the literature and thus could only be secreted, while O₂ uptake was bound to 0.003mM, as it has been shown that some members of *Pseudomonas* (the only aerobe bacteria in the community) can grow under this oxygen concentration (Alvarez-Ortega and Harwood 2007; Sun Yoon et al. 2002). In addition, the organisms that could degrade cellulose, according to the literature, were bound to uptake 10mM (the standard amount for carbohydrates uptake in FBA simulations (Babaei et al. 2014)), giving preference to this carbohydrate over others.

After several cycles of *in silico* experiments, the FBA simulations of all the individual models yielded growth (objective function > 0) and exchanged metabolites that agreed with the literature. For instance, carbon dioxide production was predicted for all the bacteria, acetate production was predicted for the models of *C. beijerinckii*, *C. saccharoperbutylacetonicum*, *L. tardivitalis*, *L. mesenteroides* and *R. albus* (Keis et al. 2001; Ward et al. 2015; Desvaux 2006), whereas D_lactate was only obtained in *L. tardivitalis* and *L. mesenteroides* (Yamada et al. 2006; Dols et al. 1997). Moreover, *P. caeni* was predicted to uptake nitrate and secrete nitrite (Xiao et al. 2009; Stoeckel et al. 2016). In these individual model simulations, EtOH was only expected to be produced by *C. beijerinckii*, *C. saccharoperbutylacetonicum* and *P. saccharofermentans*.

7.4.3 Communities draft models

Two communities were assembled for analysis through the SMETANA pipeline, the “average” highly ethanologenic community enriched after initial inoculation of microcosms after 7 days of incubation, and the “average” community enriched from 3-day transfers (see Chapter 6).

Despite sanity checks (i.e. duplicated reactions, demand reactions with negative lower bound) for growth of the individual models (Brunk et al. 2018), the integration of these by the SMETANA pipeline did not find a solution for growth after repeated simulations. Knockout communities were then simulated (eliminating one of the members at a time), showing that the individual model of *L. mesenteroides* could not be analysed by the Framed Python package (from which SMETANA is a submodule (Machado 2017)). Therefore, leaving *L. mesenteroides* aside, communities comprised by the other species were analysed.

Through the SMETANA pipeline, the FBA of the highly ethanologenic community enriched after initial inoculation showed an optimal solution for the growth reaction set as the objective function of $11.0 \text{ mmol} \cdot \text{gDW}^{-1} \cdot \text{hr}^{-1}$ (*bacterial grams of dried weight), MIP of 15 (number of possible metabolites exchanged between the individual members) and an MRO of 0.84. Since MRO values range from 0 to 1, with the latter meaning full resource competition, this result suggested a great level of competition between the members of the community, agreeing with the observations of Zelezniak *et al* (2015) of resource competition being the predominant factor shaping community’s composition.

Additionally, the SMETANA pipeline produced species couplings of possible subcommunities of interacting members (Figure 7.2).

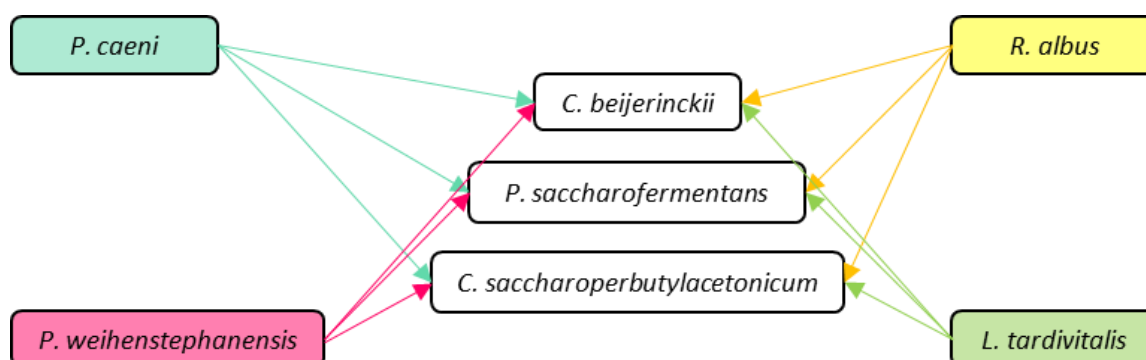


Figure 7.2 Predictions of interacting subcommunities within the “average” highly ethanologenic community enriched after initial inoculation by the SMETANA pipeline. The arrows indicate the direction of the possible interaction.

The results illustrated in Fig. 7.2 suggest no interaction between *L. tardivitalis*, *R. albus*, *P. caeni* and *P. weihenstephanensis* and some degree of association (competition or comensalism) of these bacteria with *C. beijerinckii*, *C. saccharoperbutylacetonicum* and *P. saccharofermentans*. It is important to notice that *C. beijerinckii*, *C. saccharoperbutylacetonicum* and *P. saccharofermentans* did not produce any coupling, thereby the unidirectionality of the arrows in Fig. 7.2.

Meanwhile, the simulation of the enriched community from 3-days transfers which, comprised only by *C. beijerinckii* and *P. weihenstephanensis*, showed an optimal solution for the growth reaction of $360.48 \text{ mmol} \cdot \text{gDW}^{-1} \cdot \text{hr}^{-1}$, an MIP of 7 and an MRO of 0.81. Additionally, for this community optimal growth solutions under the conditions tested were calculated for the individual species with values of $298.8 \text{ mmol} \cdot \text{gDW}^{-1} \cdot \text{hr}^{-1}$ for *Clostridium* and $61.7 \text{ gDW}^{-1} \cdot \text{hr}^{-1}$ for *Pseudomonas*. Nevertheless, no interaction between these two species was predicted to occur.

It must be noted that the results for of MIP, MRO and SMETANA couplings are only preliminary. To this date, the SMETANA pipeline is still under development and many unexpected errors were experienced during this project.

7.5 Discussion

To truly understand a bacterial community behaviour, it must be placed within its ecological context including direct interactions within its members as well as the environmental and physical location. (Jayathilake et al. 2017). In this regard, the modelling approach employed in this research faced two major drawbacks to adequately represent the communities enriched experimentally in this project: it does not count with a mechanism to account for the pH effect in growth and metabolism, factor that was shown to be a driving force to impose selective pressure in the enrichment of the communities under study (Chapters 4 and 5). While it also neglects possible community members' interactions that are not direct metabolic exchanges, for instance, biofilm formation, which was proposed as one of the mechanisms which could have allowed the 3-day transfers communities to maintain EtOH production (see Chapter 6). Since these problems have been previously recognised by the scientific community, different modelling approaches which consider these variables are under development (Jayathilake et al. 2017; Naylor et al. 2017; Millat et al. 2013; Grimm et al. 2010).

Despite these limitations, the results obtained through the SMETANA simulations help in the qualitative interpretation of the results, particularly the ones of the community enriched after 3-days transfers, where the growth was expected to be much higher than that of the initial community, and *Clostridium*'s growth rate was also importantly higher than that of *Pseudomonas*. The differences in growth rate between these two species could be attributed to the anoxic conditions constrained into the models (0.003mM O₂), thus limiting *Pseudomonas* growth while being adequate for *Clostridium*. At the same time, the lack of coupling predicted between these two species indicating no metabolic exchange between them, would not negate the hypothesis proposed previously in Chapter 6, in which *Pseudomonas* biofilm components could have protected other bacteria from the increasingly low pH as well as from inhibitors derived from the lignocellulosic substrate acid pre-treatment and, *Clostridium* EtOH production could have helped maintain the media pH value above a threshold where growth was possible for both species.

The hypothesis above stated is plausible as it has been reported that pH changes as well as the presence of toxic compounds in the environment induce biofilm matrix formation (Khiyami et al. 2005; Lund et al. 2014), and that this biofilm barrier can also protect other organisms besides the *Pseudomonas* species producing it (Marchand et al. 2012; Coughlan et al. 2016). In addition, there is literature support implying that *Clostridium*'s EtOH production could help to maintain the extracellular pH within values where growth is possible (Amador-Noguez et al. 2011; Lee et al. 2015; Ganigué et al. 2016).

However, it is more difficult to derive conclusions from the average initially inoculated enriched community results, as the predicted growth is rather low, in disagreement with the experimental results, where the most abundant OTUs at 7 days of incubation prevailed in these communities at least until 14 days, indicating their activity and possible growth was maintained. Even more, these communities displayed higher soluble fermentation production than any community enriched after transfer, which could be seen as an indirect measurement of successful growth.

In this respect, it is recognised that the accuracy of a model is highly dependent on the reconstruction process, and that the models might contain summative process-dependent errors, including missing reactions (Babaei et al. 2014, 2018). Nevertheless, although it should not be expected that a model will represent biochemical distinguishable differences as accurately as laboratory experimental results do, if a model is precise enough, the results from its simulations should be close to laboratory data. The lack of

clarity in these results can then also be attributed to the inappropriate complete curation of the genomic models.

Additionally, although the analysis of fragments of phylogenetic marker genes, such as the 16S rRNA gene has enabled important advances in the study of microbial communities, its validity to explain a community's functional capabilities, as it is the case of the approach used here, is limited in a number of ways (Langille et al. 2013; Poretsky et al. 2014). Said limitations start with the nature of 16S rRNA high-throughput sequencing itself, as identification to species level via the short-read lengths obtained after amplification of the selected variable region of this gene are not only susceptible to sequencing errors but also depend on the differences derived from different regions chosen (Poretsky et al. 2014). For instance, in Chapter 6 of this work it was shown that communities enriched and characterised in independent experiments had a highly similar composition despite the use of different variable regions (V4-V5 and V3) for their characterisation. Although many of the communities' members were consistently identified as the same species (e.g. *Leuconostoc mesenteroides*), it remained unclear if OTUs highly abundant in those independent communities that were differentially identified to closely related species (i.e. *C. beijerinckii* and *C. saccharoperbutylacetonicum*) belonged indeed to different species or the difference in identification was due to the different variable region sequenced, the limited resolution of the 16S rRNA gene among closely related species, or simply to the inherent variability in the genome of members of a single species and even in that of the members of the same strain (Vernikos et al. 2015; Poretsky et al. 2014).

Since extrapolating from fragments of phylogenetic markers to species identification is a limited process, the interpretation and use of results obtained from methods based on species identified through said process, such as the modelling approached used in this work, must be cautious. Nevertheless, the author considers that both, the conceptual model (Chapter 6, section 6.5.1) and the draft FBA-based model presented in this thesis provide an informed starting point to guide the planning of future work.

7.6 Conclusions

Individual genome scale metabolic model reconstructions able to grow in OMSW medium were computed. In spite of this, the models integrating the individual species did not provide clear information that would help elucidate the interactions between the bacteria enriched in the successful ethanologenic communities obtained previously (see Chapter 6). The latter can be attributed to the lack of modelling experience by the main researcher curating and simulating these *in silico* experiments (me), as well as to some deficiencies in the modelling approach used which have been considered as key elements for the enrichment of the afore mentioned communities, these being pH and biofilm formation.

Nevertheless, the high growth predicted for the 3-days transferred community and the agreement of *Clostridium* and *Pseudomonas* growth rates with what would be typically expected in laboratory experiments under anoxic conditions, along with the absence of direct metabolic interactions predicted for these two bacteria, supports the hypothesis that their successful co-culture observed experimentally might be mediated by pseudomonads biofilm formation and clostridial pH regulation.

Additionally, a “non-expert” step-by-step strategy to reconstruct and curate GEMs, as well as to simulate flux metabolic analysis was developed in this project, which could be beneficial for future work i.e. by creating *in silico* knock out communities thus proving insights into individual function, investigate nutrients and trace minerals addition into the medium that could enhance EtOH and biofilm formation, among others.

7.7 Acknowledgements

This stage of the PhD was carried out with the support of a FEMS Research and Training Grant award (ID: FEMS-RG-2017-0064) at the Department of Biology and Biological Engineering, Division of Systems and Synthetic Biology, Chalmers University of Technology, Göteborg, Sweden under the supervision of Dr. Aleksej Zelezniak and the invaluable help of PhD researchers Filip Buric and Parizad Babaei.

Chapter 8. Conclusions and recommendations

8.1 Conclusions

The main aim of this thesis (as outlined in Chapter1) was to enrich a robust microbial community, able to transform the organic fraction of municipal solid waste into ethanol with the potential for implementation in biorefinery projects in developed and developing countries. In an attempt to reduce biofuel production costs that would make this process economically viable, the operational conditions for the fermentation process were kept as simple as possible (low process control). As this thesis' outlook was microbiological, to avoid a "black box" approach, one of its main objectives was to characterise the enriched community in terms of composition and putative function of its members for control and optimisation of the fermentation.

8.1.1 OMSW lab-scale batch reactors operational conditions

Research on biofuels production from OMSW has focussed on pre-treatments, with a clear lack of experimental studies on the utilisation of this substrate in mixed-culture fermentation (MCF) for EtOH production, as in general for complex lignocellulosic substrates. While other authors have used mostly food waste (carrot and potato peels), here, an analogue of OMSW was produced based on its average composition in Mexico (food waste, paper and cardboard contributions) and the UK (contribution of specific categories comprising the food waste fraction i.e. fruits and bread), providing a closer approximation to the real-life challenge for the conversion of this substrate by a bacterial community.

Ethanol from OMSW was differentially produced by microbial communities from five environmental sources, where lignocellulose matter degradation is known to occur, when incubated under both, initially neutral and acidic pH values and initially aerobic and anaerobic conditions.

In this regard, it was demonstrated that initial oxygen conditions do not play a significant role in EtOH production by the inocula tested. The ability to produce EtOH at initial aerobic conditions irrespective of pH or inocula source agreed with the general

observations of the few other reports evaluating fermentation under initial aerobic conditions, this study being the first where a complex lignocellulosic substrate was tested. This finding supports the aim of this project of simplifying the production process and concomitantly reducing its costs, since the system would passively create the anaerobic conditions necessary for fermentation by itself without the need of flushing the headspace for oxygen removal.

At the same time, pH could be considered the driving environmental factor for EtOH production from OMSW in these experiments. However, it was also shown that the inocula source influenced the formation of this soluble end-product. Specifically, anaerobic granular sludge reproducibly generated the highest EtOH concentration under initial acidic pH, while EtOH production by rumen was equally high at initially neutral pH. The EtOH peak production of both inocula (~30mM) was higher than the reported in the literature for similar studies mostly conducted under neutral to alkaline conditions. Thereby confirming the disagreement previously presented (see Chapter 4) regarding optimal pH for EtOH production estimated solely by thermodynamic models that neglect the microbial composition of the system.

The successful enrichment of a mixed-source community comprised by members of both these inocula (anaerobic sludge and rumen) able to maintain the same ethanologenic activity at a range of pH values (5.5-7), could further contribute to cost reduction and streamlining of this process, since initial acidic incubation would allow the direct fermentation of acid pre-treated OMSW without previous pH adjustment.

Based on these findings, the rest of the experiments were conducted under an initial pH of 5.5. This decision was supported by an energetics-based metabolic model predicting EtOH formation preference over other soluble fermentation products at low pH. The mechanism proposed to explain this, is that EtOH contributes to the restoration of redox balance inside the cell avoiding the expense of charged molecules secretion across the cell membrane (i.e. butyrate).

8.1.2 Mixed-source microbial community characterisation

In addition to the possible significance of the robustness exhibited by the mixed-source community in terms of pH, at the moment of writing, this work is the first determining whether the initial ethanologenic mixed-source community was indeed comprised of members belonging to the original inocula sources. This information is relevant when different inocula sources are combined for MCF studies, since the combination of inocula could not be even necessary, thus simplifying the process for future reproducibility.

The 16S RNA gene sequencing analyses showed the enrichment of bacteria with functionalities involved in aerobic and anaerobic organic matter degradation. Importantly, the enrichment of OTUs closely related to aerobic species able to detoxify the medium by degrading lignocellulose-derived organic compounds, provided a further explanation for the beneficial effect of initial aerobic conditions in MCF. Thus, it is concluded that it is not only the inocula source and initial pH that are responsible for the enrichment of particular OTUs, but also the unconditioned pre-treated substrate, due to both, its nutrients composition and the toxic compounds derived from it, which impose further selective pressure on the microorganisms.

8.1.3 Reproducibility and stability of ethanologenic activity by the mixed-source community

In the experiments conducted to evaluate the stability in EtOH production and bacterial composition of the mixed-source community across transfers, it was found that the batch of microcosms directly inoculated with the combination of rumen and sludge produced about 60mM of EtOH by day 14 of incubation and reached an average total productivity of soluble fermentation products in terms of carbon and electron milliequivalents of about 200mM and 1085.2 e⁻ meq. /L, respectively, recovering about 23.2 % of the electrons feed into the system as biodegradable matter (based on BMP estimates) of which 15% ended up as EtOH regardless of the time which had elapsed in-between experimental set-ups (3 to 12 months). This consistency lead to the conclusion that the ethanologenic activity after initial inoculation with the combination of these inocula sources under the environmental conditions tested is a reproducible and repeatable process.

Furthermore, these results coincided with clear similarities in the microbial composition of the initial communities after 7 days of incubation, where more than 70% of their most

abundant members (>1% relative abundance) were comprised of: clostridial solventogenic species (*C. saccharoperbutylacetonicum* or *C. beijerinckii*) for which ethanologenic activity is enhanced by acidic conditions; the aerobes, biofilm formers and aromatic compounds degraders *Pseudomonas* (*P. caeni*, and *P. weihenstephanensis* in one of the experiments); *L. mesenteroides*, an acid resistant heterofermentative lactobacillus possibly enriched from the substrate, an OTU closely related to the cellulolytic *Ruminococcus albus*; as well as members of the facultatively anaerobic fermentative *Petrimonas* and *Leptolinea* genera.

However, a drastic loss of EtOH production as well as of diversity occurred when successive transfers of the initially inoculated microcosms were conducted at 14 and 3 days of incubation, where about 80% and 50% of the initial ethanologenic activity was lost, respectively. The resulting communities enriched were mostly comprised of 2 or 3 OTUs accounting for at least 70% of their composition. Distinctively, the 3-days transfers maintained higher EtOH production rates and an equivalent total soluble fermentation productivity than the original inoculation, with butyric acid being the second major soluble fermentation product in the five successive transfers. This differentiation in transfers behaviour could also be linked to the bacteria enriched. While the 14-days transfers were dominated by two *Lactobacillus* species, the 3-day transfers were mostly comprised of *Pseudomonas* and *Clostridium*. It was then speculated that the *Lactobacillus* might not have thrived under the incubation conditions, an assumption supported by the reduced total fermentative activity (i.e. low lactic acid production) in the 14-day transfer reactors. Alternatively, an indirect collaboration could have taken place between *Pseudomonas* and *Clostridium* in the 3-day transfers, where besides providing anaerobic conditions through O₂ consumption, *Pseudomonas* could have detoxified the media and produce shelter for growth via biofilm production. At the same time, clostridial EtOH production would have contributed to the prevention of an extracellular pH drop below a threshold where growth of these species would have been impeded. This hypothesis was supported by the fact that both species kept being enriched as the most abundant across 5 sequential transfers.

The latter 3-day transfer community had a stable ethanologenic activity, with an average EtOH concentration of 30mM as its main soluble fermentation product maintained across five successive inocula transfers. Additionally, the preliminary results obtained after a draft flux metabolic balance analysis was conducted, supported the hypothesis of

Pseudomonas and *Clostridium* indirect interaction, as good growth by the simulated community could not predict direct metabolic exchange, but a feasible growth by both members.

A modelling approach that considers effects of pH, one of the driving forces for enrichment in these experiments, and biofilm formation, a plausible mechanism for pH tolerance in the 3-days stable sequential transfers, would be more adequate to describe these communities.

Nevertheless, the present study along with the few currently found in the literature demonstrates that successive inocula transfer is not a straight forward process as commonly depicted by MCF batch studies, where the activity of the original inocula source is either qualitatively reported or not specified, and it is usually assumed that the community enriched at the end of successive transfers would be adapted and therefore better suited to produce the desired metabolite. In contrast, here the significantly higher ethanologenic activity of the initial inoculated microcosms would support the need to investigate further means to maintain the functional enriched community integrity, through a more in-depth study of the interactions within the community members and with the physical environment leading to high EtOH production.

8.1.4 Closing remarks

In summary, EtOH produced as the main soluble fermentation product from OMSW was achieved in MCF systems under minimal operational condition inputs, these being: incubation at environmental temperature, static conditions, initial acidic pH caused by unconditioned acid pre-treated substrate and initially aerobic headspace.

Two different types of bacterial communities were enriched under those conditions. The first of these relied on direct inoculation by a 1:1 w/w combination of sheep's rumen and anaerobic granular sludge, from where about 6 dominant species were reproducibly enriched, producing 0.070L_{EtOH}/Kg_{OMSW}, equivalent to 1/6 of the current corn grain-based EtOH industrial production process. This was the highest EtOH concentration achieved in the present work. The second type of community was derived from the first one after sequential 3-days transfers. This community, dominated by 2 species, was able to maintain activity and composition across successive inocula transfers producing 30mM of EtOH (50% of the originally inoculated).

Although these are promising results for the implementation of these communities in biorefinery projects, mostly in developing countries, the present work broadly leaves two open possibilities for future study: optimisation of EtOH fermentation by repeated initial direct inoculation from a mixed-source inoculum, and/or optimisation of a stable, but less productive, community maintained after successive transfers. Nevertheless, this work contributes to the literature by presenting the first report of Mixed-source Community Fermentation for Ethanol production from the Organic fraction of Municipal Solid Waste.

8.2 Limitations and Recommendations

As previously described, the focus of this work was Microbiological, however for the implementation of this technology, the determination of parameters deemed to be key in environmental bioengineering studies are required. For instance, the microcosms inoculation in the present study was based on a dry weight mass of substrate to wet weight mass of inoculum ratio, when a more suitable approach would be to inoculate these systems on the basis of the OMSW VS to R+S VSS ratio, which in this project might have imposed a selective pressure on the system (see Chapter's 6 discussion). Of equal importance is a deeper characterisation of the substrate before and after pre-treatment to evaluate the effect of the pre-treatment process and more importantly, the conversion yield achieved after inoculation through mass balance analyses. Although in the present work measurements of COD and estimates of TCOD and BMP are reported, it is highly recommended that actual measurements of the OMSW analogue's TCOD and BMP are performed. An additional test that could help compare this study to the ones available in the literature, is the determination of the substrate's elemental composition. Furthermore, cell counts, and gas measurements would highly improve any mass balance conducted and the understanding of the system's dynamics. The acknowledgement of these limitations offers opportunities for the improvement and optimisation of the system and pinpoint specific aspects that can be addressed in further experimentation.

Additionally, future research on the described communities above, EtOH production at an initial pH value of 5.5 seems promising, however, it would be advised to control the drop of this parameter to levels above 4.5 throughout a given incubation period, aiming to maintain physical conditions suitable for growth of the active community members.

To truly understand these bacterial communities' behaviour, they should be studied within their ecological context including direct interactions within their members as well as with their chemical environment and physical location. For which the cell growth of the total community as well as of the most relatively abundant members should be monitored (i.e. by flow cytometry and qPCR), and ideally complimented using multi-omics analyses (i.e. proteomics). It would also be advised to conduct microscopic analyses of the liquid and solid fractions in the culture medium (i.e. by confocal laser microscopy) to evaluate biofilm formation.

An alternative/additional approach would be to isolate the most abundant community members and assess their EtOH production as well as to conduct knockout communities to evaluate their functions.

The use of an appropriate computational modelling approach integrating the experimental data with the knowledge available in the literature would also be highly recommended, as it could allow *in silico* determination of the optimal environmental conditions for an optimised EtOH production, avoiding the time and costs necessary for laboratory tests.

Also, despite GC-FID using wax columns being a documented method employed for the quantification of soluble fermentation products in aqueous media, the multiple problems experienced throughout this project would not advise the utilisation of this method for the quantification of volatile fatty acids in fermentation studies, although it seems appropriate for short chain alcohols. It was out of the scope of this thesis to determine the cause for this lack of consistency, but trouble shooting the problems it caused took several months away from the defined time for this project and represented one of its highest costs (over £1000). The quantification of VFAs by IC is recommended instead. When available, current literature advises the use of High-Performance Liquid Chromatography (HPLC), where sugars concentration could also be determined, thus providing a more integral analysis.

Despite the promising results obtained regarding the microbial communities enriched, it must be noted the current EtOH industrial processes yields and processing times importantly outperform the findings of this work. Should the alternatives presented in here be considered for scaling up studies and industrial applications, attention must be paid in the design of the overall production process. For instance, the use of 3-day transfers would require a number of reactors to run in parallel, all producing similar

effluents needing downstream processing, thus increasing operational costs, while generating half of the EtOH concentration achieved in the initially inoculated batch. Although this fact could make the 3 day-transfer enriched community seem less appealing for EtOH production, the integration of the effluents generated into a biorefinery where other valuable products could be recovered (e.g. chemicals and biomass), could generate benefits from the overall process.

While the initial R+S inoculation might then be more attractive for further study and optimisation towards industrial application as potentially competitive EtOH concentrations could be achieved, the constant availability of sheep rumen and granular anaerobic sludge could represent a limitation to achieve reproducible EtOH yields, particularly regarding rumen's composition, as it has been shown rumen's microbial populations depend on ruminant species and their diets. It is therefore recommended to conduct comparative studies of local and reliable rumen sources (e.g. abattoirs) to select the highest producer. In addition, similarly to the 3-day transfers considerations highlighted above, it is recommended the use of R+S for EtOH production as part of a biorefinery project, as the recovery of multiple metabolic products would add value and make the entire process cost effective and part of a circular economy development.

“Utopia is on the horizon.

I move two steps closer; it moves two steps further away.

I walk another ten steps and the horizon runs ten steps further away.

As much as I may walk, I'll never reach it.

So, what's the point of pursuing utopia?

The point is this: to make me keep walking.”

Eduardo Galeano

Appendix A. Statistical analyses of physicochemical data

The R programming language and free software R version 3.4.3 (2017-11-30) -- "Kite-Eating Tree" was used to conduct statistical analyses of physicochemical data unless otherwise stated. The following diagrams (Figs. A1 and A2) illustrate the workflow for commonly used statistical tests in this work. In all cases:

- Null hypothesis: the means of the groups are not different at a significance level $\alpha = 0.05$, $p\text{-value} > 0.05$.
- Alternative hypothesis: At least one sample mean is not equal to the others at a significance level $\alpha = 0.05$, $p\text{-value} < 0.05$.

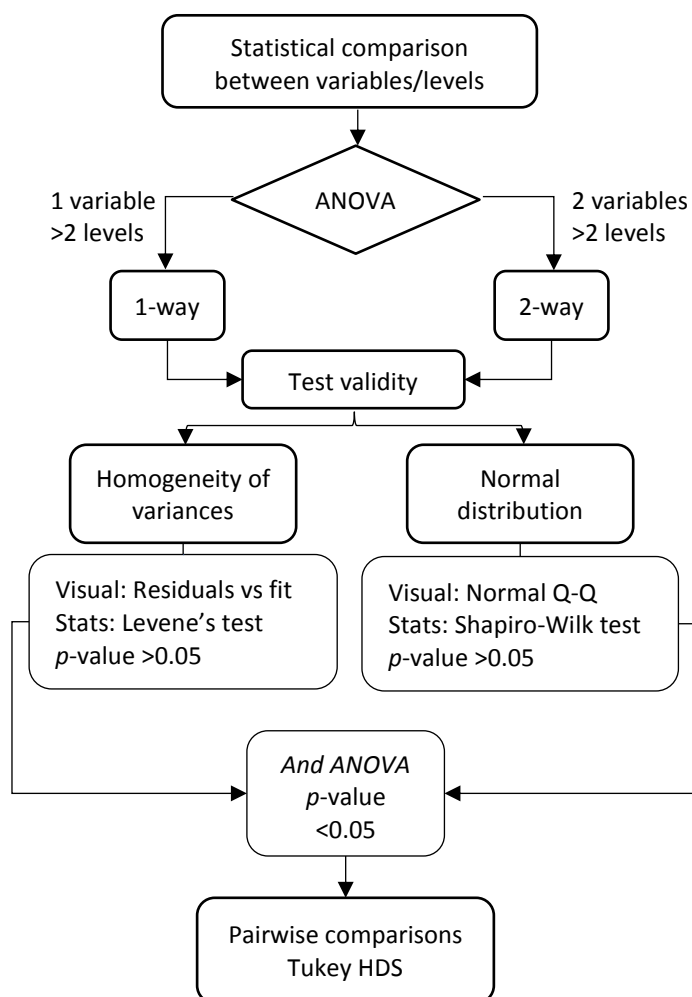


Figure A1. Workflow diagram for the statistical comparison of variables with n number of levels.

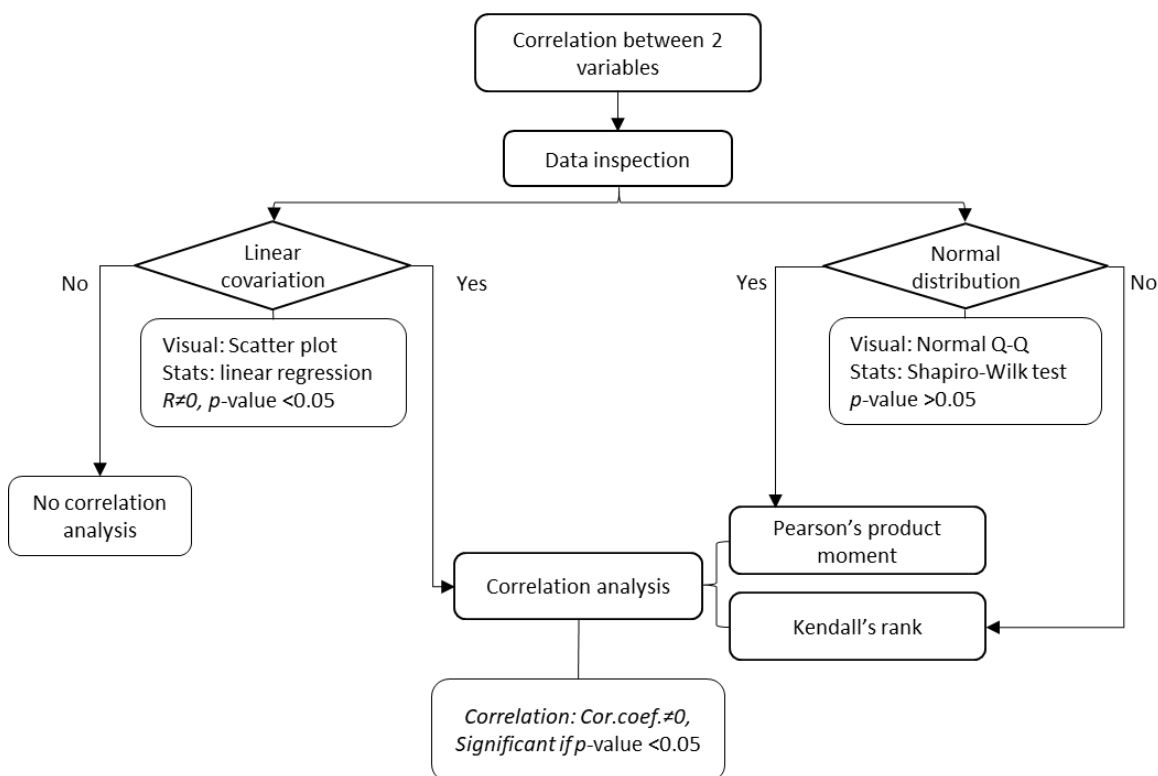


Figure A2. Workflow diagram for the statistical correlation analysis of 2 variables.

Examples following Figs. A1 and A2 based on Chapter's 4 results are presented below.

Example A1) Statistical comparison between variables. Comparing EtOH production as a function of inocula and initial aerobic or anaerobic incubation conditions.

i) 2-way ANOVA (2 variables: inocula (5 levels) and initial O₂ (2 levels)).

Anova Table

Response: EtOH_mM

	Sum Sq	Df	F value	Pr(>F)	
(Intercept)	14.55	1	1.2232	0.280174	
Inocula	1881.36	5	31.6301	1.399e-09	***
O2	135.78	1	11.4136	0.002591	**
Inocula:Treatment	227.74	5	3.8288	0.011391	*
Residuals	273.61	23			

Signif. codes:

0 '***', 0.001 '**', 0.01 '*', 0.05 '.', 0.1 ' ', 1

From the ANOVA results and based on the p -values and a significance level of 0.05, it can be concluded that EtOH production is significantly different due to the inocula, initial O₂ and their interaction.

ii) Visual inspection of the test validity.

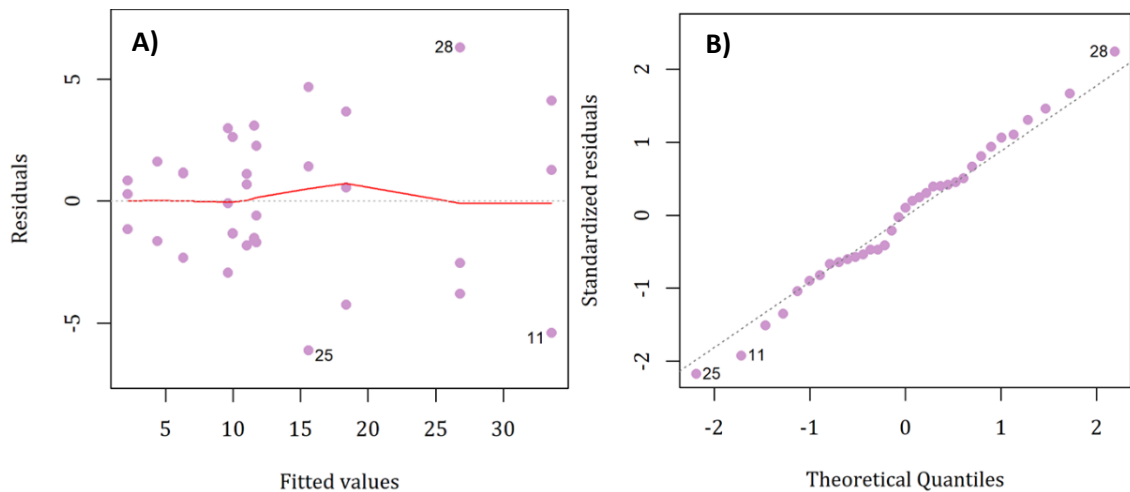


Figure A3. A) Residuals vs fits plot B) Normal Q-Q plot. the quantiles of the residuals vs the quantiles of the normal distribution along with a 45-degree reference line. This is used to verify the assumption that the residuals are normally distributed and should approximately follow the reference line. As all the points fall approximately along this reference line, normality can be assumed.

The residuals vs fits plot displays the residuals on the y-axis and the mean of each group (fitted values) on the x-axis to verify the assumption that the residuals are randomly distributed and have constant variance. The points should be randomly allocated above and below 0, with no recognisable patterns in the points. However, Fig. A3 A) shows three outliers questioning the assumption that the variances are constant. Meanwhile, in the normal Q-Q plot. the quantiles of the residuals are displayed against the quantiles of the normal distribution along with a 45-degree reference line. To visually evaluate whether the residuals are normally distributed, the data points should approximately follow the reference line. Apart from three outliers, all the points fall approximately along this reference line, and normality could be assumed.

Despite the outliers shown in Figure A3), the results of the Levene's test to evaluate the homogeneity of variance shows that there is no evidence to suggest that the variance across groups is significantly different ($p = 0.9205$), while the Shapiro-Wilk test ($p = 0.987$) shows the same for normality. Therefore, the homogeneity of variances and normality in the different treatment groups could be assumed.

iii) Tukey HDS test for performing multiple pairwise-comparison between the means of groups.

Tukey multiple comparisons of means
95% family-wise confidence level

The relevant results for this test are listed in table 4.1 of Chapter 4.

Example A2) Correlation analysis between pH of rumen inoculated microcosms and maximal EtOH production by this inoculum.

i) Visual data inspection

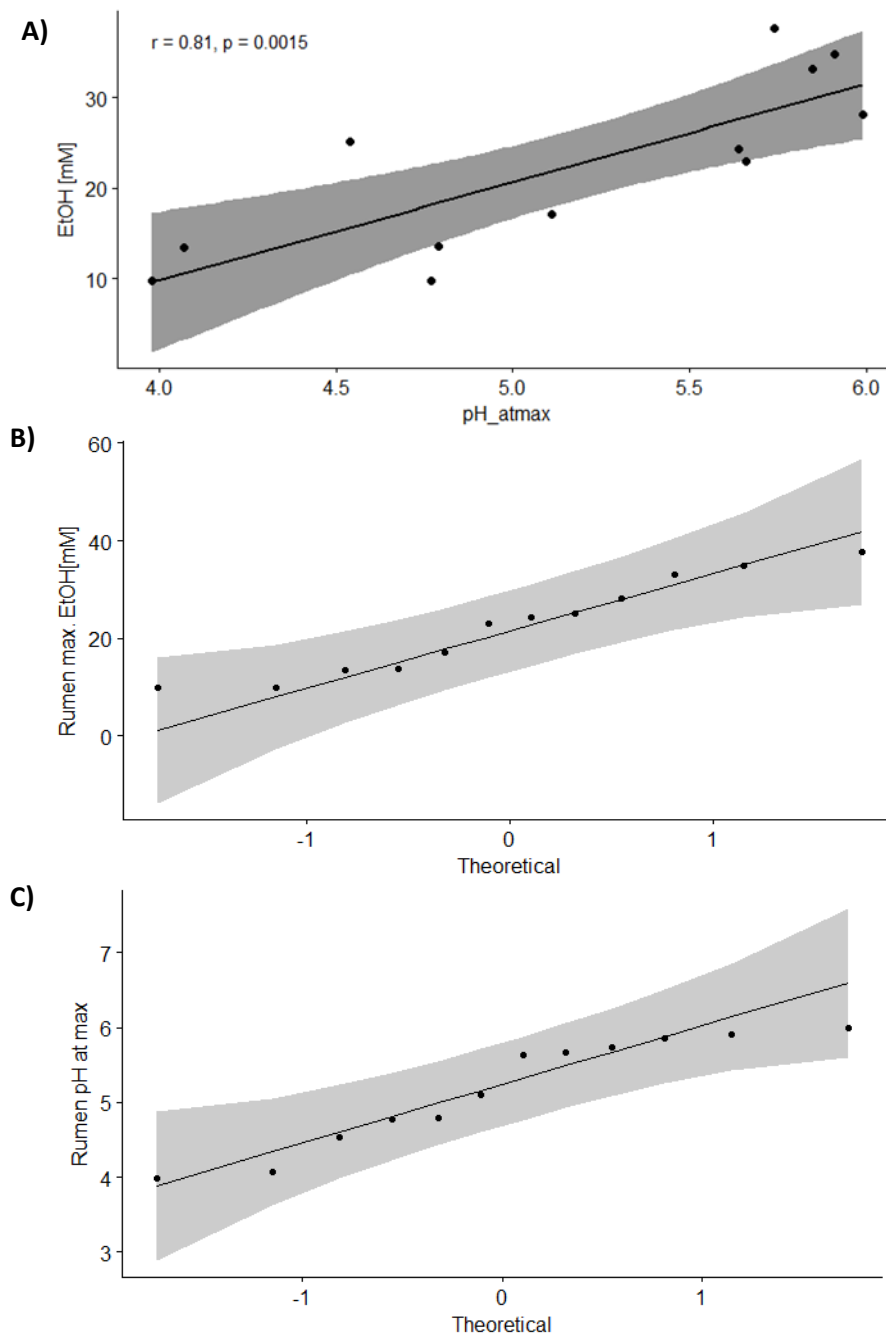


Figure A4. A) Scatter plot of maximal EtOH concentration as a function of the pH of the medium when this maximal EtOH concentration was observed. B) and C) Normal Q-Q plots of the individual variables being correlated: rumen maximal EtOH production and the pH values registered in rumen inoculated microcosms when this maximal concentration occurred.

The scatter plot shows a linear relationship between maximal EtOH concentrations as a function of pH, while in both Q-Q plots the quantiles of the residuals vs the quantiles of the normal distribution follow the reference line, suggesting a normal distribution.

To confirm these observations, the linear relationship of the continuous variables tested, and normal distribution of the data sets were examined through linear regression ($R = 0.81$, $p=0.0015$) and Shapiro-Wilk normality tests (max_EtOH p -value = 0.4031, pH_at_max p -value = 0.1132). Since the relationship between the variables was linear, the correlation test proceeded.

ii) Selection of correlation test once linearity could be assumed.

Pearson's product-moment correlation was computed since both variables data were normally distributed.

Pearson's product-moment correlation

```
data: x1n2ru$max_pH and x1n2ru$etoh
t = 4.3227, df = 10, p-value = 0.001507
alternative hypothesis: true correlation is not equal to 0
95 percent confidence interval: 0.4343972 0.9438224
sample estimates: cor 0.8070902
```

Based on these results, a significant positive correlation could be assumed between the pH of the medium in rumen inoculated microcosms and maximal EtOH concentration.

When the data of one or more variables in each data set was not normally distributed, the non-parametric Kendall's rank correlation tau was done. The relevant results for the correlation tests are presented in table 4.3 of Chapter 4.

Appendix B. OMSW medium basic chemical characterisation

B1. Solid OMSW analysis

As described in Chapter 3, section 3.2.2, the components integrating the food fraction of the OMSW analogue were first characterised by evaluating their moisture content (H₂O), total solids (TS), volatile solids (VS) and fixed solids (FS) content. The results from these analyses are presented in Table B1:

Table B1. Basic chemical characterisation of food waste fractions and acid pre-treated OMSW.

Food waste fraction	H ₂ O %	TS %	VS %	FS %
Vegetables	91.36	8.64	90.35	0.78
Fruit peelings	94.13	5.87	82.12	1.05
Bakery	26.76	73.24	97.61	1.75
Meals	61.50	38.50	98.66	0.52
Meat	62.98	37.02	97.58	0.89
Pre-treated OMSW	12.90 ± 0.37	87.10 ± 0.37	78.83 ± 0.53	9.77 ± 0.44

n=3, ± SE

Where:

- Moisture content: typically, the amount of water (and other components) lost after heating an organic sample at 105°C.
- Total solids: the amount of solids remaining after heating an organic sample at 105°C to constant weight.
- Volatile solids: the weight loss after an organic sample is ignited (heated to dryness at 550 °C).
- Fixed solids or ash content: the amount of solids remaining after heating an organic sample at 550°C to constant weight.

In addition, the total Chemical Oxygen Demand (TCOD) and Bio Methane Potential (BMP) of the solid OMSW fraction were estimated using the proportions of the general waste categories with TCOD (in gCOD/gmaterial) and BMP contents (in mLCH₄/gmaterial) as reported by Bayard *et al.*, 2018. The data used to calculate these estimations are presented in Table B2.

Table B2. Reported and estimated TCOD and BMP values of food waste fractions and acid pre-treated OMSW.

OMSW waste categories	OMSW %	TCOD ^a	BMP ^b	Es ^c TCOD ^a	Es ^c BMP ^b
Food waste	83	1.33	268	1.10	222.44
Paper ^d	10	0.95	190.66	0.10	19.07
Newspaper		1.08	142		
Office paper		1.06	273		
Magazines		0.70	157		
Cardboard	7	1.13	221	0.08	15.47
Total				1.28	256.98

^a in gCOD/gmaterial

^b in mLCH₄/gmaterial

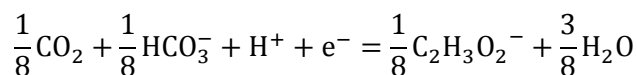
^c Es: estimated

^d The paper category TCOD and BMP values were calculated as an average of the individual fractions comprising this category, as experimentally, it was indeed comprised by newspaper, office paper and magazines.

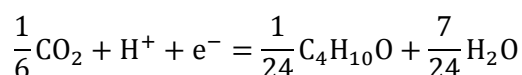
Appendix C. Electron balances

C1. Half reactions used to determine electron-equivalent balance and stoichiometry

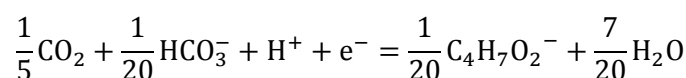
Acetate^a



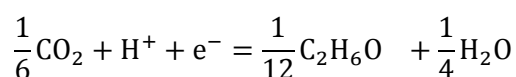
Butanol^b



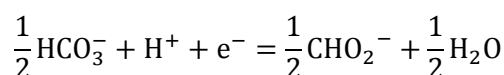
Butyrate^b



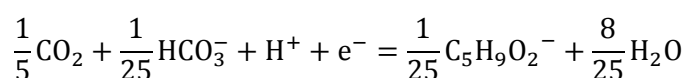
Ethanol^a



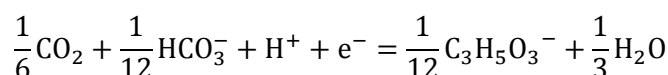
Formate^a



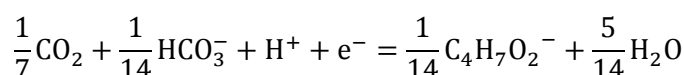
Isovalerate^b



Lactate^a

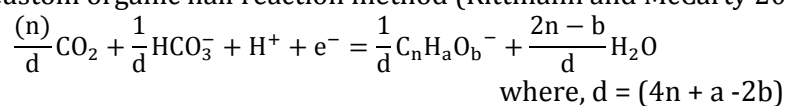


Propionate^a



^aAs described in Rittmann and McCarty, 2001.

^bDetermined via the custom organic half reaction method (Rittmann and McCarty 2001):



C2. Electron balance calculation demonstration

The following example demonstrates how the estimate of the proportion of electrons from the substrate converted into EtOH was calculated:

- Based on the EtOH half reaction above, 12 electrons (e^-) are required to oxidise EtOH to CO_2 . Regarding organic matter oxidation, these are the electron equivalents (e^- eq.) of a mol of EtOH.
- The molecular mass of EtOH is 46g, equivalent to 3.83 g/ e^- eq. (46 g/12 e^- eq.).
- Using as example the maximal concentration of EtOH produced by rumen and sludge (see Chapter 4) of 30mM, there were 1.38 g of EtOH per litre of solution, equivalent to 0.36 e^- eq./L (1.38 g/L / 3.83 g/ e^- eq.).
- As previously described (Chapter 3, section 3.2.3), the OMSW medium had an original input of 4687.5 e^- -meq./L based on the BMP estimate derived COD. Therefore, it can be assumed that about 7.68% of the electrons present initially in the medium were used for EtOH formation (360 e^- -meq./L ./ 4687.5 e^- -meq./L). This proportion would be 4.5% and 14.69% when considering TCOD (8000 e^- -meq./L) and COD in the liquid fraction (2450 e^- -meq./L) electron milliequivalent contents.

Appendix D. Samples and Golay barcodes used for Ion Torrent PGM sequencing

Table D1 lists the samples sent for amplification and the corresponding sequence of barcodes used as mentioned in Chapter 5 section 5.3.8.

Table D1 Samples and Golay barcodes used for Ion torrent PGM sequencing in Chapter 5.

Sample ID	Barcode
R1_0	ACGGATCGTCAG
R2_0	ACGGTGAGTGTC
R3_0	ACGTACTCAGTG
R1_11	ACGTCTGTAGCA
R2_11	ACGTGAGAGAAT
R3_11	ACGTGCCGTAGA
S1_0	ACGTTAGCACAC
S2_0	ACTACAGCCTAT
S3_0	ACTACGTGTGGT
S1_11	ACTAGCTCCATA
S2_11	ACTATTGTCACG
S3_11	ACTCACGGTATG
R+S 1_0	ACTCAGATACTC
R+S 2_0	ACTCGATTTCGAT
R+S 3_0	ACTCGCACAGGA
R+S 1_11	ACTCTTCTAGAG
R+S 2_11	ACTGACAGCCAT
R+S 3_11	ACTGATCCTAGT
B1_0	ACTGTACGCGTA
B2_0	ACTGTCTGAAGCT
B3_0	ACTGTGACTTCA
B1_11	ACTTGTAGCAGC
B2_11	AGAACACGTCTC
B3_11	AGACCGTCAGAC

R: rumen, S: sludge, R+S: mixed inocula, B: Inocula blank. The number right after the letter corresponds at the replicate number (1,2 or 3). Each of the samples were taken at either incubation days 0 or 11.

Table D2 lists the samples sent for amplification and the corresponding sequence of barcodes used as mentioned in Chapter 6 section 6.3.7.

Table D2 Samples from EXPs A and B and Golay barcodes used for Ion Torrent PGM sequencing in Chapter 6.

EXP A	EXP A	EXP B	EXP B
Sample ID	Barcode	Sample ID	Barcode
EXPA_110	AACGCACGCTAG	EXPB_110	ACTCAGATACTC
EXPA_210	AACTCGTCGATG	EXPB_210	ACTCGATTTCGAT
EXPA_310	AACTGTGCGTAC	EXPB_310	ACTCGCACAGGA
EXPA_111	AAGAGATGTCTGA	EXPB_111	ACTCTTCTAGAG
EXPA_211	AAGCTGCAGTCG	EXPB_211	ACTGACAGCCAT
EXPA_311	AATCAGTCTCGT	EXPB_311	ACTGATCCTAGT
EXPA_112	AATCGTGACTCG	EXPB_112	ACTGTACGCGTA
EXPA_212	ACACACTATGGC	EXPB_212	ACTGTCTGAAGCT
EXPA_312	ACACATGTCTAC	EXPB_312	ACTGTGACTTCA
EXPA_120	ACACGAGCCACA	EXPB_120	ACTTGTAGCAGC
EXPA_220	ACACGGTGTCTA	EXPB_220	AGAACACGTCTC
EXPA_320	ACACTAGATCCG	EXPB_320	AGACCGTCAGAC
EXPA_121	ACACTGTTCATG	EXPB_121	AGAGTCCTGAGC
EXPA_221	ACAGACCACTCA	EXPB_221	AGATCGGCTCGA
EXPA_321	ACAGAGTCGGCT	EXPB_321	AGCCATACTGAC
EXPA_122	ACAGCAGTGGTC	EXPB_122	AGCGACTGTGCA
EXPA_222	ACAGCTAGCTTG	EXPB_222	AGCTCCATACAG
EXPA_322	ACGGATCGTCAG	EXPB_322	AGCTCTCAGAGG
EXPA_150	ACGGTGAGTGTC	EXPB_150	AGCTGACTAGTC
EXPA_250	ACGTACTCAGTG	EXPB_250	AGGCTACACGAC
EXPA_350	ACGTCTGTAGCA	EXPB_350	AGGTGTGATCGC
EXPA_151	ACGTGAGAGAAT	EXPB_151	AGTACGCTCGAG
EXPA_251	ACGTGCCGTAGA	EXPB_251	AGTACTGCAGGC
EXPA_351	ACGTTAGCACAC	EXPB_351	AGTCACATCACT
EXPA_152	ACTACAGCCTAT	EXPB_152	AGTCCATAGCTG
EXPA_252	ACTACGTGTGGT	EXPB_252	AGTCTACTCTGA
EXPA_352	ACTAGCTCCATA	EXPB_352	AGTGAGAGAAGC

EXPA: experimental set-up A, EXPB: experimental set-up B. The number right after the underscore corresponds at the replicate number (1,2 or 3). The following number represents the sequential transfers: 1 for the initially inoculated microcosms, 2 for the first transfer and 5 for the last. The last number indicates the timepoint at which the sample was taken, 0: day 0, 1: day 7 and 2: day 14.

Appendix E. TG-DSC data analysis

The average DSC profiles were used to define boundaries for the thermal mass loss (TG) ranges which could be attributed to the labile, recalcitrant (hemicellulose-like and cellulose-like) and refractory components of the OMSW after 14 days of incubation, as illustrated by Fig. E1. The detailed average results of OMSW samples before and after steam (autoclave) pre-treatment, as well as from initially inoculated and Tr4 microcosms, along with their corresponding blanks are presented in Table E1.

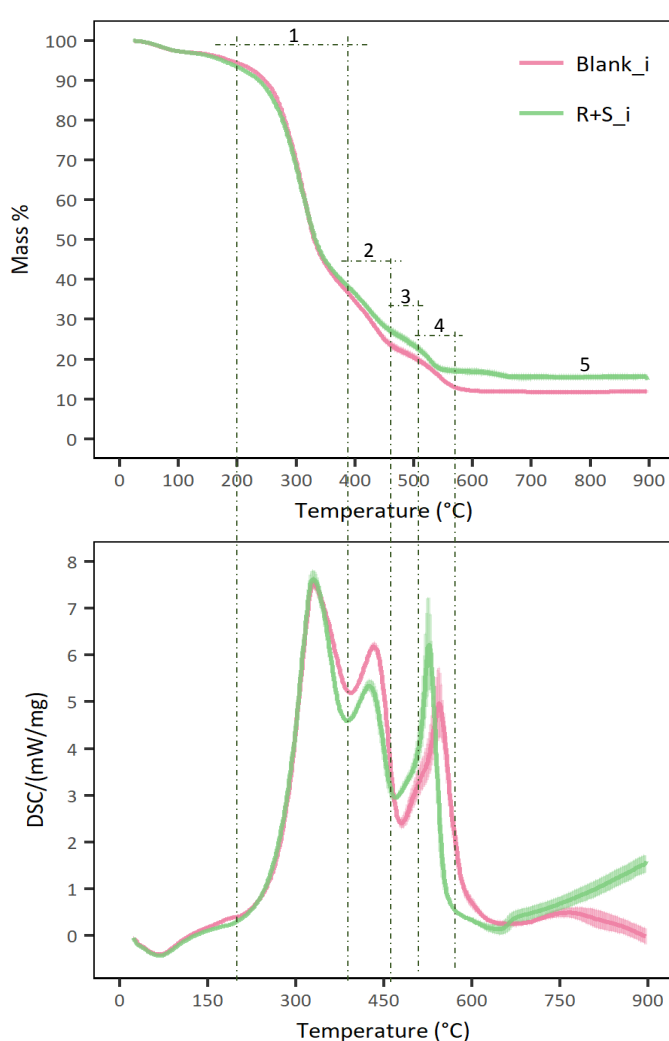


Figure E1. Average TG and DSC profiles (from top to bottom of OMSW substrate in initially inoculated microcosms and inocula blanks from Exp B after 14 days of incubation (see Chapter 6, section 6.4.3). The plots are divided into areas according to putative TG carbon fractions mass losses of the initially inoculated microcosms: 1) Loss of labile carbon, 2) Loss of recalcitrant carbon (hemicellulose-like), 3) Loss of recalcitrant carbon (cellulose-like), 4) Loss of refractory carbon (lignin), 5) Residual matter (ash, likely combined with the breakdown of inorganic carbon i.e, carbonate).

Table E1. TG-QDS results

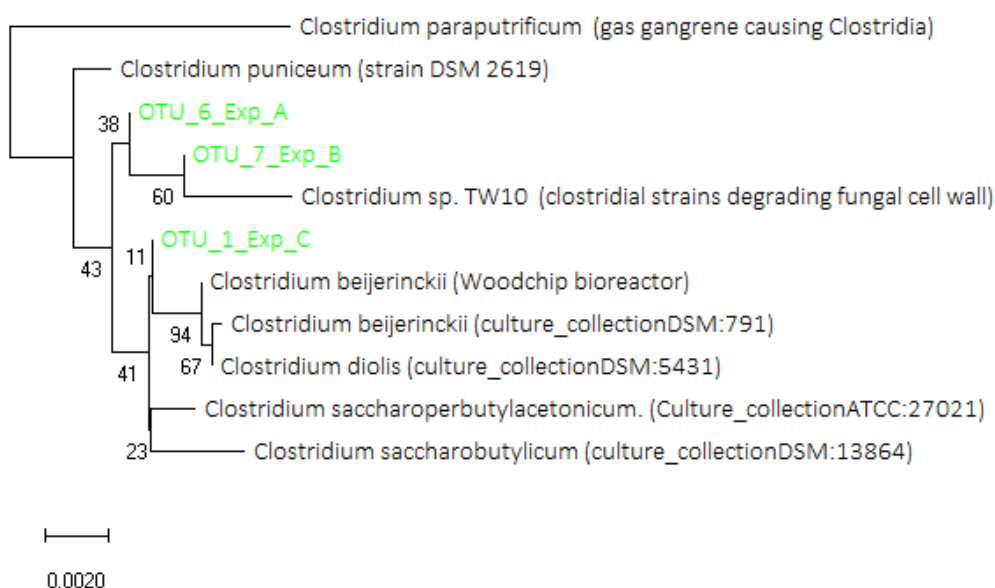
OMSW batch	Labile			Refractory (hemicellulose-like)			Refractory (cellulose-like)			Recalcitrant (lignin-like)			Residual	
	Temp. Range (°C)		Mass loss %	Temp. Range (°C)		Mass loss %	Temp. Range (°C)		Mass loss %	Temp. Range (°C)		Mass loss %	Temp. (°C)	Fixed solids %
B-auto	232.1	391.6	43.2	391.6	541.2	26.0	NA		NA	541.2±	646.1±	14.5	897.2	12.7±
A- auto	210.0±	385.7±	50.7±	385.7±	463.6±	12.3±	463.6±	497.7±	4.0±	497.7±	575.5±	7.4±	897.3	13.7±
	2.9	1.6	0.7	1.6	4.4	1.1	4.4	4.7	0.2	4.7	0.5	1.3		1.1
IBlack	204.5±	393.1±	58.4±	393.1±	480.4±	13.8±	480.4±	522.8±	3.6±	522.8±	610.4±	6.3±	897.2	11.8±
	0.1	0.1	0.5	0.1	1.6	0.5	1.5	1.6	0.2	1.6	0.4	0.4		0.3
R+Si	203.9±	389.3±	55.0±	389.3±	470.4±	11.9±	470.4±	506.5±	3.4±	506.5±	583.3±	5.9±	896.8	15.6±
	0.5	1.9	0.7	1.9	4.2	0.6	4.2	4.7	0.1	4.7	13.6	0.5		0.7
IBlack _{Tr4}	204.2±	392.3±	58.5±	392.3±	483.3±	14.9±	483.3±	524.1±	3.4±	524.1±	611.9±	5.9±	897.2	11.0±
	0.2	0.9	0.6	0.9	2.0	0.2	2.0	4.1	0.2	4.1	1.0	0.2		0.6
R+S _{Tr4}	203.6±	392.6±	58.5±	392.6±	479.8±	12.0±	479.8±	519.3±	3.4±	519.3±	613.0±	7.3±	897.2	12.8±
	0.7	0.3	0.2	0.3	2.1	0.5	2.1	3.2	0.1	3.2	3.1	0.5		0.4

B-auto: before autoclave; A-auto: after autoclave; IBlank: Initial inocula blanks; R+Si: Initially inoculated microcosms; IBlank_{Tr4}: inocula blanks Tr4; R+S_{Tr4}: inoculated microcosms Tr4.

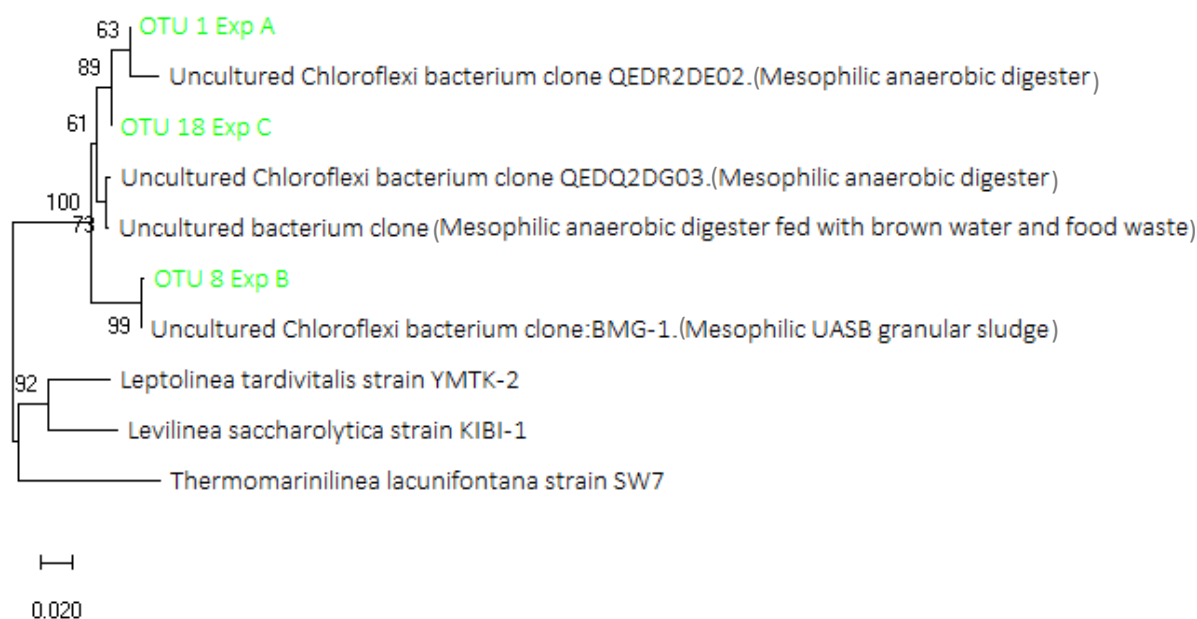
Appendix F. Phylogenetic trees of the most abundant OTUs in the enriched communities of Chapter 6.

Phylogenetic comparisons of the representative sequences from the dominant OTUs comprising the ethanologenic communities described in Chapters 6 and 7 against their closest relative sequences after BLAST alignment via MEGA X.

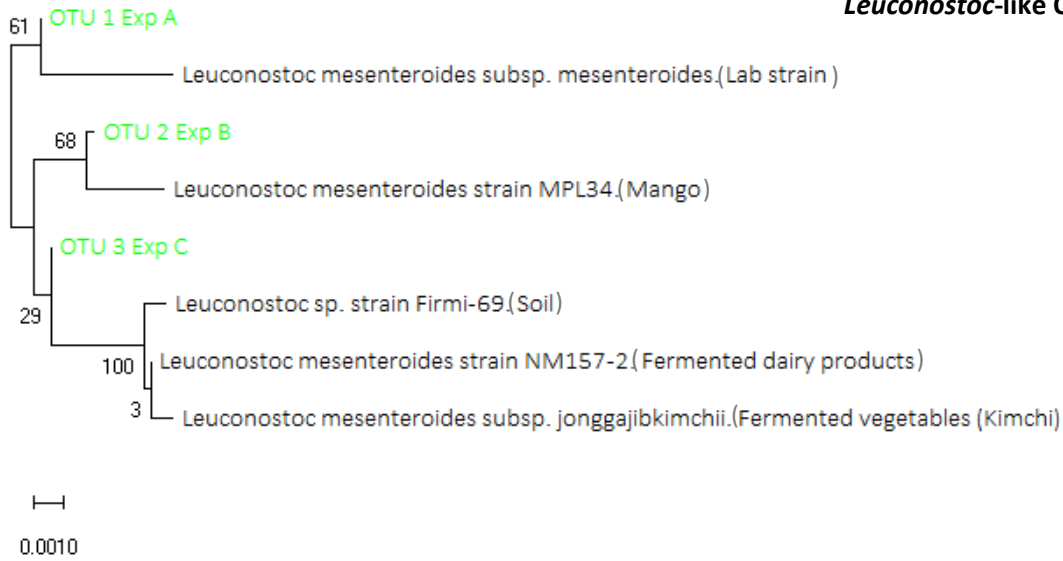
Clostridium-like OTUS



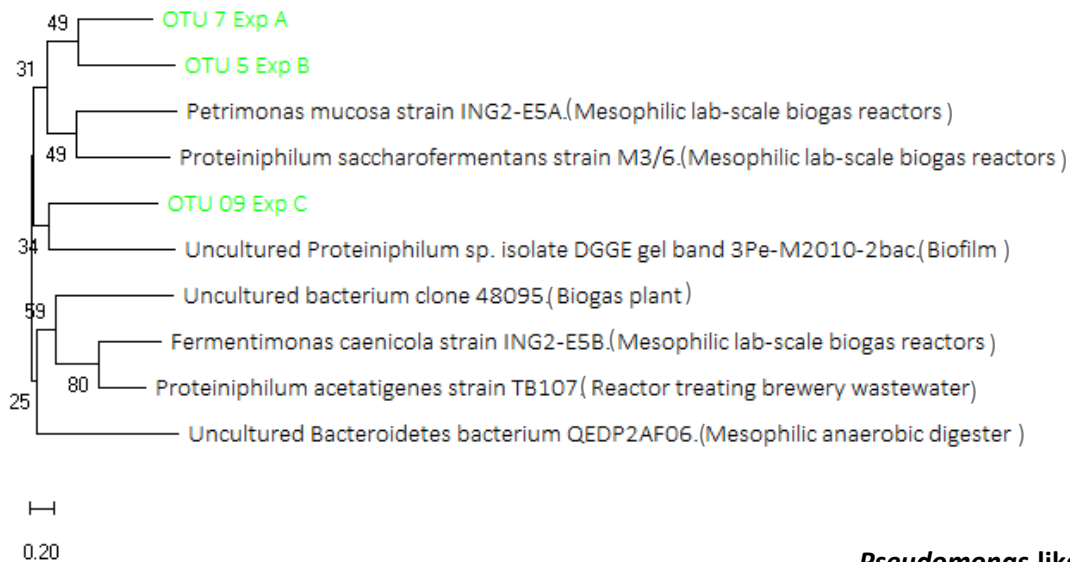
Leptolinea-like OTUS



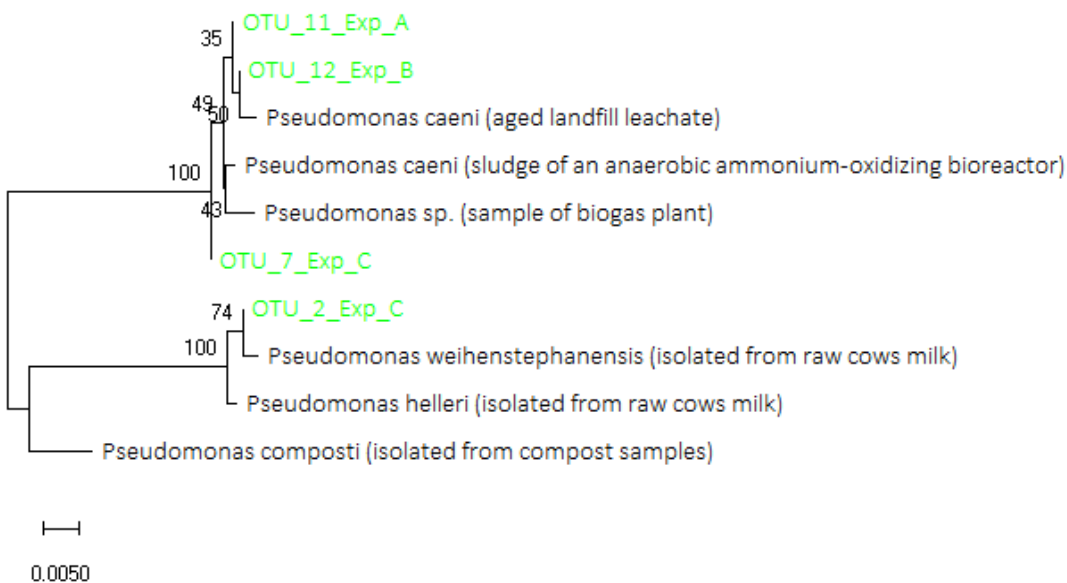
***Leuconostoc*-like OTUS**



***Petrimonas*-like OTUS**



***Pseudomonas*-like OTUS**



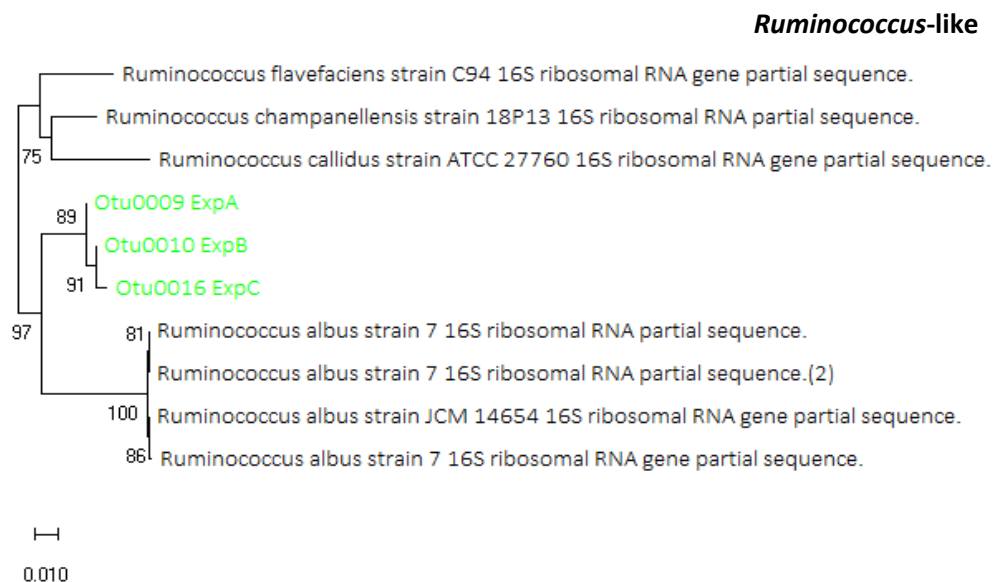


Figure F1: Neighbour-joining phylogenetic tree based on 16S rRNA gene sequences (Saitou *et al.*, 1987), showing the relationship of the different OTUs to related species. Next to the species name, a short description of the DNA source is provided. The percentage of replicate trees in which the associated taxa clustered together in the bootstrap test (500 replicates) are shown next to the branches. The tree is drawn to scale, with branch lengths in the same units as those of the evolutionary distances used to infer the phylogenetic tree. The evolutionary distances were computed using the Maximum Composite Likelihood method and are in the units of the number of base substitutions per site (Tamura *et al.*, 2004). All ambiguous positions were removed for each sequence pair. Bootstrap values (expressed as percentages of 500 replications) greater than 50 are shown at the branching points. These analyses were conducted in MEGA X (Kumar *et al.*, 2018).

Appendix G. Volatile Suspended Solids content of the R+S inoculum

Following the method described in Appendix B, the volatile suspended solids (VSS) content of the R+S inoculum was determined (x3), resulting in $0.05 \pm 0.005 \text{ g}_{\text{VSS}}/\text{g}_{\text{R+S}}$. As the volatile solids (VS) content of the OMSW was $0.78 \pm 0.005 \text{ g}_{\text{VS}}/\text{g}_{\text{OMSW}}$ (see Appendix B, Table B1), the substrate/inoculum (S/I) and inoculum to substrate (I/S) ratios, in terms of VS content, of the experiments assessing the R+S inoculum EtOH production were of 15.6 and 0.064, respectively.

References

- Abe, A., Furukawa, S., Watanabe, S. and Morinaga, Y. (2013). Yeasts and lactic acid bacteria mixed-specie biofilm formation is a promising cell immobilization technology for ethanol fermentation. *Applied Biochemistry and Biotechnology* 171 (1): 72–79. <https://doi.org/10.1007/s12010-013-0360-6>.
- Adav, S.S., Lee, D.J. and Lai, J.Y. (2009). Proteolytic activity in stored aerobic granular sludge and structural integrity. *Bioresource Technology* 100 (1): 68–73. <https://doi.org/10.1016/j.biortech.2008.05.045>.
- Adav, S.S., Lee, D.-J. and Lai, J.-Y. (2010). Potential cause of aerobic granular sludge breakdown at high organic loading rates. *Applied Microbiology and Biotechnology* 85 (5): 1601–10. <https://doi.org/10.1007/s00253-009-2317-9>.
- Agarwal, A.K. (2007). Biofuels (alcohols and biodiesel) applications as fuels for internal combustion engines. *Progress in Energy and Combustion Science* 33 (3): 233–71. <https://doi.org/10.1016/j.pecs.2006.08.003>.
- Agler, M.T., Wrenn, B.A., Zinder, S.H. and Angenent, L.T. (2011). Waste to bioproduct conversion with undefined mixed cultures: The carboxylate platform. *Trends in Biotechnology* 29 (2): 70–78. <https://doi.org/10.1016/j.tibtech.2010.11.006>.
- Agrawal, R., Satlewal, A., Gaur, R., Mathur, A., Kumar, R., Gupta, R.P., et al. (2015). Pilot scale pretreatment of wheat straw and comparative evaluation of commercial enzyme preparations for biomass saccharification and fermentation. *Biochemical Engineering Journal* 102: 54–61. <https://doi.org/10.1016/j.bej.2015.02.018>.
- AGU. (2017). Planta de Termovalorización pone a la CDMX a la vanguardia en tecnología y materia ambiental. Agencia de Gestión Urbana de La Ciudad de México. 2017. <http://www.agu.cdmx.gob.mx/busqueda?q=bordo+poniente>.
- Alamanou, D.G., Malamis, D., Mamma, D. and Kekos, D. (2015). Bioethanol from Dried Household Food Waste Applying Non-isothermal Simultaneous Saccharification and Fermentation at High Substrate Concentration. *Waste and Biomass Valorization* 6 (3): 353–61. <https://doi.org/10.1007/s12649-015-9355-6>.
- Alibardi, L. and Cossu, R. (2015). Composition variability of the organic fraction of municipal solid waste and effects on hydrogen and methane production potentials. *Waste Management* 36: 147–55. <https://doi.org/10.1016/j.wasman.2014.11.019>.
- Alrumman, S.A. (2016). Enzymatic saccharification and fermentation of cellulosic date palm wastes to glucose and lactic acid. *Brazilian Journal of Microbiology* 47 (1): 110–19. <https://doi.org/10.1016/j.bjm.2015.11.015>.
- Altschul, S.F., Gish, W., Miller, W., Myers, E.W. and Lipman, D.J. (1990). Basic local alignment search tool. *Journal of Molecular Biology* 215 (3): 403–10. [https://doi.org/10.1016/S0022-2836\(05\)80360-2](https://doi.org/10.1016/S0022-2836(05)80360-2).
- Alvarez-Ortega, C. and Harwood, C.S. (2007). Responses of *Pseudomonas aeruginosa* to low oxygen indicate that growth in the cystic fibrosis lung is by aerobic respiration. *Molecular Microbiology* 65 (1): 153–65. <https://doi.org/10.1111/j.1365-2958.2007.05772.x>.
- Amador-Noguez, D., Brasg, I.A., Feng, X.J., Roquet, N. and Rabinowitz, J.D. (2011). Metabolome remodeling during the acidogenic-solventogenic transition in *Clostridium acetobutylicum*. *Applied and Environmental Microbiology* 77 (22): 7984–97. <https://doi.org/10.1128/AEM.05374-11>.
- APHA. (2012). 2540 G. Total, fixed, and volatile solids in solid and semisolid samples. In *Standard Methods for the Examination of Water and Wastewater*.
- Atkinson, C.F., Jones, D.D. and Gauthier, J.J. (1996). Putative anaerobic activity in aerated composts. *Journal of Industrial Microbiology* 16 (3): 182–88. <https://doi.org/10.1007/BF01570002>.
- Atreya, M.E., Strobel, K.L. and Clark, D.S. (2016). Alleviating product inhibition in cellulase enzyme Cel7A. *Biotechnology and Bioengineering* 113 (2): 330–38. <https://doi.org/10.1002/bit.25809>.
- Auling, G., Pilz, F., Busse, H.J., Karrasch, S., Streichan, M. and Schon, G. (1991). Analysis of the polyphosphate-accumulating microflora in phosphorus-eliminating, anaerobic activated sludge systems by using

- diaminopropane as a biomarker for rapid estimation of *Acinetobacter* spp. *Applied and Environmental Microbiology* 57(12) (12): 3583–92.
- Babaei, P., Ghasemi-Kahrizsangi, T. and Marashi, S.A. (2014). Modeling the differences in biochemical capabilities of *Pseudomonas* species by flux balance analysis: How good are genome-scale metabolic networks at predicting the differences? *The Scientific World Journal* 2014. <https://doi.org/10.1155/2014/416289>.
- Babaei, P., Shoaie, S., Ji, B. and Nielsen, J. (2018). Challenges in modeling the human gut microbiome. *Nature Biotechnology* 36 (8): 682–86. <https://doi.org/10.1038/nbt.4213>.
- Balat, M. (2011). Production of bioethanol from lignocellulosic materials via the biochemical pathway: A review. *Energy Conversion and Management* 52 (2): 858–75. <https://doi.org/10.1016/j.enconman.2010.08.013>.
- Baldrian, P. (2017). Microbial activity and the dynamics of ecosystem processes in forest soils. *Current Opinion in Microbiology*. <https://doi.org/10.1016/j.mib.2017.06.008>.
- Ballesteros, M., Sáez, F., Ballesteros, I., Manzanares, P., Negro, M.J., Martínez, J.M., et al. (2010). Ethanol production from the organic fraction obtained after thermal pretreatment of municipal solid waste. *Applied Biochemistry and Biotechnology* 161 (1–8): 423–31. <https://doi.org/10.1007/s12010-009-8877-4>.
- Barros, S. (2017). Brazil. *Biofuels Annual 2017*. Global Agricultural Information Network. 2017. [https://gain.fas.usda.gov/Recent GAIN Publications/Biofuels Annual_Sao Paulo ATO_Brazil_9-15-2017.pdf](https://gain.fas.usda.gov/Recent%20GAIN%20Publications/Biofuels%20Annual_Sao%20Paulo%20ATO_Brazil_9-15-2017.pdf).
- Bayard, R., Benbelkacem, H., Gourdon, R. and Buffière, P. (2018). Characterization of selected municipal solid waste components to estimate their biodegradability. *Journal of Environmental Management* 216: 4–12. <https://doi.org/10.1016/j.jenvman.2017.04.087>.
- Beeck, M. Op De, Lievens, B., Busschaert, P., Declerck, S., Vangronsveld, J. and Colpaert, J. V. (2014). Comparison and validation of some ITS primer pairs useful for fungal metabarcoding studies. *PLoS ONE* 9 (6). <https://doi.org/10.1371/journal.pone.0097629>.
- Begon, M., Colin, R.T. and Harper, J.L. (2007). *Ecology – From Individuals to Ecosystems*, 4th Ed., Michael Begon, Colin R. Townsend, John L. Harper, Blackwell Publishing, Oxford, 2005, 738 Pages, Price £37.50 (Paperback) ISBN: 1405111178. *Biological Conservation*. Vol. 135. <https://doi.org/10.1016/j.biocon.2006.10.034>.
- Bekele, A.Z., Koike, S. and Kobayashi, Y. (2010). Genetic diversity and diet specificity of ruminal *Prevotella* revealed by 16S rRNA gene-based analysis. *FEMS Microbiology Letters* 305 (1): 49–57. <https://doi.org/10.1111/j.1574-6968.2010.01911.x>.
- Bertrand, E., Vandenberghe, L.P.S., Soccol, C.R., Sigoillot, J.C. and Faulds, C. (2016). First generation bioethanol. In *Green Energy and Technology*, 175–212. https://doi.org/10.1007/978-3-319-30205-8_8.
- Bertsch, J., Siemund, A.L., Kremp, F., Müller, V., Wolfgang, J. and Str, M. (2016). A novel route for ethanol oxidation in the acetogenic bacterium *Acetobacterium woodii*: the acetaldehyde / ethanol dehydrogenase pathway 18: 2913–22. <https://doi.org/10.1111/1462-2920.13082>.
- Beta Renewables. n.d. PROESATM / The scientific research. Accessed April 28, 2018. <http://www.betarenewables.com/en/proesa/the-scientific-research>.
- Bioenergy2020+. n.d. Database on facilities for the production of advanced liquid and gaseous biofuels for transport. IEA Bioenergy. Accessed April 28, 2014. <http://demoplants.bioenergy2020.eu/>.
- Bischof, R.H., Ramoni, J. and Seiboth, B. (2016). Cellulases and beyond: The first 70 years of the enzyme producer *Trichoderma reesei*. *Microbial Cell Factories*. <https://doi.org/10.1186/s12934-016-0507-6>.
- Bisson, L.F. (1999). Stuck and sluggish fermentations. *American Journal of Enology and Viticulture*.
- Blake, L.I., Halim, F.A., Gray, C., Mair, R., Manning, D.A.C., Sallis, P., et al. (2017). Evaluating an anaerobic digestion (AD) feedstock derived from a novel non-source segregated municipal solid waste (MSW) product. *Waste Management*. <https://doi.org/10.1016/j.wasman.2016.10.031>.
- Boratyn, G.M., Schäffer, A.A., Agarwala, R., Altschul, S.F., Lipman, D.J. and Madden, T.L. (2012). Domain enhanced lookup time accelerated BLAST. *Biology Direct* 7. <https://doi.org/10.1186/1745-6150-7-12>.

- Bothast, R.J. and Schlicher, M.A. (2005). Biotechnological processes for conversion of corn into ethanol. *Applied Microbiology and Biotechnology* 67 (1): 19–25. <https://doi.org/10.1007/s00253-004-1819-8>.
- Boulanger, A., Pinet, E., Bouix, M., Bouchez, T. and Mansour, A.A. (2012). Effect of inoculum to substrate ratio (I / S) on municipal solid waste anaerobic degradation kinetics and potential. *Waste Management* 32 (12): 2258–65. <https://doi.org/10.1016/j.wasman.2012.07.024>.
- Brosius, J., Palmer, M.L., Kennedy, P.J. and Noller, H.F. (1978). Complete nucleotide sequence of a 16S ribosomal RNA gene from *Escherichia coli*. *Proc Natl Acad Sci U S A* 75 (10): 4801–5. <https://doi.org/10.1073/Pnas.75.10.4801>.
- Brunk, E., Sahoo, S., Zielinski, D.C., Altunkaya, A., Dräger, A., Mih, N., et al. (2018). Recon3D enables a three-dimensional view of gene variation in human metabolism. *Nature Biotechnology*. <https://doi.org/10.1038/nbt.4072>.
- Buttigieg, P.L. and Ramette, A. (2014). A guide to statistical analysis in microbial ecology: A community-focused, living review of multivariate data analyses. *FEMS Microbiology Ecology* 90 (3): 543–50. <https://doi.org/10.1111/1574-6941.12437>.
- Cai, H., Rodriguez, B.T., Zhang, W., Broadbent, J.R. and Steele, J.L. (2007). Genotypic and phenotypic characterization of *Lactobacillus casei* strains isolated from different ecological niches suggests frequent recombination and niche specificity. *Microbiology* 153 (8): 2655–65. <https://doi.org/10.1099/mic.0.2007/006452-0>.
- Callaway, T.R., Dowd, S.E., Edrington, T.S., Anderson, R.C., Krueger, N., Bauer, N., et al. (2010). Evaluation of bacterial diversity in the rumen and feces of cattle fed different levels of dried distillers grains plus solubles using bacterial tag-encoded FLX amplicon pyrosequencing. *Journal of Animal Science* 88 (12): 3977–83. <https://doi.org/10.2527/jas.2010-2900>.
- Calvo-Flores, F.G. and Dobado, J.A. (2010). Lignin as renewable raw material. *ChemSusChem*. <https://doi.org/10.1002/cssc.201000157>.
- Cantarella, H. (2018). With Brazilian biofuels on the rise, can we keep ethanol green? *Financial Times*. 2018. <https://www.ft.com/content/16ad268e-05ac-11e8-9650-9c0ad2d7c5b5>.
- Caporaso, J.G., Lauber, C.L., Walters, W.A., Berg-Lyons, D., Lozupone, C.A., Turnbaugh, P.J., et al. (2011). Global patterns of 16S rRNA diversity at a depth of millions of sequences per sample. *Proceedings of the National Academy of Sciences*. <https://doi.org/10.1073/pnas.1000080107>.
- Carere, C.R., Sparling, R., Cicek, N. and Levin, D.B. (2008). Third generation biofuels via direct cellulose fermentation. *International Journal of Molecular Sciences* 9 (7): 1342–60. <https://doi.org/10.3390/ijms9071342>.
- Cekmecelioglu, D., Demirci, A., Graves, R.E. and Davitt, N.H. (2005). Applicability of optimised in-vessel food waste composting for windrow systems. *Biosystems Engineering* 91 (4): 479–86. <https://doi.org/10.1016/j.biosystemseng.2005.04.013>.
- Chapman, M.G. and Underwood, A.J. (1999). Ecological patterns in multivariate assemblages: Information and interpretation of negative values in ANOSIM tests. *Marine Ecology Progress Series* 180 (Clarke 1993): 257–65. <https://doi.org/10.3354/meps180257>.
- Chassard, C., Delmas, E., Robert, C., Lawson, P.A. and Bernalier-Donadille, A. (2011). *Ruminococcus champanellensis* sp. nov., a cellulose-degrading bacterium from human gut microbiota. *International Journal of Systematic and Evolutionary Microbiology* 62 (1): 138–43. <https://doi.org/10.1099/ijms.0.027375-0>.
- Cheng, J.-R. and Zhu, M.-J. (2012). A Novel Co-culture Strategy for Lignocellulosic Bioenergy Production: A Systematic Review. *International Journal of Modern Biology and Medicine* *International Journal of Modern Biology and Medicine Journal Homepage: Www.ModernScientificPress.Com/Journals/IJBioMed.Aspx* 1 (3): 166–93.
- Chester, M., Stupples, D. and Lees, M. (2008). A Comparison of the Physical and Chemical Composition of UK Waste Streams Based on Hypothetical Compound Structure. In 13th European Biosolids and Organic Resources Conference, 10–12. White Rose Research Online. <https://doi.org/10.1186/1742-7622-5-2>.

Chundawat, S.P.S., Beckham, G.T., Himmel, M.E. and Dale, B.E. (2011). Deconstruction of Lignocellulosic Biomass to Fuels and Chemicals. *Annual Review of Chemical and Biomolecular Engineering* 2 (1): 121–45. <https://doi.org/10.1146/annurev-chembioeng-061010-114205>.

Clarke, K.R. (1993). Non-parametric multivariate analyses of changes in community structure. *Austral Ecology* 18 (1): 117–43. <https://doi.org/10.1111/j.1442-9993.1993.tb00438.x>.

Clarke, K.R. and Gorley, R.N. (2006). PRIMER v6: User Manual/Tutorial. PRIMER-E, Plymouth UK. <https://doi.org/10.1111/j.1442-9993.1993.tb00438.x>.

Clarke, K.R. and Gorley, R.N. (2015). PRIMER v7 : User Manual/Tutorial. PRIMER-E Ltd.

Clarke, K.R. and Warwick, R.M. (2001). Change in marine communities: an approach to statistical analysis and interpretation. Plymouth, UK: PRIMER-E Ltd. <https://doi.org/10.1111/j.1442-9993.1993.tb00438.x>.

Coughlan, L.M., Cotter, P.D., Hill, C. and Alvarez-Ordóñez, A. (2016). New weapons to fight old enemies: Novel strategies for the (bio)control of bacterial biofilms in the food industry. *Frontiers in Microbiology* 7 (OCT): 1–21. <https://doi.org/10.3389/fmicb.2016.01641>.

Crable, B.R., Sieber, J.R., Mao, X., Alvarez-Cohen, L., Gunsalus, R., Loo, R.R.O., et al. (2016). Membrane complexes of *Syntrophomonas wolfei* involved in syntrophic butyrate degradation and hydrogen formation. *Frontiers in Microbiology* 7 (NOV): 1–9. <https://doi.org/10.3389/fmicb.2016.01795>.

D. Hoornweg and P. Bhada-Tata. (2012). WHAT A WASTE A Global Review of Solid Waste Management. Urban Development Series. Vol. 15. Washington D.C. <https://doi.org/10.1111/febs.13058>.

D'Amore, R., Ijaz, U.Z., Schirmer, M., Kenny, J.G., Gregory, R., Darby, A.C., et al. (2016). A comprehensive benchmarking study of protocols and sequencing platforms for 16S rRNA community profiling. *BMC Genomics* 17 (1). <https://doi.org/10.1186/s12864-015-2194-9>.

Das, S.P., Ghosh, A., Gupta, A., Goyal, A. and Das, D. (2013). Lignocellulosic fermentation of wild grass employing recombinant hydrolytic enzymes and fermentative microbes with effective bioethanol recovery. *BioMed Research International* 2013. <https://doi.org/10.1155/2013/386063>.

DEFRA. (2009). Municipal Waste Composition: Review of Municipal Waste Component Analyses. WR0119. Vol. 5. <http://randd.defra.gov.uk/Default.aspx?Module=More&Location=None&ProjectID=15133>.

Demirbas, A. (2009). Political, economic and environmental impacts of biofuels: A review. *Applied Energy*. <https://doi.org/10.1016/j.apenergy.2009.04.036>.

Deschamps, A.M., Mahoudeau, G. and Lebeault, J.M. (1980). Fast degradation of kraft lignin by bacteria. *European Journal of Applied Microbiology and Biotechnology* 9 (1): 45–51. <https://doi.org/10.1007/BF00500001>.

Desvaux, M. (2006). Unravelling carbon metabolism in anaerobic cellulolytic bacteria. *Biotechnology Progress* 22 (5): 1229–38. <https://doi.org/10.1021/bp060016e>.

Desvaux, M., Guedeon, E. and Petitdemange, H. (2001). Metabolic flux in cellulose batch and cellulosefed continuous cultures of *Clostridium cellulolyticum* in response to acidic environment. *Microbiology* 147 (6): 1461–71. <https://doi.org/10.1099/00221287-147-6-1461>.

Dewan, A., Li, Z., Han, B. and Karim, M.N. (2013). Saccharification and fermentation of waste sweet potato for bioethanol production. *Journal of Food Process Engineering* 36 (6): 739–47. <https://doi.org/10.1111/jfpe.12042>.

Dias, M.O.S., Junqueira, T.L., Cavalett, O., Cunha, M.P., Jesus, C.D.F., Rossell, C.E.V., et al. (2012). Integrated versus stand-alone second generation ethanol production from sugarcane bagasse and trash. *Bioresource Technology* 103 (1): 152–61. <https://doi.org/10.1016/j.biortech.2011.09.120>.

Diender, M., Stams, A.J.M., Sousa, D.Z., Robb, F.T. and Guiot, S.R. (2015). Pathways and Bioenergetics of Anaerobic Carbon Monoxide Fermentation 6 (November): 1–18. <https://doi.org/10.3389/fmicb.2015.01275>.

DOE Joint Genome Institute. (2006). *Syntrophomonas wolfei* subsp. *wolfei* str. Goettingen G311 (DSM 2245B). 2006.

- Dols, M., Chraïbi, W., Remaud-Simeon, M., Lindley, N.D. and Monsan, P.F. (1997). Growth and energetics of *Leuconostoc mesenteroides* NRRL B-1299 during metabolism of various sugars and their consequences for dextranucrase production. *Applied and Environmental Microbiology* 63 (6): 2159–65.
- Dowd, S.E., Callaway, T.R., Wolcott, R.D., Sun, Y., McKeethan, T., Hagevoort, R.G., et al. (2008). Evaluation of the bacterial diversity in the feces of cattle using 16S rDNA bacterial tag-encoded FLX amplicon pyrosequencing (bTEFAP). *BMC Microbiology* 8: 1–8. <https://doi.org/10.1186/1471-2180-8-125>.
- Du, R., Yan, J., Li, S., Zhang, L., Zhang, S., Li, J., et al. (2015). Cellulosic ethanol production by natural bacterial consortia is enhanced by *Pseudoxanthomonas taiwanensis*. *Biotechnology for Biofuels* 8 (1): 1–10. <https://doi.org/10.1186/s13068-014-0186-7>.
- Duff, S.J.B. and Murray, W.D. (1996). Bioconversion of forest products industry waste cellulose to fuel ethanol: A review. *Bioresource Technology* 55 (1): 1–33. [https://doi.org/10.1016/0960-8524\(95\)00122-0](https://doi.org/10.1016/0960-8524(95)00122-0).
- Durán-Moreno, A., Garcés, M., Velasco, A., Marín, J., Gutiérrez, R., Moreno, A., et al. (2013). Mexico City's municipal solid waste characteristics and composition analysis. *Revista Internacional de Contaminación Ambiental* 29 (1): 39–46. <https://doi.org/ISSN: 0188-4999>.
- Eiteman, M.A., Lee, S.A. and Altman, E. (2008). A co-fermentation strategy to consume sugar mixtures effectively. *Journal of Biological Engineering* 2: 1–8. <https://doi.org/10.1186/1754-1611-2-3>.
- Elshaghabee, F.M.F., Bockelmann, W., Meske, D., Vrese, M. de, Walte, H.G., Schrezenmeir, J., et al. (2016). Ethanol production by selected intestinal microorganisms and lactic acid bacteria growing under different nutritional conditions. *Frontiers in Microbiology* 7 (JAN): 47. <https://doi.org/10.3389/fmicb.2016.00047>.
- ENVIRONMENTAL PROTECTION, E.A.W. (2012). The Waste (England and Wales) (Amendment) Regulations 2012. Statutory Instruments. UK. <http://www.legislation.gov.uk/ukSI/2012/1889/made>.
- European Parliament and Council. (2008). Directive 2008/98/EC of the European Parliament and of the Council of 19 November 2008 on waste and repealing certain directives. *Official Journal of the European Union*, 3–30. <https://doi.org/2008/98/EC; 32008L0098>.
- Evangelisti, S., Lettieri, P., Borello, D. and Clift, R. (2014). Life cycle assessment of energy from waste via anaerobic digestion: A UK case study. *Waste Management* 34 (1): 226–37. <https://doi.org/10.1016/j.wasman.2013.09.013>.
- Fang, H.H.P., Zhang, T. and Liu, H. (2002). Microbial diversity of a mesophilic hydrogen-producing sludge. *Applied Microbiology and Biotechnology* 58 (1): 112–18. <https://doi.org/10.1007/s00253-001-0865-8>.
- Fetzer, I., Johst, K., Schäwe, R., Banitz, T., Harms, H. and Chatzinotas, A. (2015). The extent of functional redundancy changes as species' roles shift in different environments. *Proceedings of the National Academy of Sciences* 112 (48): 14888–93. <https://doi.org/10.1073/pnas.1505587112>.
- Fierer, N. and Jackson, R.B. (2006). The diversity and biogeography of soil bacterial communities. *Proceedings of the National Academy of Sciences of the United States of America* 103 (3): 626–31. <https://doi.org/10.1073/pnas.0507535103>.
- Flint, H.J. (1997). The rumen microbial ecosystem--some recent developments. *Trends in Microbiology* 5 (12): 483–88. [https://doi.org/10.1016/S0966-842X\(97\)01159-1](https://doi.org/10.1016/S0966-842X(97)01159-1).
- Florio, C., Pirozzi, D., Ausiello, A., Micoli, L., Toscano, G., Turco, M., et al. (2017). Effect of Inoculum / Substrate Ratio on Dark Fermentation for Biohydrogen Production from Organic Fraction of Municipal Solid Waste. *Chemical Engineering Transactions* 57.
- Frankó, B., Galbe, M. and Wallberg, O. (2016). Bioethanol production from forestry residues: A comparative techno-economic analysis. *Applied Energy*. <https://doi.org/10.1016/j.apenergy.2016.11.011>.
- Friedrich, M., Springer, N., Ludwig, W. and Schink, B. (1996). Phylogenetic positions of *Desulfotulnus glycolicus* gen. nov., sp. nov., and *Syntrophobotulus glycolicus* gen. nov., sp. nov., two new strict anaerobes growing with glycolic acid. *International Journal of Systematic Bacteriology* 46 (4): 1065–69. <https://doi.org/10.1099/00207713-46-4-1065>.
- Fuente-Hernández, A., Corcos, P.-O., Beauchet, R. and Lavoie, J.-M. (2013). Biofuels and Co-Products Out of Hemicelluloses. *Liquid, Gaseous and Solid Biofuels - Conversion Techniques*, 3–46. <https://doi.org/10.5772/52645>.

Ganigué, R., Sánchez-paredes, P., Bañeras, L. and Colprim, J. (2016). Low Fermentation pH Is a Trigger to Alcohol Production , but a Killer to Chain Elongation. *Frontiers in Microbiology* 7 (May): 1–11. <https://doi.org/10.3389/fmicb.2016.00702>.

Garcia, S.L., Jangid, K., Whitman, W.B. and Das, K.C. (2011). Transition of microbial communities during the adaption to anaerobic digestion of carrot waste. *Bioresource Technology* 102 (15): 7249–56. <https://doi.org/10.1016/j.biortech.2011.04.098>.

GBEP. (2007). Summary of WTW Energy and GHG balances. Well-to-Wheels Analysis of Future Automotive Fuels and Powertrains in the European Context WELL-TO-WHEELS Report. 2007. <http://www.globalbioenergy.org/bioenergyinfo/biofuels-for-transportation/detail/en/c/6319/>.

Ghafari, S., Hasan, M. and Aroua, M.K. (2009). Effect of carbon dioxide and bicarbonate as inorganic carbon sources on growth and adaptation of autohydrogenotrophic denitrifying bacteria. *Journal of Hazardous Materials* 162 (2–3): 1507–13. <https://doi.org/10.1016/j.jhazmat.2008.06.039>.

Ghigliazza, R., Lodi, A. and Rovatti, M. (1998). Study on biological phosphorus removal process by *Acinetobacter lwoffii*: Possibility to by-pass the anaerobic phase. *Bioprocess Engineering* 18 (3): 207–11. <https://doi.org/10.1007/s004490050432>.

Goh, C.S., Tan, K.T., Lee, K.T. and Bhatia, S. (2010). Bio-ethanol from lignocellulose: Status, perspectives and challenges in Malaysia. *Bioresource Technology* 101 (13): 4834–41. <https://doi.org/10.1016/j.biortech.2009.08.080>.

Goldemberg, J., Coelho, S.T. and Guardabassi, P. (2008). The sustainability of ethanol production from sugarcane. *Energy Policy* 36 (6): 2086–97. <https://doi.org/10.1016/j.enpol.2008.02.028>.

González-Cabaleiro, R., Lema, J.M. and Rodríguez, J. (2015). Metabolic energy-based modelling explains product yielding in anaerobic mixed culture fermentations. *PLoS ONE* 10 (5). <https://doi.org/10.1371/journal.pone.0126739>.

GrandBio. n.d. GrandBio. <http://www.granbio.com.br>.

Grimm, V., Berger, U., DeAngelis, D.L., Polhill, J.G., Giske, J. and Railsback, S.F. (2010). The ODD protocol: A review and first update. *Ecological Modelling* 221 (23): 2760–68. <https://doi.org/10.1016/j.ecolmodel.2010.08.019>.

Guerra, N.P., Fajardo, P., Fuciños, C., Amado, I.R., Alonso, E., Torrado, A., et al. (2010). Modelling the biphasic growth and product formation by *Enterococcus faecium* CECT 410 in realkalized fed-batch fermentations in whey. *Journal of Biomedicine and Biotechnology* 2010. <https://doi.org/10.1155/2010/290286>.

Guo, F., Wu, F., Mu, Y., Hu, Y., Zhao, X., Meng, W., et al. (2016). Characterization of organic matter of plants from lakes by thermal analysis in a N₂ atmosphere. *Scientific Reports* 6: 1–7. <https://doi.org/10.1038/srep22877>.

Guo, P., Zhu, W., Wang, H., Lü, Y., Wang, X., Zheng, D., et al. (2010). Functional characteristics and diversity of a novel lignocelluloses degrading composite microbial system with high xylanase activity. *Journal of Microbiology and Biotechnology* 20 (2): 254–64. <https://doi.org/10.4014/jmb.0906.06035>.

Gusakov, A. V. (2011). Alternatives to *Trichoderma reesei* in biofuel production. *Trends in Biotechnology* 29 (9): 419–25. <https://doi.org/10.1016/j.tibtech.2011.04.004>.

Haegeman, B., Hamelin, J., Moriarty, J., Neal, P., Dushoff, J. and Weitz, J.S. (2013). Robust estimation of microbial diversity in theory and in practice. *ISME Journal* 7 (6): 1092–1101. <https://doi.org/10.1038/ismej.2013.10>.

Haft, R.J.F., Keating, D.H., Schwaegler, T., Schwalbach, M.S., Vinokur, J., Tremaine, M., et al. (2014). Correcting direct effects of ethanol on translation and transcription machinery confers ethanol tolerance in bacteria. *Proceedings of the National Academy of Sciences* 111 (25): E2576–85. <https://doi.org/10.1073/pnas.1401853111>.

Haghighi Mood, S., Hossein Golfeshan, A., Tabatabaei, M., Salehi Jouzani, G., Najafi, G.H., Gholami, M., et al. (2013). Lignocellulosic biomass to bioethanol, a comprehensive review with a focus on pretreatment. *Renewable and Sustainable Energy Reviews* 27: 77–93. <https://doi.org/10.1016/j.rser.2013.06.033>.

Hahnke, S., Langer, T., Koeck, D.E. and Klocke, M. (2016). Description of *Proteiniphilum saccharofermentans* sp. nov., *Petrimonas mucosa* sp. nov. and *Fermentimonas caenicola* gen. nov., sp. nov., isolated from

mesophilic laboratory-scale biogas reactors, and emended description of the genus *Proteiniphilum*. *International Journal of Systematic and Evolutionary Microbiology* 66 (3): 1466–75. <https://doi.org/10.1099/ijsem.0.000902>.

Hall-Stoodley, L., Costerton, J.W. and Stoodley, P. (2004). Bacterial biofilms: From the natural environment to infectious diseases. *Nature Reviews Microbiology* 2 (2): 95–108. <https://doi.org/10.1038/nrmicro821>.

Hames, B., Ruiz, R., Scarlata, C., Sluiter, a, Sluiter, J. and Templeton, D. (2008). Preparation of Samples for Compositional Analysis Laboratory Analytical Procedure (LAP) Issue Date : 8 / 06 / 2008 Preparation of Samples for Compositional Analysis Laboratory Analytical Procedure (LAP). National Renewable Energy Laboratory, no. August: 1–9.

Hammes, W.P. and Hertel, C. (2006). The Genera *Lactobacillus* and *Carnobacterium*. In *The Prokaryotes*, 320–403. https://doi.org/10.1007/0-387-30744-3_10.

Hanly, T.J. and Henson, M.A. (2013). Dynamic metabolic modeling of a microaerobic yeast co-culture: Predicting and optimizing ethanol production from glucose/xylose mixtures. *Biotechnology for Biofuels* 6 (1): 1. <https://doi.org/10.1186/1754-6834-6-44>.

Haruta, S., Cui, Z., Huang, Z., Li, M., Ishii, M. and Igarashi, Y. (2002). Construction of a stable microbial community with high cellulose-degradation ability. *Applied Microbiology and Biotechnology* 59 (4–5): 529–34. <https://doi.org/10.1007/s00253-002-1026-4>.

Haruta, S., Cui, Z., Huang, Z., Li, M., Ishii, M. and Igarashi, Y. (2002). Construction of a stable microbial community with high cellulose-degradation ability. *Applied Microbiology and Biotechnology* 59 (4–5): 529–34. <https://doi.org/10.1007/s00253-002-1026-4>.

Hasunuma, T. and Kondo, A. (2012). Development of yeast cell factories for consolidated bioprocessing of lignocellulose to bioethanol through cell surface engineering. *Biotechnology Advances*. <https://doi.org/10.1016/j.biotechadv.2011.10.011>.

Hasunuma, T., Okazaki, F., Okai, N., Hara, K.Y., Ishii, J. and Kondo, A. (2013). A review of enzymes and microbes for lignocellulosic biorefinery and the possibility of their application to consolidated bioprocessing technology. *Bioresource Technology* 135: 513–22. <https://doi.org/10.1016/j.biortech.2012.10.047>.

Henan-Tianguan-Group. n.d. Henan Tianguan Group. Accessed April 28, 2018. <http://www.tianguan.com.cn/english/>.

Henderson, G., Cox, F., Ganesh, S., Jonker, A., Young, W., Janssen, P.H., et al. (2015). Rumen microbial community composition varies with diet and host, but a core microbiome is found across a wide geographical range. *Scientific Reports* 5 (April): 1–13. <https://doi.org/10.1038/srep14567>.

Hendriks, A.T.W.M. and Zeeman, G. (2009). Pretreatments to enhance the digestibility of lignocellulosic biomass. *Bioresource Technology* 100 (1): 10–18. <https://doi.org/10.1016/j.biortech.2008.05.027>.

Hoelzle, R.D., Viridis, B. and Batstone, D.J. (2014). Regulation mechanisms in mixed and pure culture microbial fermentation. *Biotechnology and Bioengineering* 111 (11): 2139–54. <https://doi.org/10.1002/bit.25321>.

Holtzapple, M.T., Lundeen, J.E., Sturgis, R., Lewis, J.E. and Dale, B.E. (1992). Pretreatment of lignocellulosic municipal solid waste by ammonia fiber explosion (AFEX). *Applied Biochemistry and Biotechnology* 34–35 (1): 5–21. <https://doi.org/10.1007/BF02920530>.

Honda, T., Fujita, T. and Tonouchi, A. (2013). *Aminivibrio pyruvatiphilus* gen. nov., sp. nov., an anaerobic, amino-acid-degrading bacterium from soil of a Japanese rice field. *International Journal of Systematic and Evolutionary Microbiology* 63 (PART10): 3679–86. <https://doi.org/10.1099/ijms.0.052225-0>.

Hui, W., Jiajia, L., Yucai, L., Peng, G., Xiaofen, W., Kazuhiro, M., et al. (2013). Bioconversion of un-pretreated lignocellulosic materials by a microbial consortium XDC-2. *Bioresource Technology* 136: 481–87. <https://doi.org/10.1016/j.biortech.2013.03.015>.

Huston, M., DeAngelis, D. and Post, W. (1988). New Computer Models Unify Ecological Theory. *BioScience* 38 (10): 682–91. <https://doi.org/10.2307/1310870>.

Hyduke, D., Hyduke, D., Schellenberger, J., Que, R., Fleming, R., Thiele, I., et al. (2011). Creation and analysis of biochemical constraint-based models the COBRA Toolbox v3.0. *Nature Protocols* 6 (9): 1290–1307. <https://doi.org/10.1038/protex.2011.234>.

IEA. (2014). FAQs: Transport. International Energy Agency. 2014. <http://www.iea.org/aboutus/faqs/transport/>.

INECC. (2007). Residuos sólidos urbanos. Instituto Nacional de Ecología y Cambio Climático. 2007. <http://www2.inecc.gob.mx/publicaciones2/libros/495/residuos.html>.

INEGI. (2015). Encuesta intercensal. Instituto Nacional de Estadística y Geografía. 2015. <http://cuentame.inegi.org.mx/monografias/informacion/DF/Poblacion/default.aspx?tema>.

Infantes, D., González Del Campo, A., Villaseñor, J. and Fernández, F.J. (2011). Influence of pH, temperature and volatile fatty acids on hydrogen production by acidogenic fermentation. *International Journal of Hydrogen Energy* 36 (24): 15595–601. <https://doi.org/10.1016/j.ijhydene.2011.09.061>.

Jabari, L., Gannoun, H., Cayol, J.L., Hedi, A., Sakamoto, M., Falsen, E., et al. (2012). *Macellibacteroides fermentans* gen. nov., sp. nov., a member of the family Porphyromonadaceae isolated from an upflow anaerobic filter treating abattoir wastewaters. *International Journal of Systematic and Evolutionary Microbiology* 62 (10): 2522–27. <https://doi.org/10.1099/ijs.0.032508-0>.

Jain, R., Pandey, A., Pasupuleti, M. and Pande, V. (2017). Prolonged Production and Aggregation Complexity of Cold-Active Lipase from *Pseudomonas proteolytica* (GBPI_Hb61) Isolated from Cold Desert Himalaya. *Molecular Biotechnology* 59 (1): 34–45. <https://doi.org/10.1007/s12033-016-9989-z>.

Janssen, P.H. (2010). Influence of hydrogen on rumen methane formation and fermentation balances through microbial growth kinetics and fermentation thermodynamics. *Animal Feed Science and Technology*. <https://doi.org/10.1016/j.anifeedsci.2010.07.002>.

Jayatilake, P.G., Gupta, P., Li, B., Madsen, C., Oyebamiji, O., González-Cabaleiro, R., et al. (2017). A mechanistic Individual-based Model of microbial communities. *PLoS ONE* 12 (8): 1–26. <https://doi.org/10.1371/journal.pone.0181965>.

Jimenez, D.J., Dini-Andreote, F. and Elsas, J.D. Van. (2014). Metataxonomic profiling and prediction of functional behaviour of wheat straw degrading microbial consortia. *Biotechnology for Biofuels* 7 (1). <https://doi.org/10.1186/1754-6834-7-92>.

Johnson, K., Jiang, Y., Kleerebezem, R., Muyzer, G. and Loosdrecht, M.C.M. Van. (2009). Enrichment of a mixed bacterial culture with a high polyhydroxyalkanoate storage capacity. *Biomacromolecules* 10 (4): 670–76. <https://doi.org/10.1021/bm8013796>.

Jönsson, L.J. and Martín, C. (2016). Pretreatment of lignocellulose: Formation of inhibitory by-products and strategies for minimizing their effects. *Bioresource Technology* 199: 103–12. <https://doi.org/10.1016/j.biortech.2015.10.009>.

Jönsson, L.J., Alriksson, B. and Nilvebrant, N.O. (2013). Bioconversion of lignocellulose: Inhibitors and detoxification. *Biotechnology for Biofuels* 6 (1): 1–10. <https://doi.org/10.1186/1754-6834-6-16>.

Kádár, Z., Maltha, S.F., Szengyel, Z., Réczey, K. and Laatsch, W. De. (2007). Ethanol fermentation of various pretreated and hydrolyzed substrates at low initial pH. In *Applied Biochemistry and Biotechnology*, 137–140:847–58. <https://doi.org/10.1007/s12010-007-9102-y>.

Kaliyan, N., Morey, R.V. and Tiffany, D.G. (2011). Reducing life cycle greenhouse gas emissions of corn ethanol by integrating biomass to produce heat and power at ethanol plants. *Biomass and Bioenergy* 35 (3): 1103–13. <https://doi.org/10.1016/j.biombioe.2010.11.035>.

Karadag, D. and Puhakka, J.A. (2010). Direction of glucose fermentation towards hydrogen or ethanol production through on-line pH control. *International Journal of Hydrogen Energy*. <https://doi.org/10.1016/j.ijhydene.2010.07.139>.

Kato, S., Haruta, S., Cui, Z.J., Ishii, M. and Igarashi, Y. (2004). Effective cellulose degradation by a mixed-culture system composed of a cellulolytic *Clostridium* and aerobic non-cellulolytic bacteria. *FEMS Microbiology Ecology* 51 (1): 133–42. <https://doi.org/10.1016/j.femsec.2004.07.015>.

- Kato, S., Haruta, S., Cui, Z.J., Ishii, M. and Igarashi, Y. (2005). Stable coexistence of five bacterial strains as a cellulose-degrading community. *Applied and Environmental Microbiology* 71 (11): 7099–7106. <https://doi.org/10.1128/AEM.71.11.7099-7106.2005>.
- Keis, S., Shaheen, R. and Jones, D.T. (2001). Emended descriptions of *Clostridium acetobutylicum* and *Clostridium beijerinckii*, and descriptions of *Clostridium saccharoperbutylacetonicum* sp. nov. and *Clostridium saccharobutylicum* sp. nov. *Int. J. Syst. Evol. Microbiol.* 51 (Pt 6): 2095–2103. <https://doi.org/11760952>.
- Kersey, P.J., Allen, J.E., Allot, A., Barba, M., Boddu, S., Bolt, B.J., et al. (2018). Ensembl Genomes 2018: An integrated omics infrastructure for non-vertebrate species. *Nucleic Acids Research* 46 (D1): D802–8. <https://doi.org/10.1093/nar/gkx1011>.
- Kersey, P.J., Lawson, D., Birney, E., Derwent, P.S., Haimel, M., Herrero, J., et al. (2009). Ensembl Genomes: Extending Ensembl across the taxonomic space. *Nucleic Acids Research* 38 (SUPPL.1). <https://doi.org/10.1093/nar/gkp871>.
- Khiyami, M. a, Pometto Iii, A.L. and Brown, R.C. (2005). Detoxification of corn stover and corn starch pyrolysis liquors by *Pseudomonas putida* and *Streptomyces setonii* suspended cells and plastic compost support biofilms. *Journal of Agricultural and Food Chemistry* 53 (Atcc 11443): 2978–87. <https://doi.org/10.1021/jf048224e>.
- Kim, D.H., Kim, S.H., Jung, K.W., Kim, M.S. and Shin, H.S. (2011). Effect of initial pH independent of operational pH on hydrogen fermentation of food waste. *Bioresource Technology* 102 (18): 8646–52. <https://doi.org/10.1016/j.biortech.2011.03.030>.
- Kim, J.K., Nhat, L., Chun, Y.N. and Kim, S.W. (2008). Hydrogen production conditions from food waste by dark fermentation with *Clostridium beijerinckii* KCTC 1785. *Biotechnology and Bioprocess Engineering* 13 (4): 499–504. <https://doi.org/10.1007/s12257-008-0142-0>.
- King, Z.A., Lu, J., Dräger, A., Miller, P., Federowicz, S., Lerman, J.A., et al. (2016). BiGG Models: A platform for integrating, standardizing and sharing genome-scale models. *Nucleic Acids Research* 44 (D1): D515–22. <https://doi.org/10.1093/nar/gkv1049>.
- Kirkegaard, R.H., McIlroy, S.J., Kristensen, J.M., Nierychlo, M., Karst, S.M., Dueholm, M.S., et al. (2017). The impact of immigration on microbial community composition in full-scale anaerobic digesters. *Scientific Reports* 7 (1): 1–11. <https://doi.org/10.1038/s41598-017-09303-0>.
- Kleerebezem, R. and Loosdrecht, M.C. van. (2007). Mixed culture biotechnology for bioenergy production. *Current Opinion in Biotechnology* 18 (3): 207–12. <https://doi.org/10.1016/j.copbio.2007.05.001>.
- Köpke, M., Held, C., Hujer, S., Liesegang, H., Wiezer, A., Wollherr, A., et al. (2010). *Clostridium ljungdahlii* represents a microbial production platform based on syngas. *Proc. Natl. Acad. Sci.* 107 (29): 15305–15305. <https://doi.org/10.1073/pnas.1011320107>.
- Kotsyurbenko, O.R., Friedrich, M.W., Simankova, M. V., Nozhevnikova, A.N., Golyshin, P.N., Timmis, K.N., et al. (2007). Shift from acetoclastic to H₂-dependent methanogenesis in a West Siberian peat bog at low pH values and isolation of an acidophilic *Methanobacterium* strain. *Applied and Environmental Microbiology* 73 (7): 2344–48. <https://doi.org/10.1128/AEM.02413-06>.
- Kozich, J.J., Westcott, S.L., Baxter, N.T., Highlander, S.K. and Schloss, P.D. (2013). Development of a dual-index sequencing strategy and curation pipeline for analyzing amplicon sequence data on the miseq illumina sequencing platform. *Applied and Environmental Microbiology* 79 (17): 5112–20. <https://doi.org/10.1128/AEM.01043-13>.
- Kumar, S., Stecher, G., Li, M., Knyaz, C. and Tamura, K. (2018). MEGA X: Molecular Evolutionary Genetics Analysis across Computing Platforms. *Molecular Biology and Evolution* 35 (6): 1547–49. <https://doi.org/10.1093/molbev/msy096>.
- Kutzner, H.J. (2000). Microbiology of Composting. In *Biotechnology: Environmental Processes III*, edited by H.-J. Rehm, G. Reed, A. Pühler and P. Stadler, Second Edi, 35–100. Weinheim, Germany: Wiley-VCH Verlag GmbH. <https://doi.org/10.1002/9783527620968.ch2>.
- Kuzyakov, Y., Friedel, J.K. and Stahr, K. (2000). Review of mechanisms and quantification of priming effects 32.

Lagkouvardos, I., Pukall, R., Abt, B., Foessel, B.U., Meier-Kolthoff, J.P., Kumar, N., et al. (2016). The Mouse Intestinal Bacterial Collection (miBC) provides host-specific insight into cultured diversity and functional potential of the gut microbiota. *Nature Microbiology* 1 (10): 1–15. <https://doi.org/10.1038/nmicrobiol.2016.131>.

Lampert, Y., Dror, B., Sela, N., Teper-Bamnolker, P., Daus, A., Sela (Saldinger), S., et al. (2017). Emergence of *Leuconostoc mesenteroides* as a causative agent of oozing in carrots stored under non-ventilated conditions. *Microbial Biotechnology* 10 (6): 1677–89. <https://doi.org/10.1111/1751-7915.12753>.

Lane, J. (2017). DowDuPont to exit cellulosic biofuels business. *Biofuels Digest*. 2017. <http://www.biofuelsdigest.com/bdigest/2017/11/02/breaking-news-dowdupont-to-exit-cellulosic-ethanol-business/>.

Langille, M.G.I., Zaneveld, J., Caporaso, J.G., McDonald, D., Knights, D., Reyes, J.A., et al. (2013). Predictive functional profiling of microbial communities using 16S rRNA marker gene sequences. *Nature Biotechnology* 31 (9): 814–21. <https://doi.org/10.1038/nbt.2676>.

Larsen, J., Haven, M.Ø. and Thirup, L. (2012). Inbicon makes lignocellulosic ethanol a commercial reality. *Biomass and Bioenergy* 46: 36–45. <https://doi.org/10.1016/j.biombioe.2012.03.033>.

Laser, M. and Lynd, L.R. (2014). Comparative efficiency and driving range of light- and heavy-duty vehicles powered with biomass energy stored in liquid fuels or batteries. *Proceedings of the National Academy of Sciences* 111 (9): 3360–64. <https://doi.org/10.1073/pnas.1314039111>.

Lauber, C.L., Hamady, M., Knight, R. and Fierer, N. (2009). Pyrosequencing-based assessment of soil pH as a predictor of soil bacterial community structure at the continental scale. *Applied and Environmental Microbiology* 75 (15): 5111–20. <https://doi.org/10.1128/AEM.00335-09>.

Lee, D.J., Show, K.Y. and Wang, A. (2013). Unconventional approaches to isolation and enrichment of functional microbial consortium - A review. *Bioresource Technology* 136: 697–706. <https://doi.org/10.1016/j.biortech.2013.02.075>.

Lee, S., Lee, J.H. and Mitchell, R.J. (2015). Analysis of *Clostridium beijerinckii* NCIMB 8052's transcriptional response to ferulic acid and its application to enhance the strain tolerance. *Biotechnology for Biofuels* 8 (1): 1–14. <https://doi.org/10.1186/s13068-015-0252-9>.

Lee, Y.J., Romanek, C.S., Mills, G.L., Davis, R.C., Whitman, W.B. and Wiegel, J. (2006). *Gracilibacter thermotolerans* gen. nov., sp. nov., an anaerobic, thermotolerant bacterium from a constructed wetland receiving acid sulfate water. *International Journal of Systematic and Evolutionary Microbiology* 56 (9): 2089–93. <https://doi.org/10.1099/ijs.0.64040-0>.

Legendre, P. and Legendre, L. (2012). *Numerical Ecology* (3rd English Edition). *Developments in Environmental Modelling* 20.

Li, A. and Khraisheh, M. (2010). Bioenergy II: Bio-Ethanol from Municipal Solid Waste (MSW): The Role of Biomass Properties and Structures During the Ethanol Conversion Process. *International Journal of Chemical Reactor Engineering* 8 (1): A85. <https://doi.org/10.2202/1542-6580.1918>.

Li, A., Antizar-Ladislao, B. and Khraisheh, M. (2007). Bioconversion of municipal solid waste to glucose for bio-ethanol production. *Bioprocess and Biosystems Engineering*. <https://doi.org/10.1007/s00449-007-0114-3>.

Li, H., Wu, S., Wirth, S., Hao, Y., Wang, W., Zou, H., et al. (2016). Diversity and activity of cellulolytic bacteria, isolated from the gut contents of grass carp (*Ctenopharyngodon idellus*) (Valenciennes) fed on Sudan grass (*Sorghum sudanense*) or artificial feedstuffs. *Aquaculture Research* 47 (1): 153–64. <https://doi.org/10.1111/are.12478>.

Li, S., Zhang, X. and Andresen, J.M. (2012). Production of fermentable sugars from enzymatic hydrolysis of pretreated municipal solid waste after autoclave process. *Fuel* 92 (1): 84–88. <https://doi.org/10.1016/j.fuel.2011.07.012>.

Liang, S., McDonald, A.G. and Coats, E.R. (2014). Lactic acid production with undefined mixed culture fermentation of potato peel waste. *Waste Management* 34 (11): 2022–27. <https://doi.org/10.1016/j.wasman.2014.07.009>.

- Lim, S.J. and Kim, T.-H. (2014). Applicability and trends of anaerobic granular sludge treatment processes. *Biomass and Bioenergy* 60: 189–202. <https://doi.org/10.1016/j.biombioe.2013.11.011>.
- Lin, C.W., Wu, C.H., Tran, D.T., Shih, M.C., Li, W.H. and Wu, C.F. (2011). Mixed culture fermentation from lignocellulosic materials using thermophilic lignocellulose-degrading anaerobes. *Process Biochemistry* 46 (2): 489–93. <https://doi.org/10.1016/j.procbio.2010.09.024>.
- Lin, C.Y. and Hung, W.C. (2008). Enhancement of fermentative hydrogen/ethanol production from cellulose using mixed anaerobic cultures. *International Journal of Hydrogen Energy* 33 (14): 3660–67. <https://doi.org/10.1016/j.ijhydene.2008.04.036>.
- Lin, X., Fan, J., Wen, Q., Li, R., Jin, X., Wu, J., et al. (2014). Optimization and validation of a GC/FID method for the determination of acetone-butanol-ethanol fermentation products. *Journal of Chromatographic Science* 52 (3): 264–70. <https://doi.org/10.1093/chromsci/bmt022>.
- Liu, Q., Ren, Z.J., Huang, C., Liu, B., Ren, N. and Xing, D. (2016). Multiple syntrophic interactions drive biohydrogen production from waste sludge in microbial electrolysis cells. *Biotechnology for Biofuels* 9 (1): 1–10. <https://doi.org/10.1186/s13068-016-0579-x>.
- LongLive Bio-Technology. n.d. LongLive Bio-Technology. Accessed April 29, 2018. <http://en.longlive.cn/a/Service/Application/>.
- Lopez-Capel, E., Sohi, S.P., Gaunt, J.L. and Manning, D.A.C. (2005). USE OF THERMOGRAVIMETRY–DIFFERENTIAL SCANNING CALORIMETRY TO CHARACTERIZE MODELABLE SOIL ORGANIC MATTER FRACTIONS. *Soil Science Society of America Journal* 140: 136–40.
- Lü, F., Shao, L.M., Bru, V., Godon, J.J. and He, P.J. (2009). Synergetic effect of pH and biochemical components on bacterial diversity during mesophilic anaerobic fermentation of biomass-origin waste. *Journal of Applied Microbiology* 106 (2): 580–91. <https://doi.org/10.1111/j.1365-2672.2008.04029.x>.
- Lund, P., Tramonti, A. and Biase, D. De. (2014). Coping with low pH: Molecular strategies in neutralophilic bacteria. *FEMS Microbiology Reviews* 38 (6): 1091–1125. <https://doi.org/10.1111/1574-6976.12076>.
- Lynd, L.R. (1996). OVERVIEW AND EVALUATION OF FUEL ETHANOL FROM CELLULOSIC BIOMASS: Technology, Economics, the Environment, and Policy. *Annual Review of Energy and the Environment* 21 (1): 403–65. <https://doi.org/10.1146/annurev.energy.21.1.403>.
- Ma, H., Wang, Q., Qian, D., Gong, L. and Zhang, W. (2009). The utilization of acid-tolerant bacteria on ethanol production from kitchen garbage. *Renewable Energy* 34 (6): 1466–70. <https://doi.org/10.1016/j.renene.2008.10.020>.
- Ma, K., Liu, X. and Dong, X. (2005). *Methanobacterium beijingense* sp. nov., a novel methanogen isolated from anaerobic digesters. *International Journal of Systematic and Evolutionary Microbiology* 55 (1): 325–29. <https://doi.org/10.1099/ijs.0.63254-0>.
- Machado, D. (2017). Framed. 0.4.0. 2017.
- Machado, D., Andrejev, S., Tramontano, M. and Patil, K.R. (2018). Fast automated reconstruction of genome-scale metabolic models for microbial species and communities. *BioRxiv*, 223198. <https://doi.org/10.1101/223198>.
- Machado, D., Kaiz Huang, Matos, M., Sonnenschein, N., Sarag Correia and Andrejev, S. (2017). Cdanielmachado/framed: Even more features, November. <https://doi.org/10.5281/ZENODO.1048261>.
- Madden, R.H., Bryder, M.J. and Poole, N.J. (1989). Isolation and Characterization of an Anaerobic, Cellulolytic Bacterium, *Clostridium papyrosolvens* sp. nov. *International Journal of Systematic Bacteriology* 39 (1): 68–71.
- Maddox, I.S., Steiner, E., Hirsch, S., Wessner, S., Gutierrez, N. a, Gapes, J.R., et al. (2000). The cause of “acid-crash” and “acidogenic fermentations” during the batch acetone-butanol-ethanol (ABE-) fermentation process. *Journal of Molecular Microbiology and Biotechnology* 2 (1): 95–100.
- Madigan, M. (2015). *Brock Biology of Microorganisms*. Fourteenth. San Francisco, CA: Pearson Education, publishing as Benjamin Cummings.
- Magee, J.A. and Herd, A.C. (1999). Internal Standard Calculations in Chromatography. *Journal of Chemical Education* 76 (2): 252. <https://doi.org/10.1021/ed076p252>.

- Magurran, A.E. (2013). *Measuring of Biological Diversity*. John Wiley & Sons, Incorporated. <https://doi.org/10.2989/16085910409503825>.
- Mann, S.O., Masson, F.M. and Oxford, a E. (1954). Facultative anaerobic bacteria from the sheep's rumen. *Journal of General Microbiology* 10 (1): 142–49. <https://doi.org/10.1099/00221287-10-1-142>.
- Marchand, S., Block, J. De, Jonghe, V. De, Coorevits, A., Heyndrickx, M. and Herman, L. (2012). Biofilm Formation in Milk Production and Processing Environments; Influence on Milk Quality and Safety. *Comprehensive Reviews in Food Science and Food Safety* 11 (2): 133–47. <https://doi.org/10.1111/j.1541-4337.2011.00183.x>.
- Martel, C.M., Parker, J.E., Jackson, C.J., Warrilow, A.G.S., Rolley, N., Greig, C., et al. (2011). Expression of bacterial levanase in yeast enables simultaneous saccharification and fermentation of grass juice to bioethanol. *Bioresource Technology* 102 (2): 1503–8. <https://doi.org/10.1016/j.biortech.2010.07.099>.
- McCann, J.C., Wickersham, T.A. and Loor, J.J. (2014). High-throughput methods redefine the rumen microbiome and its relationship with nutrition and metabolism. *Bioinformatics and Biology Insights* 8: 109–25. <https://doi.org/10.4137/BBI.Ss15389>.
- McDonald, L.C., Fleming, H.P. and Hassan, H.M. (1990). Acid tolerance of *Leuconostoc mesenteroides* and *Lactobacillus plantarum*. *Applied and Environmental Microbiology* 56 (7): 2120–24.
- McElhinny, C., Gibbons, P., Brack, C. and Bauhus, J. (2005). Forest and woodland stand structural complexity: Its definition and measurement. *Forest Ecology and Management*. <https://doi.org/10.1016/j.foreco.2005.08.034>.
- McIlroy, S.J., Kirkegaard, R.H., McIlroy, B., Nierychlo, M., Kristensen, J.M., Karst, S.M., et al. (2017). MiDAS 2.0: An ecosystem-specific taxonomy and online database for the organisms of wastewater treatment systems expanded for anaerobic digester groups. *Database* 2017 (1). <https://doi.org/10.1093/database/bax016>.
- Mielenz, J.R. (2013). CONSOLIDATED BOPROCESSING METHOD USING THERMOPHILIC MCROORGANISMS. US 2013021 0071A1, issued 2013.
- Millat, T., Janssen, H., Bahl, H., Fischer, R.J. and Wolkenhauer, O. (2013). Integrative modelling of pH-dependent enzyme activity and transcriptomic regulation of the acetone-butanol-ethanol fermentation of *Clostridium acetobutylicum* in continuous culture. *Microbial Biotechnology* 6 (5): 526–39. <https://doi.org/10.1111/1751-7915.12033>.
- Mohd Azhar, S.H., Abdulla, R., Jambo, S.A., Marbawi, H., Gansau, J.A., Mohd Faik, A.A., et al. (2017). Yeasts in sustainable bioethanol production: A review. *Biochemistry and Biophysics Reports* 10 (November 2016): 52–61. <https://doi.org/10.1016/j.bbrep.2017.03.003>.
- Morales, Y., Tortajada, M., Picó, J., Vehí, J. and Llaneras, F. (2014). Validation of an FBA model for *Pichia pastoris* in chemostat cultures. *BMC Systems Biology* 8: 142. <https://doi.org/10.1186/s12918-014-0142-y>.
- Morris, E.K., Caruso, T., Buscot, F., Fischer, M., Hancock, C., Maier, T.S., et al. (2014). Choosing and using diversity indices: Insights for ecological applications from the German Biodiversity Exploratories. *Ecology and Evolution* 4 (18): 3514–24. <https://doi.org/10.1002/ece3.1155>.
- Mousdale, D.M. (2008). *Biofuels: Biotechnology, Chemistry, and Sustainable Development*. Boca Raton: CRC Press. [https://doi.org/10.1016/S1351-4180\(10\)70185-9](https://doi.org/10.1016/S1351-4180(10)70185-9).
- Mtui, G. and Nakamura, Y. (2005). Bioconversion of lignocellulosic waste from selected dumping sites in Dar es Salaam, Tanzania. *Biodegradation* 16 (6): 493–99. <https://doi.org/10.1007/s10532-004-5826-3>.
- Müller, V. and Frerichs, J. (2013). Acetogenic Bacteria. ELS. <https://doi.org/10.1002/9780470015902.a0020086.pub2>.
- Muyzer, G., Waal, E.C. De and Uitterlinden, A.G. (1993). Profiling of complex microbial populations by denaturing gradient gel electrophoresis analysis of polymerase chain reaction-amplified genes coding for 16S rRNA. *Applied and Environmental Microbiology* 59 (3): 695–700. [https://doi.org/10.1099-2240/93/030695-06\\$02.00/0](https://doi.org/10.1099-2240/93/030695-06$02.00/0).
- Muyzer, G., Waal, E.C. De and Uitterlinden, A.G. (1993). Profiling of complex microbial populations by denaturing gradient gel electrophoresis analysis of polymerase chain reaction-amplified genes coding for 16S rRNA. *Applied and Environmental Microbiology* 59 (3): 695–700. [https://doi.org/10.1099-2240/93/030695-06\\$02.00/0](https://doi.org/10.1099-2240/93/030695-06$02.00/0).

- Naylor, J., Fellermann, H., Ding, Y., Mohammed, W.K., Jakubovics, N.S., Mukherjee, J., et al. (2017). Simbiotics: A Multiscale Integrative Platform for 3D Modeling of Bacterial Populations. *ACS Synthetic Biology* 6 (7): 1194–1210. <https://doi.org/10.1021/acssynbio.6b00315>.
- Neher, D.A., Weicht, T.R., Bates, S.T., Leff, J.W. and Fierer, N. (2013). Changes in bacterial and fungal communities across compost recipes, preparation methods, and composting times. *PLoS ONE* 8 (11). <https://doi.org/10.1371/journal.pone.0079512>.
- Nelson, M.C., Bomar, L., Maltz, M. and Graf, J. (2015). *Mucinivorans hirudinis* gen. Nov., sp. nov., an anaerobic, mucin-degrading bacterium isolated from the digestive tract of the medicinal leech *Hirudo verbena*. *International Journal of Systematic and Evolutionary Microbiology* 65 (3): 990–95. <https://doi.org/10.1099/ijms.0.000052>.
- Neubeck, M. von, Huptas, C., Glück, C., Krewinkel, M., Stoecke, M., Stressler, T., et al. (2016). *Pseudomonas helleri* sp. nov. and *Pseudomonas weihenstephanensis* sp. nov., isolated from raw cow's milk. *International Journal of Systematic and Evolutionary Microbiology* 66 (3): 1163–73. <https://doi.org/10.1099/ijsem.0.000852>.
- O'Sullivan, C.A., Burrell, P.C., Clarke, W.P. and Blackall, L.L. (2005). Structure of a cellulose degrading bacterial community during anaerobic digestion. *Biotechnology and Bioengineering* 92 (7): 871–78. <https://doi.org/10.1002/bit.20669>.
- Ogunbanwo, S.T., Sanni, A.I. and Onilude, a. a. (2003). Characterization of bacteriocin produced by *Lactobacillus plantarum* F1 and *Lactobacillus brevis* OG1. *African Journal of Biotechnology* 2 (8): 219–27. <https://doi.org/10.4314/ajb.v2i8.14770>.
- Okeke, B.C. and Lu, J. (2011). Characterization of a defined cellulolytic and xylanolytic bacterial consortium for bioprocessing of cellulose and hemicelluloses. *Applied Biochemistry and Biotechnology* 163 (7): 869–81. <https://doi.org/10.1007/s12010-010-9091-0>.
- Oksanen, J., Guillaume Blanchet, F., Friendly, M., Kindt, R., Legendre, P., McGlinn, D., et al. (2018). *Vegan: Community Ecology Package*. 2018.
- Olsson, L. and Hahn-Hägerdal, B. (1996). Fermentation of lignocellulosic hydrolysates for ethanol production. *Enzyme and Microbial Technology* 18 (5): 312–31. [https://doi.org/10.1016/0141-0229\(95\)00157-3](https://doi.org/10.1016/0141-0229(95)00157-3).
- Orth, J.D., Thiele, I. and Palsson, B.Ø. (2010). What is flux balance analysis? *Nature Biotechnology* 28 (3): 245–48. <https://doi.org/10.1038/nbt.1614>.
- Parawira, W. and Tekere, M. (2011). Biotechnological strategies to overcome inhibitors in lignocellulose hydrolysates for ethanol production: Review. *Critical Reviews in Biotechnology* 31 (1): 20–31. <https://doi.org/10.3109/07388551003757816>.
- Park, N. (2016). Revised population estimates for England and Wales : mid-2012 to mid-2016.
- Paul, E.A. (2006). *Soil Microbiology, Ecology and Biochemistry: Third Edition*. Soil Microbiology, Ecology and Biochemistry: Third Edition. <https://doi.org/10.1016/C2009-0-02816-5>.
- Peacock, J.P., Cole, J.K., Murugapiran, S.K., Dodsworth, J.A., Fisher, J.C., Moser, D.P., et al. (2013). Pyrosequencing Reveals High-Temperature Cellulolytic Microbial Consortia in Great Boiling Spring after In Situ Lignocellulose Enrichment. *PLoS ONE* 8 (3): 1–12. <https://doi.org/10.1371/journal.pone.0059927>.
- Pieragostini, C., Aguirre, P. and Mussati, M.C. (2014). Life cycle assessment of corn-based ethanol production in Argentina. *Science of the Total Environment* 472: 212–25. <https://doi.org/10.1016/j.scitotenv.2013.11.012>.
- Pietro, M. and Paola, C. (2004). Thermal analysis for the evaluation of the organic matter evolution during municipal solid waste aerobic composting process. *Thermochimica Acta* 413 (1–2): 209–14. <https://doi.org/10.1016/j.tca.2003.09.026>.
- Poehlein, A., Solano, J.D.M., Flitsch, S.K., Krabben, P., Winzer, K., Reid, S.J., et al. (2017). Microbial solvent formation revisited by comparative genome analysis. *Biotechnology for Biofuels* 10 (1): 1–15. <https://doi.org/10.1186/s13068-017-0742-z>.
- POET-DSM. n.d. POET-DSM. Accessed April 24, 2018. <http://poetdsm.com/>.

Pontes, H., Pinho, P.G. De, Casal, S., Carmo, H., Santos, A., Magalhães, T., et al. (2009). GC determination of acetone, acetaldehyde, ethanol, and methanol in biological matrices and cell culture. *Journal of Chromatographic Science* 47 (4): 272–78. <https://doi.org/10.1093/chromsci/47.4.272>.

Ponton-Lozano, S., Montoya-Gómez, N.Y., Martínez-Sepúlveda, J.A. and Cañizares-Cañizares, P. Fernández-Morales, F.J. (2014). Study of Pre-Treatments for an Enhanced Bio-Ethanol Production From the Organic Fraction of Municipal Solid Wastes. *Global NEST Journal* 16 (6): 1091–99.

Poolman, B. (1993). Energy transduction in lactic acid bacteria. *FEMS Microbiology Reviews* 12 (1–3): 125–47. [https://doi.org/10.1016/0168-6445\(93\)90060-M](https://doi.org/10.1016/0168-6445(93)90060-M).

Poretzky, R., Rodriguez-r, L.M., Luo, C., Tsementzi, D. and Konstantinidis, K.T. (2014). Strengths and Limitations of 16S rRNA Gene Amplicon Sequencing in Revealing Temporal Microbial Community Dynamics 9 (4). <https://doi.org/10.1371/journal.pone.0093827>.

PROMEGA. (2012). Buffers for Biochemical Reactions. Buffers for Biochemical Reactions. Protocols and Applications Guide. 2012. <https://doi.org/10.1111/j.1399-302X.1990.tb00645.x>.

Pruesse, E., Quast, C., Knittel, K., Fuchs, B.M., Ludwig, W., Peplies, J., et al. (2007). SILVA: A comprehensive online resource for quality checked and aligned ribosomal RNA sequence data compatible with ARB. *Nucleic Acids Research* 35 (21): 7188–96. <https://doi.org/10.1093/nar/gkm864>.

Quast, C., Pruesse, E., Yilmaz, P., Gerken, J., Schweer, T., Yarza, P., et al. (2013). The SILVA ribosomal RNA gene database project: Improved data processing and web-based tools. *Nucleic Acids Research* 41 (D1). <https://doi.org/10.1093/nar/gks1219>.

Quested, T. and Johnson, H. (2009). Household Food and Drink Waste in the UK: A Report Containing Quantification of the Amount and Types of Household Food and Drink Waste in the UK. Report Prepared by WRAP (Waste and Resources Action Programme), Banbury.

Quince, C., Lanzen, A., Davenport, R.J. and Turnbaugh, P.J. (2011). Removing Noise From Pyrosequenced Amplicons. *BMC Bioinformatics*. <https://doi.org/10.1186/1471-2105-12-38>.

Quintero, J.A., Montoya, M.I., Sánchez, O.J., Giraldo, O.H. and Cardona, C.A. (2008). Fuel ethanol production from sugarcane and corn: Comparative analysis for a Colombian case. *Energy* 33 (3): 385–99. <https://doi.org/10.1016/j.energy.2007.10.001>.

Raizen. n.d. Second Generation Ethanol. Accessed April 28, 2018. <https://www.raizen.com.br/en/energy-future/renewable-energy-technology/second-generation-ethanol>.

Ramette, A. (2007). Multivariate analyses in microbial ecology. *FEMS Microbiology Ecology* 62 (2): 142–60. <https://doi.org/10.1111/j.1574-6941.2007.00375.x>.

Rashid, G.M.M., Durán-Peña, M.J., Rahmanpour, R., Sapsford, D. and Bugg, T.D.H. (2017). Delignification and enhanced gas release from soil containing lignocellulose by treatment with bacterial lignin degraders. *Journal of Applied Microbiology* 123 (1): 159–71. <https://doi.org/10.1111/jam.13470>.

Rice, E.W., Baird, R.B., Eaton, A.D. and Clesceri, L.S. (2012). 5220 CHEMICAL OXYGEN DEMAND (COD). In *Standard Methods for the Examination of Water and Wastewater*. <https://doi.org/ISBN 9780875532356>.

Rittmann, B.E. and McCarty, P.L. (2001). *Environmental Biotechnology: Principles and Applications*. McGraw-Hill Series in Water Resources and Environmental Engineering. [https://doi.org/10.1016/S0958-1669\(96\)80047-4](https://doi.org/10.1016/S0958-1669(96)80047-4).

Rodríguez, J., Kleerebezem, R., Lema, J.M. and Loosdrecht, M.C.M. Van. (2006). Modeling product formation in anaerobic mixed culture fermentations. *Biotechnology and Bioengineering* 93 (3): 592–606. <https://doi.org/10.1002/bit.20765>.

Rodríguez, J., Lema, J.M. and Kleerebezem, R. (2008). Energy-based models for environmental biotechnology. *Trends in Biotechnology* 26 (7): 366–74. <https://doi.org/10.1016/j.tibtech.2008.04.003>.

Rodríguez, J., Lema, J.M. and Kleerebezem, R. (2008). Energy-based models for environmental biotechnology. *Trends in Biotechnology* 26 (7): 366–74. <https://doi.org/10.1016/j.tibtech.2008.04.003>.

Ronan, P., William Yeung, C., Schellenberg, J., Sparling, R., Wolfaardt, G.M. and Hausner, M. (2013). A versatile and robust aerotolerant microbial community capable of cellulosic ethanol production. *Bioresource Technology* 129: 156–63. <https://doi.org/10.1016/j.biortech.2012.10.164>.

- Sanderson, K. (2011). Lignocellulose: A chewy problem. *Nature* 474 (7352 SUPPL.). <https://doi.org/10.1038/474S012a>.
- Sarkar, N., Ghosh, S.K., Bannerjee, S. and Aikat, K. (2012). Bioethanol production from agricultural wastes: An overview. *Renewable Energy* 37 (1): 19–27. <https://doi.org/10.1016/j.renene.2011.06.045>.
- Schloss, P.D. (2016). Customize your reference alignment for your favorite region. *The Mothur Blog*. 2016. <http://blog.mothur.org/2016/07/07/Customization-for-your-region/>.
- Schloss, P.D., Gevers, D. and Westcott, S.L. (2011). Reducing the effects of PCR amplification and sequencing Artifacts on 16s rRNA-based studies. *PLoS ONE* 6 (12). <https://doi.org/10.1371/journal.pone.0027310>.
- Schloss, P.D., Westcott, S.L., Ryabin, T., Hall, J.R., Hartmann, M., Hollister, E.B., et al. (2009). Introducing mothur: Open-source, platform-independent, community-supported software for describing and comparing microbial communities. *Applied and Environmental Microbiology*. <https://doi.org/10.1128/AEM.01541-09>.
- Schmidt, J.E. and Ahring, B.K. (1996). Granular sludge formation in upflow anaerobic sludge blanket (UASB) reactors. *Biotechnology and Bioengineering* 49 (3): 229–46. [https://doi.org/10.1002/\(SICI\)1097-0290\(19960205\)49:3<229::AID-BIT1>3.0.CO;2-M](https://doi.org/10.1002/(SICI)1097-0290(19960205)49:3<229::AID-BIT1>3.0.CO;2-M).
- Schwab, A., Warner, E. and Lewis, J. (2016). 2016 Survey of Non-Starch Ethanol and Renewable Hydrocarbon Biofuels Producers. <https://www.nrel.gov/docs/fy17osti/67539.pdf>.
- SEMARNAT. (2011). Residuos Sólidos Urbanos. <http://www2.inecc.gob.mx/publicaciones2/libros/705/solidos.pdf>.
- Shou, W., Ram, S. and Vilar, J.M.G. (2007). Synthetic cooperation in engineered yeast populations. *Proceedings of the National Academy of Sciences* 104 (6): 1877–82. <https://doi.org/10.1073/pnas.0610575104>.
- Silva Lopes, W., Duarte Leite, V. and Prasad, S. (2004). Influence of inoculum on performance of anaerobic reactors for treating municipal solid waste. *Bioresource Technology* 94: 261–66. <https://doi.org/10.1016/j.biortech.2004.01.006>.
- Simmons, C.W., Reddy, A.P., Simmons, B.A., Singer, S.W. and Vanderghenst, J.S. (2014). Effect of inoculum source on the enrichment of microbial communities on two lignocellulosic bioenergy crops under thermophilic and high-solids conditions. *Journal of Applied Microbiology* 117 (4): 1025–34. <https://doi.org/10.1111/jam.12609>.
- Simpson, E.H. (1949). Diversity, Measurement of. *Nature* 163: 688. <https://pallas2.tcl.sc.edu/login?url=http://search.ebscohost.com/login.aspx?direct=true&db=hus&AN=521607977&site=ehost-live>.
- Singh, A., Pant, D., Korres, N.E., Nizami, A.S., Prasad, S. and Murphy, J.D. (2010). Key issues in life cycle assessment of ethanol production from lignocellulosic biomass: Challenges and perspectives. *Bioresource Technology* 101 (13): 5003–12. <https://doi.org/10.1016/j.biortech.2009.11.062>.
- Sluiter, a, Hames, B., Hyman, D., Payne, C., Ruiz, R., Scarlata, C., et al. (2008). Determination of total solids in biomass and total dissolved solids in liquid process samples. *National Renewable Energy Laboratory (NREL)*, no. March: 9. <https://doi.org/NREL/TP-510-42621>.
- Sluiter, A., Hames, B., Ruiz, R., Scarlata, C., Sluiter, J. and Templeton, D. (2008). Determination of ash in biomass: Laboratory Analytical Procedure (LAP). *Nrel/Tp-510-42622*, no. April 2005: 18. <https://doi.org/NREL/TP-510-42619>.
- Sluiter, J.B., Ruiz, R.O., Scarlata, C.J., Sluiter, A.D. and Templeton, D.W. (2010). Compositional analysis of lignocellulosic feedstocks. 1. Review and description of methods. *Journal of Agricultural and Food Chemistry* 58 (16): 9043–53. <https://doi.org/10.1021/jf1008023>.
- SMA. (2010). Programa de gestión integral de los residuos sólidos urbanos para el Distrito Federal. 2010. <http://www.sma.df.gob.mx/rsolidos/03/local/03clave.pdf>.
- Smolders, G.J.F., Meij, J. van der, Loosdrecht, M.C.M. van and Heijnen, J.J. (1995). A structured metabolic model for the anaerobic and aerobic stoichiometry of the biological phosphorus removal process. *Biotechnology and Bioengineering*. *Biotechnology and Bioengineering* 47 (3): 277–87. <https://doi.org/10.1002/bit.260470302>.

Song, C., Li, M., Jia, X., Wei, Z., Zhao, Y., Xi, B., et al. (2014). Comparison of bacterial community structure and dynamics during the thermophilic composting of different types of solid wastes: Anaerobic digestion residue, pig manure and chicken manure. *Microbial Biotechnology* 7 (5): 424–33. <https://doi.org/10.1111/1751-7915.12131>.

Souza Dias, M.O. de, Maciel Filho, R., Mantelatto, P.E., Cavalett, O., Rossell, C.E.V., Bonomi, A., et al. (2015). Sugarcane processing for ethanol and sugar in Brazil. *Environmental Development* 15: 35–51. <https://doi.org/10.1016/j.envdev.2015.03.004>.

Spector, M.P. (2009). Metabolism, Central (Intermediary). In *Encyclopedia of Microbiology*, 5:242–64. <https://doi.org/10.1017/CBO9781107415324.004>.

Steinbusch, K.J.J., Arvaniti, E., Hamelers, H.V.M. and Buisman, C.J.N. (2009). Selective inhibition of methanogenesis to enhance ethanol and n-butyrate production through acetate reduction in mixed culture fermentation. *Bioresource Technology* 100 (13): 3261–67. <https://doi.org/10.1016/j.biortech.2009.01.049>.

Stephanopoulos, G. (2007). Challenges in engineering microbes for biofuels production. *Science* 315 (5813): 801–4. <https://doi.org/10.1126/science.1139612>.

Stoeckel, M., Lidolt, M., Achberger, V., Glück, C., Krewinkel, M., Stressler, T., et al. (2016). Growth of *Pseudomonas weihenstephanensis*, *Pseudomonas proteolytica* and *Pseudomonas* sp. in raw milk: Impact of residual heat-stable enzyme activity on stability of UHT milk during shelf-life. *International Dairy Journal* 59: 20–28. <https://doi.org/10.1016/j.idairyj.2016.02.045>.

Suen, G., Stevenson, D.M., Bruce, D.C., Chertkov, O., Copeland, A., Cheng, J.F., et al. (2011). Complete genome of the cellulolytic ruminal bacterium *Ruminococcus albus* 7. *Journal of Bacteriology*. <https://doi.org/10.1128/JB.05621-11>.

Sun Yoon, S., Hennigan, R.F., Hilliard, G.M., Ochsner, U.A., Parvatiyar, K., Kamani, M.C., et al. (2002). *Pseudomonas aeruginosa* Anaerobic Respiration in Biofilms: Relationships to Cystic Fibrosis Pathogenesis of toxic NO, a byproduct of anaerobic respiration. Proteomic analyses identified an outer membrane protein. *Developmental Cell* 3: 593–603. [https://doi.org/10.1016/S1534-5807\(02\)00295-2](https://doi.org/10.1016/S1534-5807(02)00295-2).

Sun, L., Pope, P.B., Eijsink, V.G.H. and Schnürer, A. (2015). Characterization of microbial community structure during continuous anaerobic digestion of straw and cow manure. *Microbial Biotechnology* 8 (5): 815–27. <https://doi.org/10.1111/1751-7915.12298>.

Sun, L., Toyonaga, M., Ohashi, A., Turlousse, D.M., Matsuura, N., Meng, X.Y., et al. (2016). *Lentimicrobium saccharophilum* gen. nov., sp. nov., a strictly anaerobic bacterium representing a new family in the phylum bacteroidetes, and proposal of *lentimicrobiaceae* fam. nov. *International Journal of Systematic and Evolutionary Microbiology* 66 (7): 2635–42. <https://doi.org/10.1099/ijsem.0.001103>.

Sun, Y. and Cheng, J. (2002). Hydrolysis of lignocellulosic materials for ethanol production : a review q. *Bioresource Technology* 83 (1): 1–11. [https://doi.org/10.1016/S0960-8524\(01\)00212-7](https://doi.org/10.1016/S0960-8524(01)00212-7).

Talebna, F., Karakashev, D. and Angelidaki, I. (2010). Production of bioethanol from wheat straw: An overview on pretreatment, hydrolysis and fermentation. *Bioresource Technology*. <https://doi.org/10.1016/j.biortech.2009.11.080>.

Tang, Y., Shigematsu, T., Ikbal, Morimura, S. and Kida, K. (2004). The effects of micro-aeration on the phylogenetic diversity of microorganisms in a thermophilic anaerobic municipal solid-waste digester. *Water Research*. <https://doi.org/10.1016/j.watres.2004.03.012>.

Tanner, R.S., Miller, L.M. and Yang, D. (1993). *Clostridium ljungdahlii* sp-Nov, an Acetogenic Species in Clostridial Ribosomal-RNA Homology Group-I . *International Journal of Systematic Bacteriology* 43 (2): 232–36. <https://doi.org/10.1099/00207713-43-2-232>.

Temudo, M.F., Kleerebezem, R. and Loosdrecht, M. Van. (2007). Influence of the pH on (Open) mixed culture fermentation of glucose: A chemostat study. *Biotechnology and Bioengineering* 98 (1): 69–79. <https://doi.org/10.1002/bit.21412>.

Temudo, M.F., Muyzer, G., Kleerebezem, R. and Loosdrecht, M.C.M. Van. (2008). Diversity of microbial communities in open mixed culture fermentations: Impact of the pH and carbon source. *Applied Microbiology and Biotechnology* 80 (6): 1121–30. <https://doi.org/10.1007/s00253-008-1669-x>.

- Teugjas, H. and Väljamäe, P. (2013). Product inhibition of cellulases studied with ¹⁴C-labeled cellulose substrates. *Biotechnology for Biofuels* 6 (1). <https://doi.org/10.1186/1754-6834-6-104>.
- Thakur, V.K., Thakur, M.K., Raghavan, P. and Kessler, M.R. (2014). Progress in green polymer composites from lignin for multifunctional applications: A review. *ACS Sustainable Chemistry and Engineering* 2 (5): 1072–92. <https://doi.org/10.1021/sc500087z>.
- Thamelis, N. and Bourtsalas, A. (2013). UK Waste Management: Growing old or Growing Clean? *Waste Management World*. 2013. <https://waste-management-world.com/a/uk-waste-management-growing-old-or-growing-clean>.
- Thurston, B. and Dawson, K.A. (1993). Cellobiose versus Glucose Utilization by the Ruminant Bacterium *Ruminococcus albus*. *Applied Environment Microbiology* 59 (8): 2631–37.
- Todhanakasem, T., Sangsutthiseree, A., Areerat, K., Young, G.M. and Thanonkeo, P. (2014). Biofilm production by *Zymomonas mobilis* enhances ethanol production and tolerance to toxic inhibitors from rice bran hydrolysate. *New Biotechnology* 31 (5): 451–59. <https://doi.org/10.1016/j.nbt.2014.06.002>.
- U.S. Energy Information Administration. (2015). Corn ethanol yields continue to improve. 2015. <https://www.eia.gov/todayinenergy/detail.php?id=21212>.
- Varrone, C., Heggeset, T.M.B., Le, S.B., Haugen, T., Markussen, S., Skiadas, I. V., et al. (2015). Comparison of Different Strategies for Selection/Adaptation of Mixed Microbial Cultures Able to Ferment Crude Glycerol Derived from Second-Generation Biodiesel. *BioMed Research International* 2015. <https://doi.org/10.1155/2015/932934>.
- Vartoukian, S.R., Palmer, R.M. and Wade, W.G. (2007). The division “Synergistes.” *Anaerobe* 13 (3–4): 99–106. <https://doi.org/10.1016/j.anaerobe.2007.05.004>.
- Vasilopoulos, C., Mey, E. De, Dewulf, L., Paelinck, H., Smedt, A. De, Vandendriessche, F., et al. (2010). Interactions between bacterial isolates from modified-atmosphere-packaged artisan-type cooked ham in view of the development of a bioprotective culture. *Food Microbiology* 27 (8): 1086–94. <https://doi.org/10.1016/j.fm.2010.07.013>.
- Vernikos, G., Medini, D., Riley, D.R. and Tettelin, H. (2015). Ten years of pan-genome analyses. *Current Opinion in Microbiology* 23: 148–54. <https://doi.org/10.1016/j.mib.2014.11.016>.
- Vos, P. De, Garrity, G.M., Jones, D., Krieg, N.R., Ludwig, W., Rainey, F.A., et al. (2009). *Bergey's Manual of Systematic Bacteriology Volume Three The Firmicutes*. *Bergey's Manual of Systematic Bacteriology*. Vol. 3. <https://doi.org/10.1007/978-0-387-68489-5>.
- Wahyudi, a, Cahyanto, M.N., Soejono, M. and Bachruddin, Z. (2010). Potency of lignocellulose degrading bacteria isolated from buffalo and horse gastrointestinal tract and elephant dung for feed fiber degradation. *J.Indonesian Trop.Anim.Agric.* 35 (1): 34–41. [file:///c:/Documents and Settings/Danie/My Documents/Reference Manager/1167 Potency of lignocellulose degrading bacteria isolated from buffalo and horse GIT and elephant dung for feed fiber degradation.pdf](file:///c:/Documents%20and%20Settings/Danie/My%20Documents/Reference%20Manager/1167%20Potency%20of%20lignocellulose%20degrading%20bacteria%20isolated%20from%20buffalo%20and%20horse%20GIT%20and%20elephant%20dung%20for%20feed%20fiber%20degradation.pdf).
- Wahyudi, a, Cahyanto, M.N., Soejono, M. and Bachruddin, Z. (2010). Potency of lignocellulose degrading bacteria isolated from buffalo and horse gastrointestinal tract and elephant dung for feed fiber degradation. *J.Indonesian Trop.Anim.Agric.* 35 (1): 34–41. [file:///c:/Documents and Settings/Danie/My Documents/Reference Manager/1167 Potency of lignocellulose degrading bacteria isolated from buffalo and horse GIT and elephant dung for feed fiber degradation.pdf](file:///c:/Documents%20and%20Settings/Danie/My%20Documents/Reference%20Manager/1167%20Potency%20of%20lignocellulose%20degrading%20bacteria%20isolated%20from%20buffalo%20and%20horse%20GIT%20and%20elephant%20dung%20for%20feed%20fiber%20degradation.pdf).
- Walker, G.M. (2011). 125th anniversary review: Fuel alcohol: Current production and future challenges. *Journal of the Institute of Brewing* 117 (1): 3–22. <https://doi.org/10.1002/j.2050-0416.2011.tb00438.x>.
- Wang, A., Gao, L., Ren, N., Xu, J. and Liu, C. (2009). Bio-hydrogen production from cellulose by sequential co-culture of cellulosic hydrogen bacteria of *Enterococcus gallinarum* G1 and *Ethanoigenens harbinense* B49. *Biotechnology Letters* 31 (9): 1321–26. <https://doi.org/10.1007/s10529-009-0028-z>.
- Wang, L., Lai, L., Ouyang, Q. and Tang, C. (2011). Flux Balance Analysis. *PLoS ONE* 58: 1–29. <https://doi.org/10.1371/journal.pone.0016362>.
- Ward, L.M., Hemp, J., Pace, L.A. and Fischer, W.W. (2015). Draft Genome Sequence of *Leptolinea tardivitalis* YMTK-2, a Mesophilic Anaerobe from the Chloroflexi Class Anaerolineae. *Genome Announcements* 3 (6): e01356-15. <https://doi.org/10.1128/genomeA.01356-15>.

Wen, Z., Wu, M., Lin, Y., Yang, L., Lin, J. and Cen, P. (2014). Artificial symbiosis for acetone-butanol-ethanol (ABE) fermentation from alkali extracted deshelled corn cobs by co-culture of *Clostridium beijerinckii* and *Clostridium cellulovorans*. *Microbial Cell Factories* 13 (1): 1–11. <https://doi.org/10.1186/s12934-014-0092-5>.

White, D. (2007). Fermentations. In *The Physiology and Biochemistry of Prokaryotes*, Third edit, 383–403. New York: Oxford University Press.

White, T. J., Bruns, T. D., Lee, S. B. and Taylor, J. W. (1990). Amplification and direct sequencing of fungal ribosomal RNA Genes for phylogenetics. In *PCR - Protocols and Applications - A Laboratory Manual*, edited by Innis, MA, Gelfand, DH, JJ, Sninsky, and TJ, White, 315–22. United States: Academic Press.

Wongwilaiwalin, S., Rattanachomsri, U., Laothanachareon, T., Eurwilaichitr, L., Igarashi, Y. and Champreda, V. (2010). Analysis of a thermophilic lignocellulose degrading microbial consortium and multi-species lignocellulolytic enzyme system. *Enzyme and Microbial Technology* 47 (6): 283–90. <https://doi.org/10.1016/j.enzmictec.2010.07.013>.

Wu, Y., Wang, C., Zheng, M., Zuo, J., Wu, J., Wang, K., et al. (2017). Effect of pH on ethanol-type acidogenic fermentation of fruit and vegetable waste. *Waste Management* 60: 158–63. <https://doi.org/10.1016/j.wasman.2016.09.033>.

Xia, Y., Wang, Y., Wang, Y., Chin, F.Y.L. and Zhang, T. (2016). Cellular adhesiveness and cellulolytic capacity in Anaerolineae revealed by omics-based genome interpretation. *Biotechnology for Biofuels* 9 (1): 1–13. <https://doi.org/10.1186/s13068-016-0524-z>.

Xiao, Y.P., Hui, W., Wang, Q., Roh, S.W., Shi, X.Q., Shi, J.H., et al. (2009). *Pseudomonas caeni* sp. nov., a denitrifying bacterium isolated from the sludge of an anaerobic ammonium-oxidizing bioreactor. *International Journal of Systematic and Evolutionary Microbiology* 59 (10): 2594–98. <https://doi.org/10.1099/ijs.0.005108-0>.

Xu, Z., He, H., Zhang, S. and Kong, J. (2017). Effects of inoculants *Lactobacillus brevis* and *Lactobacillus parafarraginis* on the fermentation characteristics and microbial communities of corn stover silage. *Scientific Reports* 7 (1): 1–9. <https://doi.org/10.1038/s41598-017-14052-1>.

Yamada, T., Sekiguchi, Y., Hanada, S., Imachi, H., Ohashi, A., Harada, H., et al. (2006). *Anaerolinea thermolimosa* sp. nov., *Levilinea saccharolytica* gen. nov., sp. nov. and *Leptolinea tardivitalis* gen. nov., sp. nov., novel filamentous anaerobes, and description of the new classes Anaerolineae classis nov. and Caldilineae classis nov. in the . *International Journal of Systematic and Evolutionary Microbiology* 56 (6): 1331–40. <https://doi.org/10.1099/ijs.0.64169-0>.

Yanagida, F., Suzuki, K.-I., Kozaki, M. and Komagata, K. (1997). Proposal of *Sporolactobacillus nakayamae* subsp. *nakayamae* sp. nov., subsp. nov., *Sporolactobacillus nakayamae* subsp. *racernicus* subsp. nov., *Sporolactobacillus terrae* sp. nov., *Sporolactobacillus kofiensis* sp. nov., and *Sporolactobacillus lactosus* sp. nov. *INTERNATIONAL JOURNAL OF SYSTEMATIC BACTERIOLOGY* 47 (2): 499–504.

Yang, B., Dai, Z., Ding, S.-Y. and Wyman, C.E. (2014). Enzymatic hydrolysis of cellulosic biomass. *Biofuels* 2: 421–49. <https://doi.org/10.4155/bfs.11.116>.

Yang, Q. and Chen, G.Q. (2012). Nonrenewable energy cost of corn-ethanol in China. *Energy Policy* 41: 340–47. <https://doi.org/10.1016/j.enpol.2011.10.055>.

Yang, S., Fei, Q., Zhang, Y., Contreras, L.M., Utturkar, S.M., Brown, S.D., et al. (2016). *Zymomonas mobilis* as a model system for production of biofuels and biochemicals. *Microbial Biotechnology*. <https://doi.org/10.1111/1751-7915.12408>.

Yao, D., Dong, S., Wang, P., Chen, T., Wang, J., Yue, Z.B., et al. (2017). Robustness of *Clostridium saccharoperbutylacetonicum* for acetone-butanol-ethanol production: Effects of lignocellulosic sugars and inhibitors. *Fuel* 208 (November): 549–57. <https://doi.org/10.1016/j.fuel.2017.07.004>.

Ye, N.F., Lü, F., Shao, L.M., Godon, J.J. and He, P.J. (2007). Bacterial community dynamics and product distribution during pH-adjusted fermentation of vegetable wastes. *Journal of Applied Microbiology* 103 (4): 1055–65. <https://doi.org/10.1111/j.1365-2672.2007.03321.x>.

Zech, K.M., Meisel, K., Brosowski, A., Toft, L.V. and Müller-Langer, F. (2016). Environmental and economic assessment of the Inbicon lignocellulosic ethanol technology. *Applied Energy* 171: 347–56. <https://doi.org/10.1016/j.apenergy.2016.03.057>.

- Zelezniak, A., Andrejev, S., Ponomarova, O., Mende, D.R., Bork, P. and Patil, K.R. (2015). Metabolic dependencies drive species co-occurrence in diverse microbial communities. *Proceedings of the National Academy of Sciences* 112 (20): 6449–54. <https://doi.org/10.1073/pnas.1421834112>.
- Zhang, B., Xu, X. and Zhu, L. (2017). Structure and function of the microbial consortia of activated sludge in typical municipal wastewater treatment plants in winter. *Scientific Reports* 7 (1). <https://doi.org/10.1038/s41598-017-17743-x>.
- Zhang, F., Zhang, Y., Chen, M. and Zeng, R.J. (2012). Hydrogen supersaturation in thermophilic mixed culture fermentation. *International Journal of Hydrogen Energy* 37 (23): 17809–16. <https://doi.org/10.1016/j.ijhydene.2012.09.019>.
- Zhang, H. and Cai, Y. (2014). *Lactic Acid Bacteria: Fundamentals and Practice*. Lactic Acid Bacteria: Fundamentals and Practice. <https://doi.org/10.1007/978-94-017-8841-0>.
- Zhang, Q. and Bao, J. (2017). Industrial cellulase performance in the simultaneous saccharification and co-fermentation (SSCF) of corn stover for high-titer ethanol production. *Bioresources and Bioprocessing* 4 (1): 17. <https://doi.org/10.1186/s40643-017-0147-7>.
- Zhang, Y. and Ezeji, T.C. (2014). Elucidating and alleviating impacts of lignocellulose-derived microbial inhibitors on *Clostridium beijerinckii* during fermentation of *Miscanthus giganteus* to butanol. *Journal of Industrial Microbiology and Biotechnology* 41 (10): 1505–16. <https://doi.org/10.1007/s10295-014-1493-5>.
- Zhang, Z., Schwartz, S., Wagner, L. and Miller, W. (2000). A Greedy Algorithm for Aligning DNA Sequences. *Journal of Computational Biology* 7 (1–2): 203–14. <https://doi.org/10.1089/10665270050081478>.
- Zhou, K., Qiao, K., Edgar, S. and Stephanopoulos, G. (2015). Distributing a metabolic pathway among a microbial consortium enhances production of natural products. *Nature Biotechnology* 33 (4). <https://doi.org/10.1038/nbt.3095>.
- Zhou, L., Xia, S., Zhang, Z., Ye, B., Xu, X., Gu, Z., et al. (2014). Effects of pH, Temperature and Salinity on Extracellular Polymeric Substances of *Pseudomonas aeruginosa* Biofilm with N- (3-Oxooxetanoyl) -L-Homoserine Lactone Addition. <https://doi.org/10.11912/jws.4.2.91-100>.
- Zomorodi, A.R. and Maranas, C.D. (2012). OptCom: A multi-level optimization framework for the metabolic modeling and analysis of microbial communities. *PLoS Computational Biology* 8 (2). <https://doi.org/10.1371/journal.pcbi.1002363>.
- Zuroff, T.R. and Curtis, W.R. (2012). Developing symbiotic consortia for lignocellulosic biofuel production. *Applied Microbiology and Biotechnology* 93 (4): 1423–35. <https://doi.org/10.1007/s00253-011-3762-9>.